FACULDADE DE FARMÁCIA
UNIVERSIDADE DO PORTO

RUA DE JORGE VITERBO
FERREIRA N.º 228
4050-313 PORTO - PORTUGAL
WWW.FF.UP.PT

SELF-ASSEMBLED POLYMERIC MICELLES AS POWDERS FOR PULMONARY ADMINISTRATION OF INSULIN

FERNANDA RAQUEL DA SILVA ANDRADE
PH.D IN PHARMACEUTICAL SCIENCES
PHARMACEUTICAL TECHNOLOGY

FACULDADE DE FARMÁCIA
UNIVERSIDADE DO PORTO

SELF-ASSEMBLED POLYMERIC MICELLES AS POWDERS FOR PULMONARY ADMINISTRATION OF INSULIN

Fernanda Raquel da Silva Andrade

THESIS SUBMITTED TO THE FACULTY OF PHARMACY OF THE
UNIVERSITY OF PORTO FOR APPROVAL OF THE PHD DEGREE

PORTO 2015

This page was intentionally left in blank


FCT
Fundação para a Ciência e a Tecnologia
MINISTÉRIO DA EDUCAÇÃO E CIÊNCIA


U.PORTO
FACULDADE DE FARMÁCIA
UNIVERSIDADE DO PORTO


FACULTAT DE
FARMÀCIA


Universitat de Barcelona


IBEC
Institute for Bioengineering of Catalonia


INEB
Instituto de Engenharia Biomédica


CESPU
INSTITUTO SUPERIOR
DE CIÊNCIAS DA SAÚDE
NORTE


iMed.
ULisboa
Research
Institute for
Medicines

Fernanda Raquel da Silva Andrade

Self-assembled polymeric micelles as powders for pulmonary administration of insulin

Thesis Submitted in fulfilment of the requirements to obtain the PhD degree in Pharmaceutical Sciences, Pharmaceutical Technology Specialty

Tese do 3.º Ciclo de Estudos Conducente ao Grau de Doutoramento em Ciências Farmacêuticas na Especialidade de Tecnologia Farmacêutica

Work developed under supervision of Prof. Dr. Bruno Sarmento and co-supervision of Prof. Dr. Domingos de Carvalho Ferreira and Prof. Dr. Mafalda Videira

May, 2015

“To try and fail is at least to learn; to fail to try is to suffer the inestimable loss of what might have been.”

Chester Barnard

Acknowledgments

I would like to express my gratitude to all the people and institutions that receive me, help me and support me during the performance of this work. Thus, I would like to acknowledge:

My supervisor Professor Bruno Sarmento and my co-supervisors Professor Domingos de Carvalho Ferreira and Professora Mafalda Videira for believe in my capabilities and for accepting the challenge of participate and supervise this work and the present thesis.

Professor Bruno Sarmento from Instituto de Engenharia Biomédica (INEB) and Instituto de Investigação e Inovação em Saúde (I3S) da Universidade do Porto, Porto, Portugal, and from Instituto de Investigação e Formação Avançada em Ciências e Tecnologias da Saúde (IINFACTS) do Instituto Superior de Ciências de Saúde do Norte (ISCS-N) da Cooperativa de Ensino Superior Politécnico e Universitário (CESPU), Gandra Portugal, for all the guidance and support in the easiest and most difficult moments. All the friendship and trust placed in me to perform this and other works and for all the opportunities provided to make me grow as a researcher. Also for all the scientific discussions, comments and corrections performed to the common publications and the present thesis.

Professor Domingos de Carvalho Ferreira from Laboratório de Tecnologia Farmacêutica da Faculdade de Farmácia, Universidade do Porto (FFUP), Porto, Portugal, for all the friendship, understanding and support in the most fun and boring moments of the work. All the availability provided to make possible the progression of this work.

Professor Mireia Oliva from Departament de Farmàcia i Tecnologia Farmacèutica, Facultat de Farmàcia, Universitat de Barcelona (UB), Barcelona, España, from Nanoprobes and Nanoswitches Group, Institute for Bioengineering of Catalonia (IBEC), Barcelona, España, and from Centro Investigación Biomédica en Red – Bioingeniería, Biomateriales y Nanomedicina (CIBER-BBN), Madrid, España for all the availability to receive me in her laboratory at UB and to introduce me in IBEC to perform part of the work. For all the hospitality, friendship, and trust and all the scientific discussions, comments and corrections performed to the common papers and the present thesis.

Professor Mafalda Videira from Instituto de Investigação do Medicamento da Faculdade de Farmácia, Universidade de Lisboa (iMed.ULisboa), Lisboa Portugal for all the support and for receiving me for a stay to perform part of the work in her research group. For all the comments and corrections performed to the common papers and the present thesis.

The members of Laboratório de Tecnologia Farmacêutica da FFUP, especially to its Director, for accepting me as PhD student in the department and for their support to this work.

The members of Departament de Farmàcia i Tecnologia Farmacèutica, Facultat de Farmàcia, and Servei de Desenvolupament del Medicament (SDM) at UB for their support to this work.

The members of Nanoprobes and Nanoswitches group from IBEC, especially Professor Fausto Sanz, Professor Pau Gorostiza, and Dr. Marina Giannotti, for receiving me in the group for a stay and their support to this work.

The members of ISCS-N/CESPU, especially Professor Vítor Seabra for all the support to this work and for allowing me to perform the *in vivo* experiments at ISCS-N.

The members of Departament de Farmàcia i Tecnologia Farmacèutica, Facultat de Farmàcia, UB, especially Professor Ana Calpena and Mireia Mallandrich, and Departament de Fisicoquímica, Facultat de Farmàcia, UB, especially Professor Marisa García for their support to this work.

The members of REQUIMTE, Departamento de Ciências Químicas da FFUP, especially Professor Salette Reis, Dr. Marina Pinheiro, Ana Rute Neves, and Ana Catarina Alves for their support to this work.

The members of Centre d'Investigacions en Bioquímica I Biologia Molecular en Nanomedicina (CIBBIM-Nanomedicina), Vall d'Hebron Institut de Recerca (VHIR), especially Dr. Simó Schwartz, Dr. Petra Gener, Diana Rafael, Dr. Juan Sayos and Dr. Aroa Ejarque for the assistance in the uptake studies with macrophages.

Pedro Fonte from REQUIMTE and ISCS-N/CESPU for assistance in the Fourier transform infrared experiments and *in vivo* experiments.

Dr. José das Neves from FFUP and INEB for assistance in the *in vitro* toxicity studies.

Dr. Cassilda Cunha Reis from ISCS-N/CESPU for assistance in the *in vivo* experiments.

Ana Costa and Rute Nunes from INEB for assistance in the *in vivo* experiments.

Carla Pereira from INEB for the assistance in preparing histology slides.

Clara Myrla Abreu from Universidade Federal do Ceará, Fortaleza, Brasil for assistance in the *in vivo* experiments.

Diana Rafael from iMed.ULisboa and VHIR, for assistance in the design of the figures for the present thesis and for all the friendship, support and everyday life sharing during my stays in Lisboa and Barcelona.

Dr. José das Neves from FFUP and INEB, Dr. Yogeeta Babu da Rocha and Ana Patrícia Neto from Inovapotek – Pharmaceutical Research and Development, Porto, Portugal, for their friendship, support, and moments of relax during the shared lunch times.

The members of Professor Karim Amighi group at the Faculté de Pharmacie, Université Libre de Bruxelles, Bruxelles, Belgique, especially Dr. Nathalie Wauthoz and Rémi Rosière, for receiving me in their laboratory to teach me the techniques of endotracheal instillation and bronchoalveolar lavage used in *in vivo* experiments.

All the friends and colleagues of work (including Alexandra Machado, Alexandre Couto, Ana Margarida Costa, Ana Vanessa Nascimento, Bárbara Mendes, Carla Pereira, Catarina Moura, Diana Rafael, Dr. Cassilda Cunha Reis, Dr. Cláudia Marques, Dr. José das Neves, Dr. Sara Baptista da Silva, Dr. Susana Martins, Filipa Antunes, Francisca Araújo, Francisca Rodrigues, Helena Xandri Monje, João Albuquerque, Luise Lopes, Maria João Gomes, Patrick Kennedy, Pedro Fonte, Rute Nunes, Teófilo Vasconcelos) for their friendship, help,

assistance, scientific discussions, and moments of relax in the laboratory and outside in an almost daily basis.

My closest friends for their friendship, support, companionship, complicity, and for putting me up in the most difficult moments.

My family, mother (Filomena), father (Vítor), sister (Isabel), grandmother (Dolores) and my nephew (my little prince Francisco), for their unconditional love, patience, support, and for bear my long periods of absence.

BASF, Ludwigshafen, Germany for kindly provide Soluplus®, Pluronic® F68, Pluronic® F108 and Pluronic® F127.

Abbot Laboratories, Portugal for kindly provide the Precision Xtra® blood glucose meter and test strips.

Vétoquinol, Barcarena, Portugal for kindly provide Clorketam 1000®.

Fundação para a Ciência e a Tecnologia (FCT) for financial support through the grant SFRH/BD/73062/2010 financed by the Programa Operacional Potencial Humano (POPH) do Quadro de Referência Estratégico Nacional (QREN) Portugal 2007-2013, and by funds from the Ministério da Educação e Ciência. This work was also financed by the European Regional Development Fund (ERDF) through the Programa Operacional Factores de Competitividade (COMPETE), by Portuguese funds through FCT in the framework of the project PEst-C/SAU/LA0002/2013, and co-financed by North Portugal Regional Operational Programme (ON.2 – O Novo Norte) in the framework of project SAESCTN-PIIC&DT/2011, under the National Strategic Reference Framework (NSRF).

Abstract

Over the last decades, inhalation of compounds has gained new attention since it holds the potential to deliver drugs, namely biopharmaceuticals, for both local and systemic action to treat a variety of diseases. Despite being extensively studied to formulate hydrophobic drugs, polymeric micelles present characteristics poorly exploited towards the systemic administration of biopharmaceuticals by inhalation. In particular, polymeric micelles might protect proteins against thermal denaturation, or avoid phagocytosis by alveolar macrophages due to small size. Thus, this work aims to explore the use of polymeric micelles in the development of powders as vehicles for pulmonary delivery of therapeutic peptides and proteins, using insulin as a model protein.

Different amphiphilic polymers (Soluplus®, Pluronic® F68, Pluronic® F108 and Pluronic® F127) were used to produce lyophilized nanocomposites for inhalation. The development of glucose-sensitive formulations was also attempted with the addition of phenylboronic acid (PBA) to the micelles.

Results showed that size and polydispersity of micelles were dependent on the amphiphilic polymer used, being all lower than 300 nm in size, while all the formulations displayed spherical shape and surface charge close to neutrality. Association efficiency (AE) and loading capacity (LC) ranging from 49.3% to 94.6% and from 5.6% to 8.6%, respectively, were obtained. X-ray photoelectron spectroscopy (XPS) analysis confirmed that insulin was partially present at the hydrophilic shell of the micelles, while PBA in its hydrophobic inner core, as expected taking into account their water solubility. Despite influencing the *in vitro* release of insulin from micelles, PBA did not confer glucose-sensitive properties to formulations.

Upon lyophilization, micelle formulations retained their physical characteristics, further providing easily dispersion when in contact to aqueous medium. The native-like conformation of insulin was highly maintained after lyophilization as indicated by Fourier transform infrared spectroscopy (FTIR) and far-ultraviolet circular dichroism (far-UV CD). Moreover, differential scanning calorimetry (DSC) and Raman spectroscopy did not evidence significant interactions among the formulation components.

Amorphous state formulations showed to be physically stable upon storage up to 6 months both at room-temperature (20 ºC) and fridge (4ºC), with only a slight loss (maximum of 15%) of the secondary structure of the protein.

The aerosolization and aerodynamic properties of nanocomposites varied according to the formulation, presenting aerodynamic diameters lower than 6.6 µm and fine particle fraction (FPF) up to 48 % of the administered dose, predicting good deposition pattern of particles in the lungs.

Solid formulations showed to be compatible with the respiratory tract owing to the absence of *in vitro* toxicity for epithelial respiratory cell lines (A549 and Calu-3) and macrophages (Raw 264.7). Additionally, some formulations, in particular Pluronic® F127-based formulations, enhanced the permeation of insulin through pulmonary epithelial models and underwent minimal *in vitro* internalization by macrophages, as evaluated by confocal microscopy and flow cytometry.

The efficacy and safety of formulations were assessed *in vivo* using a streptozotocin-induced diabetic rat model. Endotracheally instilled powders have shown a faster onset of action than subcutaneous administration of insulin at a dose of 10 IU/kg, with pharmacological availabilities up to 32.5% of those achieved by subcutaneous route. A significant improvement of hypoglycemic effect following inhaled insulin was observed when associated to polymeric micelles as compared to its free solution form. In a 14-day sub-acute toxicity study, bronchoalveolar lavage screening for cell count, protein content, lactate dehydrogenase (LDH), cytokines, and chemokines revealed no signs of lung inflammation and cytotoxicity. Histological analysis of lungs, heart and liver showed the absence of tissue damage.

Overall, powder formulations based on polymeric micelles presenting promising characteristics for the delivery of therapeutic peptides and proteins by inhalation were achieved. Among the polymers tested, Pluronic® F127 produced the more promising carrier formulations for systemic delivery of therapeutic proteins.

Keywords: Polymeric micelles, Pulmonary administration, Insulin, Nanocomposites, Dry powder inhalers

Resumo

Ao longo das últimas décadas a inalação de fármacos, incluindo biofármacos, tem sido alvo de atenção por parte de investigadores e indústrias farmacêuticas uma vez que permite a administração de compostos com ação local e também sistémica, contribuindo assim para o tratamento de várias doenças. Apesar de bastante utilizadas na formulação de fármacos hidrófobos, as micelas poliméricas possuem características vantajosas pouco exploradas para a administração sistémica de biofármacos por via inalatória. Entre essas vantagens encontram-se a proteção térmica conferida pelos polímeros presentes na sua constituição e a capacidade de evasão à internalização por macrófagos conferida pelos seus reduzidos tamanhos. Desta forma, o presente trabalho explora a utilidade das micelas poliméricas no desenvolvimento de pós para administração pulmonar de péptidos e proteínas terapêuticas, sendo a insulina utilizada como proteína modelo.

Diferentes polímeros anfifílicos, nomeadamente Soluplus®, Pluronic® F68, Pluronic® F108 e Pluronic® F127 foram utilizados para o desenvolvimento de nanocompósitos obtidos por liofilização. O desenvolvimento de formulações glucose-sensitivas foi explorado através da adição de ácido fenilborónico ao sistema. Os resultados demonstraram a obtenção de micelas esféricas com uma carga superficial perto da neutralidade. O tamanho e polidispersão mostraram ser dependentes do polímero utilizado, no entanto obtiveram-se sempre micelas com diâmetro inferior a 300 nm. Foram também verificadas eficiências de associação variando de 49,3% até 94,6% e capacidade de carga variando de 5,6% até 8,6%. Ensaios de espectroscopia fotoelectrónica de raio X confirmaram a presença parcial de insulina e ausência de ácido fenilborónico na corona hidrófila das micelas, tal como se poderia prever tendo em consideração a solubilidade de ambos compostos. Apesar de contribuir para libertação *in vitro* da insulina associada às micelas, o ácido fenilborónico não conferiu às formulações as propriedades glucose-sensitivas desejadas.

O processo de liofilização não alterou significativamente as propriedades físicas das micelas que facilmente se dispersam em contacto com meio aquoso. Após liofilização uma elevada percentagem de insulina manteve a sua estrutura secundária, como evidenciado pela análise de espectroscopia de infravermelho por transformada de Fourier e dicroismo circular no UV-longínquo. Adicionalmente, a análise por calorimetria diferencial de varrimento e espectroscopia de Raman não evidenciaram a existência de interações significativas entre os diferentes componentes da formulação. As formulações liofilizadas em estado amorfo mostraram ser fisicamente estáveis durante o período de armazenamento de 6 meses à

temperatura ambiente (20 ºC), bem como refrigeradas (4 ºC), apresentando apenas uma reduzida perda da estrutura secundária da proteína (máximo 15%). As propriedades aerodinâmicas e a capacidade de aerossolização dos nanocompósitos variam de acordo com a formulação, apresentando diâmetros aerodinâmicos inferiores a 6,6 µm e fração de partículas finas até 48% da dose administrada, prevendo assim um bom perfil de deposição das partículas no sistema respiratório após inalação.

In vitro, as formulações sólidas mostraram ser compatíveis com o sistema respiratório devido à ausência de toxicidade significativa em linhas celulares epiteliais respiratórias (A549 e Calu-3) e macrófagos (Raw 264.7). Adicionalmente, algumas formulações, em particular as baseadas em Pluronic® F127, promoveram a permeação da insulina através de modelos epiteliais *in vitro* e sofreram reduzida internalização por parte de macrófagos como determinado por microscopia de confocal e citometria de fluxo.

A segurança e a eficácia terapêutica das formulações foram também avaliadas in vivo através de um modelo murino de diabetes induzido por estreptozotocina. Os pós administrados por instilação endotraqueal demonstraram um início de ação mais rápido do que a administração subcutânea de insulina a uma dose de 10 IU/kg, obtendo disponibilidades farmacológicas até 32,5% relativamente às observadas para a via subcutânea. A associação da insulina às micelas conduziu a um aumento significativo do seu efeito hipoglicémico relativamente à insulina livre em solução.

A toxicidade sub-aguda das formulações foi avaliada após administração múltipla durante um período de 14 dias. A análise do fluido de lavagem bronco-alveolar no que diz respeito à contagem total de células, teor proteico, e níveis de citoquinas e lactato desidrogenase revelou a ausência de sinais de inflamação e toxicidade. Adicionalmente, a análise histológica não revelou qualquer dano tecidular em órgãos como pulmões, coração e fígado.

Em suma, foram conseguidas formulações sólidas baseadas em micelas poliméricas que apresentam características promissoras para a administração de proteínas por inalação. Entre os polímeros usados, o Pluronic® F127 demonstrou dar origem às formulações com as melhores características para administração pulmonar de proteínas terapêuticas com ação sistémica.

Palavras-chave: Micelas poliméricas, Administração pulmonar, Insulina, Nanocompósitos, Pós para inalação

Table of contents

List of figures

Chapter 1 State-of-art

Chapter 2 Aims and Goals

Chapter 3 Design and characterization of self-assembled micelles for insulin delivery

Chapter 4 Micelle-based nanocomposites as solid formulations for pulmonary insulin delivery: design and characterization

Chapter 5 *In vitro* biological assessment of powder formulations for inhalation of insulin

Chapter 6 *In vivo* pharmacological and toxicological assessment of powder formulations for inhalation of insulin

List of tables

Chapter 1 State-of-art

Chapter 2 Aims and Goals

Chapter 3 Design and characterization of self-assembled micelles for insulin delivery

Chapter 4 Micelle-based nanocomposites as solid formulations for pulmonary insulin delivery: design and characterization

Chapter 5 *In vitro* biological assessment of powder formulations for inhalation of insulin

Chapter 6 *In vivo* pharmacological and toxicological assessment of powder formulations for inhalation of insulin

Abbreviations

5-DTAF – 5-([4,6-dichlorotriazin-2-yl]amino)fluorescein hydrochloride

AAC – Area above the curve

AE – Association efficiency

AFM – Atomic force microscopy

AmB – Amphotericin B

AO – Area of overlap

AUC – Area under the curve

BALF – Bronchoalveolar lavage fluid

BALT – Bronchus-associated lymphoid tissue

BCA – Biocinchoninic acid

BSA – Bovine serum albumin

bw – Body weight

CC_{50} - half maximal cytotoxic concentration

CINC-3 – Cytokine-induced neutrophil chemoattractant 3

C_{max} – Maximum concentration observed

CMC – Critical micelle concentration

CMT – Critical micellization temperature

COPD – Chronic obstructive pulmonary disease

CsA – Cyclosporin A

CSO-SA – Chitosan oligosaccharide-stearic acid

d_{ae} – Aerodynamic diameter

DAPI – 4′,6-diamidino-2-phenylindole

DDS – Drug delivery system

DLS – Dynamic light scattering

DMEM – Dulbecco's modified eagle medium

DMSO – Dimethyl sulfoxide

DPI – Dry powder inhaler

DSC – Differential scanning calorimetry

DSPE-PEG – 1,2-Distearoyl-sn-glycero-3-phosphoethanolamine-N-methoxy(poly(ethylene glycol))

DSPE-PEG-PHEA – 1,2-Distearoyl-sn-glycero-3-phosphoethanolamine-N-methoxy(poly(ethylene glycol))-α,β-poly(N-2-hydroxyethyl)-DL-aspartamide

EDTA – Ethylenediaminetetraacetic acid

ELISA – Enzyme-linked immunosorbent assay

EMA – European Medicines Agency

EPR effect – Enhanced permeability and retention effect

F108 – Pluronic® F108 (PEG-PPO-PEG)

F127 – Pluronic® F127 (PEG-PPO-PEG)

F68 – Pluronic® F68 (PEG-PPO-PEG)

FACS – Fluorescence-activated cell sorting

FAE – Follicle associated epithelium

far-UV CD – far-ultraviolet circular dichroism

FBS – Fetal bovine serum

Fc – Fragment crystallizable

FDA – US Food and Drug Administration

FELASA – Federation of Laboratory Animal Science Associations

FE-SEM – Field emission scanning electron microscopy

FPF – Fine particle fraction

FTIR – Fourier transform infrared spectroscopy

GLP-1 – Glucagon-like peptide 1

GnRH – Gonadotropin-releasing hormone

GRAS – Generally recognized as safe

GSD – Geometrical standard deviation

H&E – Hematoxylin and eosin

H40-PCL-PEG – Hyperbranched aliphatic polyester Boltorn H40-poly(ε-caprolactone)-poly(ethylene glycol)

HA-C18 – Hyaluronic acid-g-octadecyl

HbA1c – Glycated hemoglobin

HIV-TAT – Human immunodeficiency virus-transactivator of transcription

HLB – Hydrophilic-lipophilic balance

HPAE-co-PLA/DPPE – Poly[(amine-ester)-co-(D,L-lactide)]/1,2-dipalmitoyl-sn-glycero-3-phosphoethanolamine

HPESO – Hydrolyzed polymers of epoxidized soybean oil

HPLC – High-performance liquid chromatography

HPSO – Hydrolyzed polymers of soybean oil

IAA – Insulin autoantibodies

IC_{50} – Half maximal inhibitory concentration

ICH – International Conference on Harmonization

IL-1 – Interleukin 1

IL-2 – Interleukin 2

IL-4 – Interleukin 4

IL-6 – Interleukin 6

IL-13 – Interleukin 13

INF-α – Interferon-α

INF-γ – Interferon-γ

LC – Loading capacity

LD_{50} – Median lethal dose

LDH – Lactate dehydrogenase

LEBP – Lung epithelial binding peptides

LHRH – Luteinizing-hormone-releasing hormone

MALT – Mucosa-associated lymphoid tissue

MBCP-2 – Pluronic P104-b-di(ethylene glycol) divinyl ether

MIC – Minimal inhibitory concentration

MMAD – Mass median aerodynamic diameter

mPEG-b-PVL – Methoxy poly(ethylene glycol)-b-poly(valerolactone)

mPEG–DSPE – Methoxy poly(ethylene oxide)-b-distearoyl phosphatidyl-ethanolamine

MRP – Multidrug resistance–associated protein

MRW – Mean residual weight

MTT – 3-(4,5-Dimethylthiazol-2-yl)-2,5-diphenyltetrazolium bromide

MW – Molecular weight

NALT – Nasal-associated lymphoid tissue

nanoDDS – Nanothechnology-based drug delivery system

NLC – Nanostructured lipid carriers

P(MAA-g-EG) – Poly(methacrylic acid-grafted-poly(ethylene glycol))

PA – Pharmacological availability

PAGE-b-PLA – Poly(allyl glycidyl ether)-b-polylactide

Papp – Apparent permeability coefficient

PBA – Phenylboronic acid

PBCA – Poly(n-butyl cyanoacrylate)

PBS – Phosphate buffer saline pH 7.4

PC – Phosphatidylcholine

PCL – Poly(ε-caprolactone)

PCL-b-COS-b-PEG – Poly(epsilon-caprolactone)-b-chitooligosaccharide-b-poly(ethylene glycol)

PCL-PEG-PCL – Poly(ε-caprolactone)-b-poly(ethylene glycol)-b-poly(ε-caprolactone)

PDE – Permitted daily exposure

PDEAEMA-PAEMA – Poly(diethylaminoethyl methacrylate)-poly(aminoethyl methacrylate)

PdI – Polydispersity index

PDT – Photodynamic therapy

PE – Phosphatidylethanolamine

PEG – Poly(ethylene glycol)

PEG-b-PAA – Poly(ethylene glycol)-b-polyacrylic acid

PEG-b-(PLL-IM) – Iminothiolane-modified poly(ethylene glycol)-b-poly(L-lysine)

PEG-b-PBC – Poly(ethylene glycol)-b-poly(α-benzyl carboxylate- ε-caprolactone)

PEG-b-PCL – Poly(ethylene glycol)-b-poly(ε-caprolactone)

PEG-b-PHOHH – Poly(ethylene glycol)-b-poly(3-hydroxyoctanoate-co-3-hydroxyhexanoate)

PEG-chitosan – Poly(ethylene glycol)-chitosan

PEG-DACH-platin – Poly(ethylene glycol)-dichloro(1,2-diaminocyclohexane)platinum(II)

PEG-g-PAE – Poly(ethylene glycol)-g-poly(b-amino ester)

PEG-MOG – Poly(ethylene glycol)-monooleylglyceride

PEG-PAsp – Poly(ethylene glycol)-poly(aspartic acid)

PEG-PBCA – Poly(ethylene glycol)-poly(n-butylcyano acrylate)

PEG-PDLA – Poly(ethylene glycol)–poly(d-lactide)

PEG-PEI – Poly(ethylene glycol)-poly(ethylene imine)

PEG-PGlu – Poly(ethylene glycol)-poly(L-glutamic acid)

PEG-PHis – Poly(ethylene glycol)-poly(L-histidine)

PEG-PLA – Poly(ethylene glycol)–polylactic acid

PEG-PLLA – Poly(ethylene glycol)–poly(l-lactide)

PEG-PPO-PEG – Poly(ethylene glycol)-b-polypropylene oxide-b-poly(ethylene glycol) (also known as Pluronic®)

PEG-PPS – Poly(ethylene glycol)-b-poly(propylene sulfide)

PEG-PPS-PEG – Poly(ethylene glycol)-b-poly(propylene sulfide)-b-poly(ethylene glycol)

PEI – Polyethylenimine

PER – Permeability enhancement ratio

PGA-co-PDL – Poly(glycerol adipate-co-ω-pentadecalactone)

PHEA – α,β-poly(N-2-hydroxyethyl)-DL-aspartamide

PHEA-g-PDTC – Poly-a,b-[N-(2-hydroxyethyl)-L-aspartamide]-g-poly(2,2-dimethyltrimethylene carbonate)

PHOHH – Poly(3-hydroxyoctanoate-co-3-hydroxyhexanoate)

PLA – Polylactide or polylactic acid

PLA-b-PEG-b-PHis – Poly(L-lactic acid)-b-poly(ethylene glycol)-b-poly(L-histidine)

PLA-chitosan – Polylactide-chitosan

PLGA – Poly(D,L-lactide-co-glycolic acid)

PLGA-chitosan – Poly(D,L-lactide-co-glycolide)-chitosan

PLGA-PEG – Poly(D,L-lactide-co-glycolide)-b-poly(ethylene glycol)

PLGA-PEG-PLGA – Poly(D,L-lactide-co-glycolide)-b-poly(ethylene glycol)-b-poly(D,L-lactide-co-glycolide)

PLLF-g-(PLF-b-PLG) – Poly(l-lysine-co-l-phenylalanine)-g-poly(l-phenylalanine)-b-poly(l-glutamic acid)

PMA – Phorbol 12-myristate 13-acetate

pMDI – Pressurized metered-dose inhaler

PPEGMEA-g-PMOMMA – Poly[poly(ethylene glycol) methyl ether acrylate]-g-poly(methacrylate acid)

PPO – Polypropylene oxide

PVA – Polyvinyl alcohol

PVA-acyl chains – Polyvinyl alcohol-modified with acyl chains

PVP – Polyvinylpyrrolidone

PVP-b-PDLLA – Poly(N-vinyl-2-pyrrolidone)-b-poly(D,L-lactide)

RAFT – Reversible addition-fragmentation chain transfer

RES – Reticuloendothelial system

RGD – Arginine-Glycine-Aspartic acid

rhDNase – Recombinant human desoxyribonuclease I

ROP – Ring-opening polymerization

SA-BPEI – Stearic acid-branched polyethyleneimine

SAGly-DA – Poly[(sodium N-acryloyl-L- glycinate)-co-(N-dodecylacrylamide)]

SALeu-DA – Poly[(sodium N-acryloyl-L- leucinate)-co-(N-dodecylacrylamide)]

SAPhe-DA – Poly[(sodium N-acryloyl-L- phenylalaninate)-co-(N-dodecylacrylamide)]

SAVal-DA – Poly[(sodium N-acryloyl-L-valinate)-co-(N-dodecylacrylamide)]

SAVal-OA – Poly[(sodium N-acryloyl-L-valinate)-co-(N-octylacrylamide)]

SCC – Spectral correlation coefficient

SEDDS – Self-emulsifying drug delivery systems

SEM – Scanning electron microscopy

SIMS – Secondary ion mass spectroscopy

SIS – Styrene-isoprene-styrene

SLN – Solid lipid nanoparticles

SOD – Superoxide dismutase

SOL – Soluplus® – Polyvinyl caprolactam-polyvinyl acetate-poly(ethylene glycol) graft copolymer

SP-A – Surfactant protein A

SP-D – Surfactant protein D

$t_{1/2}$ – Half-life time

TEER – Transepithelial electrical resistance

TEM – Transmission electron microscopy

TFA – Trifluoroacetic acid

THALWHT – Threonine-Histidine-Alanine-Leucine-Tryptophan-Histidine-Threonine

T_{max} – Time of maximum concentration observed

TNF-α – Tumor necrosis factor alpha

TPGS – D-alpha-tocopheryl-co-PEG 1000 succinate

VEGF – Vascular endothelial growth factor

XPS – X-ray photoelectron spectroscopy

XRD – X-ray diffraction

ZO-1 – Zonula occludens-1

Chapter 1

State-of-art

The information presented in this chapter was partially published in the following publications:

Fernanda Andrade, Mafalda Videira, Domingos Ferreira, and Bruno Sarmento, Nanocarriers for pulmonary administration of peptides and therapeutic proteins, Nanomedicine (Lond), 6(1):123-41, 2011.

Fernanda Andrade, Mafalda Videira, Domingos Ferreira, and Bruno Sarmento, Micelle-based systems for drug pulmonary delivery and targeting, Drug Delivery Letters, 1 (2):171-185, 2011.

Fernanda Andrade, Diana Rafael, Mafalda Videira, Domingos Ferreira, Alejandro Sosnik, and Bruno Sarmento, Nanotechnology and pulmonary delivery to overcome resistance in infectious diseases, Advanced Drug Delivery Reviews, 65 (13–14):1816–1827, 2013.

Fernanda Andrade, Catarina Moura, Bruno Sarmento, Pulmonary Delivery of Biopharmaceuticals in *Mucosal Delivery of Biopharmaceuticals*: *Biology, Challenges and Strategies*, José das Neves and Bruno Sarmento (Eds), Springer, 2014, ISBN 978-1-4614-9524-6.

Diana Rafael, Mafalda Videira, Mireia Oliva, Domingos Ferreira, Bruno Sarmento, Fernanda Andrade, Amphiphilic Polymers in Drug Delivery in *Encyclopedia of Biomedical Polymers and Polymeric Biomaterials*, Munmaya Mishra (Ed.), CRC Press, 2015, ISBN 9781439898796.

1. Drug delivery systems: innovation and technology

The advent of pharmaceutical industry brought the nececity to control the biodistribution of drugs, aiming to enhance their therapeutic efficacy. The concept of drug delivery system (DDS) that control the release of the drugs and target them to specific locations in the body represents a major clinical breakthrough. This concept is in close agreement with those predicted by Paul Ehrlich in the early 20th century; however, we still cannot achieve the desired 'magic bullet' (1, 2). The pharmacological properties, clinical use, marketability, and competitiveness of drugs are highly dependent on the nature and properties of the DDS used. Thus, pharmaceutical companies are continuously seeking for new and improved DDS to deliver both new and existing drugs, focusing on its effectiveness, safety and market value. Since the success of a DDS relies on several aspects related to the route of administration, specific drug properties or disease physiopathology, distinct strategies must be applied during its rational development according to the desired application. Ideally, a DDS should possess characteristics such as (i) appropriate circulation time in the body to promote a therapeutic or diagnostic action, (ii) protect the drug from degradation and from premature clearance, (iii) organ/tissue selectivity, (iv) therapeutic concentration of the drug at the target anatomical site, (v) release the compound in response to specific stimuli, and (vi) improve the therapeutic index of the drug (2-4). Although some studies already refer the development of multi-functional systems (Figure 1.1), the development of the ideal DDS is still in its infancy.

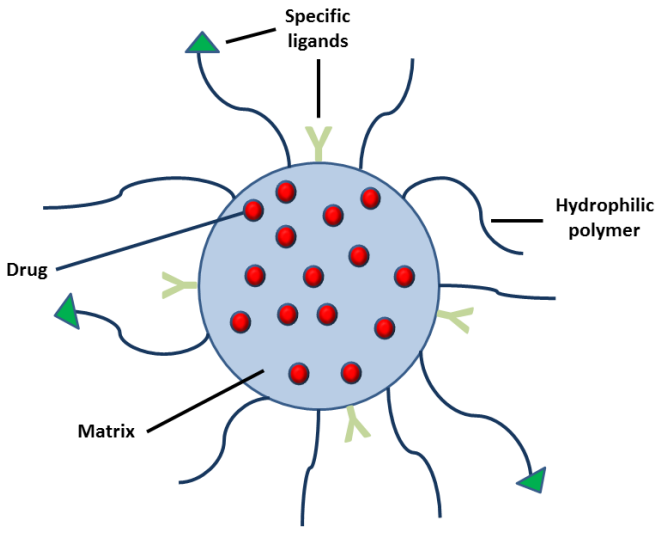

Figure 1.1 Schematic representation of a multi-functional DDS.

Passive or active targeting of drugs to specific organs and tissues, enhancing its therapeutic efficacy and decreasing the side effects, can be achieved via different mechanisms. By increasing the systemic circulation time of drugs through a reduction of their uptake by the reticuloendothelial system (RES) (e.g. by conjugating drugs or coating particles with poly(ethylene glycol) (PEG), i.e. PEGylation), drugs are more likely to suffer an enhanced permeability and retention effect (EPR effect). Thus, there will be a passive targeting to tissues with increased vascular permeability such as solid tumors, being this mechanism extensively used by DDS of anticancer drugs. It can also occur at infection or inflammation sites. On the other hand, active targeting can be achieved using carriers with stimuli-sensitiveness once several pathological processes are characterized by changes in pH, temperature or redox potential. Thus, an active targeting can be achieved by using carriers that release drugs only after exposed to certain conditions (stimulus-sensitive). Other potential approach for active targeting might be achieved through the use of specific antibodies, molecules recognized by certain cell receptors, or receptors for molecules that are overexpressed in certain disease states. These include integrins and vascular endothelial growth factor (VEGF) presented in vascular cells of various solid tumors, as well as transferrin and folate residues, whose receptors are overexpressed on the surface of various tumor cells (4-8).

The translation of this concept to pulmonary administration leads, for instance, to the identification and selection of lung epithelial binding peptides (LEBP), namely LEBP-1, LEBP-2 and LEBP-3 as peptides that bind selectively to receptors of the alveolar epithelium cells, therefore promoting a specific alveolar targeting (9). LEBP-binding DNA complexes presented higher *in vitro* transfection efficiency to lung epithelial cells (L2 cell line) when compared to the same formulation without LEBP (10). In another study, Jost and co-workers identified a peptide with the amino acid sequence Threonine-Histidine-Alanine-Leucine-Tryptophan-Histidine-Threonine (THALWHT) that selectively binds to airway epithelial cell lines and can be used as targeting moiety for gene delivery (11). Several reports on moieties explored to achieve active targeting to lungs like surfactant protein A (SP-A) (12), transferrin (13), lectin (14), folate (15) or human immunodeficiency virus-transactivator of transcription (HIV-TAT) peptide (16) can be found on the literature. Mannose and its derivatives have been also proposed to target the mannose receptor present at the surface of alveolar macrophages and improve the treatment of intracellular pathogens like *Mycobacterium tuberculosis* (17, 18).

In the last decades, several studies have been conducted with the aim of developing innovative pharmaceutical forms, arising some of the most promising advances from the application of nanotechnology to the production of DDS (19-21).

1.1. Nanotechnology in the development of drug delivery systems

The application of nanotechnology in medicine has been capturing growing interest over recent years, having emerged the concept of nanomedicine. This is explained by the nano and micrometer scale of cellular and subcellular structures (6). The goal of nanomedicine is to allow a more accurate and timely diagnosis and to provide the most effective treatment without side effects (22). Currently, the main application areas of nanomedicine are imaging and cancer therapy. However, studies in various areas such as peptides and proteins delivery, vaccination, gene therapy, tissue engineering or production of devices for the administration of drugs are also being carried out (6).

Both pharmacokinetics and pharmacodynamics of a drug are highly dependent on its physical and chemical features, and are influenced by the type of formulation and dosage form used to deliver it. NanoDDS like nanoparticles, liposomes or micelles can modulate and improve the performance of many drugs to an extent not achievable by conventional formulations. For example, nanoDDS can be capitalized to encapsulate drugs and thereby (i) increase their solubility, (ii) protect them from degradation, (iii) enhance their epithelial absorption, (iv) escape from the *in vivo* defensive systems, thus increasing their blood circulation time, (v) target the drugs to specific cells/tissues/organs, releasing them in a controlled manner as a response to a specific stimulus, or (vi) enhance their uptake by cells (19, 23). They also allow the reduction of the immunogenicity of proteins, thus decreasing the toxicity of the formulation (24). In addition, combined nanoDDS can simultaneously detect and treat a disease by encompassing both imaging and therapeutic compounds, an emerging field known as theranostics (25). In the near future, nanomedicine could play a key role to achieve the so desired personalized medicine.

Table 1.1 Examples of nanoDDS with market authorization. AmB is Amphotericin B.

Type of nanocarrier	Drug	Tradename
Polymeric nanoparticles and polymer conjugates	Glatiramer acetate	Copaxone
	Pegademase bovine	Adagen
	Peginterferon α-2a	Pegasys
	Peginterferon α-2b	PEG-Intron
	Pegaspargase	Onscaspar
	Pegaptanib sodium	Macugen
	Pegfilgrastim	Neulasta
	Pegvisomant	Somavert
	Neocarzinostatin (Smancs)	Zinostatin Stimalmer
	PEG -epoetin beta	Micera
	Peginesatide	Omontys
	Pegloticase	Krystexxa
	Certolizumab pegol	Cimzia
Liposomes	AmB	Abelcet
	AmB	AmBisome
	Beractant	Survanta
	Bovactant	Alveofact
	Cisplatin	Lipoplatin
	Cytarabine	DepoCyt
	Daunorubicin	Daunoxome
	Doxorubicin	Myocet
	Doxorubicin	Doxil/Caelyx
	Inactivated surface Influenza virus antigen	Inflexal V
	Inactivated hepatitis A virus	Epaxal
	Mitoxantrone	Novantrone
	Morfin	DepoDur
	Paclitaxel	EndoTAG-1
	Poractant α	Curosurf
	Verteporfin	Visudyne

Type of nanocarrier	Drug	Tradename
Liposomes	Vincristine	Marqibo
	Mifamurtide	Mepact
	Factor VIII	Octocog alfa
	Octafluoropropane	Definity
Micelles	Estradiol	Estrasorb
Nanocrystals	Megestrol acetate	Megace ES
	Aprepitant	Emend
	Fenofibrate	Tricor
	Sirolimus	Rapamune
	Fenofibrate	Triglide
Albumin nanoparticles	Paclitaxel	Abraxane
Lipidic coloidal dispersion	AmB	Amphotec
Antibody or protein-drug conjugate	Gemtuzumab-ozogamicin	Mylotarg
	Tositumomab-iodine I131	Bexxar
	Ibritumomab-tiuxetan	Zevalin
	Denileukin-diftitox	Ontak
	Brentuximab vedotin	Adcetris
Inorganic particles	Superparamagnetic iron oxide	Feridex
	Superparamagnetic iron oxide	Endorem
	Superparamagnetic iron oxide	GastroMARK
	Superparamagnetic iron oxide	Lumirem
	Superparamagnetic iron oxide	Resovist

Over the last decades, the usefulness of nanoDDS design and development to overcome a variety of pharmaceutical drawbacks in the diagnosis, prevention, immunization and treatment of diseases has been intensively explored by a large number of research groups and companies worldwide, generating a high number of patents and scientific papers published in international scientific journals. However, and despite the fact that nanomedicine began as a discipline almost half century ago, only some nanothechnology-based drug delivery system (nanoDDS) paved their way to the market (Table 1.1) (26). This phenomenon could be explained by the poor financial profitability, consumer distrust and the lack of confidence due to poor information/education, ineffective regulation of new and generic

products, and weak patent protection (27). At the moment, regulatory agencies are in process of developing specific guidelines and regulations regarding nanotechnology-based products in order to develop new tools, standards, and approaches to assess the safety, efficacy, quality, and performance of such products (28, 29). Nonetheless, the relatively few marketed nanoDDS have been successful in their respective therapeutic areas, especially in cancer therapy. According to BCC Research, the global nanomedicine market has been growing steadily, reaching a value of $72.8 billion in 2011, being expected to increase at annual growth rate of 12.5% until 2016 reaching $130.9 billion (30).

Currently used technologies at both laboratory and industrial level, including high-pressure homogenization, emulsification/solvent evaporation, emulsification/solvent diffusion, nanoprecipitation/solvent displacement, salting-out, layer-by-layer synthesis, ionic complexation/coacervation, ionotropic gelation, thin-film hydration, supercritical fluids technology or microfluidics have been reported as effective methods to produce nanoDDS (20, 22, 31, 32).

1.1.1. Lipid-based nanoparticles

Liposomes are spherical vesicles composed of bilayers of phospholipids, cholesterol, and/or other lipids (22). Lecithin, phosphatidylglycerol, phosphatidylinositol, phosphatidylethanolamine, and phosphatidylserine are the mainly used phospholipids (8). They can be classified according to their lamellarity as uni, oligo and multilamellar, or by size as small, intermediate and large. Due to its structure, they allow the incorporation of hydrophilic drugs in the aqueous core, and lipophilic drugs within the lipid bilayer (Figure 1.2) (32). Possessing higher core, unilamellar liposomes are preferred for encapsulation of hydrophilic drugs, while multilamellar liposomes are especially used to encapsulate hydrophobic drugs due to the higher lipid content (33). Depending on the number and composition of the bilayers and the presence of coating, it is possible to obtain systems with modified release characteristics (34, 35). Although liposomal-based formulations represent the higher number of nanoDDS currently available on the market, they were first commercialized for cosmetic purposes (35). Besides the marketed formulations, liposomes have been suggested for the administration of several drugs, including peptides and therapeutic proteins, as well as for gene therapy (8).

Stealth liposomes like Doxil/Caelyx®, Novantrone® or Lipoplatin® are a good example of how the previously mentioned PEGylation allows the improvement of blood circulation time and the therapeutic efficacy of many drugs through the avoidance of opsonization and escape from RES (33).

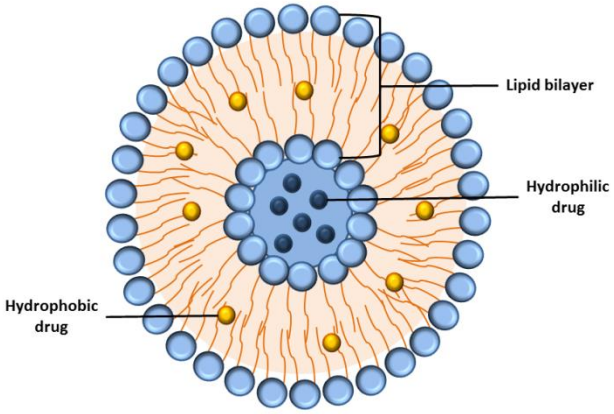

Figure 1.2 Schematic representation of a liposome.

Nanoemulsions are nanometric scale lipid droplets dispersed in water that were initially developed for parental nutrition. They possess the advantage of large-scale production through the high-pressure homogenization technique, but lack on controlled release properties of drugs (32). More recently, self-emulsifying drug delivery systems (SEDDS) composed by mixtures of drugs, oils and surfactants that emulsify with the water present on the gastrointestinal tract, have been proposed as nanoDDS. They are easy to produce and generally stable, but the high percentage of surfactants on its composition arise toxicity concerns (32).

Lipid nanoparticles generally comprise two types of structures, solid lipid nanoparticles (SLN) and nanostructured lipid carriers (NLC) (32, 36). They comprise a solid lipid matrix at both room and body temperatures, dispersed in aqueous solution and stabilized with a layer of emulsifier agent, usually phospholipids (35). Lipid nanoparticles emerged as an alternative to liposomes and pharmaceutical emulsions because of the superior stability in biological fluids. They are also less toxic than the inorganic and polymeric particles due to its biocompatibility and biodegradability (35). Unlike the SLN, the NLC are composed not only of solid lipids, but also by a mixture of solid and liquid lipids, resulting in a solid matrix less rigid and ordered. This difference will allow NLC to increase the loading capacity of drugs and the stability during storage (Figure 1.3) (32, 36).

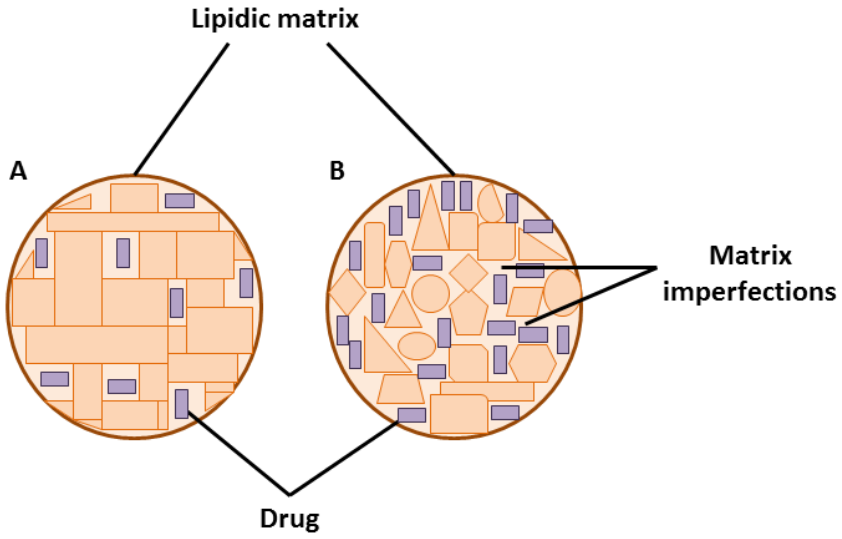

Figure 1.3 Schematic representation of SLN (S) and NLC (B).

1.1.2. Polymer-based nanoparticles

Polymeric nanocarriers have been adopted as the preferred drug delivery systems mostly by the fact that they overcome some of the disadvantages presented by liposomes and lipid particles, namely low encapsulation efficiency and stability during storage and rapid release of encapsulated compounds. They can be obtained through polymerization of monomers or polymer dispersion (Figure 1.4) (31, 35). Among polymeric nanocarriers, those containing natural polysaccharides, including chitosan, alginate or hyaluronic acid, receive high popularity among drug delivery researchers owing its biocompatible, biodegradable, and non-toxic properties. Moreover, they possess hydrophilic properties, having in general low cost production and many sources in nature (37). Among the synthetic polymers, PEG, poly(D,L-lactide-co-glycolic acid) (PLGA) or poly(ε-caprolactone) (PCL) are some of the most well studied and explored. PLGA is accepted by regulatory authorities and widely used in biomedical applications due to its biocompatibility, biodegradation and utility in the production of modified release formulations (24, 38).

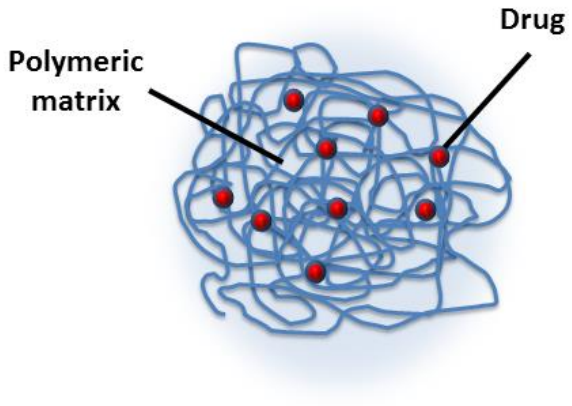

Figure 1.4 Schematic representation of a polymeric nanoparticle.

1.1.3. Polymeric micelles

Micelles are spherical nanosized colloidal dispersions having a hydrophobic core coated by a hydrophilic shell (Figure 1.5). Normally, they arise from the self-assembly of amphiphilic molecules above the critical micelle concentration (CMC) and critical micellization temperature (CMT) (5). The amphiphilic molecules used can be composed by graft and block copolymers (generally di- and triblock-copolymers) and/or polymers conjugated with lipids (5, 22) originating polymeric micelles or phospholipids (22), in the case of conventional micelles. Recently, most attention has been paid to polymeric micelles as drug delivery systems, especially for poorly water-soluble drugs (39, 40). Due to the higher core hydrophobicity and viscosity as well as an highly hydrated shell, polymeric micelles are thermodynamically and kinetically more stable then surfactant micelles, presenting slower and delayed disintegration and drug release in circulation even upon dilution below the CMC value (41). Therefore, they present a promising approach to eliminate the use of excipients such as Cremophor EL® which has been associated to hypersensitivity reactions, aggregation of erythrocytes, peripheral neuropathy, among others (42). By varying the composition of micelles, namely the type and size of the polymers, it is possible to modulate their characteristics such as size, encapsulation efficiency and release profile. The most common component of micelle surface is PEG but it is possible to use other hydrophilic polymers such as chitosan (43-46), polyvinyl alcohol (PVA) (47-49), or polyvinylpyrrolidone (PVP) (50, 51). The hydrophobic core is constituted by polymers such lactic acid (52, 53), PCL (44, 54, 55), propylene oxide (56, 57), aspartic acid (58), or lipids such as phosphatidylethanolamine (59, 60).

Polymeric micelles have been developed to modify several major intrinsic characteristics of incorporated drugs, i.e. drug aqueous solubility, *in vivo* stability, release pattern, pharmacokinetics and biodistribution (5, 39). They allow the formulation and administration of highly hydrophobic drugs that would be withdrawn from development in the stage of drug formulation using conventional formulations (61). Despite being especially used to formulate hydrophobic drugs, like liposomes, polymeric micelles allow the encapsulation of drugs with different polarities. Hydrophobic drugs are incorporated into the micelle core being the solubilization capacity of drugs proportional to the hydrophobicity of the micelle core, while water-soluble drugs are adsorbed on the micelle shell and/or surface. Drugs with intermediate polarity are distributed along the amphiphilic molecules (62, 63). In addition to the higher stability compared to liposomes, micelles present low size and high encapsulation efficiency, which, together with the possibility of being sterilized by filtration, make these systems an interesting alternative to drug delivery (5, 62, 64).

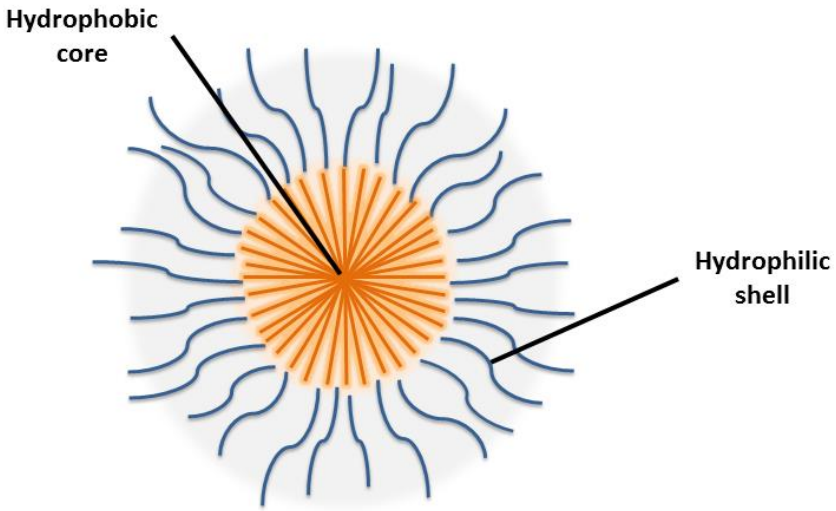

Figure 1.5 Schematic representation of a micelle.

A few polymeric micelles-based formulations are currently in clinical trials (Table 1.2) (65, 66), one of them (Genexol-PM®, Samyang Co.) granted a pre-market authorization in Korea for the treatment of breast cancer and non-small cell lung cancer (67-69), while SP1049C (Surpatek Pharma, Inc.) granted orphan drug designation by US Food and Drug Administration (FDA) for the treatment of gastric cancer (70). Besides the formulations that are ongoing on clinical trials, polymeric micelles have successfully enhanced the therapeutic

index of various drugs from anticancer and anti-inflammatory drugs (71-75), to genetic material (76). They are also been proposed as delivery systems for diagnostic agents (77). Due to its small size, generally lower than 200 nm, and hydrophilic surface, micelles are poorly recognized by RES and present long circulation times in bloodstream suffering the EPR effect at solid tumor sites, reason why have been extensively exploited as drug delivery systems for anticancer agents (78-80). Promoting drug selective targeting to specific organs and tissues can be also achieved either using stimuli-responsive micelles (63, 79, 81, 82), or by modulating their surface with active-targeting ligands (79, 83). By sharing some structural and functional features with natural transport systems, e.g. virus and lipoproteins, polymeric micelles can be a useful strategy to solve the problem of drug resistance (84). Pluronic®-based micelles have shown to interfere with the activity of P-glycoprotein and multidrug resistance–associated protein (MRP), increasing the therapeutic effectiveness of anticancer agents in multidrug resistant cancer cell lines (56, 85-87).

Table 1.2 Examples of polymeric micelles-based formulations that enrolled in clinical trials.

Formulation	Polymer	Drug	Indication	Clinical phase	Reference
SP1049C	Pluronic® L61 and F127	Doxorubicin	Advanced adenocarcinoma of the esophagus, gastroesophageal junction and stomach	II/III	(70)
Genexol-PM®	PEG-PLA	Paclitaxel	Breast cancer, non-small cell lung cancer, advanced pancreatic cancer, ovarian cancer, and head and neck cancer	I/II/III/IV	(68, 88-90)
NK012	PEG-PGlu-SN-38 conjugated	SN-38	Breast cancer, colorectal cancer and small cell lung cancer	I/II	(65, 91, 92)
NK105	PEG-PAsp	Paclitaxel	Advanced or recurrent gastric cancer and breast cancer	I/II/III	(66, 93)
NC-4016	PEG-DACH-platin	Oxaliplatin	Advanced solid tumors and lymphoma	I	(94)

Formulation	Polymer	Drug	Indication	Clinical phase	Reference
NC-6004 (Nanoplatin®)	PEG-PGlu-cisplatin conjugated	Cisplatin	Solid tumors, breast cancer, pancreatic cancer	I/II/III	(95, 96)
Paxceed®	PEG-PLA	Paclitaxel	Rheumatoid arthritis, psoriasis	II	(97, 98)
CRLX101	Polymer-cyclodextrin-camptothecin conjugated	Camptothecin	Advanced solid tumors, ovarian cancer	I/II	
AquADEK®	TPGS	Vitamins and antioxidants	Multivitamin supplement in cystic fibrosis	I/II	(99, 100)
BIND-014	PEG-PLA and PLGA-PEG	Docetaxel	Non-small cell lung Cancer and prostate cancer	I/II	(101-103)

PEG-DACH-platin – Poly(ethylene glycol)-dichloro(1,2-diaminocyclohexane)platinum(II); PEG-PAsp – Poly(ethylene glycol)-poly(aspartic acid); PEG-PGlu – Poly(ethylene glycol)-poly(L-glutamic acid); PEG-PLA – Poly(ethylene glycol)-polylactic acid; PLGA-PEG – Poly(D,L-lactide-co-glycolide)-b-poly(ethylene glycol); TPGS – D-alpha-tocopheryl-co-PEG 1000 succinate

1.2. The role of amphiphilic polymers in the development of drug delivery systems

Amphiphilic copolymers are heterogeneous compounds composed by both hydrophilic and hydrophobic units disposed in sequential blocks (generally di- and triblock-copolymers) or grafts. By varying either the type or the chain length of the units, it is possible to modulate the polymer properties (41, 104). It is their versatility that makes them suitable for industrial and pharmaceutical applications. Regarding the last one, they have been used for a long time in different pharmaceutical dosage forms as excipients like emulsifiers, wetting, thickening or gel forming agents, and stabilizing agents of suspensions and colloidal dispersions. Still, they gained an increased interest in the last decades in the development of new DDS driven by the progresses seen in the pharmaceutical sciences and nanomedicine field (41, 105). Amphiphilic polymers are used in the development of different types of DDS, such as tablets, capsules, gels, microparticles, with emphasis in nanoDDS, namely polymeric micelles. Table 1.3 presents examples of DDS in development using amphiphilic polymers.

Table 1.3 Examples of DDS in development using amphiphilic polymers.

Type of DDS	Polymer	Drug	Reference
Micelles	CSO-SA	Doxorubicin, paclitaxel and AmB	(106-108)
	DSPE-PEG	Calcitonin	(59)
	HA-C_{18}	Paclitaxel	(109)
	mPEG-b-PVL	Camptothecin	(110)
	PCL-PEG-PCL	Rifampicin	(111, 112)
	PEG-b-PAA	Mitoxantrone and doxorubicin	(113)
	PEG-b-(PLL-IM)	siRNA	(114)
	PEG-b-PBC	Paclitaxel	(115)
	PEG-b-PCL	Paclitaxel, indomethacin, curcumin, plumbagin and etoposide	(61, 115)
	PEG-Phis	Doxorubicin	(116, 117)
	PEG-chitosan	Methotrexate	(118)
	PEG-g-PAE	Doxorubicin	(119)
	PEG-PAsp	Lysozyme, irinotecan	(120, 121)
	PEG-PEI	DNA	(122)
	PEG-PLA	Paclitaxel and CsA	(53, 123, 124)
	PHEA-g-PDTC	Prednisone and tegafur	(125)
	PLA-b-PEG-b-Phis	Doxorubicin	(126)
	PLGA-PEG-PLGA	Curcumin, DNA	(127, 128)
	Pluronic® F68, F127, L61 and P85	DNA	(76, 128-130)
	Pluronic® P105 and P105/L101 mix and Pluronic® P105/PCL mix	Paclitaxel	(131, 132) (133)
	Poly(sodium N-acryloyl-L-aminoacidate-co-alkylacrylamide)s	Griseofulvin and non-steroidal anti-inflammatory drugs	(134-136)
	PVA-acyl chains	Doxorubicin	(137)
Cylindrical brushes	PLLF-g-(PLF-b-PLG)	Doxorubicin	(138)

Type of DDS	Polymer	Drug	Reference
Microparticles	PEG-PLA	BSA	(139)
	Pluronic® F68	BSA	(140)
Nanoparticles	H40-PCL-PEG	5-fluorouracil and Paclitaxel	(141)
	HPAE-co-PLA/DPPE	Paclitaxel	(142)
	HPESO and Pluronic® F68	Doxorubicin and mitomycin C	(143, 144)
	PDEAEMA-PAEMA	siRNA and proteins	(145)
	PEG-PBCA	Docetaxel	(146)
	PEG-PLA	Paclitaxel, DNA	(147, 148)
Hydrogels	MBCP-2	DNA	(149)
	P(MAA-g-EG)	Insulin, interferon β and calcitonin	(150-152)
	PEG-chitosan	BSA	(153)
	PLGA-PEG-PLGA	Dexamethasone and calcitonin	(154, 155)
	Pluronic® F127	Deslorelin, GnRH, Vitamin B12 and naproxen	(156-158)
Patches	SIS	Methyl salicylate, capsaicin, and diphenhydramine hydrochloride	(159)
Capsules	PEG-MOG	Risperidone, ketoconazole, indomethacin, hydrocortisone and CsA	(160)
Solid solutions (Extrudates)	Soluplus®	Danazol, fenofibrate and itraconazole	(161)
Tablets	Soluplus®, Pluronic® and Vitamin E-TPGS®	Amine drugs like donepezil, olanzapine or tamsulosin	(162)

AmB - Amphotericin B; BSA – Bovine serum albumin; CsA – Cyclosporin A; CSO-SA – Chitosan oligosaccharide-stearic acid; DSPE-PEG – 1,2-Distearoyl-sn-glycero-3-phosphoethanolamine-N-methoxy(poly(ethylene glycol); GnRH – Gonadotropin-releasing hormone; H40-PCL-PEG – Hyperbranched aliphatic polyester Boltorn H40-poly(ε-caprolactone)-poly(ethylene glycol); HA-C18 – Hyaluronic acid-g-octadecyl; HPAE-co-PLA/DPPE – Poly[(amine-ester)-co-(D,L-lactide)]/1,2-dipalmitoyl-sn-glycero-3-phosphoethanolamine; HPESO – Hydrolyzed polymers of epoxidized soybean oil; MBCP-2 – Pluronic P104-b-di(ethylene glycol) divinyl ether; mPEG-b-PVL – Methoxy poly(ethylene glycol)-b-poly(valerolactone); P(MAA-g-EG) – Poly(methacrylic acid-grafted-poly(ethylene glycol)); PCL – Poly(ε-caprolactone); PCL-PEG-PCL – Poly(ε-caprolactone)-b-poly(ethylene glycol)-b-poly(ε-caprolactone); PDEAEMA-PAEMA – Poly(diethylaminoethyl methacrylate)-poly(aminoethyl methacrylate); PEG-b-(PLL-IM) – Iminothiolane-modified poly(ethylene glycol)-b-poly(L-lysine); PEG-b-

PAA – Poly(ethylene glycol)-b-polyacrylic acid; PEG-b-PBC – Poly(ethylene glycol)-b-poly(α-benzyl carboxylate- ε-caprolactone); PEG-b-PCL – Poly(ethylene glycol)-b-poly(ε-caprolactone); PEG-chitosan - Poly(ethylene glycol)-chitosan; PEG-g-PAE – Poly(ethylene glycol)-g-poly(b-amino ester); PEG-MOG – Poly(ethylene glycol)-monooleylglyceride; PEG-PAsp – Poly(ethylene glycol)-poly(aspartic acid); PEG-PBCA – Poly(ethylene glycol)-poly(n-butylcyano acrylate); PEG-PEI – Poly(ethylene glycol)-poly(ethylene imine); PEG-PHis – Poly(ethylene glycol)-poly(L-histidine); PEG-PLA – Poly(ethylene glycol)–polylactic acid; PHEA-g-PDTC – Poly-a,b-[N-(2-hydroxyethyl)-L-aspartamide]-g-poly(2,2-dimethyltrimethylene carbonate); PLA-b-PEG-b-PHis – Poly(L-lactic acid)-b-poly(ethylene glycol)-b-poly(L-histidine); PLGA-PEG-PLGA – Poly(D,L-lactide-co-glycolide)-b-poly(ethylene glycol)-b-poly(D,L-lactide-co-glycolide); PLLF-g-(PLF-b-PLG) – Poly(l-lysine-co-l-phenylalanine)-g-poly(l-phenylalanine)-b-poly(l-glutamic acid); PVA-acyl chains – Polyvinyl alcohol-modified with acyl chains; SIS – Styrene-isoprene-styrene.

Among the different structures available, the most extensively explored for the production of DDS are composed of PEG as hydrophilic block and (i) polypropylene oxide (PPO); (ii) poly(ester)s like PCL or PLGA; (iii) poly(amino acid)s such as poly(L-aspartic acid) and poly(L-glutamic acid); or (iv) lipids like phosphatidylethanolamine (PE) as hydrophobic block (5). Particular interest has been given to poly(ethylene glycol)-b-polypropylene oxide-b-poly(ethylene glycol) (PEG-PPO-PEG) block copolymers (poloxamers and poloxamines) (163, 164), mainly due to their commercial accessibility in a wide range of compositions and molecular weight (MW) (Pluronic®/Lutrol®/Kolliphor P® and Tetronic®).

1.2.1. Synthesis of copolymers

Due to environmental concerns, the synthesis of these polymers has evolved in the last decades, in order to achieve a cleaner production, in the scope of the "green-chemistry". Among the different methods, reversible addition-fragmentation chain transfer (RAFT) polymerization and ring-opening polymerization (ROP) of lactones, lactides and cyclic anhydrides are extensively used, mainly due to its ability to prepare both homo- and copolymers of different MW and architectures with well-defined structures or end-groups (165-167). Enzyme-catalyzed ROP has also been used to eliminate the use of organometallic catalysts, but only low MW polymers can be obtained using this method (168, 169). The ROP can be performed either as a bulk polymerization, in solution, emulsion or dispersion (166), while RAFT is commonly performed in emulsions (167). Copolymers can be produced by the sequential addition of monomers or by the conjugation of the preformed homopolymers, e.g. by reactive extrusion using transesterifcation at high temperature (166). For example,

poloxamers are synthesized using anionic polymerization in the presence of an alkaline catalyst, generally sodium or potassium hydroxide. The PPO central unit is formed by the polymerization of propylene oxide monomers followed by the addition of ethylene glycol to the PPO end-groups (105).

1.2.2. Characteristics of copolymers and copolymer-based structures

1.2.2.1. Stimuli-responsiveness

These polymers present some characteristics that make them suitable for human administration, namely their water-solubility, biodegradability, biocompatibility and low immunogenicity. Among all characteristics presented by some amphiphilic polymers for the development of advanced controlled nanoDDS, one of the most interesting is the stimuli-responsiveness (170, 171). Stimuli-responsive polymers are a class of “smart” polymers that undergo physical or chemical changes as response to a specific stimulus, e.g. temperature, pH, redox potential, magnetic field or light (172, 173). Monomers of N-alkyl substituted acrylamides and acrylate/methacrylate derivatives are commonly used in the development of thermo-responsive and pH-responsive copolymers, respectively (171, 174). pH-responsive hydrogels were able to protect proteins from the harsh gastric environment, promoting their release only at distal parts of intestine. At acidic pH the existence of intermolecular polymer complexes lead to the formation of compact gels that swells just at basic pH (150, 152). Due to their properties, the hydrogels enhanced the *in vivo* intestinal absorption and hypoglycemic effects of oral insulin (152).

1.2.2.2. Self-assembly: the crucial phenomenon

Amphiphilic copolymers are able to form nanoscopic structures with different morphologies, e.g. polymersomes, nanocapsules, nanospheres, nanogels or dendrimers, although polymeric micelles are the most commonly used and studied (105, 175, 176). Polymeric micelles are supramolecular structures formed by self-assembly of amphiphilic copolymers into spherical nanosized particles with a hydrophilic corona and hydrophobic core. The self-assembly or micellization occurs at or above a threshold level of concentration (CMC) and temperature (CMT), which are specific for the polymer (Figure 1.6) (5).

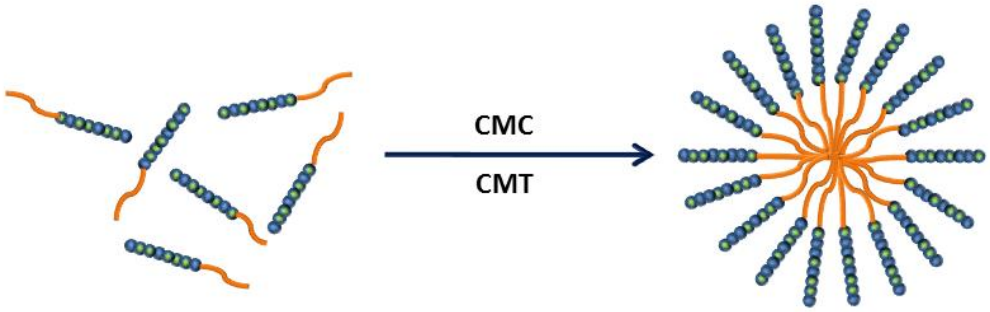

Figure 1.6 Schematic representation of micellization.

In water, this process is driven by an increase in entropy of the solvent molecules in contact to the hydrophobic units and a consequent decrease of free energy in the system as the hydrophobic components are withdrawn from the aqueous media to form the micelle core (39, 177). Two forces are involved in the micelle formation, an attractive force that leads to the association of molecules and a repulsive force that prevents unlimited growth of the micelles (178). The free energy of the micellization process, Δ°Gm, is given by the follow Equation 1.1.

$$\Delta^{\circ}Gm = RT \ln CMC \qquad \textbf{Equation 1.1}$$

where R is the gas constant and T is the temperature of the system.

MW, molecular architecture, temperature, solvent-polymer interactions or salt concentration are parameters that influence the self-assembly of polymers. Increasing temperature of the system, the solvency of hydrophilic unit as well as the CMC value will decrease, promoting the micellization. Similarly, this phenomena is favored when the attractive hydrophobic interactions increases as a result of a gain in the MW of the hydrophobic domain (179). For example, poly(ethylene glycol)-b-poly(3-hydroxyoctanoate-co-3-hydroxyhexanoate) (PEG-b-PHOHH) copolymers present a CMC value of 5.50 and 0.93 mg/L for poly(3-hydroxyoctanoate-co-3-hydroxyhexanoate) (PHOHH) segments with 1500 and 7700 g/mol, respectively (180). During the development of amphiphilic copolymers for DDS is imperative to determine the CMC value, which is generally estimated by a steady-state fluorescence method using pyrene as a probe. In Table 1.4 are presented estimated CMC values of some amphiphilic copolymers.

Table 1.4 Estimated critical micelle concentration (CMC) values for some amphiphilic copolymers.

Copolymer$_{Mw\ (g/mol)\ or\ mol\%}$	**CMC (mg/L or *mM*)**	**Reference**
CSO-SA	140	(106)
HA-C_{18}*	10-37.3	(109)
HPESO$_{4866}$	0.075-0.080	(181)
HPSO$_{3800}$	0.055	(181)
mPEG-b-PVL$_{2000-10000}$	*0.01-0.1*	(110)
PAGE-b-PLA	60-160	(182)
PCL$_{1050-7850}$-PEG$_{6000-20000}$-PCL$_{1050-7850}$	*$2.2.10^{-3}$-39.10^{-3}*	(111)
PEG$_{5000}$-b-PHOHH$_{1500-7700}$	5.50-0.93	(180)
PEG-MOG$_{5-10}$	300-4000	(160)
PEG-PPS	*0.0076-0.027*	(183)
PEG-PPS-PEG	*0.0015-0.015*	(183)
PLGA-PEG-PLGA	5	(128)
Pluronic® F108	*3.08*	(184)
Pluronic® F127	*0.56*	(184)
Pluronic® P103	*0.14*	(184)
Pluronic® P105	*0.46*	(184)
Pluronic® P123	*0.05*	(184)
PPEGMEA-g-PMOMMA	1.63	(185)
PVP-b-PDLLA$_{27\ or\ 38}$	4.3 and 2.6	(186)
SAGly-DA$_{16}$	2.9	(134)
SALeu-DA$_{16}$	0.4	(134)
SAPhe-DA$_{16}$	1.5	(134)
SAVal-DA$_{9\ or\ 16}$	0.9 and 4.5	(187)
SAVal-OA$_{16}$	22	(136)

CSO-SA – Chitosan oligosaccharide-stearic acid; HA-C_{18} – Hyaluronic acid-g-octadecyl (* Octadecyl moiety with various substitution degrees); HPESO – Hydrolyzed polymers of epoxidized soybean oil; HPSO – Hydrolyzed polymers of soybean oil; mPEG-b-PVL – Methoxy poly(ethylene glycol)-b-poly(valerolactone); PAGE-b-PLA – Poly(allyl glycidyl ether)-b-polylactide; PCL-PEG-PCL – Poly(ε-caprolactone)-b-poly(ethylene glycol)-b-poly(ε-caprolactone); PEG-b-PHOHH – Poly(ethylene glycol)-b-poly(3-hydroxyoctanoate-co-3-hydroxyhexanoate); PEG-MOG – Poly(ethylene glycol)-monooleylglyceride; PEG-PPS – Poly(ethylene glycol)-b-poly(propylene sulfide); PEG-PPS-PEG –

Poly(ethylene glycol)-b-poly(propylene sulfide)-b-poly(ethylene glycol); PLGA-PEG-PLGA – Poly(D,L-lactide-co-glycolide)-b-poly(ethylene glycol)-b-poly(D,L-lactide-co-glycolide); PPEGMEA-g-PMOMMA – Poly[poly(ethylene glycol) methyl ether acrylate]-g-poly(methacrylate acid); PVP-b-PDLLA – Poly(*N*-vinyl-2-pyrrolidone)-b-poly(D,L-lactide); SAGly-DA – Poly[(sodium N-acryloyl-L- glycinate)-co-(N-dodecylacrylamide)]; SALeu-DA – Poly[(sodium N-acryloyl-L- leucinate)-co-(N-dodecylacrylamide)]; SAPhe-DA – Poly[(sodium N-acryloyl-L- phenylalaninate)-co-(N-dodecylacrylamide)]; SAVal-DA – Poly[(sodium N-acryloyl-L-valinate)-co-(N-dodecylacrylamide)]; SAVal-OA – Poly[(sodium N-acryloyl-L-valinate)-co-(N-octylacrylamide)].

1.2.2.3. Hydrophilic surface: stability and functional role

While the hydrophobic core of micelles, in addition to the solubilization and protection of drugs, provides appropriate mechanical properties for the desired application, hydrophilic shell masks the particle from the biological environment, reducing the protein absorption and cellular adhesion, thereby enhancing the particle stability (188, 189).

Opsonin proteins present in the blood serum promptly bind to particles, allowing their recognition by macrophages that will quickly remove the encapsulated drugs from bloodstream (190). The presence of hydrophilic layer on the surface of particles (stealth particles) will reduce or delay the opsonization via steric repulsion forces, thus increasing the plasma circulation time of particles and the half-life time ($t_{1/2}$) of drugs (190, 191). PEG and poloxamers are generally used as hydrophilic polymers to cover the surface of many nanoDDS (146). Although PEGylation presents advantages, may not always be necessary. Indeed, unnecessary or excessive PEGylation could lead to a non-desirable increase in the particle size. Additionally, an increase in the cost of the final product could also be noticed. Thus, the quantification of hydrophilic groups at the surface of particles must be performed using techniques like XPS or secondary ion mass spectroscopy (SIMS) (192, 193) in order to assess the convenience of PEGylation (or other method to increase hydrophilicity) and to predict the nanoDDS behavior *in vivo*.

From the technological point of view, the importance of the hydrophilic surface on nanoDDS relies not only in the stealth properties but also in their functionalization potential by chemical modification or bioconjugation. The functionalization is mainly used to bind targeting moieties to the particles surface that allows the biodistribution control of nanoDDS (194) and different ligands can be used accordingly to the required application (195), as referred before. The conjugation of folate at the surface of hyperbranched aliphatic polyester Boltorn H40-poly(ε-caprolactone)-poly(ethylene glycol) (H40-PCL-PEG) nanoparticles enhances the *in vitro* drug

uptake and therapeutic efficacy of anticancer agents in Hela and A549 cells. The presence of acid folic in the media reduces the particles uptake by receptor saturation, proving the effectiveness of folate in the targeting of tumor cells (141). Similarly, Arginine-Glycine-Aspartic acid (RGD) peptide and transferrin improved the cytotoxicity of paclitaxel-loaded micelles against $\alpha_v\beta_3$ integrin and transferrin over-expressed human cells, respectively (115, 142).

1.3. Safety of nanocarriers

The growing development of nanotechnology in the last decades is intensifying the use of materials whose security profile is not completely clarified. Although some of the materials possess toxicological data, their chemical, physical and biological properties can suffer changes when at the nanometric scale. Some studies suggest the development of side effects to health derivate from the occupational or environmental exposure to nanomaterials (196, 197). Despite the advantages presented by nanocarriers, their small size provides high surface area and possible higher reactivity with celular components. *In vitro* and *in vivo* studies showed induction of inflamatory responses and damage to the pulmonary epitelium, as well as extrapulmonary effects like increase in the blood coagulation and oxidative stress derived from the translocation of inhaled nanoparticles to the circulation and accumulation in other organs (197-200). These could result in alterations of respiratory, cardiovascular and immune systems. However, such studies are based on high doses of nanoparticles, not corresponding to the normal doses of exposition (198), yet the possibility of deleterious effects for health due to inhalation of nanocarriers should not be overlooked, requiring further detailed studies. Also, some researchers mention the urgent need for the development of standardized procedures for the analysis of biological samples of people exposed to nanoparticles, with a view to characterizing their safety profile (197).

Regardless of all the potential of nanotechnology in various areas of health, the euphoria observed must give way to conscious and carefull decisions regarding its safety based in evidence. During the development of new nanomaterials the health side effects and the environmental impact resultant from secondary production and disposal might be considered (196, 201). Thus, a risk assessment should be carried out before the marketing of such materials, as well as a review and monitoring of long-term effects of whose already on the market.

2. Therapeutic peptides and proteins

2.1. Properties

Biopharmaceuticals, including therapeutic peptides and proteins have emerged as useful and promising drugs in the treatment of various diseases such as diabetes, cancer or autoimmune diseases (202). The first biotechnologically derived product approved for market was recombinant human insulin (Humulin®, Eli Lilly) in 1982 (203) and since then, many efforts and investment have been located to the research of biopharmaceuticals. In 2013, around 900 biopharmaceuticals targeting more than 100 diseases were under development by American's research companies (204). This is explained by the overall improvement in quality of life and reduced burden of complex and challenging diseases achieved by these specific and selective medicines in an extent sometimes not reached by conventional drugs (205). Consequently, many biopharmaceutical products have granted market authorization over the years (206) and gain an increased share in global pharmaceutical market year-by-year (207). For example, peptides, proteins, enzymes and monoclonal antibodies together account for 26% of the total approved medicines by FDA between 2009 and 2011 (208). This is due to the development of molecular biology that allowed the understanding of the role of biopharmaceuticals in pathophysiological processes as well as the growing development of biotechnology, bioengineering and recombinant DNA technology, which allowed their large-scale production. Despite the tendency to classify peptides and proteins as new therapeutic agents, insulin extracted from animal's pancreas was produced at industrial level for the first time in 1923 by the company E. Lilly (209).

Sequences with fewer than 50 amino acids (< 5 kDa) are considered to originate peptides, while proteins are composed by bigger amino acid sequences (> 5 kDa). By that, both peptides and proteins by far exceed the 500 Da of MW cutoff of molecules generally assumed to be orally absorbed (210). Thus, and

regardless of all the therapeutic potential associated with peptides and proteins, they have physicochemical characteristics that limit their therapeutic applications. Due to their high MW and general hydrophilicity, peptides and proteins have limited ability to cross biological membranes and consequently reduced permeability and bioavailability (211). Also, they complex structure makes difficult its formulation and administration in the active conformation as discussed below.

2.2. Stability and formulation challenges

Due to its complex structure, peptides and proteins have limited chemical stability *in vivo*, undergoing aggregation, degradation and proteolytic cleavage, being further removed from the bloodstream, thus presenting reduced systemic $t_{1/2}$. Apart from the above characteristics that determine its pharmacokinetics and pharmacodynamics, they also present *in vitro* barriers to their stability during the pharmaceutical development. The reactivity of some aminoacids results in degradation reactions such as deamination, racemization, oxidation or hydrolysis, that are dependent of production and storage condition such as pH, temperature, agitation, ionic strength, shear stress, light exposure, presence of metal ions, surfactants or solvents. This could lead to changes in the primary, secondary and tertiary structure of the molecules, originating a loss of their activity. When unstable, they tend to undergo aggregation with possible precipitation, adsorption and denaturation, which will limit its concentration and therapeutic levels after administration, and could present safety problems (209, 211, 212).

The problems of *in vitro* and *in vivo* instability of proteins can be solved with the addition of excipients that act as stabilizers by different mechanisms. Examples are sugars and salts that increase the thermal stability of proteins, the non-ionic surfactants that reduce its aggregation, metal chelators and enzyme inhibitors that reduce the ability of various proteolytic enzymes (211, 213). Attention should be paid to the addition of sugars, since glycation of the peptides and proteins could occasionally occur by reaction of the sugars with the amino groups of the amino acids (214). In addition to the referred excipients, the drying of the final product using techniques like lyophilization and spray-freeze-drying reduce the instability mechanisms occurring in liquid medium. Also, chemical modification of proteins such as conjugation with PEG or Fc fusion protein, glycosylation or acylation has shown to decrease the immunogenicity of peptides and proteins, and improve their stability and the $t_{1/2}$ by increasing their resistance to proteolysis by conformational restriction *in vivo* (211, 213).

2.3. Administration routes of therapeutic peptides and proteins

Parenteral administration can overcome the problem of reduced bioavailability of peptides and proteins through biological membranes, being its usual route of administration. However, it does not eliminate the instability in the bloodstream (211). Moreover, this is an invasive

route, which can lead to a reduced acceptance by patients and, consequently, increased costs of therapy, especially when it required a prolonged or chronic treatment. Besides, there is a need for sterilization and cold chain transport and storage of various formulations of peptide drugs, as well as the need for specialized personnel for its administration (215, 216).

The problems associated with parenteral administration boosted industrial and academic researchers to seek for needle-free and user-friendly formulations for non-invasive administration of peptides and proteins. Among the different non-invasive routes of administration appears oral, buccal, pulmonary, nasal, transdermal, ocular, rectal or vaginal (211). Oral administration is considered the most attractive route for drug administration and the preferred/accepted by patients due of its ease and convenience of administration. However, the harsh gastric environment (acidic pH and proteolysis) and the intestinal epithelia arise as strong barriers to efficient delivery of macromolecules (217). The bioavailability of proteins and peptides after oral administration is very low due to its instability in the gastrointestinal tract and low permeability through the intestinal mucosa (218, 219). Actually several studies are focused on oral administration of proteins, many of them using nanotechnology to increase their bioavailability.

Parallel to the oral, inhalation is seen as an effective way to deliver peptides and proteins and appears as an alternative route to parenteral administration, as demonstrated by the several experimental and clinical assays proposed so far (213, 220) and mentioned in the section 4 of the present chapter.

3. Pulmonary administration as non-invasive route for systemic delivery of therapeutic peptides and proteins

3.1. Brief history of inhalation

Inhalation of compounds as a means to treat diseases is used since ancient times. The oldest reports came from China and India around 2000 BC and are related to the inhalation of smoke from burned herbal preparations based on *Ephedra sinica*, *Atropa belladonna* or *Datura stramonium* to treat throat and chest diseases like asthma (221-224). Pedanus Discorides (40-90 AD) the Greek physician, surgeon, pharmacologist, botanist and author of *De Materia Medica* (considered the first pharmacopeia) as well as Aelius Galenus (129-199/217 AD) prescribed inhaled sulfur vapors to their patients (225). Although the word

"inhaler" was used for the first time by the English physician John Mudge in 1778 to describe his invention, the first therapeutic inhalation device is attributed to Hippocrates (460–377 BC) (221, 222). Through the years, many compounds and mixtures were proposed and used to treat distinct diseases using various methods for inhalation, from ceramic inhalers, to combustible powders, burning papers and liquid atomizers. A very curious and popular way to inhale compounds in the 19th and 20th centuries was based on the use of asthma cigarettes, which were withdrawn from the market in 1992 (221, 225). The inhalation of vapor from solutions of picric acid, tar, iodine or sulfuric acid was very popular in the 20th century to treat tuberculosis and other infections, especially in spa's (225). The first mentions regarding inhalation of antibiotics such as penicillin by nebulization to treat pulmonary infections were published in the 1940s (225-229). Nowadays, inhaled drugs are preferentially administered via dry powder inhaler (DPI) and pressurized metered-dose inhaler (pMDI), being also used nebulizers in hospitals.

Despite inhalation started as a route to treat diseases confined to the respiratory tract, with the observed scientific and technology advances, a change in paradigm took place over the years, and inhalation has been evaluated and used to treat both local and systemic diseases (230) such as asthma (231), tuberculosis (232), other bacterial infections (233), influenza virus infection (234), fungal infections (235), cystic fibrosis (236), chronic obstructive pulmonary disease (237), diabetes (238) or cancer (239, 240). Moreover, inhalation has been also tested as a non-invasive vaccination platform (241-243).

3.2. Anatomo-physiological characteristics of lungs and airways

Over the past 20 years, the research focus on inhalation shifted from the almost exclusive local treatment to include drugs with systemic action. However, the understanding and characterization of pulmonary administration of drugs is a complex task that involves not only the release of the drug from inhalation devices, but also the mechanisms of drug deposition and absorption, which are related to the physiology of the respiratory system (244).

The respiratory system consists in the upper and lower airways and lungs. The upper airways consist on the nose, mouth, pharynx and larynx. The trachea follows the larynx and branch into two bronchi. The bronchi divide consecutively in bronchioles which branch into alveolar ducts and terminate in alveolar sacs (245). The gas exchange with blood occurs through approximately 300 million alveoli (246), occupying a surface area of 75-150 m^2 (245, 247),

which corresponds to approximately 98% of the adult lungs (248). These begin to emerge in smaller bronchioles, which are called respiratory bronchioles. The lower airways are divided into conduction zone and the respiratory zone. The respiratory zone is comprised by the respiratory bronchioles and the alveolar ducts and sacs (246).

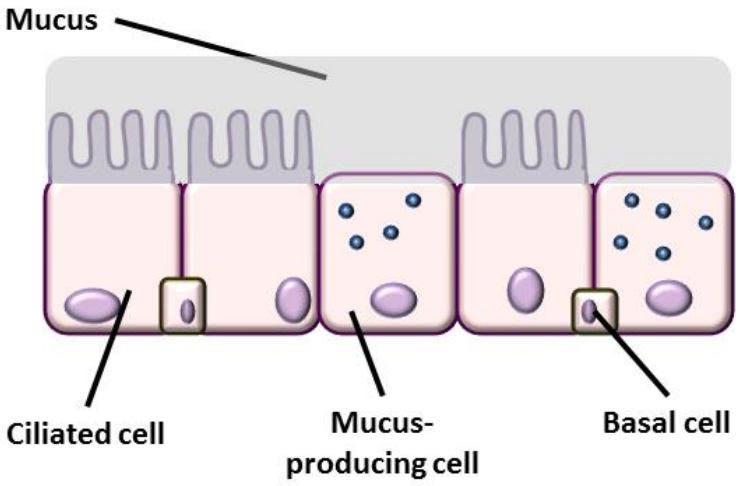

Figure 1.7 Schematic representation of the bronchial epithelium.

The airways, with the exception of the alveoli, possess a pseudostratified epithelium composed of ciliated cells, basal cells and mucus-producing cells (goblet cells and Clara cells) (246) (Figure 1.7). The alveolar wall consists of three tissue components: epithelium (around 0.3 µm of thickness), supporting tissue/basement membrane (around 1.2 µm of thickness) and blood capillaries (endothelium with around 0.4 µm of thickness) (249). The epithelium is composed of two types of cells called pneumocytes (Figure 1.8). The alveolar type I pneumocytes occupy most of the alveolar surface and have the function of barrier while type II pneumocytes, interspersed with type I, are responsible for secreting surfactant. This consists of phospholipids (90%) and protein (10%), forming a 0.1-0.2 µm thick film that is responsible for the decrease in surface tension existing in the alveoli, thereby preventing its collapse. In several areas of the alveolar wall, the tissue support is absent allowing the fusion of the basement membrane with the alveolar capillary endothelium of the extensive blood capillaries plexus surrounding alveoli. Thus, a very low thickness barrier separates the alveolar air from the bloodstream (245, 246, 250).

The epithelium of the respiratory system has also lymphoid tissue called mucosa-associated lymphoid tissue (MALT) that is responsible for its immunological activity. The lymphoid follicles present in the airways (nasal-associated lymphoid tissue (NALT) and bronchus-associated lymphoid tissue (BALT)) have many immune cells such as dendritic cells and T and B lymphocytes. The epithelium covering the lymphoid follicles called follicle associated epithelium (FAE) possesses M cells that are involved in uptake, transport and presentation of antigens in the respiratory lumen (216).

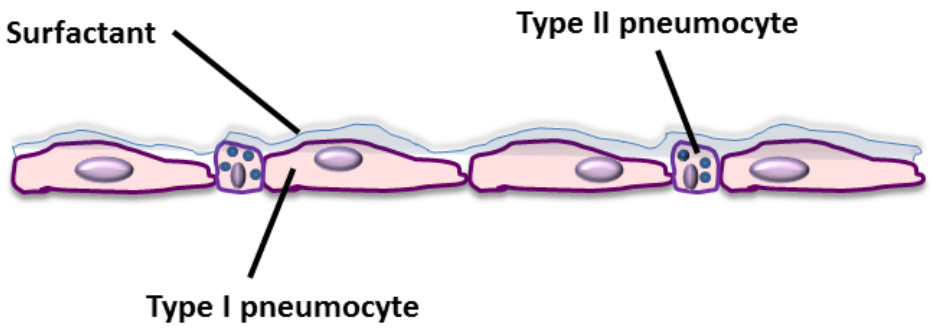

Figure 1.8 Schematic representation of the alveolar epithelium.

Taking into account the physiological characteristics of the respiratory system, it becomes clear that this route provides a non-invasive alternative presenting a large surface area, a thin epithelial barrier, extensive blood supply (flow 5 L/min), and lower enzymatic activity and efflux systems compared to other organs and tissues (e.g., gastrointestinal tract). Moreover, the reduced volume of fluid allows high concentrations of drug near the bloodstream, and the first-pass metabolism is avoided by pulmonary administration, which is especially useful for drugs that suffer high hepatic metabolism (251). These features are the reason for the higher bioavailability of inhaled peptides and proteins (10-200 times higher) compared with other non-invasive routes (84, 252).

3.3. Pulmonary biodistribution of inhaled peptides and proteins

After inhalation, particles will undergo lung deposition and be subjected to the existing clearance mechanisms of the respiratory system. Being the place of gas exchange and constant contact with the exterior ambient, respiratory system developed complex and not

fully clarified defense mechanisms working as barrier for foreign particles that could impair the efficient delivery of drugs (248). The complex geometry and humidity of the airways hampers the passage of the larger particles to the deep lung, and the movement of the bronchial cilia, known as mucociliary escalator, transports the particles trapped in the mucus layer to the gastrointestinal tract. Particles/compounds capable of evade the mentioned barriers and reach the deep lung have to face other defense mechanisms like phagocytosis by alveolar macrophages, alveolar lining fluid, intra- and extra-cellular catabolism, and the epithelium to attain the bloodstream (253, 254). Phagocytized compounds can be transported through the alveolar surface, undergo translocation to the lymphatic system or degradation by the intracellular enzymatic lysosomal system (69).

In some studies, the rate of protein clearance did not significantly change in the presence or absence of an endotracheal tube, suggesting a reduced role of mucociliary escalator in the lung's protein clearance (255). Also, demonstrate that only small amounts of proteins are found in macrophages (255). Despite the higher phagocytic capacity of macrophages compared to the endocytic capacity of pneumocytes, the first ones do not play an important role in clearance of proteins before 48 hours after exposure (254, 255). In addition, several large-sized proteins reach the circulation in intact form after instillation, suggesting a lower impact of catabolism in lung protein clearance (248, 254). However, degradation by proteolysis is relevant for proteins with small MW (< 3 kDa) (256). The use of enzyme inhibitors such as bacitracin, chymostatin, leupeptin or nafmostato mesylate reduces proteolysis and, thereby, increase the bioavailability of proteins prone to suffer high catabolism (8).

In addition to the mechanisms/barriers described above and able to influence the permeability of compounds from the respiratory tract to the bloodstream and their bioavailability, the alveolar and airway epithelium arise as a major barrier to absorption of drugs. The absorption of macromolecules through the respiratory tract is a complex and enigmatic process that involves various mechanisms that are not yet well characterized, being apparently dependent on the hydrophilicity and the size of macromolecules (257-259). Different studies suggest that the rate of absorption is inversely proportional to the MW of the macromolecule. This influence not only the percentage of drug absorbed, but also the time necessary to the absorption occurs. For example, the $t_{1/2}$ of the alveolar absorption of macromolecules increases with their MW (inulin with MW: 5250 Da and $t_{1/2}$: 225 min; dextran with MW: 20000 Da and $t_{1/2}$: 688 min; dextran with MW: 75000 Da and $t_{1/2}$: 1670 min) (260).

Two major mechanisms were proposed to characterize pulmonary absorption of proteins: paracellular diffusion and transcytosis (Figure 1.9). Transcytosis may further be classified into vesicular endocytosis or pinocytosis, and receptor dependent transcytosis. Proteins with small MW are apparently absorbed by the paracellular route, diffusing through the tight junctions, while molecules with higher MW seem to suffer endocytosis (248). Peptides can be absorbed by receptor mediated transcytosis using the high-affinity peptide transporter 2 (247), while immunoglobulins are absorbed by a conjugation of pinocytosis with receptor mediated transcytosis. After suffer endocytosis, immunoglobulins bind with the fragment crystallizable (Fc) receptors that prevent the fusion with lysosomes and are release in the basolateral side of epithelial cells (261). This immunoglobulin transport pathway is used to deliver proteins by conjugation of the therapeutic macromolecule with Fc regions of immunoglobulins (261, 262). Other strategy proposed to enhance the pulmonary absorption of proteins is their coupling with specific peptidic sequences that not alter the biologic activity but promote their translocation through the epithelium probably by receptor mediated transport (263).

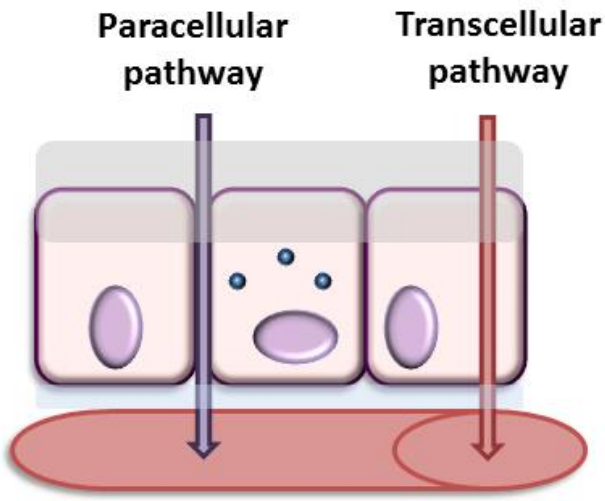

Figure 1.9 Schematic representation of absorption routes.

3.4. Formulation requirements for pulmonary delivery of drugs

Different aspects related to the formulation, inhalation device, and patient influence the aerosolization and deposition of drugs and, consequently, their therapeutic efficacy. The airways geometry, respiratory capacity (tidal volume, inspiratory flow rate and breathing

frequency), inhaler handling, smoking, and pathologies affecting the lungs will be responsible for therapeutic inter-individual variations.

Formulation plays an important role in the inhaled drugs performance, in terms of stability, deposition and absorption. It should maintain the drug in the active state and deliver it to a specific site of action to be absorbed or released for systemic or local action, respectively. Additionally, the formulation must be stable upon storage. Since proteins are labile drugs, suitable to lose their activity through physical and chemical instability, maintenance of the active conformation is a challenge and a series of considerations should be taken into account during their production and storage. Temperature, pH, agitation, ionic strength or presence of surfactants needs to be controlled in order to avoid aggregation, degradation or conformation lost (264, 265). The stability of proteins and their therapeutic performance can be improved through the incorporation of some excipients to the formulation as detailed in the section 3.4.2.

3.4.1. Aerodynamic properties of particles

Among the different formulation characteristics, aerodynamic diameter (d_{ae}) plays a key role in the deposition pattern and therapeutic efficiency of the aerosolized particles. Aerodynamic diameter is the diameter of a unit density sphere that has the same terminal settling velocity in still air as the particle in consideration (266) and is defined by the following Equation 1.2.

$$\mathrm{d}ae = \mathrm{d}eq\sqrt{\frac{\rho p}{\rho o \chi}} \qquad \textbf{Equation 1.2}$$

where d*eq* is the geometric diameter of an equivalent volume sphere of unit density, ρ*p* and ρ*o* are particle and unit densities, respectively, and χ is the dynamic shape factor.

When determined based on the mass size of particles through methods like aerosolization using impactors, d_{ae} receives the denomination of mass median aerodynamic diameter (MMAD).

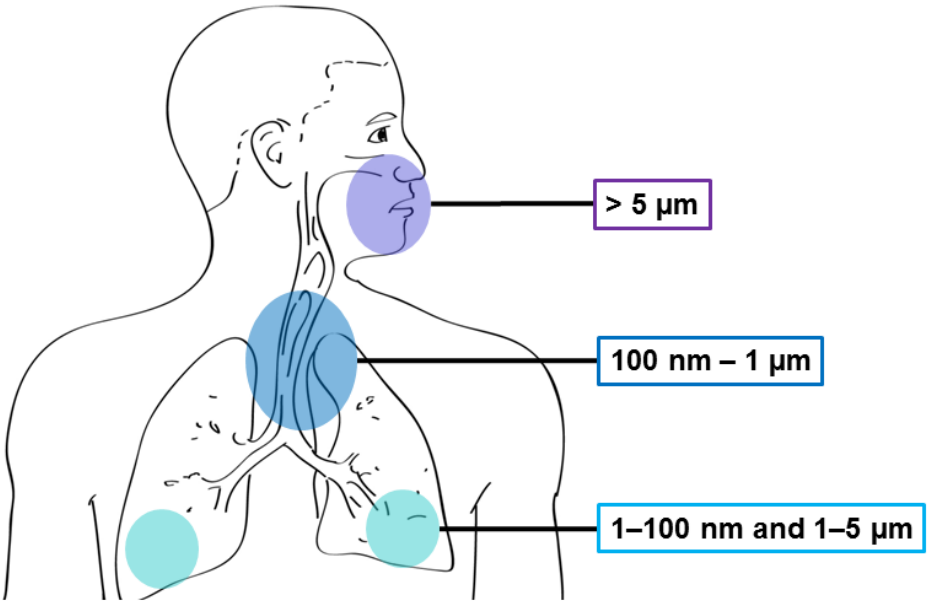

Figure 1.10 Deposition profile of particles on the different areas of the respiratory system according to their aerodynamic diameter.

After inhalation, depending on d_{ae} or MMAD, particles will move through the airways and deposit in different parts of the respiratory track or be exhaled. For deposition at the lower regions of lungs, particles in the range of 1–100 nm and 0.5–5 µm are required. Particles larger than 5 µm will impact in the throat and be swallowed, while the middle sized particles will be essentially exhaled (Figure 1.10) (198, 267). Different forces, namely inertial impaction, sedimentation, diffusion and interception, will govern the particles fate and are related to the aerodynamic and hydrophilic properties of particles and shape of airways (253, 268, 269). By manipulating the particle size, is possible to target specific regions of the respiratory tract (more than 50% of deposition). For systemic delivery, alveolar deposition is needed, while for local action, delivery at bronchial level is preferred. As referred before, although alveolar macrophages are part of the respiratory defense system, they are sometimes the therapeutic target, for example in the treatment of tuberculosis. Targeting of alveolar macrophages could be achieved by surface-decoration with ligands of the lectin-like receptors present at the membrane of macrophages (17), or by deliver particles with a size that promote their phagocytosis (270, 271).

Formulations based on peptides and proteins loaded into nano- or microparticles have been widely proposed in the last years as strategies to overcome the limitations of conventional formulations. Since a wide range of the developed nanoparticles falls within the particle's size range liable to suffer exhalation, the agglomeration of nanoparticles into micron-sized particles (nanocomposites) with proper aerodynamic characteristics that disaggregate after deposition have been exploited (34, 272). One possible advantage of use agglomerates of nanoparticles instead of microparticles relies on the capacity of nanoparticles to easily evade mucociliary clearance and phagocytosis by alveolar macrophages. Some studies show that smaller particles are internalized at a lower extent than particles higher in size (273, 274).

3.4.2. Excipients used in the development of inhalatory formulations

Besides drugs, pharmaceutical excipients constitute an integral part of pharmaceutical formulations. They provide physical, chemical or microbiological stability, bulk properties that improve handling and metering, while controlling the mechanical and pharmaceutical properties of formulations such as release and permeation (267, 275). At the moment, only a small number of excipients are authorized for pulmonary delivery, but a variety of new excipients is under evaluation. Since lungs have limited buffer capacity, only compounds that are biocompatible or endogenous to the lung and that are easily metabolized or cleared can be used in inhaled formulations (275).

Since formulations for nebulization are liquid solutions or suspensions, the common excipients used are salts (e.g., NaCl) to adjust the osmolarity (300 mosmol/L), HCl, NaOH, phosphates to adjust the pH to neutrality, and surfactants such as polysorbates, sorbitan monostearate, oleic acid, and soya lecithin to facilitate the formation of liquid droplets. Ethanol can be used as co-solvent and permeation enhancer only in small concentration due to its irritation potential. Preservatives such as parabens and benzalkonium chloride, antioxidants like ascorbic acid or chelating agents such as ethylenediaminetetraacetic acid (EDTA) can also be used to enhance stability (267).

The excipients used in pMDI are similar to those found in preparations for nebulization excepting the gas propellants. The most widely excipient used as propellant in pMDI is hydrofluoroalkane, a non-toxic, non-flammable, and chemically stable gas without carcinogenic or mutagenic effects. Due to the absence of ozone-depleting properties, hydrofluoroalkane have been replacing chlorofluorocarbon-based propellants (276). DPI were

developed as a response to the limitations regarding stability and environmental aspects of pMDI and nebulizers (275).

DPI are considered the most advantageous devices for inhalation regarding long-term stability of formulation, absence of gas propellants and patient convenience since are breath-actuated and easy to use without the need of hand-lung inhalation co-ordination (277, 278). However, the development of particles with a narrow particle-size distribution and good flowability, suitable for aerosolization and lung deposition of peptides and proteins in the active state is challenging and depends on the appropriate use of powder technology and particle engineering. Techniques like microcrystallization, micronization by jet- or ball-milling, lyophilization, spray-drying, spray-freeze-drying or supercritical fluid technology can be used to produce solid particles (267, 279). All the methods present advantages and disadvantages, and should be chosen according to the effect on the stability of the proteins, the characteristics of particles required to a specific formulation, scale-up, cost-effectiveness and safety issues (279). As stated before, the capacity to produce an aerosol with a narrow particle-size distribution will influence the deposition pattern of the drugs. Taking this in consideration, it is crucial to produce powders with good dispersibility. Solid particles are subject to cohesive and adhesive interactions with the surrounding environment, that need to be break during the aerosolization. Different forces are involved in particle's interactions and include electrostatic and van der Waals forces, capillary forces from to the presence of residual water at the surface of particles, and mechanical interlocking due to surface roughness (275). Distinct aerosolization properties could be obtained playing with these forces by specific particle engineering. For example, an efficient drying of the particles needs to be provided by the production method to reduce moisture and capillary forces, but extra drying should be avoided due to the formation of charges at the surface of particles that promote electrostatic interactions. One of the main factors affecting the particle's interactions is their surface area. The larger surface area, the greater will be the interactions between particles, and lower will be the flowability. Surface area is dependent on size, shape and morphology of particles (269, 275). Particles in the size range suitable for inhalation possess high surface areas and are generally mixed with larger coarse carrier particles of excipients to improve their flow properties. In DPI, the coarse carrier particle is the major component of the formulation (>95%, w/w). It provides bulk properties and reduces the cohesion forces between drug particles, facilitating the aerosol dispersion and defining deposition pattern (280). Lactose is the main excipient used as coarse and larger carrier particles and, to a lower extent, as cryoprotectant when particles are prepared using lyophilization (281). There

are commercially available a variety of inhalation grade lactose with different characteristics and narrow particle size distribution (Flowlac®, Granulac®, Respitose®, Lactohale®, Inhalac®, etc.) that should be carefully selected during the development of the formulation (282, 283). Other sugars such as glucose, trehalose and mannitol are also used as cryoprotectants and coarse carriers (267). Magnesium stearate is approved for inhalation to protect drug from moisture and to reduce the cohesion and adhesion between particles (284). The characteristics of the carriers and the adhesive forces between carrier and drug particles influence the performance of the formulation and need to be assessed and optimized. Blending of drugs with coarse carriers is a critical point during the development of a DPI and also object of optimization (285-289).

Regarding inhaled nanoDDS, most of the components are generally not approved for inhalation. In this case, new excipients proposed for inhalatory formulations need to pass through the entire process of safety evaluation, including complete *in vitro* toxicological evaluation and *in vivo* assessment of non-clinical and clinical safety prior to licensing. Unfortunately, there is a lack of specific regulatory guidance regarding the toxicological assessment of excipients for inhalation (290-292). Excipients generally recognized as safe (GRAS) or those approved for other routes of administration need a more limited number of experiments for safety evaluation, being its acceptance by regulatory agencies usually easier. This is the case of phosphatidylcholine (PC), a lipid surfactant and one of the constituents of lung surfactant that is commonly used in the production of liposomes. Studies show that PC-based liposomes do not affect or slightly decrease the viability of human A549 alveolar cells after 24h of exposure. The effects on cell viability are dependent on the PC derivate and the concentration used (293). Other compounds used in the development of nanoDDS such as dextran, alginate, carrageenan or gelatin also possess GRAS status. It should be mentioned that those regulations apply not only to the material itself but also to its source. For example, contrary to what happen with shrimp-derived chitosan, chitosan obtained from *Aspergillus niger* is in the process to obtain GRAS status (294). Chitosan does not present significant toxicity to pulmonary tissue and cell lines after inhalation (295, 296). In fact, some studies showed some protective effect against oxidative stress (295). PLGA is another biodegradable polymer extensively used in the production of nanoDDS and present in various approved medicines including Trelstar® Depot (Pfizer), Risperidal® Consta (Johnson & Johnson), Sandostatin LAR® Depot (Novartis), Suprecur® MP (Aventis) or Lupron Depot® (TAP). The cytotoxicity of PLGA nanoparticles with different coatings and surface charges was assessed. Results showed that the cytotoxicity of the nanoparticles to human bronchial Calu-3 cells was

very limited, with the absence of inflammatory response (297). Cyclodextrins have been tested as complexing agent and excipient of inhalatory formulations. Various approved formulations containing cyclodextrins such as Voltaren® (Novartis), Clorocil® (Laboratório Edol), Brexin® (Chiesi Farmaceutici) or Vfend® (Pfizer), are daily used in the clinical practice for administration routes other than inhalation (298).

Recently, carrier-free formulations that presented good aerosolization properties and deposition patterns have been developed and proposed as promising inhalatory formulations (299, 300). This "carrierless" strategy prevented the need of long and expensive safety studies, facilitating the authorization by regulatory agencies. Some engineered drug particles alone fulfill the requirements for inhalation, which is possible by the development of large porous/hollow particles (301-303). Due to its small density, particles with high geometric size and, consequently, reduced cohesive forces, present appropriate aerodynamic diameters. For example, salbutamol particles prepared by thermal ink-jet spray-freeze-drying with mean geometric diameter of 35 µm and mean aerodynamic diameter lower than 8.7 µm, present a percentage of FPF comparable to a salbutamol commercial formulation (302). At the moment, there are commercially available carrier-free DPI composed by agglomerates of pure terbutalin and budesonide particles, namely Bricanyl Turbohaler® (AstraZeneca) and Pulmicort Turbohaler ® (AstraZeneca), respectively.

3.4.3. Inhalation devices

Apart from the characteristics of particles, pulmonary administration demands an inhaler device that produces an appropriate aerosol. There are numerous devices available with distinct properties and specifications that are more appropriate for each type of formulation – nebulizer for liquids, pMDI for liquids and powders, and DPI for powders (280, 304, 305). Since the device greatly influences the particle aerosolization and deposition pattern, the choice of the right inhaler for a specific formulation is one of the most time-consuming and challenging stages during the development of inhalable medicines, and it is imperative to ensure the appropriate drug efficacy (280, 306). For example, Alexander and co-workers tested the aerosolization efficacy of Ambisome® (Gilead Sciences) using different nebulizers and they found differences among all of them (307). The ideal inhaler should generate an aerosol with a FPF and reproducible drug dosage, guaranty protection and stability of the product during storage, be accurate, small, easy to handle, discrete, and user friendly in order to be accepted. One of the claimed reasons for the market failure of Exubera® (Pfizer) was

the low patient compliance partially due to the complex inhaler device (308). Owing to the great therapeutic potential of this alternative administration route, the last decades witnessed the development of devices with greater FPF and lung deposition patterns of approximately 40–50% of the nominal dose as compared with the low levels between 10 and 15% verified in the past (276).

However, it is worth mentioning that this is a growing and dynamic field and innovative technologies are emerging. For example, power-assisted devices activated by vibration (309, 310) or pneumatic technology (311), called active inhalers, have been developed for the delivery of systemically proteins and active drugs that have narrow therapeutic windows as well as for inhalatory nanoDDS (275). Examples of such devices are the AERx® from Aradigm, Respimat® from Boehringer or AeroDose® from Aerogen Inc (8). Also, the development of adjusted inhalers that present specific inhalation patterns that are useful for the treatment of certain pulmonary diseases can be faced (276). It is also important to consider the cost relative to the production of the device and its impact on the final product price. A balanced price/therapeutic efficacy relationship is a crucial factor that can limit the clinical application of a certain product.

3.5. Limitations of pulmonary administration

The main limitation faced by pulmonary administration of drugs relates to the reproducibility of the dose. From the delivery device until be absorbed in the lungs, the drug undergoes consecutive losses during aerosolization and deposition. Thus, the absorbed dose is usually lower than the dose present in the delivery device.

As stated before, the deposition of particles at the lower respiratory tract is a complex phenomenon and its efficiency depends on several factors like the type of formulation, delivery device used and their capacity to produce the aerosol (250, 277, 312, 313). Unfortunately, there is no inhaler device producing only particles within the size limits appropriate to the lung deposition which results in a very low rate of dose emitted (277). Another issue of relevance arises from the fact that more than 50% of patients improperly uses the delivery device, leading to non-reproducibility (312). Thus, an intensive education of patients by health care professionals is required to an increase the effectiveness of the treatment (277).

The respiratory capacity of patients also plays an important role on the delivery efficiency of particles, being reduced in patients with lower respiratory capacity like children, elderly

persons or adults with certain disease conditions that compromises the lungs functions, resulting in non-reproducible pharmacokinetics and pharmacodynamic responses (314).

4. State-of-art on therapeutic peptides and proteins for inhalation

In 1993 the FDA approved the first protein administered via inhalation, a highly purified solution of recombinant human desoxyribonuclease I (rhDNase), also known as dornase alpha (Pulmozyme® from Genentech), for treatment of cystic fibrosis (315). Despite the promise and advantages presented by pulmonary delivery, only Pulmozyme® and, more recently, Afrezza® (insulin DPI from MannKind) granted market authorization. This could be attributed to the formulation and delivery challenges of inhalable drugs referred previously. However, the rational design of particles with appropriate characteristics for inhalation enabled the development of many formulations some of which already entered in clinical evaluation.

Insulin has branded the history of the development of inhaled protein therapeutics with cycles of hope and disappointment. Attempts to develop an inhaled insulin formulation to substitute the current treatment of diabetes by subcutaneous injection have been made by dozens of researchers and companies all over the world during decades. The apogee of inhaled insulin was reached in 2006 when FDA and European Medicines Agency (EMA) granted market authorization to Exubera® (Pfizer/Nektar), a spray-dried mixture of insulin, sodium citrate (dihydrate), sodium hydroxide, mannitol and glycine (308, 316). During clinical trials, patients treated with Exubera® presented similar postprandial glycemic control and values of glycated hemoglobin (HbA1c), faster onset of action, lower weight gain, lower incidence and severity of hypoglycaemia and greater satisfaction (higher comfort and convenience) compared with patients receiving subcutaneous injection of regular insulin (238, 317-319). However, less than two years later, the product was withdrawn without achieving the excepted market success (308). This decision had as casualty the development's interruption of AERx iDMS® (Novo Nordisk/Aradigm) and AIR® (Eli Lilly/Alkermes) both at phase III clinical trials, few months after Pfizer decision (320). Because of its short-term action, there was the necessity to inject a long-acting insulin for overnight glycemic control (24, 321). Moreover, Exubera® showed a bioavailability of only 10-20% compared to subcutaneous injection. The big size of the inhaler device and its complex handling also contribute to the low acceptance of the product by both patients and clinicians (215, 322). Although Pfizer argued that the decision was due to a commercial failure related to limitations of the formulation and the inhaler device

hampering the acceptance of the product; the development of serum insulin autoantibodies and the emergence of lung cancer cases in patients treated with Exubera® raised questions regarding the immunological effects and safety of inhaled proteins (238, 319, 323). Pfizer stated that patients that developed lung cancer had a history of smoking. It could be related to vasodilator and growth promoting capacities of insulin (238). However, due to the low number of cases was not possible to establish a causal relationship between the emergence of lung cancer and the use of Exubera®. Nonetheless, some companies continued the development of their products with different and improved technologies, hoping to succeed were Exubera® failed.

Afrezza® (MannKind), a DPI based on Technosphere® technology (324) using a next-generation inhaler device (Dreamboat®) recently granted FDA approval. The change of the inhaler device from MedTone® to Dreamboat® over of the clinical studies raised concerns by FDA about the equivalence of the two devices, which delayed the product approval. Technosphere® technology is based on fumaryl diketopiperazine large porous particles with a MMAD of 2-2.5 µm, suitable for delivery at deep lung, where small proteins can be absorbed onto the surface. Pharmacodynamic and pharmacokinetic analysis of Afrezza® showed a rapid absorption (time of maximum concentration observed (t_{max}) = 12–14 min), short onset of action (20–30 min) and action duration time (2–3 hours) that mimic the physiological insulin requirements to cover prandial glucose absorption in type 2 diabetic patients (325). In a pilot study an optimal dose of inhaled insulin was able to control the postprandial glycemic levels of type 2 diabetes patients regardless the meal carbohydrate content (326). In addition, the absorption and pharmacokinetics of insulin after inhalation was not significantly altered in patients with mild-to-moderate chronic obstructive pulmonary disease (COPD) (maximum concentration observed (C_{max}) = 34.7 µU/mL and area under the curve (AUC) = 2037 µU/mL·min) compared to healthy patients (C_{max} = 39.5 µU/mL and AUC = 2279 µU/mL·min) (327). Concerning safety, in a 2-years study, Afrezza® showed to be well tolerated, promoting slightly changes in lung function, comparable to the usual treatment and mild, transient cough after inhalation (328). However, the results of the study should be analyzed carefully, since a high percentage of treatment discontinuation owing to adverse events was higher in the Afrezza® treated group.

Other inhalable insulin products are under clinical stage such as Aerodose (phase II), Abbott Labs' inhaled insulin (phase II), QDose (phase I), Alveair® (phase I), BioAir® (phase I) or ProMaxx® (phase I) (320). Insulin is commonly used as drug model in the development of

formulations for delivery of proteins, which explains the high number of studies at preclinical stage published (34, 322, 329-337).

Besides Afrezza®, MannKind is also developing a glucagon-like peptide 1 (GLP-1)-based product to treat type 2 diabetes by inhalation based on the same Technosphere® system. The product (MKC253) is currently at phase I stage and, so far, proved to be able to stimulate the insulin secretion and, consequently, reduce the postprandial glycemic levels. Also, the gastrointestinal adverse effects usually observed with the subcutaneous or oral administration of GLP-1 and its analogs used in clinical practice are absent with this inhaled formulation (338).

Aerovance is a biopharmaceutical company that is also exploiting the potential of biopharmaceuticals' inhalation to treat local diseases. Presently, two DPI are at phase II clinical studies for the treatment of asthma (pitrakinra) and cystic fibrosis and COPD (bikunin). Pitrakinra is a recombinant human interleukin 4(IL-4) variant that efficiently inhibits both IL-4 and interleukin 13 (IL-13) activity, reducing the inflammation in asthma and eczema (339, 340). At the first studies both liquid and powder formulations were tested, but the last news available are related to a DPI (Aerovant®) formulation to treat exacerbations in patients with eosinophilic asthma. Bikunin is a truncated human SPINT2 serine protease inhibitor that presents the capacity to reduce the airway epithelial sodium ion channels activity, thereby reducing sodium hyper absorption in cystic fibrosis patients and COPD (341). Is currently under development with the name Aerolytic® and Pulmolytic®.

Inhalable proteins to treat viral infections have also been proposed. DAS181 is a recombinant sialidase fusion protein that inactivates viral receptors on the cells of the human respiratory tract, thus preventing and treating infection by various influenza virus subtypes, including H5N1, and parainfluenza (342-344). In a phase II clinical trial, DAS181 was able to reduce the lung viral load in patients infected with influenza B, H3N2 and H1N1 without significant side effects (342). DAS181 was formulated using TOSAP® technology into dry powder microspheres for pulmonary delivery (Fludase®).

In Table 1.5 are presented examples of formulations and products proposed for inhalation of therapeutic peptides and proteins that are currently in clinical trials.

Table 1.5 Formulations for pulmonary administration of therapeutic peptides and proteins ongoing clinical trials.

Peptide/protein	Therapeutic indication	Name/System	Inhalation mode	Clinical phase	Reference
Bikunin	Cystic fibrosis and COPD	Aerolytic and Pulmolytic	Nebulizer and DPI	phase II	(345)
CsA	Lung transplant rejection	Liquid solution	Nebulizer	phase III	(346)
CsA	Lung transplant rejection	Sugar-based particles	DPI	phase 0	(347)
DAS181	Influenza virus infection	Fludase/TOSAP	DPI	phase II	(342)
GLP-1	Diabetes mellitus	MKC253/Technosphere	DPI	phase I	(338)
INF-γ	Cystic fibrosis, lung infection	Liquid solution	Nebulizer	phase II	(348, 349)
Insulin	Diabetes mellitus	Aerodose/liquid solution	Nebulizer	phase II	(350, 351)
Insulin	Diabetes mellitus	Dry crystals	pMDI	phase II	(352)
Insulin	Diabetes mellitus	QDose	DPI	phase I	(353)
Insulin	Diabetes mellitus	Alveair/liquid solution	Nebulizer	phase I	(238)
Insulin	Diabetes mellitus	BioAir/pegylated calcium phosphate nanoparticles	DPI	phase I	(354)
Insulin	Diabetes mellitus	ProMaxx/microspheres	DPI	phase I	(355)
IL-2	Metastatic or unresectable solid tumors	Liquid solution	Nebulizer	phase I	(356)
Pitrakinra	Asthma	Aerovant	DPI	phase II	(340)

Peptide/protein	Therapeutic indication	Name/System	Inhalation mode	Clinical phase	Reference
Sargramostin	Metastatic cancer, sarcoma	Liquid solution	Nebulizer	phase II	(357)
α_1-antitrypsin	Cystic fibrosis	Liquid solution	Nebulizer	phase I	(358)

COPD – Chronic obstructive pulmonary disease; CsA – Cyclosporin A; DPI – Dry powder inhaler; GLP-1 – Glucagon-like peptide 1; INF- γ – Interferon-γ; IL-2 – Interleukin 2; pMDI – Pressurized metered-dose inhaler.

A variety of formulations for inhalation of therapeutic peptides and proteins have been developed at preclinical stage. Some examples include calcitonin (359-361), parathyroid hormone (362), detirelix (363, 364), erythropoietin (262), interferon-α (INF-α) (365), follicle-stimulating hormone (366), glucagon (367), among others.

4.1. The new era of pulmonary administration: nanomedicine-based formulations

Driven by the progresses in the nanomedicine field, many researchers have consolidated the concept of pulmonary delivery of drugs using nanoDDS by developing innovative formulations with improved biopharmaceutical features (23, 368). For example, mucoadhesive (369) and mucus-penetrating particulates (370, 371) showed to increase the residence time of drugs into the lungs and improve their absorption and/or therapeutic efficacy. The last approach could have great impact in the pulmonary delivery of drugs to treat diseases with high mucus production like cystic fibrosis (372, 373). Preliminary results are promising and it is expected that the clinical relevance of such products could be proven in clinical trials (19, 84, 240). In this context, a new door has been opened in the field of inhalation therapy and new advances could be expected in the near future. Still, several issues such as large scale production, batch-to-batch reproducibility, variable lung deposition pattern, or cost- effectiveness balance of the treatment need to be addressed and optimized in order to ensure the bench-to-bedside translation of inhalatory nanoDDS.

4.1.1. Lipid-based formulations

From the lipid-based nanoDDS for inhalation, liposomes appear as the preference of researchers owing to its interaction with endogenous surfactant phospholipids, promoting an increased retention of drugs in the lungs. Furthermore, the use of phospholipids similar to the surfactant promotes the absorption of the incorporated drugs, although the mechanism underlying the permeation enhancing is not yet clear (34).

As discussed above, insulin is the most studied protein for pulmonary delivery. Several formulations containing nanocarriers have been developed for pulmonary delivery of insulin in order to overcome the problems associated with conventional formulations (238, 319). Huang and co-workers produced liposomes using the membrane destabilization/dialysis method with an average diameter of 200 nm and encapsulation efficiency of 52% (335). *In vivo* studies demonstrate a homogeneous deposition of liposomes in alveoli with reduction of systemic levels of glucose and absence of immunoreaction of lung tissue (335). In another study, the liposomes obtained using the reverse phase evaporation technique possessing an average diameter of 295 nm and an encapsulation efficiency of 43%, were subjected to spray congealing before solvent evaporation (336). The formulation proved to be stable after three months of storage, promoting a decrease in systemic levels of glucose for 12 hours when compared with solutions for pulmonary administration of insulin and subcutaneous injection (336). Chono and co-workers produced liposomes containing different derivatives of phosphatidylcholine by hydration of lipid film technique (337). *In vivo* studies using rats as an animal model showed a greater reduction of serum glucose after intratracheal administration of insulin encapsulated in liposomes as compared to insulin solution. However, this reduction was only significant for liposomes containing the derivative dipalmitoylphosphatidylcholine. In this study it was also assessed the influence of the size of liposomes in the absorption of insulin. There was a greater reduction in levels of plasma glucose and increased serum insulin after administration of liposomes with an average diameter of 100 nm. In the case of liposomes of 1000 nm, it was observed an increased retention by macrophages. *In vitro* tests performed in cell cultures of Calu-3 showed the existence of an absorption promoting effect of liposomes, possibly by opening of tight junctions (337).

Leuprolide, also called leuprorrelin, is a highly hydrophilic luteinizing-hormone-releasing hormone (LHRH) agonist peptide with a MW of 1.2 kDa, used in treatment of prostate cancer, endometriosis, and precocious puberty (374). In order to develop a DPI for pulmonary administration of leuprolide, Shahiwala and co-workers produced liposomes by reverse phase

evaporation technique followed by lyophilization (374). The diameter of the aggregates of liposomes obtained lies within the limits compatible with alveolar deposition of particles from 3.5 to 4.3 μm possessing high encapsulation efficiency (66-72%). After intratracheal instillation in rats, liposomes promoted higher serum luteinizing hormone levels than the solution of leuprolide and an increased $t_{1/2}$ when compared to solutions for pulmonary and subcutaneous administration. However, the bioavailability of liposomes was only 50% compared with subcutaneous injection and it is necessary to change the formulation in order to increase the bioavailability of leuprolide (374).

Liposomal inhaled cyclosporin A (CsA) to treat rejection of lung transplants was also proposed.. Pulmonary administration to dogs resulted in higher concentration of CsA in the lungs instead of the liver, kidneys, spleen, heart and blood compartment. However, three hours after administration, there was some accumulation of CsA in the kidney and spleen, so the effects on the kidney should be studied (375). In another study, pulmonary delivery of liposome-encapsulated CsA promoted an accumulation of CsA in the lungs. The formulation was stable after nebulization and maintains the immunosuppressive activity of CsA after encapsulation (376). Gilbert and co-workers administered liposomal CsA by inhalation to healthy humans and found a preferential deposition of the particles in the alveolar region (70% of inhaled dose) (377). When the formulation was administered via a mouth-only face mask for 45 minutes, no changes were observed in pulmonary function. In contrast, the administration using a nebulizer mouthpiece has proved troublesome, leading to coughing and throat irritation and a slight decrease in lung function. This may be due to the fact of particles, when administered by a nebulizer mouthpiece suffer greater impaction in the throat. The observed differences do not appear to be due to the formulation, because in both cases were used the same formula, with the same particle size at the same dose (377).

In an *in vivo* study conducted by Khanna and co-workers in healthy dogs, the pulmonary administration of interleukin 2 (IL-2)-loaded liposomes led to an activation of the immune response by a significant increase in leukocyte levels in the lung and serum mononuclear cells (378). This response was more efficient compared to inhaled free IL-2. The observed differences may be due to increased cellular uptake or decreased clearance of liposomal IL-2. *In vitro* studies showed that activation of pulmonary leukocytes leads to inhibition of proliferation of tumor cells (378). Another study of the same researchers conducted in dogs with primary lung carcinoma or lung metastasis of other carcinomas, has shown that there is no significant toxicity associated with pulmonary administration of liposomal IL-2 (379). It was also found that liposomal Il-2 stimulates the immune system after inhalation. Moreover, in

some animals it was observed the complete regression of metastasis and the non-progression of primary lung carcinoma in another animal. Most significantly results were observed in treating pulmonary metastasis from osteosarcoma (379). In a phase I clinical trial, the pulmonary delivery of liposomes containing IL-2 to patients with various carcinomas affecting the lungs (pulmonary sarcoma, renal cell carcinoma, melanoma and metastatic osteosarcoma) was well tolerated and there was no significant toxicity observed at doses that may possess therapeutic effect (380). However, in this study it was not determined the clinical efficacy of the formulation. In another phase I clinical trial was studied the utility of inhaled lipossomal IL-2 in patients with common variable immunodeficiency (381). IL-2 retained its biological activity after encapsulation. No changes were observed in pulmonary function or significant side effects during treatment. Although the patients treated with IL-2 liposome declare sense of improving their condition was not detected alterations of the immune response within the blood compartment. Such lack of response evidence may be due to low specificity of the markers used in the study (381).

Superoxide dismutase (SOD) is an antioxidant enzyme, kidnapper of free radicals, ubiquitous in mammalian cells. It causes a decrease of reactive oxygen species responsible for oxidative stress, involved in phenomena such as carcinogenesis, inflammation and neurodegeneration (382). Studies demonstrate the success of the use of SOD in the treatment of rheumatoid arthritis and ischemia-reperfusion injury. However, after intravenous and oral administration, the SOD has a reduced circulation $t_{1/2}$ and a high-level gastrointestinal degradation, respectively. With the aim of developing a non-invasive formulation that promotes an increased $t_{1/2}$ of SOD, Kaipel and co-workers produced liposomes for pulmonary administration (382). *In vivo* studies conducted in pigs showed a prolonged release of SOD into the systemic circulation and an increase in its $t_{1/2}$. There were no side effects such as irritation or inflammation in the lung, as well as changes in pH and plasmatic O_2 and CO_2 pressure (382).

Different liposomal formulations were developed for aerosol delivery of a cationic α-helical peptide called CM3 with antimicrobial and antiendotoxin activity (383). The pulmonary delivery of CM3 allows the treatment of local infections and reduction of systemic effects. Of the several formulations developed, the best results in terms of the encapsulation and nebulization efficiencies and maintenance of liposomal integrity during nebulization were achieved with the combination of dimyristoyl phosphatidylcholine and dimyristoyl phosphatidylglycerol with a 3:1 molar ratio. With this formulation liposomes with diameter of 262 nm were obtained, presenting an encapsulation efficiency of 73%. Using a mathematical

model it was possible to predict the deposition profile and distribution in lungs of liposomes in adults and children of different ages. Data showed a pulmonary deposition in the all lungs, particularly in the tracheobronchial region. In this region, the minimum inhibitory levels of CM3 can be reached in the adult model, and can be exceeded in pediatric model subjects (383).

SLN have been proposed for pulmonary administration of insulin. Examples are the nanoparticles of lecithin obtained by emulsification method with an average diameter of 300 nm, and alveolar deposition of 45% (w/w) of the dose delivered after lyophilization. It was confirmed the retention of the primary, secondary and tertiary structure of insulin after processing (322). In another study, Liu and co-workers produced SLN containing micelles inside by double emulsion with an average diameter 115 nm and an encapsulation efficiency of 98% (329). *In vitro* studies showed prolonged release of insulin. It was also demonstrated to retain the integrity of insulin after encapsulation and stability of the formulation after 6 months of preparation at 4 °C (329).

4.1.2. Polymeric nanoparticles

A variety of polymeric nanocarriers have been explored for the pulmonary administration of proteins. A study compared six different types of nanocarriers composed by gelatin, chitosan, alginate, PLGA, poly(D,L-lactide-co-glycolic acid)-chitosan (PLGA-chitosan), and Poly(D,L-lactide-co-glycolide)-b-poly(ethylene glycol) (PLGA-PEG), as DDS for inhalation of proteins using bovine serum albumin (BSA) and erythropoietin as model proteins (384). Excepting those of PLGA-PEG and alginate, particles presented a mean diameter lower than 300 nm. Gelatin and PLGA nanoparticles presented the best *in vitro* cytocompatibility and uptake by human type I alveolar epithelial cells. Additional in vivo studies in rats, showed that inhalation of these systems led to the release and retention of the proteins in lung tissue up to 10 days (384). Thus, these systems could be explored for the pulmonary administration of proteins with local therapeutic activity. In another study, powders for inhalation based on poly(glycerol adipate-co-ω-pentadecalactone) (PGA-co-PDL) nanoparticles co-spray with L-leucine were assessed (385). Powder presenting high FPF (> 75%) and a MMAD compatible to deep lung deposition (1.21 ± 0.67 μm) had shown to be compatible with pulmonary cell lines (A549 and 16HBE14o-). Also, the primary and secondary structure of the encapsulated BSA was maintained (385). The same research group developed a similar system based on poly(ethylene glycol)-co-poly(glycerol adipate-co-ω-pentadecalactone) (PEG-co-(PGA-co-

PDL)) for pulmonary administration of α-chymotrypsin and DNase I. The obtained powders maintain the activity of both enzymes and presented characteristics compatible with good lung deposition after inhalation (386).

Inhalation of insulin encapsulated in polymeric nanoDDS has also been proposed. Huang and co-workers have developed nanoparticles of low MW chitosan using the emulsification/solvent evaporation technique (330). The resulting particles have a spherical shape with average diameter of approximately 400 nm, zeta potential of about +42 mV and encapsulation efficiency of 96%. The release profile of insulin was characterized by a burst effect followed by prolonged release for 24 hours. When administered to diabetic rats, the formulation has demonstrated a hypoglycemic effect similar to subcutaneous administration of insulin solution but prolonged in time (330). In a series of studies, Grenha and co-workers produced chitosan nanoparticles with and without lipid coating obtained by ionic gelation and then spray-dried to obtain nanocomposites. The nanoparticles obtained had an average diameter between 380 and 450 nm and encapsulation efficiency between 65 and 81%, while the spray-dried powder particles a d_{ae} of 2.5 – 2.8 µm (34, 272, 333). *In vitro* studies demonstrate a rapid release of insulin in the case of lipid nanoparticles without coating and a prolonged release in formulation containing lipid coating (34, 333). Additionally, formulations showed to be compatible with the epithelial respiratory A549 and Calu-3 cell lines (296). *In vivo* studies in rats show that after intratracheal administration, uncoated lipid nanoparticles reach the alveolar region and promote a greater reduction of systemic levels of glucose, compared to insulin solution (272, 387). Kawashima and co-workers obtained PLGA nanoparticles with average diameter of 400 nm, and alveolar deposition of 75% (w/w) using the modified emulsification/solvent evaporation method (332). *In vitro* dissolution tests showed an insulin release profile characterized by an initial burst effect followed by extended release. *In vivo* studies show a significant reduction in systemic levels of glucose which lasts for a period exceeding 48 hours, compared with an aqueous solution of insulin for inhalation (332). This biphasic release of insulin can mimic the marketed injectable insulin mixtures of short and long duration of action. In another study, PLGA nanoparticles were produced using the emulsification/solvent evaporation technique followed by granulation (331). *In vitro* and *in vivo* showed an alveolar deposition of approximately 45% (w/w) of emitted dose and pharmacological effect of prolonged over 12 hours when compared with solutions of insulin administered intratracheally and intravenously (331). Poly(n-butyl cyanoacrylate) (PBCA)/dextran nanoparticles obtained by Zhang and co-workers using the in situ polymerization method have a diameter of 255 nm and an encapsulation efficiency of 79%

(334). *In vitro* assays demonstrate an insulin release profile characterized by an initial burst effect followed by prolonged release. *In vivo* studies are characterized by a prolonged therapeutic effect over time when compared to insulin solution administered intratracheally and a bioavailability of 57% compared with subcutaneous administration (334).

PLGA nanoparticles coated with chitosan obtained by the emulsion and solvent diffusion technique have been proposed to administer calcitonin by pulmonary route (388). Due to the mucoadhesion promoted by chitosan, coated nanoparticles were eliminated more slowly from the lung compared to those not coated. Moreover, the opening of tight junctions also promoted by chitosan led to an increased absorption of calcitonin and a decreased in *in vivo* systemic levels of calcium (388). The pharmacological effect was prolonged for 24 hours after inhalation. The particles with a diameter of 650 nm and were nebulized with success and the release profile of calcitonin is characterized by a burst effect followed by prolonged release over time (388). Based in the previous study and to enjoy the advantages of solid calcitonin formulations for inhalation over the liquid ones (389), chitosan-modified PLGA nanocomposites were produced by spray drying fluidized bed granulation (Agglomaster®) and dry powder coating technique (Mechanofusion®) (390). Powders obtained with the Agglomaster® showed improved redispersibility of powders in liquid media and higher *in vivo* lung retention and hypocalcemic effect, which could be explained by the lower strong aggregation of particles using the spray drying fluidized bed granulation technique (390). Chitosan nanoparticles co-sprayed with mannitol as powders for inhalation of calcitonin were also proposed by other research group, presenting appropriate aerodynamic properties and good absorption to the systemic circulation after pulmonary administration to rats (391).

5. State-of-art of micelles as drug delivery systems by inhalation

In the last two decades, pulmonary administration of nanoDDS has been a growing topic of interest among researchers (278, 384, 392). However, micelles as platforms for inhalation of drugs have been poorly explored. Numerous examples of liposomes intended for inhalation have been proposed over the years presenting good results (393, 394), with at least two formulations enrolling clinical trials Arikace® (Insmed at phase I/II) (395) and Pulmaquin® (Aradigm at phase III) (396). Since polymeric micelles presented advantages over liposomes, like higher stability and high capacity of solubilization of hydrophobic drugs, as described before, they possess the potential for pulmonary delivery of drugs. Additionally, the capacity demonstrated by some micelles to overcome multidrug resistance (56, 397) and enhance the

transfection of genetic material to cells (130), make them promising vehicles for local delivery of anticancer drugs to treat lung cancer, and genetic material to target cells. Also, the small size of micelles confers them the opportunity to escape easily from phagocytosis by alveolar macrophages and allow the delivery and absorption of drugs with systemic action through an epithelium with high surface area and reduced enzymatic activity. Thus, the feasibility of micelles as DDS for pulmonary administration of drugs has been explored in the last years with some studies reviewed in this section. Taking into account the results so far, is expected an increase in the upcoming years of the studies using formulations based on polymeric micelles as inhaled DDS. As referred before, a careful and detailed assessment of the safety of such formulations should be performed, especially in the case of the ones expected to be chronically administered.

5.1. Lipid-polymer micelles

As referred previously, lipid-polymer micelles are composed by polymers conjugated with phospholipids or long-chain fatty acids. Several combinations of polymers and lipids/phospholipids have been tested for the preparation and application of micelles. Chitosan oligosaccharide-stearic acid (CSO-SA) micelles were developed by Gilani and co-workers, for the pulmonary administration of amphotericin B (AmB) to treat invasive pulmonary fungal infections in some patients receiving immune suppressive treatments (108). Local administration avoids the systemic side effects of AmB and improves their bioavailability (398). After encapsulation into micelles, AmB presented the same antifungal activity of Fungizone® but lower toxicity (108), a phenomenon intimately related to its aggregation state (399). The micelles possessed positive charges with mean diameters between 100-250 nm, and were efficiently nebulized using an Air-jet nebulizer to particles with FPF up to 52%, making them suitable for pulmonary delivery of AmB (108). The same research group developed chitosan-stearic acid micelles encapsulating itraconazole for pulmonary delivery (400). Positively charged micelles with mean diameters inferior to 200 nm were efficiently and stably nebulized presenting FPF up to 48%. The antifungal activity of itraconazole against *C. albicans*, *A. fumegatus*, and *A. niger* was maintained after its encapsulation into micelles (400). Thus, the solubilization of hydrophobic itraconazole into polymeric micelles could be an effective approach to deliver the drugs by inhalation in order to treat pulmonary fungal infections.

Different research groups have been studying the administration of drugs to treat tuberculosis using polymeric micelles. Stearic acid-branched polyethyleneimine (SA-BPEI) micelles encapsulating rifampicin were spray-dried and powders with a drug content of 48%, a MMAD lower than 2.5 µm, and FPF of 67% obtained. Moreover, micelles showed *in vitro* biocompatibility up to 75 µg/mL concentration and taken up by THP-1 cells differentiated to macrophages (401). Thus this system could be explored to target alveolar macrophages, the reservoir of *Mycobacterium tuberculosis*. Methoxy poly(ethylene oxide)-b-distearoyl phosphatidyl-ethanolamine (mPEG–DSPE) micelles where also proposed as carriers for rifampicin, although its therapeutic efficacy was not assessed (60). Rifampicin was entrapped with high encapsulation efficiency into these micelles that sustained its release over 3 days *in vitro*. Formulations presented a fraction of fine particles of approximately 40% after nebulization (60).

The potential of 1,2-distearoyl-sn-glycero-3-phosphoethanolamine-N-methoxy(poly(ethylene glycol)) (DSPE-PEG) as pulmonary DDS was evaluated. Paclitaxel was successfully encapsulated in DSPE-PEG micelles with an encapsulation efficiency of 95% and was slowly released in simulated surfactant lung fluid, reaching 90% of drug release after 8 hours. Additionally, micelles showed to be stable in water during 3 months of storage. After intratracheal administration of paclitaxel-loaded micelles in rats, the lung concentration of paclitaxel was significantly higher as compared to intravenous administration of micelles and intratracheal administration of Taxol®. While paclitaxel is mainly accumulated in organs such liver and spleen and rapidly cleared from lungs after intravenous administration of micelles and intratracheal administration of Taxol®, respectively, around 50% of the paclitaxel concentration remains in lungs 12 hours after intratracheal administration of paclitaxel-loaded micelles. These results show that pulmonary administration of paclitaxel leave to low systemic exposure, resulting in localized chemotherapy to the lungs and avoiding the unwanted side effects to other tissues (402). In another study, inhaled DSPE-PEG micelles of 16 nm in size encapsulating doxorubicin showed higher accumulation in the lungs and lower distribution in non-target organs compared to its intravenous administration (403). These results reinforce the usefulness of local administration of anticancer drugs through inhalation to treat lung cancer. In addition, micelles showed a strongest tendency to be accumulated to the lungs for the longer periods of time compared to mesoporous silica nanoparticles, dendrimers, and quantum dots (403), demonstrating the feasibility of micelles as nanoDDS for inhalations of drugs.

DSPE-PEG micelles have also been proposed for pulmonary delivery of anti-inflammatory drugs like beclomethasone dipropionate (404, 405) or budesonide (406). Gaber and co-workers developed micelles of 22 nm diameter and a high encapsulation efficiency (> 96%) presenting a sustained release profile and a FPF suitable for pulmonary delivery, with lower deposition of particles in the throat (404). In another study DSPE-PEG was conjugated with α,β-poly(N-2-hydroxyethyl)-DL-aspartamide (PHEA) in order to further improve the pulmonary delivery of corticosteroids to treat bronchial inflammatory diseases (407). Beclomethasone dipropionate was efficiently encapsulated in 1,2-distearoyl-sn-glycero-3-phosphoethanolamine-N-methoxy(poly(ethylene glycol))-α,β-poly(N-2-hydroxyethyl)-DL-aspartamide (DSPE-PEG-PHEA) micelles presenting a sustained release *in vitro* with less than 30% of the drug being released after 48 hours. The obtained micelles showed to be biocompatible with human bronchial epithelial cells (16HBE14o-) and enhanced the drug uptake by the same cell line after 48 hours of incubation (407).

Due to its cationic nature, chitosan can be complexed with negatively charged DNA and be used as non-viral vector for gene therapy. Hu and co-workers synthesized CSO-SA in order to produce polymeric micelles to delivery pEGFP-C1 (408). The CSO-SA/DNA micelles efficiently protected the condensed DNA from enzymatic degradation by DNase I, presented lower cytotoxicity and comparable transfection efficiency in A549 cells compared to Lipofectamine® 2000 (408), making these micelles a promising gene delivery system in the treatment of pulmonary diseases. The same research group developed CSO-SA micelles for the delivery of drugs like paclitaxel (107) or doxorubicin (106, 409). The encapsulation of doxorubicin in CSO-SA micelles resulted in higher uptake and accumulation by A549 cells and a decreasing in the half maximal inhibitory concentration (IC_{50}) value (45). Although the promising results, the feasibility of such formulations as inhaled or intravenous delivery systems needs to be confirmed with *in vivo* studies.

5.2. Copolymer-based micelles

As referred previously, besides the use of lipids as hydrophobic segment of polymeric micelles, is possible to produce this kind of micelles with amphiphilic copolymers composed by segments with different water affinity nature, being ones hydrophilic and others hydrophobic.

Laouini and co-workers developed different systems, namely polymeric micelles, liposomes, SLN and nano-emulsions, intended for pulmonary administration of vitamin E and assess their aerodynamic properties using different techniques (410). PEG-b-PCL micelles of 154 nm in size, low PdI (0.09) and high AE (87.4%) (411), presented a d_{ae} of 5.8 µm and a FPF of 29% as determined by laser diffraction analysis of the nebulized micelles dispersion (410). On the other hand, a MMAD of 3.2 µm and a FPF of 78% were obtained when the formulations were assessed by cascade impaction. Additionally, an *in silico* prediction of the aerodynamic behavior of nebulized micelles using the multiple-path particle dosimetry, resulted in ~52% of lung deposition (410). These results evidence the importance of multiple technique assessment of the aerodynamic properties of inhaled formulations, in order to better predict its *in vivo* behavior. The incorporation of a hydrazone bond between the PEG and PCL blocks allowed the development of pH-sensitive micelles (411), that could be explored for the targeting of drugs to cancer or inflammation tissues.

As referred previously, polymeric micelles have been proposed as platforms for the inhalation of antitubercular drugs. Wu and co-workers synthesized and characterized polylactide-chitosan (PLA-chitosan) copolymers with different molar ratios for delivery of rifampicin (412). As polylactide (PLA) molar ratio increased, the micelle size and drug-loading content increased with a decreasing in rifampicin release rate (412). In another study, enantiomeric poly(ethylene glycol)–polylactic acid (PEG-PLA) stereocomplex micelles composed by a equimolar mixture of enantiomeric poly(ethylene glycol)–poly(l-lactide) (PEG-PLLA) and poly(ethylene glycol)–poly(d-lactide) (PEG-PDLA) were developed to sustained release of rifampicin (413). The stereocomplex micelles presented lower CMC and mean diameter, higher stability in water and encapsulation efficiency than those observed with the single enantiomeric micelles. *In vitro* drug delivery release was characterized by an initial burst release followed by a sustained release until 48 hours (413). Silva and co-workers evaluated the feasibility of poly(ethylene glycol)-poly(aspartic acid) (PEG-Pasp) micelles as delivery system for tuberculostatic agents. The conjugation of isoniazid and pyrazinamide with PEG-Pasp improved the activity against *Mycobacterium tuberculosis* by reducing the minimal inhibitory concentration (MIC) of the drug (58, 414). Poly(ε-caprolactone)-b-poly(ethylene glycol)-b-poly(ε-caprolactone) (PCL-PEG-PCL) micelles surface modified with chitosan and galatomannan were also proposed as nanoDDS for delivery of rifampicin. The presence of galatomannan increased the uptake by macrophages, being these micelles proposed for improved therapy of tuberculosis by targeting alveolar macrophages (18).

For the treatment of fungal infections, in a 12 days study in mice, the inhalation of itraconazole:polysorbate 80:F127 nanostructured aggregates triggered higher lung concentrations and lung-to-serum ratios of itraconazole, improved survival of infected animals while decreasing toxicity compared with orally administered itraconazole formulations (415-418). No signs of lung inflammation or changes in pulmonary histology were detected (419). It is worth stressing that a lower drug dose was required to achieve lung and serum therapeutic levels using inhaled formulation comparing to oral administration (416).

Liu and co-workers developed an tri-block copolymer consisting of Poly(epsilon-caprolactone)-b-chitooligosaccharide-b-poly(ethylene glycol) (PCL-b-COS-b-PEG) for delivery of doxorubicin (420). The obtained polymer presents the capacity to form micelles with encapsulation efficiency of doxorubicin close to 50%. Genipin post-crosslinking did not affect the macroscopic characteristics of the micelles but delayed the *in vitro* release of doxorubicin from the micellar reservoir (420). Similar results were obtained by Chen and co-workers using chitosan-poly(ε-caprolactone)-poly(ethylene glycol) to encapsulate paclitaxel and rutin with glutaraldehyde post-crosslinking (44). In another study, Kontoyianni and co-workers synthesized a new type of amphiphilic polymer based on the PEGylation of a hyperbranched aliphatic polyester (BH40-PEG polymer) (421). The polymer produces micelles presenting 20 nm of mean diameter that could encapsulate paclitaxel. Paclitaxel water solubility significantly increased after encapsulation into micelles, and the polymer showed to be non-toxic to A549 cells up to a concentration of 1.75 mg/mL, while the median lethal dose (LD_{50}) was 3.5 mg/mL (421). The obtained results make these systems promising for administration of anticancer agents, however, further studies are required in order to assess their feasibility as inhaled drug delivery systems.

Besides the conventional chemotherapy, it is possible resort to photodynamic therapy (PDT) to treat lung cancer. PDT consists in the administration of photosensitizer agents that generate reactive oxygen species after activation of the system by light exposure at the targeted tissues. Pluronic L122 was used by Yang and co-workers to encapsulate hematoporphyrin for pulmonary delivery. Micelles with 98% of encapsulation efficiency exhibited higher cellular uptake and cytotoxicity against A549 cells as compared to the free drug. In addition, micelles were efficiently incorporated into lactose microparticles with ~2 μm by spray-drying, making the system a suitable DPI for pulmonary administration (422).

Gene therapy aiming to treat pulmonary pathologies was also explored. An amphiphilic polyethylenimine (PEI) derivative was synthesized by Roesler and co-workers (423). Although PEI is one of the most effective polycations for gene delivery due to is high-density

charge, it presents short $t_{1/2}$ and systemic cytotoxicity due to adherence to cell membranes and aggregation with blood components. PEGylation of PEI reduces their cytotoxicity and improves their stability. In addition, the micelles produced efficiently condensed the DNA and presented higher transfection efficiency of PEI/DNA complexes after intratracheally instillation in mice (423). Chao and co-workers study the feasibility of PEG-PPO-PEG micelles as inhaled gene delivery systems (424). DNA was efficiently encapsulated into micelles and their degradation by DNase I was delayed. Significant gene expression in mice lungs was detected 48 hours after the inhalation of DNA-micelles co-formulated with 10% ethanol as permeation enhancer. After 6 doses, gene expression was also detected in other tissues such trachea, stomach and duodenum (424).

Chapter 2

Aims and Goals

Recent advances in biotechnology and genetic engineering have resulted in the promotion of peptides and proteins as an important class of therapeutic agents. Despite the emergence of several peptides and proteins with therapeutic potential, their administration in the active conformation has been shown to be an enormous challenge for the pharmaceutical industry. There are several limitations that are imposed as low bioavailability, physical or chemical instability and side effects (425). Currently, due to instability and reduced permeability of proteins through biomembranes, the parenteral route is the most used for the administration of such drugs. However, this is an invasive route, which can lead to a reduced acceptance by patients and, consequently, increased costs of therapy, especially when is required a prolonged or chronic treatment (215, 216). Alternative routes for administration of proteins have been the focus of many research groups, being respiratory system receiving special attention due to its physiological characteristics (19). Several formulations for inhalation of peptides and proteins are currently under development and in clinical trials. Some of them showed positive results. However, conventional formulations have some limitations, namely reduced bioavailability (215, 322).

Polymers such as gums, cellulose derivatives, acrylates or PVP have been used from decades in the development of conventional DDS, in order to control the release pattern of drugs from the polymeric matrix (170, 426). With the advent of new technologies applied to health, namely nanomedicine, and the progresses seen in chemical and surface engineering, new and improved polymers have been produced and the older ones have gained new functionalities (7). Controlling the size and molecular architecture of polymers is possible to obtain formulations with distinct properties. The incorporation or conjugation of therapeutic or imaging agents with polymers modifies their pharmacokinetics and pharmacodynamics (127, 426, 427). Characteristics of drugs such as hydrophilicity, release and degradation profile,

stability, transport across biological membranes, plasma circulation time, and biodistribution can be tailored to specific needs (428, 429). In addition, recent DDS have been designed as responsive and recognitive systems that can target drugs to specific sites and deliver them in response to a stimulus (35, 430). Among polymers, those possessing amphiphilic properties have been rediscovered in the last years and used in the development of intelligent and advanced systems in the field of nanomedicine (79, 431).

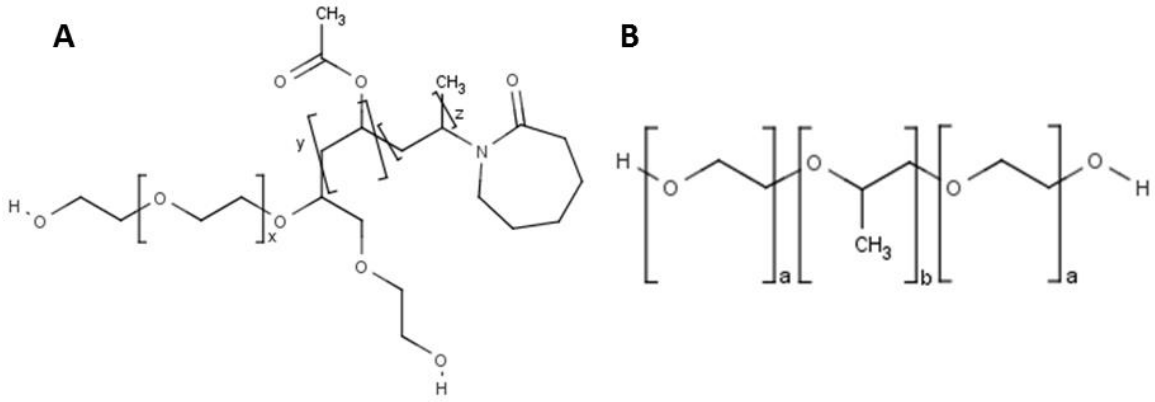

Figure 2.1 General structure of Soluplus® (A) and Pluronic® (B).

In this thesis we explore the utility of amphiphilic polymers in the development of solid formulations for pulmonary administration of proteins, using insulin as model drug. The system comprised polymeric micelles composed by polyvinyl caprolactam-polyvinyl acetate-poly(ethylene glycol) graft copolymer (Soluplus® (SOL), Figure 2.1) or PEG-PPO-PEG (Pluronic® F68 (F68), Pluronic® F108 (F108), and Pluronic® F127 (F127)) (Figure 2.1 and Table 2.1) in which insulin was encapsulated.

Table 2.1 Poly(ethylene glycol) (a) and polypropylene oxide (b) units of the different Pluronic® used (according to the manufacturer).

Type of Pluronic®	a	b
F68	80	27
F108	141	44
F127	101	56

The main objectives undertaken on the present thesis were:

i) Develop polymeric micelles as delivery systems for insulin, as model therapeutic protein. Different polymers, production conditions and polymer:protein ratio were tested;

ii) Explore the possibility of develop stimuli-sensitive formulations. For that, PBA was added to the system, since boronic acid derivatives have been proposed as excipients to control the release of insulin from formulations as response to glucose concentration;

iii) Develop solid formulations presenting appropriate characteristics for inhalation. Lyophilization was used as technique for the production of nanocomposites based on polymeric micelles and its effect on the conformation of insulin evaluated;

iv) Assess the biological efficiency and biocompatibility of formulations. Pulmonary cell lines and macrophages were used to study the toxicity, pulmonary permeability and phagocytosis of formulations;

v) Evaluate the *in vivo* efficacy and safety of the insulin-loaded polymeric micelles. Thereunto, powders were administered by intratracheal instillation to diabetic murine models.

Chapter 3

Design and characterization of self-assembled micelles for insulin delivery

The information presented in this chapter was partially published in the following publication:

Fernanda Andrade, Pedro Fonte, Mireia Oliva, Mafalda Videira, Domingos Ferreira, Bruno Sarmento, Solid state formulations composed by amphiphilic polymers for delivery of proteins: characterization and stability, International Journal of Pharmaceutics, 2015, 486:195-206

1. Introduction

In the last decades, the use of polymers in the development of drug delivery systems has gained a new breath as consequence of the progresses seen in the fields of polymer engineering and nanotechnology applied to health. Among them, amphiphilic polymers have emerged as platforms for advanced delivery of a variety of drugs (41). A multitude of monomers and polymers can be conjugated in order to obtain amphiphilic polymers with modulated characteristics (136). The most commonly used are poloxamers, triblock copolymers of polyoxyethylene and polyoxypropylene, commercially known as Pluronic® (164). However, PLGA-PEG, poly(ethylene glycol)-b-poly(ε-caprolactone) (PEG-b-PCL) as well as their derivatives (18, 127) are also commonly used.

Nanotechnology-based delivery systems have been explored to solve the drawbacks of conventional formulations such as instability and degradation, reduced permeation through biomembranes and bioavailability (25, 428). Polymeric micelles are spherical shape nano-sized structures composed by amphiphilic polymers or polymers conjugated with lipids that are suitable as drug delivery systems. The inner core of micelles presents the capacity to encapsulate hydrophobic drugs, while the shell can associate the hydrophilic ones (79). Due to its small size, micelles generally escape from the reticulo-endothelial system, presenting higher bloodstream circulation time (40). Also, some studies suggest the capacity of polymeric micelles to inhibit the drug efflux mechanisms and consequently multidrug resistance (113, 397). In addition, as liposomes, the surface of polymeric micelles can be easily tailored with specific ligands for targeted delivery (141). Nevertheless, micelles present the advantage of being more stable than liposomes (63). The versatility of micelles explains why they have been proposed as vehicles for solubilization and delivery of a variety of drugs like doxorubicin (119), paclitaxel (66, 68), rifampicin (18), calcitonin (59), CsA (124) among others, being some formulations in clinical trials (66, 68).

Due to the development noted in the biotechnology field, biopharmaceuticals have emerged as an alternative to conventional drugs in the treatment of many diseases. Since the commercialization of insulin obtained by biotechnology processes in 1982, biopharmaceuticals have gained an increased share in the global pharmaceutical market (207). Despite their well-known therapeutic efficacy, the major drawback of biopharmaceutical drugs is the difficulty of administration via non-invasive routes in their active conformation. Among the different non-invasive routes of administration, inhalation appears as a promise one due to the physiological characteristics of lungs and airways resulting in higher

bioavailability than for other non-invasive routes (213). In addition, inhalation of insulin presented better therapeutic results when compared to the oral administration. As a result, an insulin-based formulation (Exubera®) achieved market authorization from FDA and EMA. However, the product was withdrawn due to commercial and financial reasons, being also reported cases of adverse effects and lung cancer after the use of this product (238). More recently, FDA approved a new and improved powder formulation for insulin inhalation (Afrezza®).

In this chapter the production of micelles with characteristics appropriated to pulmonary delivery and the association of insulin to the system was explored.

2. Experimental

2.1. Materials

SOL, F68, F108 and F127 were kindly provided by BASF (Ludwigshafen, Germany). Lyophilized human insulin, PBA and phosphate buffer saline pH 7.4 (PBS) were purchased from Sigma-Aldrich (St. Louis, MO, USA). The other reagents used were methanol and ethanol absolute from analytical grade; acetonitrile and trifluoroacetic acid (TFA) from high-performance liquid chromatography (HPLC) grade (Merck, Germany) and Type 1 ultrapure water (18.2 MΩ.cm at 25 ºC, Milli-Q®, Billerica, MA, USA).

2.2. Production of micelles

Micelles were prepared using the thin-film hydration technique. Briefly, each polymer was individually weight and dissolved in methanol or a mixture of methanol:ethanol (1:1). Then, the solvent was removed under vacuum and the film was left to dry overnight at room-temperature to eliminate any remained solvent. The film was then hydrated with Type I ultrapure water or PBS at 37 ºC in order to obtain a 1 % (w/v) solution and vortexed for 5 min. The obtained dispersion was filtered through a 0.22 µm syringe filter to remove possible dust and aggregates. PBA containing micelles were prepared by dissolving PBA with the polymers in the solvents prior to the production of the film at a ratio of 10:1 (polymer:PBA). Insulin formulations were prepared by adding different amounts of insulin in the form of solution in PBS during the film hydration, to obtain polymer:insulin ratios ranging from 10:0.1 to 10:1

(w/w). The other steps were the same as for plain formulations. After preparation, the pH of all formulations was measured, ranging between 6.1 and 7.1.

2.3. Determination of size, zeta potential, association efficiency, and osmolality of formulations

Particle mean hydrodynamic diameter and polydispersity index (PdI) were measured without previous sample dilution by dynamic light scattering (DLS) at both 25 °C and 37 °C using a detection angle of 173° and zeta potential by laser doppler micro-electrophoresis using a NanoZS (Malvern Instruments, UK). For each type of formulation were produced and analyzed at least three replicates. The osmolality of formulations was determined at room temperature using a Micro-Osmometer M3320 (Advanced Instruments, Inc., MA, USA). Triplicates of each formulation were analyzed.

AE, i.e. the amount of insulin associated with the micelles, and the LC, i.e. the mass percentage of insulin of the total mass of the particles was calculated according to the Equation 3.1 and 3.2, respectively. The free insulin in filtrate was recovered after filtration of the formulations by centrifugation for 10 min at 10,000 rpm at 37 ºC, using a 30k pore filter (Nanosep® Centrifugal Devices, Pall Corporation, Spain). A previously validated HPLC method was used to quantify the insulin (432). Briefly, the mobile phase consists of acetonitrile:0.1% (v/v) TFA aqueous solution initially set to a ratio of 30:70 (v/v), which was linearly changed to 40:60 (v/v) over 5 min. From 5 to 10 min the ratio was kept constant at 40:60 (v/v). The mobile phase was pumped at a constant flow rate of 1 ml/min, the injection volume was 20 µl and the detection wavelength used was 214 nm. The HPLC (UltiMate® 3000 UHPLC+ focused, Dionex, USA) system was equipped with a Purospher® STAR RP-18e (5µm) LiChroCART® 250-4.6 (Merck, Germany) and a LiChrospher® 100 RP-18 (5 µm) LiChroCART® 4-4 guard column (Merck, Germany). All experiments were performed at 20 ºC and the total area of the peak was used to quantify insulin. For each type of formulation were analyzed at least three replicates.

$$AE = \frac{\text{total amount of insulin} - \text{free insulin in filtrate}}{\text{total amount of insulin}} \times 100 \qquad \textbf{Equation 3.1}$$

$$LC = \frac{\text{total amount of insulin} - \text{free insulin in filtrate}}{\text{total weight of micelles}} \times 100 \qquad \textbf{Equation 3.2}$$

2.4. Morphological characterization of micelles

Different microscopic techniques, namely atomic force microscopy (AFM), field emission scanning electron microscopy (FE-SEM) and transmission electron microscopy (TEM), were used to characterize the morphology of the micelles.

AFM imaging was performed using a MultiMode VIII microscope (Bruker AXS Inc., Madison, WI, USA) with a NanoScope V controller (Veeco Instruments Inc., Plainview, NY, USA). One drop of formulation was placed on top of freshly cleaved highly oriented pyrolytic graphite and left for 15 min before being removed and replaced with PBS, with no drying step in between. Analysis was conducted under fluid tapping mode using sharp silicon tips on nitride levers (model SLN-10 A, Bruker AFM Probes) with pyramidal shape and nominal tip radius of 2 nm and nominal spring constant 0.35 $N.m^{-1}$.

For FE-SEM performed in a Hitachi H-4100FE (Hitachi Ltd., Tokyo, Japan), a drop of formulation was placed on top of freshly cleaved highly oriented pyrolytic graphite and dried in a desiccator overnight prior to carbon coating.

Regarding TEM, samples were placed on a grid, treated with uranil acetate and then observed in a JEM-1400 Transmission Electron Microscope (JEOL Ltd., Tokyo, Japan).

2.5. Statistical analysis

One-way ANOVA was used to investigate the differences between formulations. Post hoc comparisons were performed according to Tukey's HSD test ($p<0.05$ was accepted as significant different) using Prism 6.02 software (GraphPad Software, Inc., CA, USA).

3. Results

3.1. Size, surface charge and association efficiency of micelles

For the production of micelles, a first screening with different combinations of polymers (SOL, F68, F108 and F127) evaporation solvents, namely methanol and a mixture of methanol and ethanol (1:1), and hydration solvent (H_2O or PBS) were tested and the characteristics of the micelles are presented in Table 3.1. No significant differences were observed in respect to the evaporation and hydration solvents used. Thus, in order to control the pH of formulations

and reduce the percentage of methanol used, the combination of methanol:ethanol (1:1) and PBS was chosen for further studies. Also, a filtration step after the hydration of the polymeric film was added to the production protocol to eliminate the aggregates observed for Pluronic®-based micelles.

Table 3.1 Mean hydrodynamic diameter, polydispersity index (PdI) and zeta potential of micelles produced with different evaporation and hydration solvents. Samples were analyzed at 25 ºC. The results are expressed as mean values ± SD, n≥3.

Polymer	Evaporation Solvent	Hydration Solvent	Hydrodynamic Diameter (nm)	PdI	Zeta Potential (mV)
SOL	Methanol	H_2O	53.6±11.4	0.031±0.007	-4.9±15.1
		PBS	43.0±1.9	0.063±0.042	-7.8±8.3
	Methanol: Ethanol	H_2O	50.4±2.5	0.022±0.001	-2.7±1.0
		PBS	50.9±6.6	0.038±0.015	-8.9±11.3
F68	Methanol	H_2O	56.4±20.8	0.566±0.161	-5.7±7.4
		PBS	337.9±219.5	0.364±0.060	-9.2±2.1
	Methanol: Ethanol	H_2O	148.3±39.1	0.203±0.036	-20.1±4.7
		PBS	87.0±21.6	0.294±0.122	-4.3±4.8
F108	Methanol	H_2O	417.1±98.3	0.279±0.387	-22.5±22.9
		PBS	400.8±312.2	0.680±0.267	-2.3±2.3
	Methanol: Ethanol	H_2O	550.6±268.0	0.406±0.029	-16.9±30.9
		PBS	455.6±105.3	0.345±0.148	0.2±3.6
F127	Methanol	H_2O	283.6±112.7	0.144±0.081	-2.6±2.5
		PBS	165.1±118.2	0.360±0.100	-4.2±3.4
	Methanol: Ethanol	H_2O	268.4±159.1	0.254±0.308	-9.1±22.0
		PBS	131.6±76.3	0.356±0.070	-1.9±6.2

The results regarding the characterization of the selected micelles in terms of size and surface charge are presented in Figure 3.1. Empty micelles of SOL presented a mean hydrodynamic diameter of 55.10 ± 7.72 nm and 288.80 ± 37.35 nm, and a PdI of 0.026 ± 0.015 and 0.298 ±0.115 at 25 ºC and 37 ºC, respectively, showing a clear temperature dependence behavior ($p<0.05$). The incorporation of insulin at different ratios up to 10:1 reduced the size of micelles although no statistical differences were observed ($p>0.05$). In the

same way, the incorporation of PBA to micelles did not produce significant differences compared to the plain micelles ($p>0.05$). All micelles presented higher mean diameters and PdI at 37 ºC compared to 25 ºC ($p<0.05$). Regarding the surface charge, particles showed negative zeta potential values near zero without significant differences among formulations ($p>0.05$).

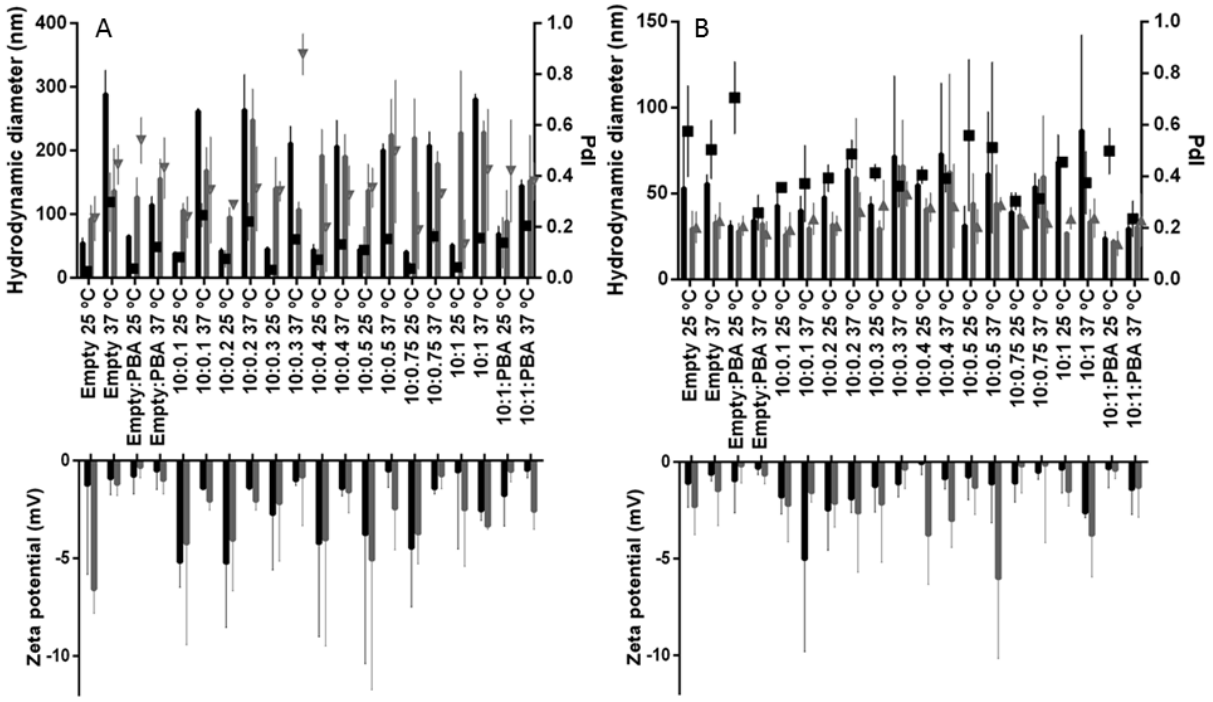

Figure 3.1 Mean hydrodynamic diameter, polydispersity index (PdI) and zeta potential of SOL (black bars and squares) (A), F68 (grey bars and triangles) (A), F108 (black bars and squares) (B) and F127 (grey bars and triangles) (B) empty micelles, containing just PBA micelles (empty:PBA), insulin-loaded micelles with different polymer:insulin ratio (10:0.1, 10:0.2, 10:0.3, 10:0.4, 10:0.5, 10:0.75 and 10:1) and insulin-loaded containing PBA micelles with 10:1 polymer:insulin ratio (10:1:PBA) after production (mean ± SD, n≥3).

Pluronic®-based micelles presented different results depending of the polymer used. The mean diameter and PdI of empty micelles at 25 ºC was 92.47 ± 21.46 nm and 0.233 ± 0.087 for F68; 53.19 ± 29.91 nm and 0.575 ± 0.176 for F108; and 29.54 ± 10.09 nm and 0.202 ± 0.060 for F127. At 37 ºC the micelles were somewhat larger in size, presenting higher polydispersity, being the differences not significant ($p>0.05$) for the majority of formulations. The incorporation of insulin up to 10:1 increased the diameter of micelles prepared by F68 ($p<0.05$), and did not promote significant changes in micelles prepared by F108 and F127

(p>0.05). On the other hand, the incorporation of PBA did not significantly alter the characteristics of F68, F108 and F127 micelles (p>0.05). Pluronic®-based micelles also presented a surface charge slightly negative and close to neutrality without significant differences among the formulations (p>0.05).

Micelles composed by 10:1 polymer:insulin ratio were chosen to proceed with the production and characterization, since they showed to possess similar values of size, PdI and surface charge of the ones containing lower insulin payloads.

The AE and LC were determined for micelles with a polymer:insulin ratio of 10:1. As seen in Table 3.2, excepting for F68, all the formulations presented an AE higher than 80% and LC of at least 7%. The presence of PBA didn´t affect the values of AE and LC (p>0.05).

Table 3.2 Association efficiency (AE), loading capacity (LC) and osmolality of the different insulin-loaded formulations. Results are presented as mean values ± SD (n≥3).

Sample	AE (%)	LC (%)	Osmolality (mOsm/Kg)
SOL:Ins	94.63±3.24	8.60±0.29	397±15
SOL:Ins:PBA	84.03±5.14	7.31±0.45	402±6
F68:Ins	76.22±14.56	6.93±1.32	325±12
F68:Ins:PBA	49.31±36.80	5.60±3.13	314±9
F108:Ins	87.28±11.57	7.93±1.05	316±10
F108:Ins:PBA	87.63±3.63	7.62±0.32	330±14
F127:Ins	80.90±14.92	7.35±1.36	325±18
F127:Ins:PBA	83.15±10.05	7.23±0.87	322±10

The osmolality of formulations was superior to 300 mOsm/Kg, being SOL-based samples similar between them (p>0.05) and different from the Pluronic®-based micelles (p<0.05). No differences were observed between the different Pluronic®-based formulations (p>0.05).

3.2. Morphological characterization

The morphology of micelles was analyzed with different microscopy techniques. FE-SEM images are presented in Figure 3.2, while TEM images presented in Figure 3.3 and 3.4, and AFM images depicted in Figure 3.5 and 3.6. All the microscopy techniques used showed that the micelles of the different polymers are mainly spherical in shape.

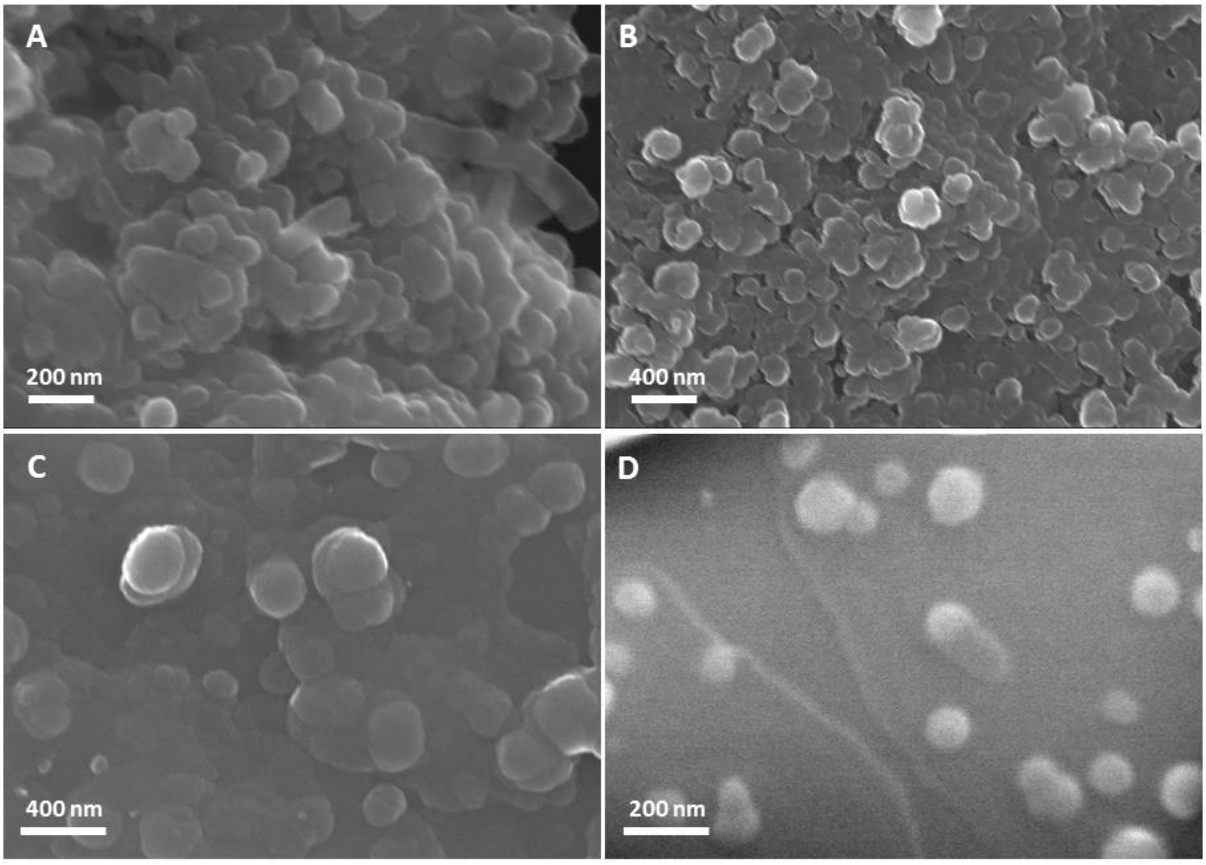

Figure 3.2 FE-SEM micrographs of SOL (A), F68 (B), F108 (C) and F127 (D) insulin-loaded micelles.

It also revealed the presence of some aggregates of smaller particles. FE-SEM analysis revealed a higher degree of aggregation compared to TEM and AFM due to the dried state of samples during the analysis. No visible differences between empty, insulin-loaded micelles and micelles containing PBA were observed.

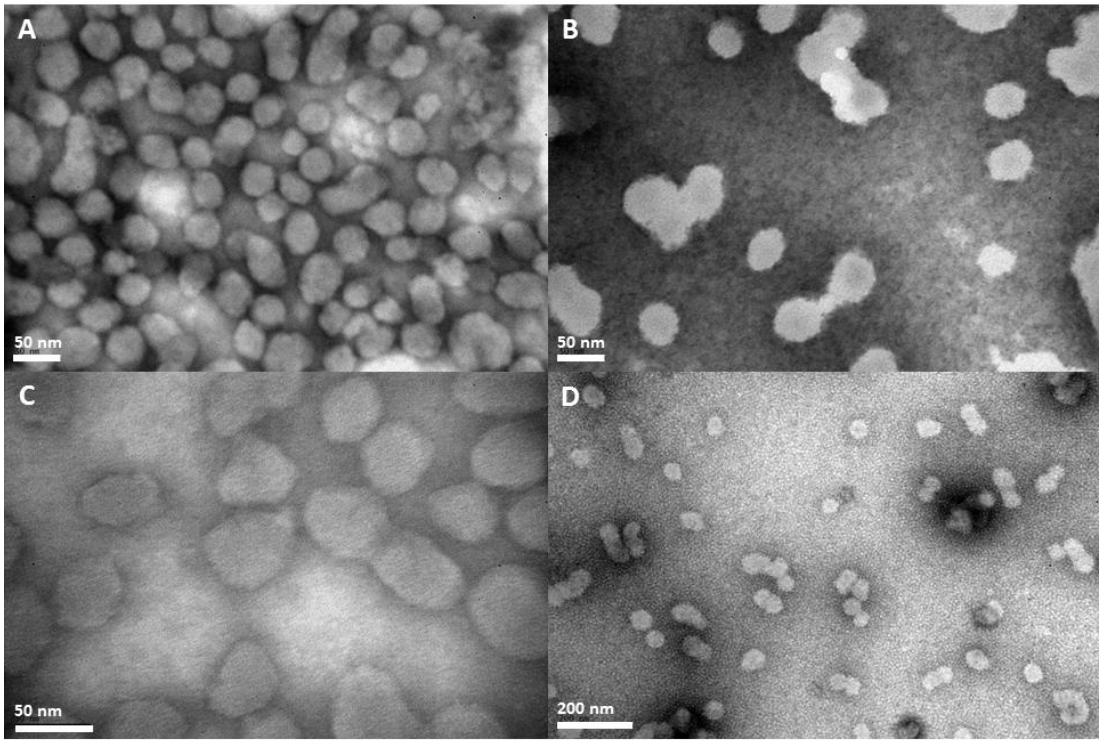

Figure 3.3 TEM images of SOL (A-C) and F68 (B-D) empty micelles (A-B) and insulin-loaded micelles (C-D).

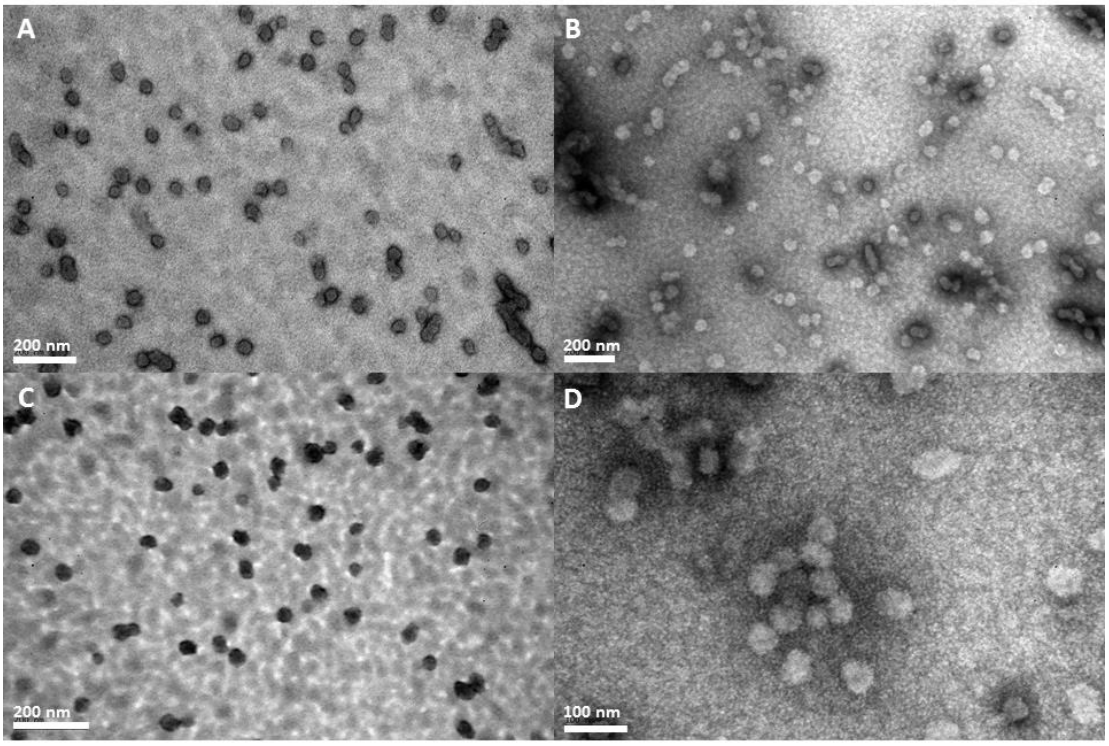

Figure 3.4 TEM images of F108 (A-C) and F127 (B-D) empty micelles (A-B) and insulin-loaded micelles (C-D).

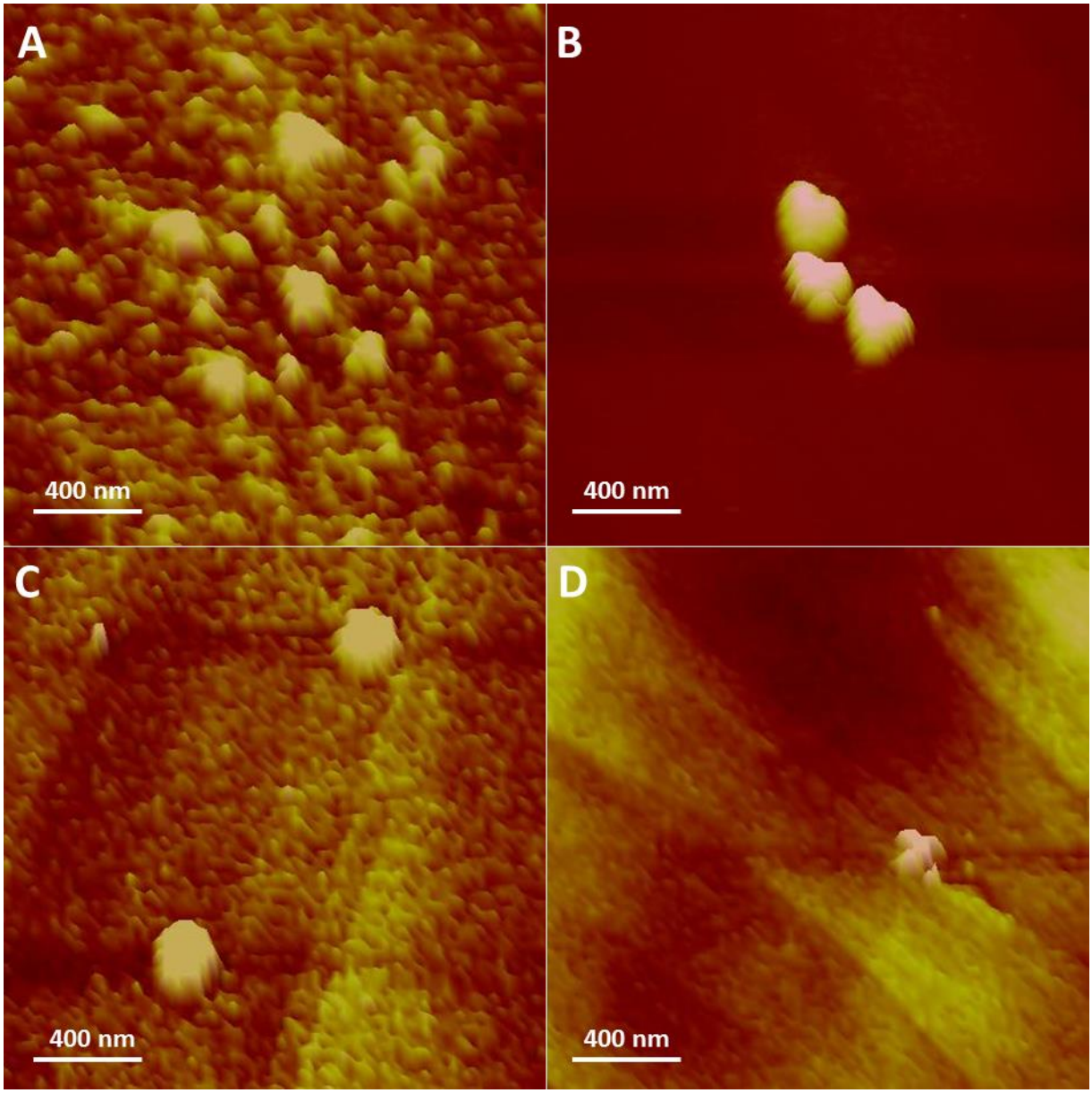

Figure 3.5 AFM images of SOL (A-B) and F68 (C-D) insulin-loaded micelles (A-C) and insulin-loaded micelles containing PBA (B-D).

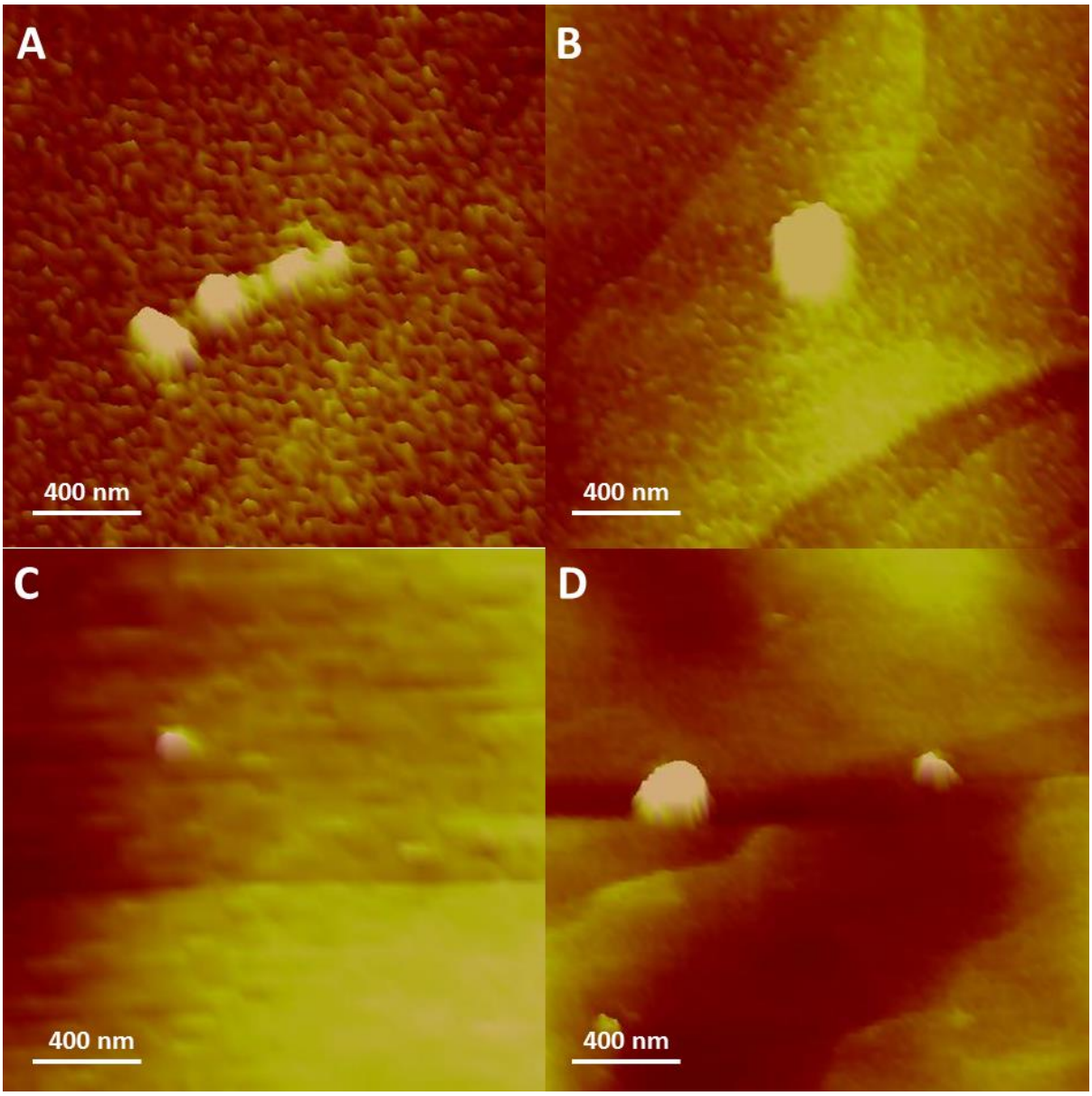

Figure 3.6 AFM images of F108 (A-B) and F127 (C-D) insulin-loaded micelles (A-C) and insulin-loaded micelles containing PBA (B-D).

4. Discussion

This study aimed to develop nanoformulations for the pulmonary administration of insulin, based on polymeric micelles. Different polymers with amphiphilic nature were tested namely SOL, F68, F08 and F127. The MW and CMC values of the polymers are summarized in Table 3.3. Although SOL possesses higher MW, is the one that present lower CMC value, which could be explained by the lower percentage of hydrophilic content: 13% of PEG against

the ~70% in F127, and ~80% in F68 and F108. For Pluronic® copolymers, F127 possess the higher number PPO units and lower percentage of PEG and, consequently, lower CMC and hydrophilic-lipophilic balance (HLB), whereas F68 presents the smaller number of PPO units and higher CMC.

Table 3.3 Molecular weight (MW) and critical micelle concentration (CMC) values of the polymers used (according to the manufacturer).

Type of polymer	Average MW of the polymer (g/mol)	CMC (M)	Approximate MW of PEG chains (g/mol)
Pluronic® F68	7,680 – 9,510	$4.8x10^{-4}$	4000
Pluronic® F108	12,700 – 17,400	$2.2x10^{-5}$	7000
Pluronic® F127	9,840 – 14,600	$2.8x10^{-6}$	5000
Soluplus®	90,000 – 140,000	$6.4x10^{-8}$	6000

In these work, PBA was added to micelles to provide them with glucose-sensitive properties. Boronic acid derivatives have been proposed as excipients to control the release of drugs, including insulin, from formulations as response to glucose concentration (433-436). Neutral boronic moieties convert to anionic boronate esters upon reaction with the diol group of sugars, increasing the hydrophilicity of the system. Many hydrogels containing boronic acid derivatives have been shown to swallow and release insulin as response to the increase in the hydrophilicity (433). At pH of 7.4, PBA (pKa ~9) will present predominantly neutral moieties to react with glucose and is expected that the differences in hydrophilicity of the micelles as a response to the glucose concentration, may control the release of insulin.

Micelles were produced using the thin-film hydration technique, previously described for the production of both liposomes and micelles (164, 437). The organic solvents generally used to prepare the films are chloroform and dichloromethane. However, according to the guideline from International Conference on Harmonization (ICH) “Impurities: Guideline for Residual Solvents Q3C (R5)”, the use of these solvents (class 2) in the production of pharmaceutical products should be limited due to its toxicity. The permitted daily exposure (PDE) and residual concentration limit are 0.6 mg/day and 60 ppm for chloroform and 6.0 mg/day and 600 ppm for dichloromethane, respectively (438). In order to substitute these solvents, ethanol was proposed since it is a class 3 solvent, with low toxic potential. Unfortunately, the polymers showed to be insoluble in pure ethanol, but soluble in ethanol:methanol (1:1)

mixture and methanol alone. By that methanol, a class 2 solvent with higher PDE (30 mg/day) and residual concentration limits (3000 ppm) compared to chloroform and dichloromethane (438) was used to prepare the films in pure form or as a mixture with ethanol.

Since particles produced using methanol presented similar mean hydrodynamic diameter and PdI values of those prepared using the methanol:ethanol mixture (Table 3.1), the mixture of solvents was selected. This decision was related to the objective of reduce the amount of class 2 solvents used in the production of particles. Also, similar results were obtained when water (Table 3.1) or PBS were used to produce empty micelles. For this reason, and in order to have a higher control in the pH of formulations, PBS was used to produce the insulin-loaded micelles.

Micellization of amphiphilic polymers in aqueous solution occurs at concentrations higher than the CMC, and since is an entropic process, namely for Pluronic®, is favored at temperatures higher than the CMT at a fixed concentration. As the CMT values of 1 wt. % solutions of F68, F108 and F127 are 54-56.21 ºC, 30-34.55 ºC (439) and 24 ºC (440), respectively, it was decided to hydrate the films with solutions at 37 ºC. This body temperature, although lower than the CMT of F68, is expected to favor the micellization of the polymers without promote significant loss of insulin conformation.

Two different temperatures, 25 and 37 ºC, were selected for the determination of the hydrodynamic diameter of particles, with the objective of study the influence of temperature in the characteristics of micelles and also to determine its size at body temperature. The obtained micelles presented different hydrodynamic diameters and PdI, according to the polymer used (Figure 3.1). The size of micelles composed by Pluronic® seems to be directly related to the CMC and CMT values of the copolymer used, since F127 presented the lower CMC and CMT values and the smaller micelles, whereas F68 presented the higher CMC and CMT values and micelles bigger in size. As the temperature increase above the CMT, Pluronic® copolymers tend to present a reduced surface tension and be more hydrophobic, aggregating with the consequent formation of micelles. Both 25 ºC and 37 ºC are above the CMT of F127, explaining its small size of micelles. Also, the small changes observed when the temperature increase from 25 ºC to 37 ºC can be explained by the effect of small concentrations of NaCl (presented in the PBS at 0.14 M) in reducing the influence of temperature in the size of F127 micelles (441). In the case of F108, is possible to observe a slightly increase in mean hydrodynamic diameter and reduction in PdI from 25 ºC to 37 ºC, as a consequence of the aggregation of unimers with small size and the formation of higher amount of micelles or aggregates as the temperature goes above the CMT. For F68, since

both 25 ºC and 37 ºC are below its CMT value and is the polymer that presents higher surface tension and lower viscosity when in solution, the system will be composed by unimers, aggregates and some micelles less hydrophobic, and consequently, less compact than the ones obtained by the other two copolymers used, resulting in micelles of higher size and PdI. Although the presence of salts such NaCl is known to reduce the CMT values of many Pluronic® copolymers, the effect of the NaCl concentration used is not enough to decrease the CMT values of F68 below 37 ºC, since a reduction of 20 ºC in CMT is observed only for NaCl concentrations of 1 M (442). The mean hydrodynamic diameters obtained for F108 and F127-based micelles were in agreement of those described by others (10-100 nm) (178, 443). The high PdI values observed are related to the fact that above CMC and CMT both unimers and micelles co-exist at different percentages since both values are the mean of a range of values, due to the copolymer polydispersity and the existence of some diblocks copolymers in the composition of the final product (441, 444).

SOL is a recently commercial available polymer that has been proposed as enhancer of the aqueous solubility of hydrophobic drugs in solid dispersions (161). Due to its amphiphilic nature it was studied its usefulness in the development of micelles to deliver proteins. To our knowledge these is the first work regarding the use of SOL as vehicle for biopharmaceutical drugs. SOL produces micelles of small and uniform size at 25 ºC, as seen by the low PdI values (Figure 3.1). At 37 ºC is possible to observe an increase in the opacity of formulations accompanied by an increase in the size and polydispersity of micelles, which is due to a reduction in the viscosity of the polymer with the temperature increase. However, the PdI values still remain lower than the ones observed for Pluronic®-based micelles, which is explained by the low CMC and high glass transition temperature of SOL (around 70 ºC as determined by DSC, Figure 4.2, *Chapter 4*), resulting in more compact and stable particles even at body temperature.

The different polymers produced micelles with surface charge close to neutrality. The near neutral charge is expected since is well documented by many authors that PEG confers hydrophilic and neutral charge to particles when at its surface (190, 445). Also, the polymers used do not present major ionic species at the work pH, as estimated *in silico* using the Marvin Suite software (ChemAxon, Hungary). The hydrophilic surface of particles confers them stealth properties, predicting that they should not suffer significant uptake by alveolar macrophages after inhalation (190). In addition, PEGylation of particles was reported to increase the retention and bioavailability of inhaled drugs in lungs by promoting their uptake by alveolar type II cells and increasing its penetration through surfactant and mucus layer

(371, 446). The high observed standard deviation of zeta potential values could be consequence of the difficulty on the equipment in determines neutral charges with precision.

Excepting for F68-based micelles, all the formulations presented high AE values (>80%) (Table 3.1). The smaller MW of F68 and the less compact micelles can be the reason to its lower capacity to load the protein between the PEG chains. In addition the protein presented at the surface of the micelles, as evidenced by XPS (Table 4.2, *Chapter 4*), can be easily released during the filtration by centrifugation step used to determine both AE and LC. Some anionic moieties of PBA could be competing with insulin for the spaces in the PEG shell, resulting in a reduced protein association and loading capacity in PBA-containing formulations.

The osmolality values of formulations were slightly hyper-osmolal with blood plasma, although within the range of tolerable values for inhaled formulations (447), thus, no changes on the osmolality of lung fluids derived from inhalation of these formulations are expected.

Microscopic imaging of micelles (Figure 3.2 – 3.6) showed general spherical shape and demonstrated that, mainly for Pluronic®-based formulations, some bigger particles are, in fact, aggregates of smaller ones, which can results is values of mean hydrodynamic diameters determined by DLS bigger than the reality. Also, this aggregation, in addition to the co-existence of unimers and micelles already referred, explains the high PdI values observed. Micelles composed by SOL presented a uniform size and lower polydispersity, which is in accordance with the values of PdI from DLS measurements. FE-SEM images showed higher aggregation of particles owing to the drying overnight step used in the preparation of samples prior to analysis (Figure 3.2). Since TEM and AFM images were taken using liquid samples, they are more appropriate to conclude about the aggregation of micelles.

5. Conclusions

Polymeric micelles containing insulin composed with different amphiphilic polymers were prepared using thin film hydration technique. The incorporation of PBA and insulin up to a polymer:protein ratio of 10:1 didn't affect the size of micelles. Neutral charged and spherical micelles with sizes in general smaller than 200 nm were obtained. In addition, high association of insulin to the system and osmolalities compatible with pulmonary administration were achieved. These interesting characteristics triggered further development and characterization of formulations for insulin inhalation.

Chapter 4

Micelle-based nanocomposites as solid formulations for pulmonary insulin delivery: design and characterization

The information presented in this chapter was partially published in the following publications:

Fernanda Andrade, Pedro Fonte, Mireia Oliva, Mafalda Videira, Domingos Ferreira, Bruno Sarmento, Solid state formulations composed by amphiphilic polymers for delivery of proteins: characterization and stability, International Journal of Pharmaceutics, 2015, 486:195-206

Fernanda Andrade, José das Neves, Petra Gener, Simó Schwartz Jr, Domingos Ferreira, Mireia Oliva, Bruno Sarmento, Biological assessment of self-assembled polymeric micelles for pulmonary administration of proteins, submitted for publication

Fernanda Andrade, Pedro Fonte, Ana Costa, Cassilda Cunha Reis, Rute Nunes, Carla Pereira, Domingos Ferreira, Mireia Oliva, Bruno Sarmento, In vivo pharmacological and toxicological assessment of self-assembled polymeric micelles as powders for inhalation of proteins, submitted for publication

1. Introduction

Inhalation of compounds has been performed since ancient cultures to treat diseases mainly affecting the respiratory system like asthma. However, a change in the paradigm is occurring and pulmonary administration of drugs with systemic action has been proposed (84, 448). Recently, a large extent of research has been performed regarding the development of formulations for inhalation and improved delivery devices, especially dry powder inhalers, due to their advantages over liquid formulations, namely long-term stability and patients convenience (449). The efficacy of an inhaled drug is dependent on its deposition pattern in the respiratory system, which is affected by several factors related to the properties of the formulation and the inhaler device, as well as physiologic characteristics of patients. Particles with a MMAD lower than 5 μm are assumed to deposit in the lungs and reach the alveoli if MMAD is below 3 μm, therefore becoming available to either exert a local effect or to undergo systemic absorption (275, 277, 449, 450). It was already demonstrated that the *in vitro* particle size and aerosolization profiles correlate in an acceptable way with *in vivo* lung deposition pattern (451), reason why the regulatory agencies require *in vitro* data regarding particle size distribution and aerosolization properties of the inhalable formulations before approval. Accordingly, FPF (particles < 5 μm), defined as the percentage of particles from the total emitted dose that are able to reach and deposit in the airways and deep lung, is used as an indicator for formulation efficiency. Compendial devices like the eight-stage Andersen non-viable Cascade Impactor are commonly used to assess the deposition profile of inhaled formulations.

In this chapter it is described the development and characterization of powders through the lyophilization of the insulin-loaded micelles described in the *Chapter 3*.

2. Experimental

2.1. Materials

SOL, F68, F108 and F127 were kindly provided by BASF (Ludwigshafen, Germany). Lyophilized human insulin, PBA, PBS, and D-glucose were purchased from Sigma-Aldrich (St. Louis, MO, USA). The other reagents used were acetonitrile and TFA from HPLC grade (Merck, Germany) and Type 1 ultrapure water (18.2 MΩ.cm at 25 ºC, Milli-Q®, Billerica, MA, USA).

2.2. Production of micelles and lyophilization

Micelles were prepared using the thin-film hydration technique. Briefly, each polymer was individually weight and dissolved in a mixture of methanol:ethanol (1:1). Then, the solvent was removed under vacuum and the film was left to dry overnight at room-temperature to eliminate any remained solvent. The film was then hydrated with PBS at 37 ºC in order to obtain a 1 % (w/v) solution and vortexed for 5 min. The obtained dispersion was filtered through a 0.22 µm syringe filter to remove possible dust and aggregates.

PBA containing micelles were prepared by dissolving PBA with the polymers in the solvents prior to the production of the film at a ratio of 10:1 (w/w) (polymer:PBA). Insulin-loaded micelles were prepared by hydrating the polymeric films with an insulin solution in PBS to obtain polymer:insulin ratios of 10:1 (w/w). The other steps were the same as for plain formulations.

After production micelles were lyophilized in an AdVantage 2.0 BenchTop Freeze Dryer (SP Scientific, Warminster, PA, USA). The cycle used was the follow: the samples were frozen at -30 ˚C and the temperature maintained for 60 min, the primary drying was set at 20 ˚C for 480 min at 150 mTorr and the secondary drying for another 480 min at 30 ˚C and 100 mTorr.

2.3. Determination of size and zeta potential of formulations

Particle mean hydrodynamic diameter and PdI was measured without dilution of the samples by DLS at both 25 °C and 37 °C using a detection angle of 173° and zeta potential by laser doppler micro-electrophoresis using a NanoZS (Malvern Instruments, UK). For each type of formulation were produced and analyzed at least three replicates.

2.4. Thermal analysis

The thermal behavior of the pure compounds, physical mixtures (1:1) and lyophilized formulations was assessed by DSC. Thermograms were obtained using a Shimadzu DSC-60 system (Shimadzu, Kyoto, Japan). 5 mg of each powder sample in an aluminum crimp was exposed to a controlled thermal treatment, specifically heated from 30 to 300ºC at a rate of 10ºC/min under constant purging of nitrogen at 40 mL/min, and the heat flow measured.

2.5. X-ray diffraction (XRD) experiments

Crystallization properties of powder samples were analyzed by XRD. Spectra were acquired using X'Pert PRO MPD θ/θ powder diffractometer of 240 mm of radius (PANalytical B.V., Almelo, Netherlands) in a configuration of convergent beam with a focalizing mirror and a transmission geometry. Samples were sandwiched between films of polyester of 3.6 µm of thickness and scanned at 45 kV, 40 mA using Cu $K\alpha_1$ radiation (λ = 1.5418 Å) at the range 2θ/θ scans from 2 to 60 º2θ with a step size of 0.026 º2θ and a measuring time of 400 s per step.

2.6. Raman spectroscopy

The micro-Raman spectra of powder formulations were acquired using dispersive high resolution micro Raman spectrometer (Jobin-Yvon LabRam HR 800) coupled with an optic microscope (Olympus BXFM) with a 50X objective. A laser of 532 nm wavelength and 2.5 mW of potency and a charge coupled device detector cooled at -70 ºC were used. The spectra were acquired and analyzed with the software LabSpec 5 (Horiba, Kyoto, Japan).

2.7. Surface analysis

The elemental composition of the surface of particles in powder state was analyzed by XPS. XPS experiments were performed in a PHI 5500 Multitechnique System (Physical Electronics, MN, USA) equipped with a monochromatic X-ray source (Aluminium Kalfa line of 1486.6 eV energy and 350 W), placed perpendicular to the analyzer axis and calibrated using the 3d5/2 line of Ag with a full width at half maximum of 0.8 eV. The analyzed area was a circle of 0.8 mm diameter, and the selected resolution for the survey spectra was 187.85 eV of pass energy and 0.8 eV/step. A low energy electron gun (less than 10 eV) was used in order to discharge the surface when necessary. All measurements were made in an ultra-high vacuum chamber with a pressure between $5x10^{-9}$ and $2x10^{-8}$ torr. The spectra were acquired, analyzed, and the atomic concentration of the elements quantified using the MultiPak 6 software (Physical Electronics, MN, USA).

2.8. Assessment of insulin conformation

FTIR and far-UV CD were used to analyze the conformation of insulin in the formulations in order to assess its stability after lyophilization.

Infrared spectroscopy analysis was conducted in a FTIR spectrometer ABB MB3000 (ABB, Switzerland) equipped with a deuterated triglycine sulphate detector and using a MIRacle single reflection horizontal attenuated total reflectance accessory (PIKE Technologies, USA) with a diamond/Se crystal plate. All spectra were acquired with 256 scans and 4 cm^{-1} resolution in the region of 4000–600 cm^{-1} using a triplicate set of samples and the related blank sample (raw polymer) after a background, and insulin spectra were obtained by a double subtraction procedure (452). After subtraction, spectra were derived using a 15 points Savitzky–Golay second-derivative and the amide I region (1590–1710 cm^{-1}) was selected. The spectra were baseline corrected using a 3–4 point adjustment and area-normalized. All spectra treatment was executed using the Horizon MB FTIR software (ABB, Switzerland). Quantitative comparison of the overall similarity of the FTIR spectra between native insulin and insulin-loaded micelles was assessed by using spectral correlation coefficient (SCC) and area of overlap (AO) algorithms (Origin software, OriginLab Corporation, MA, USA) (453).

The far-UV CD spectra were acquired using a Jasco J-815 spectropolarimeter (JASCO International Co., Ltd., Japan) at 20 ºC. In the far-UV region the spectra were recorded in a 1 cm cell from 250 to 190 nm, using a step size of 0.5 nm, a bandwidth of 1.5 nm and a speed of 50 nm/min with the lamp housing purged with nitrogen flow at 10 mL/min to remove oxygen. For all spectra and average of 5 scans was obtained. Appropriate references were used to subtract the signal of the polymers from the spectra of the protein-loaded. The mean residue ellipticity [θ] for insulin was calculated as the CD signal (θ) × mean residual weight (MRW) (116 Da for each insulin residue)/[10 × cell pathlength (cm) × insulin concentration (g/ml)] (454).

2.9. Scanning electron microscopy

The shape and morphology of lyophilized formulations was observed by scanning electron microscopy (SEM) on a FEI ESEM Quanta 200 (FEI, Hillsboro, USA). Samples were mounted onto metal stubs and coated with a carbon layer prior to observation.

2.10. Powder's particle size distribution and aerodynamic diameter

The geometrical particle size distribution of the 20 mg samples of lyophilized formulations was determined by laser diffraction using a Malvern Mastersizer 2000® laser diffractometer equipped with a dry sampling system (Scirocco® 2000, Malvern Instruments, UK) The powders were passed through a 840 µm sieve prior to analysis to eliminate possible aggregates.

The volume particle size distribution was characterized by $D_{0.1}$ (10% of the particles volume has a diameter below that value), $D_{0.5}$ also known as mass median diameter (50% of the particles volume has a diameter below that value), and $D_{0.9}$ (90% of the particles volume has a diameter below that value). Values presented are the average of at least three replicates.

The theoretical d_{ae}, Carr's index, and Hausner ratio were estimated from the geometrical particle size and tapped density (ρ, determined by tap density measurements) data according to Equation 4.1, 4.2, and 4.3, respectively.

$$\mathrm{dae} = D0.5\sqrt{\frac{\rho}{\rho o \chi}} \qquad \textbf{Equation 4.1}$$

where $D_{0.5}$ is assumed as geometrical mean diameter, ρ_0 is the reference density of a 1 g/cm^3 sphere, and χ is the dynamic shape factor.

$$\mathrm{Carr's\ index} = \frac{\text{tap density} - \text{bulk density}}{\text{tap density}} \times 100 \qquad \textbf{Equation 4.2}$$

$$\mathrm{Hausner\ ratio} = \frac{\text{tap density}}{\text{bulk density}} \qquad \textbf{Equation 4.3}$$

2.11. *In vitro* aerosolization and deposition properties

An eight-stage Andersen non-viable Cascade Impactor (ACI, Copley Scientific, UK) was used to determine the aerosolization and deposition properties of formulations *in vitro*. Hard gelatin nº 4 capsules were manually filled with the powder formulations sieved through a 300 µm sieve, and individually loaded into a Rotahaler® (GlaxoSmithKline, RTP, NC) inhaler device.

The experiments were performed at a flow rate of 28.3 L/min and four liters of air passed through the system, as recommended by European Pharmacopoeia (2.9.18. Preparations for inhalation: aerodynamic assessment of fine particles) (455). The stages were individually weighted and the FDF calculated as the amount of the particles deposited in stage 3 or lower in the cascade impactor (particles < 4.7 μm) as a percentage of the initial amount of particles. MMAD and geometrical standard deviation (GSD) were estimated through the cumulative masses of powder deposited in the impactor using a mathematic software (MMADcalculator) developed by Dr. Jay Holt (456). Each experiment was run in triplicate.

2.12. Insulin *in vitro* release study

Insulin-loaded micelles were dispersed in 10.0 mL of PBS with and without D-glucose (1.2 mmol/L) and incubated at 37°C under magnetic stirring. Samples of 0.5 mL were taken at predetermined time intervals of 15, 30, 45 min, 1, 2, 4, 6, 8 and 24 hours and replaced with fresh medium maintained at the same temperature. The collected samples were centrifuged for 10 min at 10,000 rpm and 37 ºC, using 100k pore filters (Nanosep® Centrifugal Devices, Pall Corporation, Spain) and insulin quantified by the HPLC methodology described in *Chapter 3*. All samples were run in triplicate.

The similarity factor (f_2) used for comparison of the different formulations was calculated according to the Equation 4.4.

$$f2 = 50 \times \log\left\{\left[1 + \left(\frac{1}{n}\right)\sum_{t=1}^{n}(Rt - Tt)\right]^{-0.5} \times 100\right\} \qquad \textbf{Equation 4.4}$$

where *n* is the number of time-points considered, and *Rt* and *Tt* are the percentage of insulin released at each time-point (*t*) for reference and test formulations, respectively. Insulin release profiles with values of f_2 between 50 and 100 were assumed to be similar (457).

2.13. Stability studies

In order to assess the stability of formulations, samples were stored in closed vials and in the dark at both 20 ºC and 4 ºC after production and lyophilization. At predetermined times (1, 3

and 6 months), formulations were characterized regarding mean hydrodynamic diameter and zeta potential after redispersion in liquid, and the insulin structure assessed by FTIR and far-UV CD as described previously.

2.14. Statistical analysis

One-way ANOVA was used to investigate the differences between the formulations and controls. Post hoc comparisons were performed according to Tukey's HSD test ($p<0.05$ was accepted as significant different) using Prism 6.02 software (GraphPad Software, Inc., CA, USA).

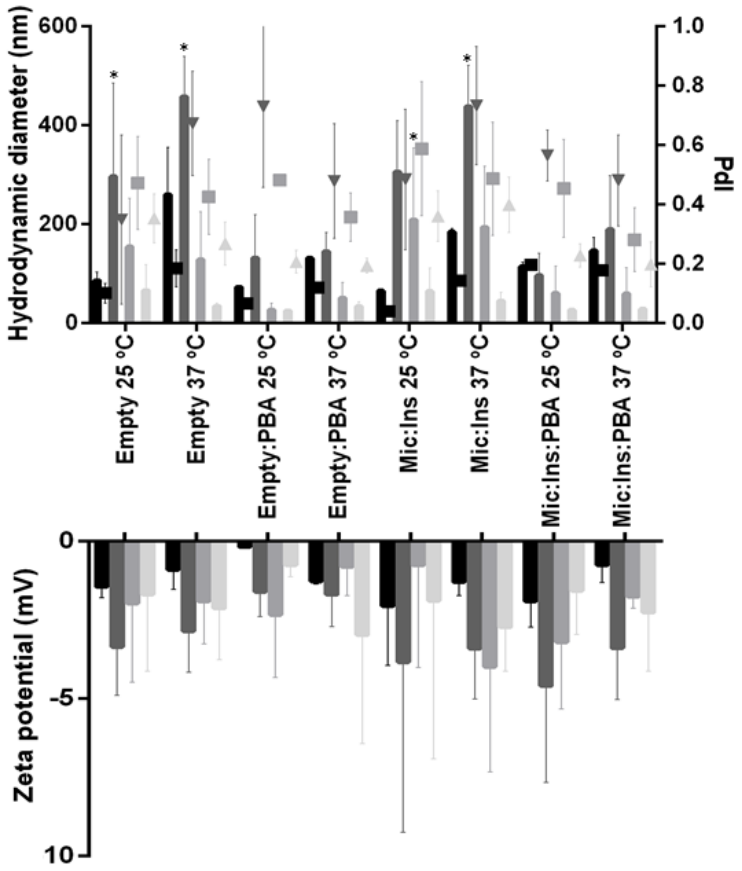

Figure 4.1 Mean hydrodynamic diameter, polydispersity index (PdI) and zeta potential of SOL (black bars and squares), F68 (dark grey bars and triangles), F108 (medium grey bars and squares) and F127 (light grey bars and triangles) based empty, containing just PBA (empty:PBA), insulin-loaded (Mic:Ins) and insulin-loaded containing PBA (Mic:Ins:PBA) lyophilized micelles after dispersion in water (mean ± SD, n≥3). * $p<0.05$ compared to the liquid micelles.

3. Results

3.1. Determination of size and zeta potential of formulations

Nanocomposites were dispersed in water and the size and surface charge of redispersed micelles analyzed to study the effect of lyophilization on their characteristics. Results expressed in Figure 4.1 showed an increase in the size of micelles, being this increase not significant for the majority of formulations. Also, no changes on the surface charge of micelles were observed ($p>0.05$).

3.2. Thermal analysis

DSC thermograms of insulin, polymers, PBA, physical mixtures and micelles with a polymer:insulin ratio of 10:1 are presented in Figure 4.2. Insulin thermogram showed a board endothermic peak at 94.16 ºC corresponding to the glass transition and denaturation of insulin and, at some extent, water lost (218). After 230 ºC a group of peaks can be detected, as a result of the degradation of the protein. PBA presented a sharp endothermic peak at 221.26 ºC, as a result of its melting. SOL presented a board endothermic peak at 69.2 ºC corresponding to the glass transition of the polymer. Thermograms of F68, F108 and F127 presented melting endothermic peaks at 46.89 ºC, 58.33 ºC and 50.84 ºC, respectively. In both physical mixtures and micelles the peaks corresponding to insulin glass transition and denaturation and melting of PBA are not detected, while the peaks of Pluronic® copolymers shifted to 51.43 ºC, 52.38 ºC and 47.62 ºC for F68, 57.3 ºC, 57.12 ºC and 51.77 ºC for F108, and 51.51 ºC, 57.62 ºC and 49.23 ºC for F127, in physical mixtures, insulin-loaded micelles and insulin-loaded micelles containing PBA, respectively.

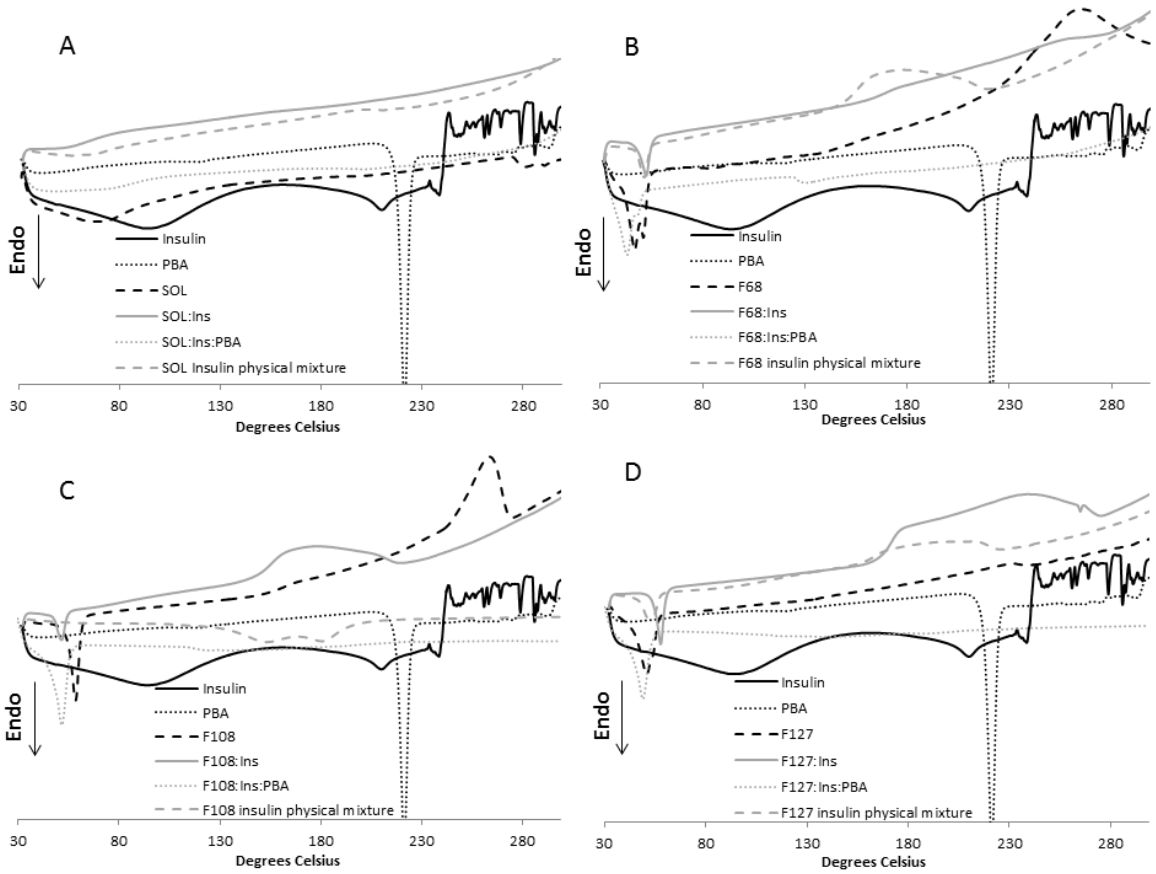

Figure 4.2 DSC thermograms of raw materials, polymer insulin physical mixture, insulin-loaded (polymer:Ins) and insulin-loaded lyophilized micelles containing PBA (polymer:Ins:PBA) of SOL (A), F68 (B), F108 (C), and F127 (D).

3.3. XRD analysis

The X-ray diffractograms of the pure compounds and lyophilized micelles with a polymer:insulin ratio of 10:1 are depicted in Figure 4.3. All samples presented two small peaks at around 2θ of 16.30º and 42.90º derivate from the polystyrene films. The crystalline nature of PBA was confirmed by the numerous sharp peaks between 2θ of 10º and 30º. Two main peaks at 2θ of 19.13º and 23.27-23.32º also indicated that Pluronic® copolymers possess a crystalline nature. On the other hand, the absence of distinct peaks in SOL spectra indicates its amorphous nature. Insulin presented few small peaks between 2θ 2-10º indicating a low degree of crystallization. Regarding micelles, distinct peaks at 2θ of 27.4º, 31.7º, 45.54º, 53.9º and 56.5º deriving from the NaCl existent in the PBS used to produce the formulations, can be detected. On the contrary, the peaks of PBA as well as the ones

respecting insulin disappeared, while the distinct peaks of Pluronic® copolymers presented a reduction in intensity compared to the pure polymers.

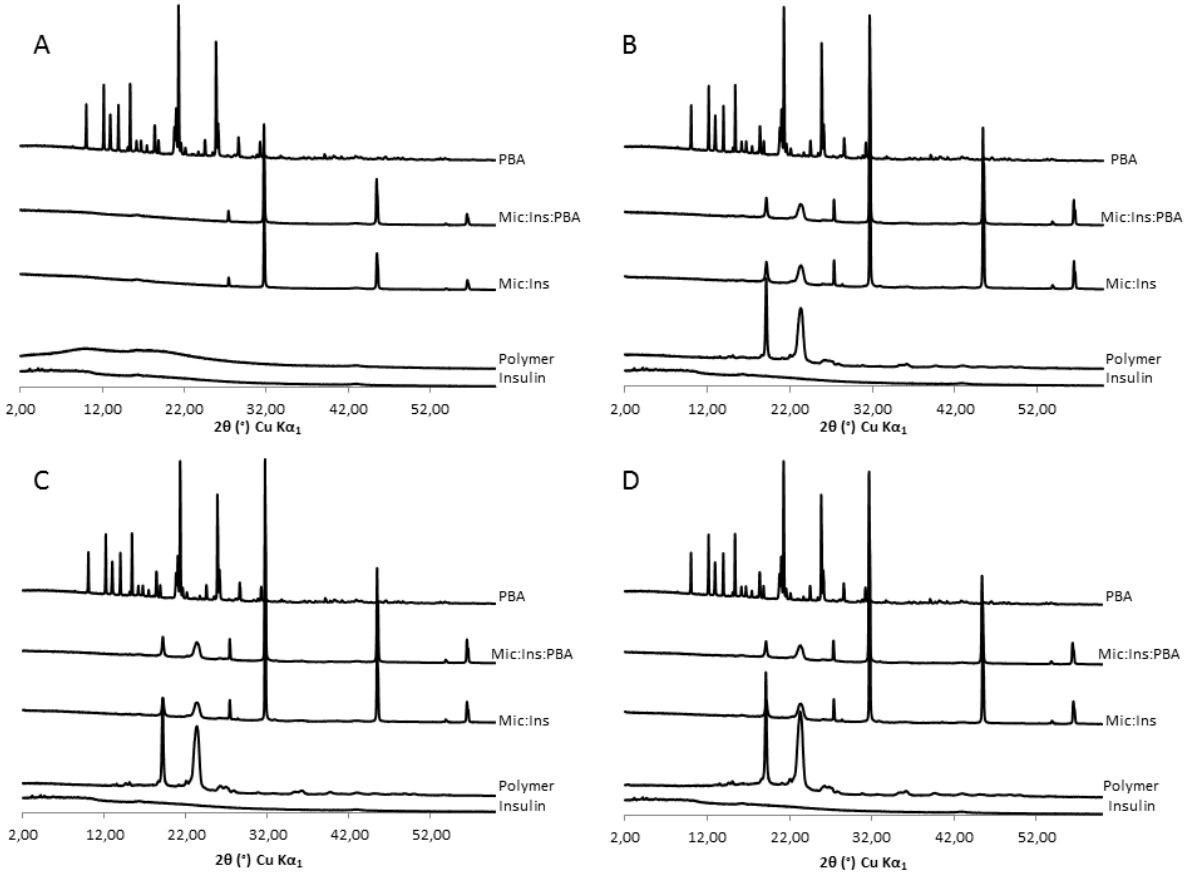

Figure 4.3 XRD patterns of insulin-loaded lyophilized micelles (Mic:Ins) and insulin-loaded containing PBA (Mic:Ins:PBA) lyophilized micelles of SOL (A), F68 (B), F108 (C), and F127 (D).

3.4. Raman spectroscopy

Raman spectroscopy was used to study possible interactions between the components of the formulations. The spectra of insulin, PBA, polymers and lyophilized micelles (10:1 polymer:insulin ratio) are presented in Figure 4.4 and the major peak assignments detailed in Table 4.1. In the spectrum of insulin, characteristic peaks related to amide I (1659 and 1673 cm^{-1}) and the aromatic rings of phenylalanine (1005 and 1606-1612 cm^{-1}) and tyrosine (832 cm^{-1}) can be identified. The B-O assymetrical stretch (1313-1368 cm^{-1}) and the vibration (994 cm^{-1}) and stretch (1602 cm^{-1}) of the aromatic ring are characteristic peaks of PBA. The characteristic peaks regarding ester C-O stretch (1029-1267 cm^{-1}), C=O stretch of the tertiary amide (1631 cm^{-1}) and ester carbonyl stretch (1732 cm^{-1}) can be identified in the SOL

spectra. In Pluronic® spectra are presented the characteristic peaks of C-O and C-C stretch (1127-1144 cm^{-1}) and CH2 twist (1234-1280 cm^{-1}).

For frequencies above 2000 cm^{-1}, board and large peaks related to CH, CH_2 and CH_3 aliphatic stretching, as well as water molecules can be detected (data not shown).

The characteristic peaks of insulin are not present in the spectra of insulin-loaded formulations, while small peaks related to PBA (1000 and 1602 cm^{-1}) can be detected in the spectra of insulin-loaded PBA containing micelles. Neither the appearance of new peaks nor the significant shift of the existing peaks is perceived in the spectra of micelles.

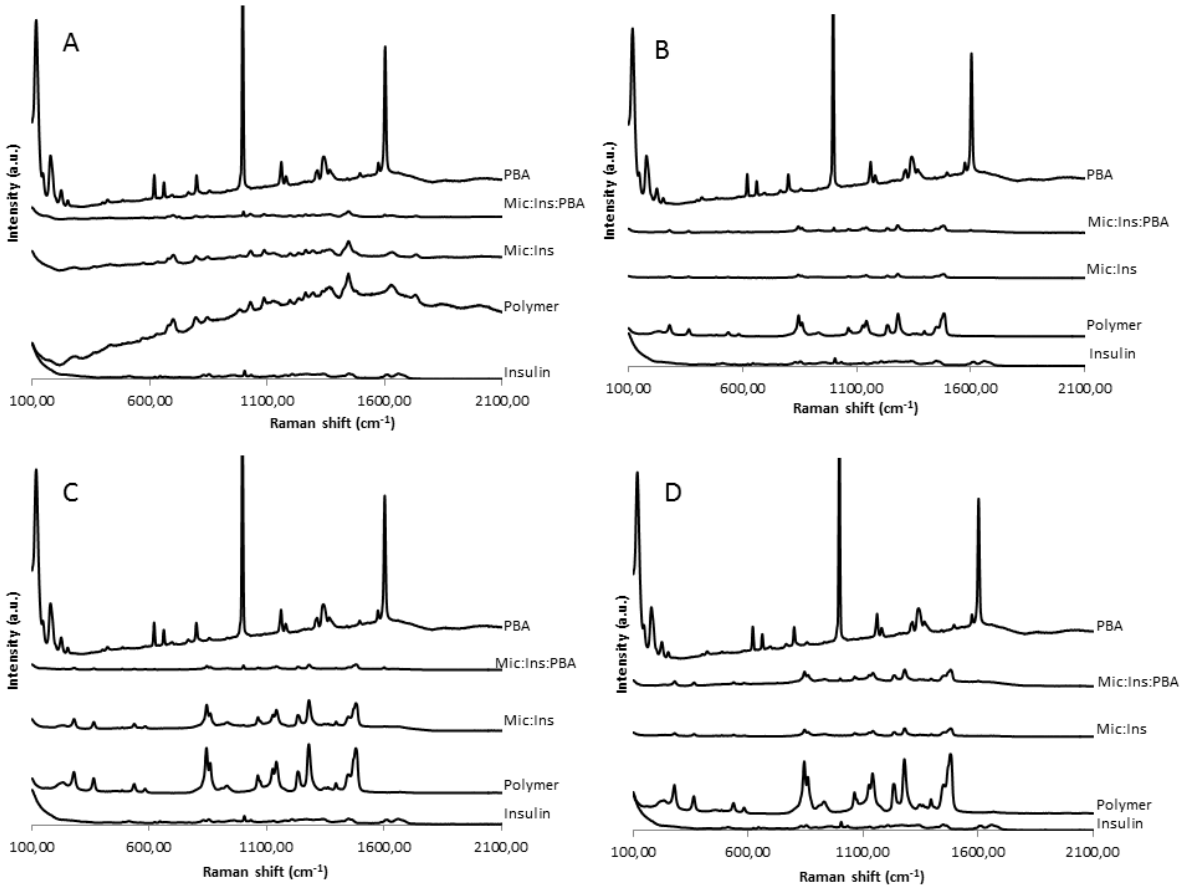

Figure 4.4 Raman spectra of insulin-loaded (Mic:Ins) and insulin-loaded containing PBA (Mic:Ins:PBA) lyophilized micelles of SOL (A), F68 (B), F108 (C), and F127 (D).

Table 4.1 Major peak assignments in the Raman spectra of the insulin, polymers and micelles.

Frequencies (cm^{-1})														Assignments
Native insulin	**PBA**	**SOL**	**SOL: Ins**	**SOL:Ins :PBA**	**F68**	**F68: Ins**	**F68:Ins :PBA**	**F108**	**F108: Ins**	**F108:Ins :PBA**	**F127**	**F127: Ins**	**F127:Ins :PBA**	
832														Tyr
		799-848	799-848	799-848	845	845	845	845	845	845	845	845	845	C-O-C stretch
1005	994			1000			1000			1000			1000	Aromatic ring vibration (Phe in insulin)
		1029-1264	1029-1267	1029-1264										Ester C-O stretch
					1127-1144	1127-1141	1125-1141	1125-1141	1127-1144	1127-1144	1125-1141	1127-1144	1127-1144	C-O and C-C stretch
	1160-1180													CH3 and CH2 assymetrical deformation
					1234-1280	1231-1280	1234-1280	1231-1280	1234-1280	1234-1280	1231-1280	1234-1280	1234-1280	CH2 twist
	1313-1368													B-O assymetrical stretch
1450		1449	1447	1449	1482	1482	1479	1482	1482	1482	1482	1482	1482	O-CH3 and/or CH2 deformation
1606-1612	1602			1602			1602			1602			1602	Aromatic ring quadrant strech (Phe in insulin)
		1631	1634	1632										C=O stretching (tertiary amide)
1657														Amide I - α helix
1673														Amide I - β sheet
		1732	1735	1735										Ester carbonyl stretch

3.5. Surface analysis

XPS was used to determine the elemental surface composition of the lyophilized formulations from the survey spectra. The atomic concentration of each sample as well as the raw materials is presented in Table 4.2. For raw materials, the elements identified are in good agreement with its molecular formula, although the atomic concentration can vary slightly from the theoretical values due to polymer polydispersion and the presence of dimers/conjugates in the case of insulin and PBA.

Table 4.2 Atomic concentration of the powders' surface.

Sample	C	O	N	Cl	Na	S	B
Insulin	66.40	18.89	13.68			1.02	
PBA	75.27	12.86					11.87
SOL raw	72.96	20.77	6.27				
SOL mic	62.42	22.72	5.24	4.17	5.45		
SOL:Ins	63.50	22.76	5.71	3.74	4.30		
SOL:PBA	68.56	22.22	3.76	2.64	2.81		
SOL:Ins:PBA	69.00	21.41	5.28	1.67	2.65		
F68 raw	68.63	31.37					
F68 mic	66.67	32.33		0.42	0.58		
F68:Ins	67.09	30.95	0.67	0.61	0.69		
F68:PBA	67.11	31.18		0.79	0.91		
F68:Ins:PBA	68.28	29.52	0.96	0.73	0.52		
F108 raw	67.34	32.66					
F108 mic	66.06	31.20		1.66	1.07		
F108:Ins	70.22	27.91		1.23	0.64		
F108:PBA	68.95	28.83		1.18	1.04		
F108:Ins:PBA	70.29	28.42		0.70	0.59		
F127 raw	69.15	30.85					
F127 mic	67.83	29.49		1.59	1.09		
F127:Ins	67.70	29.56	0.64	1.36	0.74		
F127:PBA	70.42	27.93		0.96	0.69		
F127:Ins:PBA	69.41	28.96	0.09	1.07	0.47		

The results are expressed as a percentage of the total amount of atoms detected in each sample. B – boron; C – carbon; Cl – chlorine; Ins – insulin; mic – empty lyophilized micelles; N – nitrogen; Na – sodium; O – oxygen; PBA – phenylboronic acid; raw – raw polymers without processing; S – sulphur.

Variations in the elemental composition of loaded micelles compared to empty micelles and from the last ones to raw materials can be observed. In all formulations is possible to identify the presence of chlorine and sodium derived from the PBS used during its production. Excepting for F108, all the formulations containing insulin showed the presence of nitrogen at the surface.

3.6. Protein conformation

FTIR spectra of the area-normalized second-derivative amide I region of native insulin in solution, lyophilized insulin, and lyophilized insulin-loaded micelles are presented in Figure 4.5. The spectrum of native insulin is dominated by a peak at 1655 cm^{-1} related to the major α-helix content of the protein.

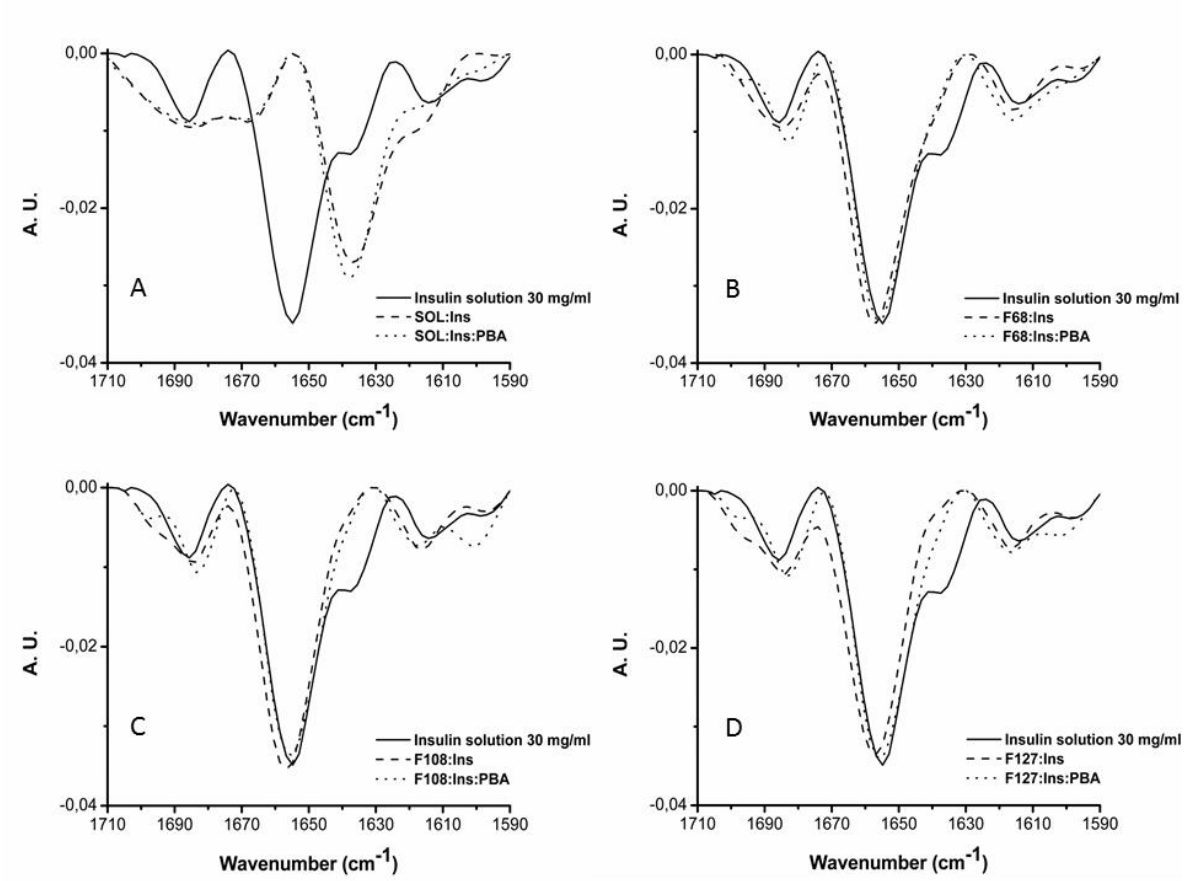

Figure 4.5 Area-normalized second-derivative amide I spectra of insulin solution 30 mg/mL, insulin-loaded (polymer:Ins), and insulin-loaded containing PBA (polymer:Ins:PBA) lyophilized micelles of SOL (A), F68 (B), F108 (C), and F127 (D).

β-sheet assignments from high-frequency at 1685 cm^{-1} and low-frequency at 1616 cm^{-1} and β-turn (1632 cm^{-1}) minor components are also present (453). Visual comparison of

the spectra of Pluronic®-based micelles had showed a narrow and a slight shift of the peaks. For SOL-based micelles is possible to observe a shift of the peak of α-helix to 1637 cm^{-1}, corresponding to a random coil, and the disappearance of the peaks related to β-sheet and β-turn. The incorporation of PBA into the micelles did not affect the secondary structure of insulin.

In order to facilitate the comparison of the spectra of native insulin and formulations, AO and SCC (indicators of the maintenance of the secondary structure of insulin) were calculated and the results obtained are expressed in Table 4.3. SOL-based micelles presented AO and SCC values lower than the lyophilized insulin and Pluronic®-based micelles ($p<0.05$). The presence of PBA increased the AO in a significant manner ($p<0.05$), but not the SCC ($p>0.05$). The differences observed between the AO values of Pluronic®-based micelles and lyophilized insulin, and between the three polymers are just statistical significant in the absence of PBA ($p<0.05$). Regarding SCC values, F127 insulin-loaded micelles differ from lyophilized insulin, F68 and F108 insulin-loaded micelles and F127 insulin-loaded micelles containing PBA ($p<0.05$). For PBA containing micelles no differences are observed ($p>0.05$).

Table 4.3 Area of overlap (AO) and spectral correlation coefficient (SCC) of lyophilized insulin, insulin-loaded (polymer:Ins) and insulin-loaded containing PBA (polymer:Ins:PBA) lyophilized micelles. Values are expressed as mean values ± SD, n=3.

Formulation	AO	SCC
SOL:Ins	50.09±0.88	49.73±0.90
F68:Ins	85.16±0.32	96.81±0.11
F108:Ins	83.01±1.60	95.32±0.49
F127:Ins	78.77±0.76	93.03±0.35
SOL:Ins:PBA	53.50±0.13	51.49±0.47
F68:Ins:PBA	87.39±1.38	97.05±0.49
F108:Ins:PBA	86.29±0.53	96.51±0.13
F127:Ins:PBA	86.89±1.53	96.82±0.47
Lyophilized insulin	87.26±0.28	97.61±0.12

The far-UV CD spectra of standard insulin solution, lyophilized insulin and lyophilized formulations showed two minima peaks around 208-209 and 220-222 nm and a maximum at 193-195 nm, related to the α-helix and β-sheet, respectively (Figure 4.6). Both lyophilized insulin and insulin-loaded micelles present less intense negative and positive

peaks and a shift in the positive peak, indicating a slight loss in the secondary structure of the protein.

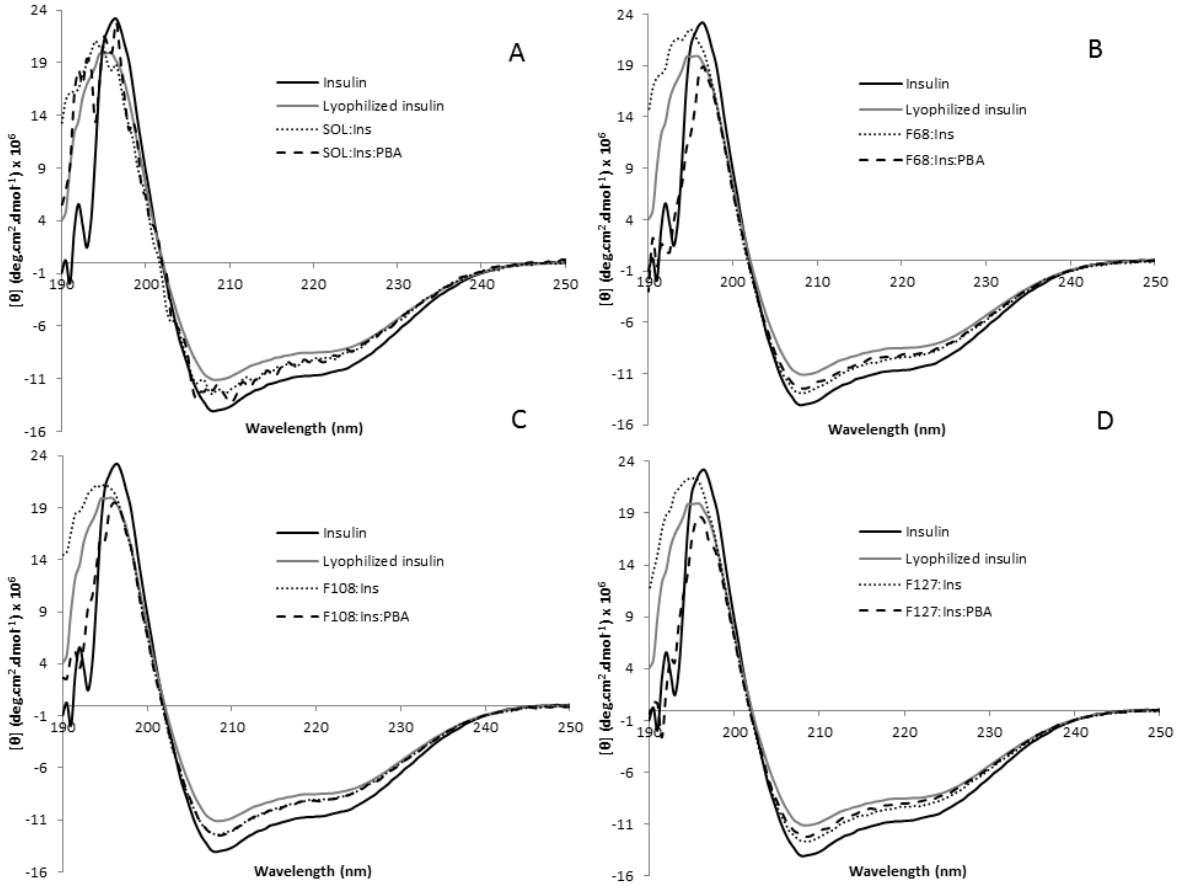

Figure 4.6 far-UV CD spectra of insulin-loaded (polymer:Ins) and insulin-loaded containing PBA (polymer:Ins:PBA) lyophilized micelles of SOL (A), F68 (B), F108 (C), and F127 (D).

3.7. Morphology and particle size distribution of powders

The shape and morphology of lyophilized formulations was analyzed by SEM. Micrographs of formulations are presented in Figure 4.7, evidencing the presence of a mixture of needle-shape and plate-shape structures resembling parts of an incomplete polymeric network. The incorporation of PBA to the systems did not affect the morphology and structure of powders. It can be noted the presence of pores and spherical nanocomposites smaller than 5 µm attached to the surface of bigger structures. SOL-based formulations presented smaller and more needle-shape structures, while F68 seemed to produce more compact and bigger particles, explaining the differences observed in the particle size distribution of powders (Table 4.3).

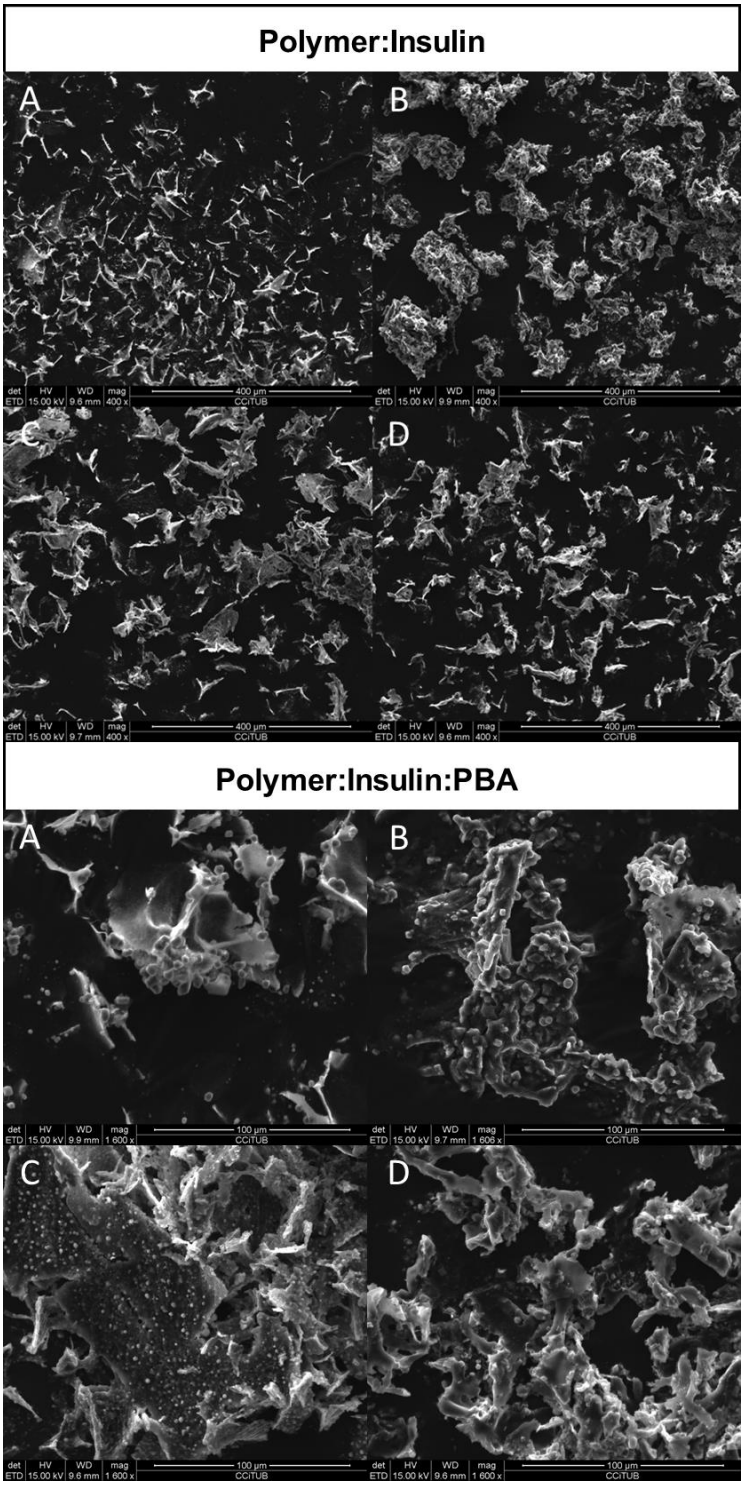

Figure 4.7 SEM micrographs of insulin-loaded formulations composed of SOL (A), F68 (B), F108 (C), and F127 (D), without (top panel) or with (bottom panel) PBA. Scale bar: 400 µm in formulations without PBA and 100 µm in formulations with PBA.

As seen in Table 4.4, all the formulations presented d_{ae} smaller than the geometric diameter due to their low densities ($p < 0.22$ g/cm^3, data not shown). SOL led to the formation of powder particles with lower $D_{0.5}$ and d_{ae}, while F68 and F108-based

formulations showed higher amount of larger particles/aggregates ($D_{0.9}$). Both F68 and F108 formulations present higher CMC and size of micelles at 25ºC before lyophilization, which could be influencing the final particle size and percentage of aggregates of powders. On the other hand, SOL and F127 could be originating more compact and stable micelles that suffer lower degree of aggregation during lyophilization. Nevertheless, no significant differences were observed between different samples ($p>0.05$). With the exception of F68-based particles, all the formulations presented $D_{0.5}$ values lower than 25µm and d_{ae} values lower than 6 µm.

All formulations presented high Carr's index (≥ 26) and Hausner ratio values (≥ 1.35), predicting poor flowability of powders according to European Pharmacopoeia (2.9.36. Powder flow) (455).

Table 4.4 Particle size distribution over the volume, aerodynamic diameter, Carr's index, and Hausner ratio of the different insulin-based formulations. Results are presented as mean values ± SD (n=3).

Sample	$D_{0.1}$ (µm)	$D_{0.5}$ (µm)	$D_{0.9}$ (µm)	d_{ae} (µm)	Carr's index	Hausner ratio
SOL:Ins	4.5±0.6	15.3±0.1	44.3±1.9	3.1±0.2	49.2±11.3	2.03±0.45
SOL:Ins:PBA	4.6±0.9	16.0±2.6	42.8±6.9	2.9±0.4	51.1±1.9	2.05±0.08
F68:Ins	9.5±2.3	39.1±11.3	328.9±127.8	13.8±4.6	44.4±19.3	2.00±0.87
F68:Ins:PBA	8.7±0.3	29.7±0.1	410.9±314.1	8.1±0.3	50.0±7.1	2.03±0.29
F108:Ins	6.5±0.5	23.4±2.8	358.3±304.5	5.8±0.2	55.7±5.2	2.28±0.25
F108:Ins:PBA	6.9±0.3	23.3±1.3	235.9±153.0	5.4±0.8	49.2±8.0	2.00±0.29
F127:Ins	6.7±1.1	21.6±3.6	81.9±31.0	5.6±0.8	51.9±3.2	2.08±0.14
F127:Ins:PBA	7.4±0.3	24.2±1.3	68.3±7.2	5.5±0.1	47.7±9.3	1.95±0.33

3.8. Deposition profile of formulations

The aerosolization properties of formulations were assessed *in vitro* following pharmacopeial instructions using an ACI impactor and a Rotahaler® as inhaler device and are presented in Table 4.5. Powders composed by SOL and F127 presented the higher FPF (around 48% and 44%, respectively) while F68 and F108 showed lower FPF (around 27% and 26%, respectively). Expecting for F108-based powders, the presence of PBA did not affect the FPF of powders ($p>0.05$). All the formulations showed a MMDA lower than 6.6 µm and GSD under 2.1 µm.

Table 4.5 Deposition profile of formulation powders after aerosolization into an Andersen Cascade Impactor via a Rotahaler® and estimation of mass median aerodynamic diameter (MMDA) and geometrical standard deviation (GSD). The results of aerosolization profile and fine particle fraction (FPF) are expressed as the amount of particles deposited in each stage as a percentage of the initial amount of particles, and the results of MMAD expressed as size in micrometers (mean ± SD, n=3). T+C+D is composed by throat, capsule and inhaler device.

Stage	Size (µm)	SOL:Ins	SOL:Ins: PBA	F68: Ins	F68:Ins: PBA	F108: Ins	F108:Ins: PBA	F127: Ins	F127:Ins: PBA
T+C+D	> 10	6.2±10.7	10.8±9.4	12.7±20.6	8.4±8.2	20.6±6.9	0.6±1.0	1.0±1.0	8.0±7.7
0	9.0-10.0	23.5±8.4	19.6±4.8	29.7±7.9	25.3±5.6	21.7±7.6	20.0±8.4	20.2±3.8	30.9±6.9
1	5.8-9.0	8.4±1.4	11.5±2.0	13.6±2.4	18.4±0.6	20.5±2.4	21.0±3.0	22.0±3.9	20.3±4.3
2	4.7-5.8	18.0±2.8	20.8±5.4	16.9±4.7	14.7±1.8	11.3±1.7	19.8±1.7	14.6±2.1	11.0±7.1
3	3.3-4.7	18.7±5.0	19.4±3.1	17.0±3.1	15.3±4.5	10.9±0.5	17.7±3.5	14.1±1.8	13.3±1.8
4	2.1-3.3	3.9±2.1	1.3±2.2	4.1±3.7	5.5±2.5	3.4±1.5	3.8±0.2	4.6±2.3	1.2±1.1
5	1.1-2.1	7.2±6.4	5.3±3.2	3.0±5.2	8.3±8.0	4.6±2.7	7.7±2.2	8.1±5.4	6.8±4.2
6	0.65-1.1	7.8±5.2	6.1±9.0	1.2±2.1	4.7±3.1	2.2±2.0	9.5±1.6	10.4±4.1	2.8±1.1
7	0.43-0.65	10.2±2.5	8.6±8.2	1.7±1.7	1.5±2.6	4.7±5.4	5.1±1.0	6.9±2.9	7.0±1.3
FPF	<4.7	47.8±15.8	40.6±16.6	27.1±12.0	35.3±7.8	25.8±1.3	43.9±3.1	44.0±10.3	31.2±6.5
MMAD		4.8±0.7	4.9±0.5	5.8±0.2	5.6±0.2	6.1±0.3	5.1±0.3	5.1±0.6	6.6±1.1
GSD		1.8±0.2	1.7±0.7	1.9±0.5	1.7±0.3	1.9±0.3	1.5±0.0	2.1±0.2	2.1±0.5

The presence of PBA did not affect the MMAD and GSD values of formulations ($p>0.05$). No differences ($p>0.05$) in the MMAD and GSD values were observed between the different powders.

3.9. Determination of the insulin release pattern from micelles

Release studies of insulin from micelles were performed at physiological pH and temperature (pH 7.4 and 37 °C) in the absence or presence of glucose (1.2 mM). Results of *in vitro* release studies are reported in Figure 4.8 as percentage of protein released over time. Insulin release presented a biphasic pattern, with notorious burst release in the first 15 minutes followed by a sustained release of the protein over the following 24 hours. Both F68:Ins and F68:PBA:Ins formulations released around 85-95 % of insulin in the absence of glucose (Figure 4.8A), presenting similar release profiles (f_2>50, Table 4.5). SOL:Ins and SOL:PBA:Ins released 40-55 % and 50-65 % of the total insulin, respectively. The high difference in the percentage of insulin released between SOL and F68-based formulations could be related to the MW of polymers and the structure of micelles. Having higher MW and lower CMC, SOL could present more compacted micelles which difficult the release of insulin. The presence of PBA seemed to affect specially F108 and F127-based formulations since, in both cases, the totality of insulin was released from PBA containing micelles (f_2>50), whereas only 80 % and 60 % of the protein was release after 24 hours from F108:Ins and F127:Ins formulations, respectively. Despite the different percentage of total insulin release, F108:Ins and F127:Ins also presented similar release profiles (f_2>50).

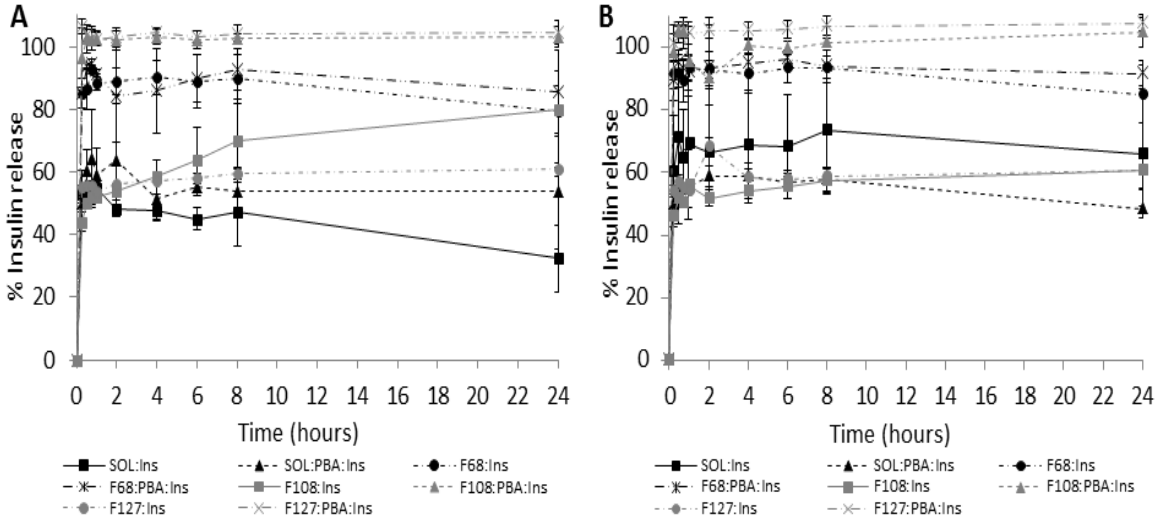

Figure 4.8 *In vitro* release profiles of insulin from different formulations in PBS (pH 7.4) without glucose (A) and with 1.2 mM glucose (B). Results are presented as mean ± SD (n=3).

The presence of glucose did not affect the release of insulin (f_2>50) from formulations (Figure 4.8B and Table 4.6), excepting for SOL:Ins formulations (f_2<50). Although the presence of PBA did not confer glucose-sensing properties to the formulations, it seemed to increase the release of insulin for the majority of formulations by a mechanism independent of glucose concentration.

Table 4.6 Similarity factor (f_2) values between insulin release profiles of the different formulations in PBS (pH 7.4) without glucose (white columns) and with 1.2 mM glucose (grey columns).

	SOL: Ins	**SOL:Ins: PBA**	**F68: Ins**	**F68:Ins: PBA**	**F108: Ins**	**F108:Ins: PBA**	**F127: Ins**	**F127:Ins: PBA**
SOL:Ins	---	44.1	31.1	29.5	42.1	24.2	48.4	21.2
SOL:Ins: PBA	48.0	---	22.0	20.9	62.6	17.1	62.6	14.9
F68:Ins	20.0	25.3	---	72.9	21.1	48.3	23.8	42.2
F68:Ins :PBA	19.1	24.3	68.7	---	20.1	54.1	22.7	45.8
F108:Ins	35.6	44.2	24.6	23.9	---	16.6	58.0	14.4
F108:Ins: PBA	13.3	17.2	41.7	43.9	17.4	---	18.6	58.4
F127:Ins	45.9	60.8	25.3	24.3	52.6	17.3	---	16.4
F127:Ins: PBA	12.6	16.2	38.9	40.7	16.4	71.9	16.4	---

3.10. Stability of formulations upon storage

In order to assess the stability of the lyophilized formulations upon storage, samples of each formulation were produced and stored at two different temperatures, namely 20 ºC and 4 ºC, and characterized after 1, 3 and 6 months. Results regarding mean hydrodynamic diameter and surface charge of micelles after the dispersion of powders in water are presented in Figure 4.9 and 4.10. The results of the majority of samples stored for 1 month were similar to the ones obtained for redispersed powders after lyophilization (p>0.05), excepting for F68-based insulin-loaded micelles containing PBA and F108-

based micelles that presented higher micelles size when stored at 20 ºC and analyzed at 25 ºC ($p<0.05$).

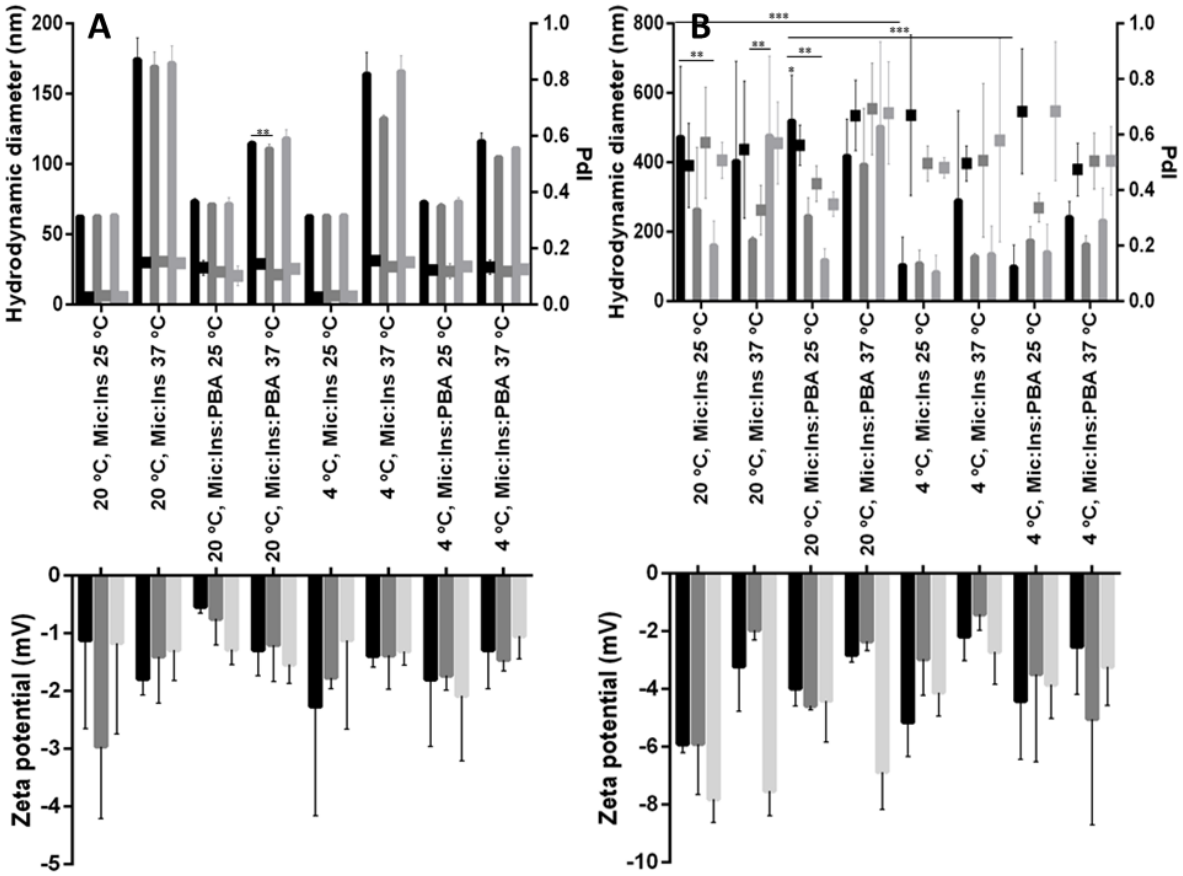

Figure 4.9 Mean hydrodynamic diameter, polydispersity index (PdI) and zeta potential of SOL (A) and F68 (B)-based lyophilized insulin-loaded (Mic:Ins) and insulin-loaded containing PBA (Mic:Ins:PBA) micelles stored for 1 month (black bars and squares), 3 months (medium grey bars and squares), and 6 months (light grey bars and squares) at 4 ºC and 20 ºC after redispersion in water (mean ± SD, n=3). * $p<0.05$ compared to the formulations after lyophilization, ** $p<0.05$ between different months of storage, *** $p<0.05$ between 20 ºC and 4 ºC.

Neither time nor temperature of storage affected in a high extension the characteristics of SOL and F127-based micelles ($p>0.05$, for almost all formulations). On the other hand, F68 and F108-based micelles stored at 20 ºC seems to be more sensitive to the time and temperature of storage, since some formulations stored at 4 ºC presented smaller mean hydrodynamic diameter ($p<0.05$), and had variable size upon storage. The zeta potential of the formulations remained slightly negative as at liquid state and recently lyophilized samples.

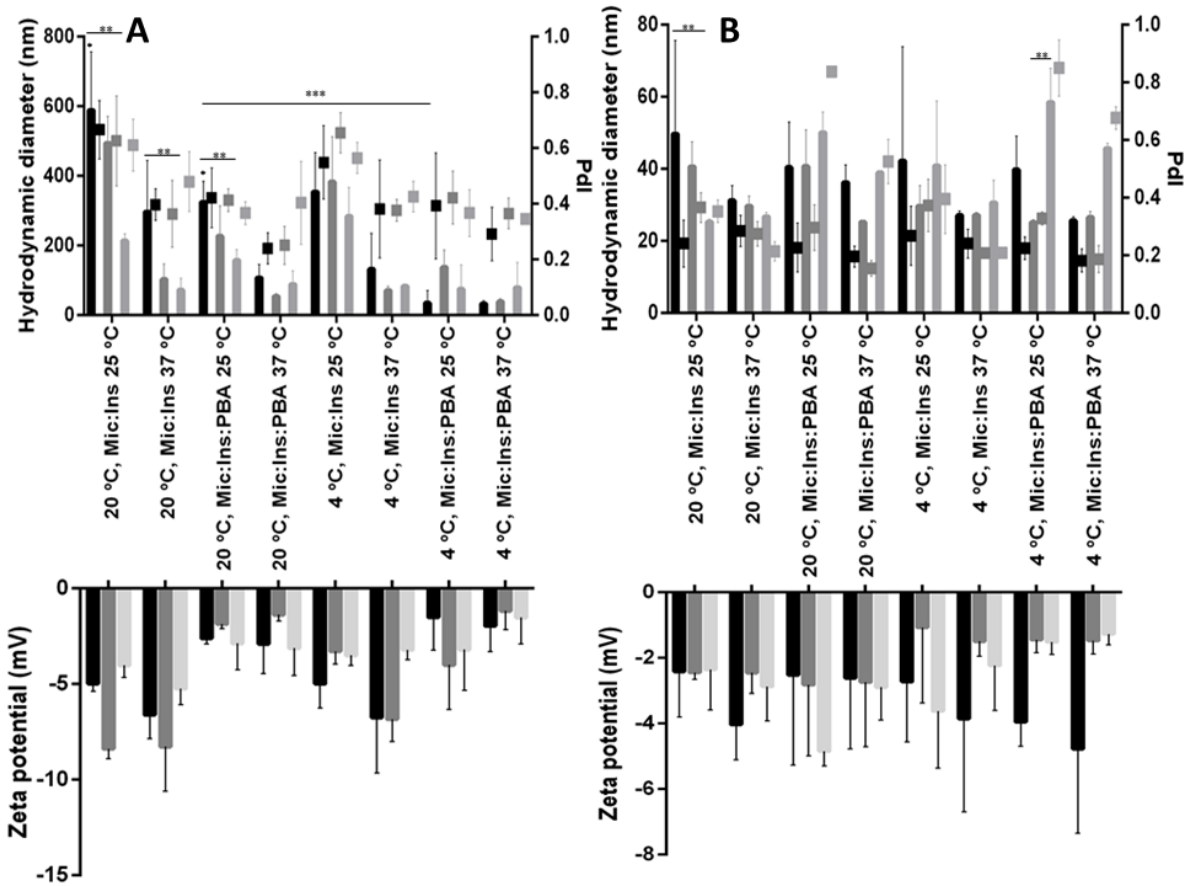

Figure 4.10 Mean hydrodynamic diameter, polydispersity index (PdI) and zeta potential of F108 (A) and F127 (B)-based lyophilized insulin-loaded (Mic:Ins) and insulin-loaded containing PBA (Mic:Ins:PBA) micelles stored for 1 month (black bars and squares), 3 months (medium grey bars and squares), and 6 months (light grey bars and squares) at 4 ºC and 20 ºC after redispersion in water (mean ± SD, n=3). * $p<0.05$ compared to the formulations after lyophilization, ** $p<0.05$ between different months of storage, *** $p<0.05$ between 20 ºC and 4 ºC.

Regarding the protein conformation, FTIR spectra of the area-normalized second-derivative amide I region of native insulin without storage and lyophilized insulin-loaded micelles and insulin-loaded micelles containing PBA stored up to 6 months at both 4 ºC and 20 ºC are presented in Figure 4.11 and 4.12, respectively.

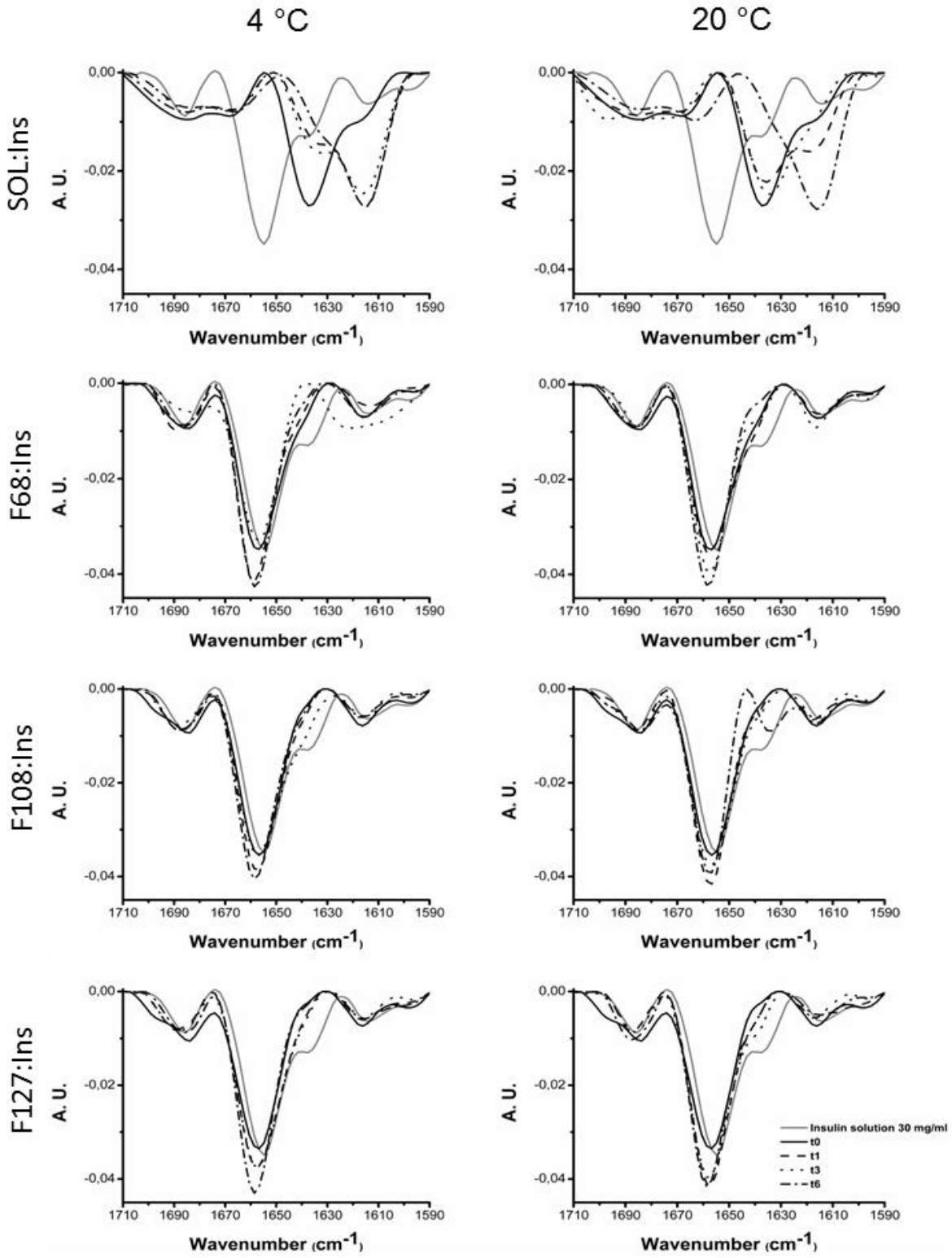

Figure 4.11 Area-normalized second-derivative amide I spectra of insulin solution 30 mg/mL and insulin-loaded micelles (polymer:ins) after lyophilization (t0) and upon 1 month (t1), 3 months (t3) and 6 months (t6) of storage at 4 ºC and 20 ºC.

AO and SCC values depicted in Table 4.7 show that, similarly to micelles after production and lyophilization, SOL-based micelles presented the lower percentage of native-like insulin conformation. After 6 months of storage, both AO and SCC values were lower ($p<0.05$) than the ones obtained after production and lyophilization, expecting for F127 insulin-loaded micelles stored at both temperatures as well as F108 insulin-loaded micelles, and SOL and F127 insulin-loaded micelles containing PBA stored at 4 ºC ($p>0.05$). The storage temperature did not seemed to affect extensively the secondary conformation of insulin, since differences ($p<0.05$) in AO values were only observed for F68 and F127 insulin-loaded micelles containing PBA, while for SCC values were observed for F127 insulin-loaded micelles containing PBA. In addition, the presence of PBA only affected the AO values of SOL and F68 insulin-loaded micelles stored at 4 and 20 ºC, respectively; the SCC values of SOL and F108 insulin-loaded micelles stored at 4 ºC and the SCC values of F68 insulin-loaded micelles stored at 20 ºC. In Table 4.8 are presented the values related to the percentage of reduction in the AO and SCC values of freeze-dried micelles after 6 months of storage. It is possible to notice that SOL-based micelles suffered the higher reduction in the conformation of insulin upon storage with a decrease of 15.0 and 22.7% in the AO and SCC values, respectively.

Regarding the spectra it was noticed that, for SOL insulin-loaded micelles, at 4 ºC insulin structure changed from a random coil organization at t0 to a dominant low-frequency β-sheet assignment at 1616 cm^{-1} after 1 month of storage, while at 20 ºC this modification was just observed after 6 months. For SOL insulin-loaded micelles containing PBA a similar pattern of insulin structural modifications was observed. At 4 ºC the modification of random coil structure into a low-frequency assignment after 1 month was observed, but after 3 and 6 months was observed a tendency to an organization of both random coil and β-sheet. At 20 ºC this latter structural organization of a random coil and β-sheet bands was observed since 1 month until 6 months of storage. Considering the Pluronic® formulations, just a few changes were observed in the α-helix band intensity, which seemed to increase during time up to 6 months of storage, both for 4ºC and 20ºC storage conditions. However, a band peak at 1600 cm^{-1} appeared after 1 month of storage in all the Pluronic®-based micelles containing PBA.

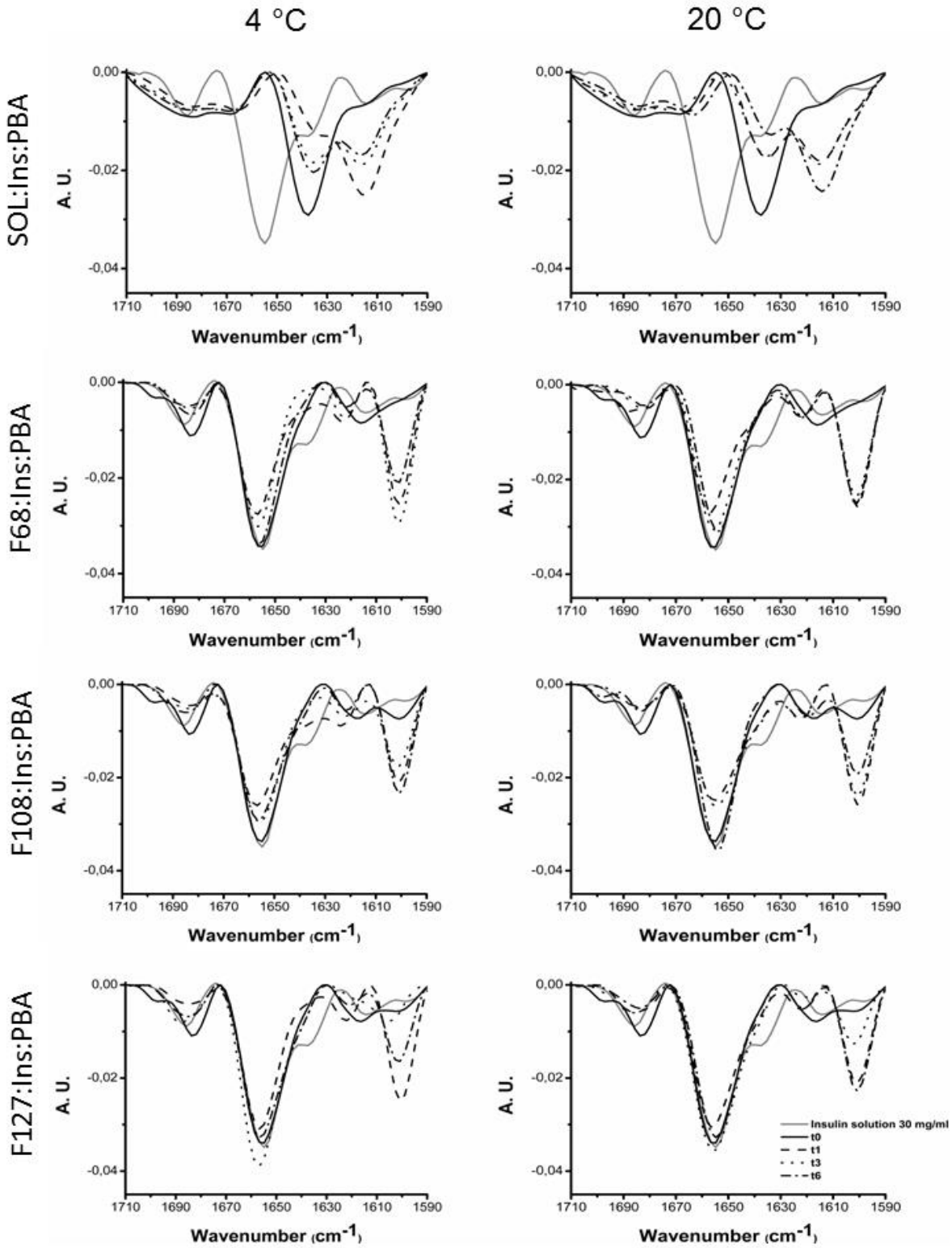

Figure 4.12 Area-normalized second-derivative amide I spectra of insulin solution 30 mg/mL and insulin-loaded micelles containing PBA (polymer:ins:PBA) after lyophilization (t0) and upon 1 month (t1), 3 months (t3) and 6 months (t6) of storage at 4 ºC and 20 ºC.

Table 4.7 Area of overlap (AO) and spectral correlation coefficient (SCC) of insulin-loaded freeze-dried micelles after storage at 4 ºC and 20 ºC. Values are expressed as mean ± SD, n=3.

Formulation	Temperature of storage	1 month		3 months		6 months	
		AO	SCC	AO	SCC	AO	SCC
Sol:Ins	4 ºC	44.5±0.9	37.9±1.4	46.2±1.4	40.6±2.2	42.6±0.2	38.5±1.2
F68:Ins	4 ºC	78.7±4.1	93.1±1.9	76.4±0.8	91.0±0.5	79.9±0.0	93.2±0.0
F108:Ins	4 ºC	83.4±1.0	95.6±0.5	86.5±2.2	97.2±1.0	80.1±1.2	93.7±0.7
F127:Ins	4 ºC	84.4±1.2	95.7±0.5	84.1±2.6	95.9±0.9	79.2±0.5	92.4±0.3
Sol:Ins:PBA	4 ºC	45.6±1.5	39.8±0.9	49.6±1.0	44.6±1.8	50.2±0.6	45.9±1.1
F68:Ins:PBA	4 ºC	70.8±2.0	83.1±2.3	66.5±1.5	77.9±2.4	77.6±1.3	90.1±1.4
F108:Ins:PBA	4 ºC	73.5±0.3	87.2±0.4	77.6±1.2	89.9±1.7	76.3±1.4	87.9±1.1
F127:Ins:PBA	4 ºC	71.9±2.3	84.8±2.0	86.8±0.4	97.1±0.2	83.6±0.1	94.3±0.2
Sol:Ins	20 ºC	48.3±0.5	45.8±1.0	45.6±0.8	43.3±1.3	43.8±1.1	42.2±3.8
F68:Ins	20 ºC	86.4±2.9	96.8±1.1	82.9±1.3	95.4±1.0	80.2±4.1	93.2±2.1
F108:Ins	20 ºC	81.5±1.8	94.6±1.2	83.8±2.0	96.0±1.3	78.4±0.3	91.5±0.3
F127:Ins	20 ºC	83.4±0.5	95.1±0.2	82.8±2.0	95.6±0.9	79.9±0.8	93.7±0.4
Sol:Ins:PBA	20 ºC	50.5±0.8	46.8±1.1	49.3±1.9	44.7±2.8	47.7±0.9	44.4±1.7
F68:Ins:PBA	20 ºC	69.3±2.5	82.2±2.7	74.1±1.7	87.2±1.3	71.8±3.8	85.2±3.2
F108:Ins:PBA	20 ºC	70.9±3.2	83.2±3.6	72.8±2.1	85.7±2.1	76.6±0.5	90.6±1.3
F127:Ins:PBA	20 ºC	77.8±4.6	89.9±3.8	86.2±0.6	96.6±0.4	77.2±2.6	89.1±2.0

Table 4.8 Percentage of reduction in the area of overlap (AO) and spectral correlation coefficient (SCC) of insulin-loaded freeze-dried micelles after 6 months of storage at 4 ºC and 20 ºC when compared to micelles after production. Values are expressed as mean ± SD, n=3.

Formulation	Temp (ºC)	AO	SCC	Temp (ºC)	AO	SCC
SOL:Ins	**4**	15.0±0.2	22.7±1.1	**20**	12.5±2.2	15.2±7.6
F68:Ins		6.2±0.0	3.7±0.0		5.8±4.7	3.7±2.2
F108:Ins		3.5±1.2	1.7±0.7		5.5±0.4	4.0±0.4
F127:Ins		-0.5±0.5	0.7±0.3		-1.4±1.0	-0.7±0.4
SOL:Ins:PBA		6.2±0.6	10.8±1.0		10.8±1.7	13.7±3.2
F68:Ins:PBA		11.2±1.3	7.2±1.4		17.9±4.4	12.2±3.3
F108:Ins:PBA		11.6±1.4	8.9±1.1		11.2±0.5	6.1±1.3
F127:Ins:PBA		3.8±0.1	2.6±0.2		11.2±2.9	8.0±2.1

Regarding far-UV CD, the pattern of spectra of formulations after 6 months of storage were similar to the ones obtained after lyophilization (Figure 4.13).

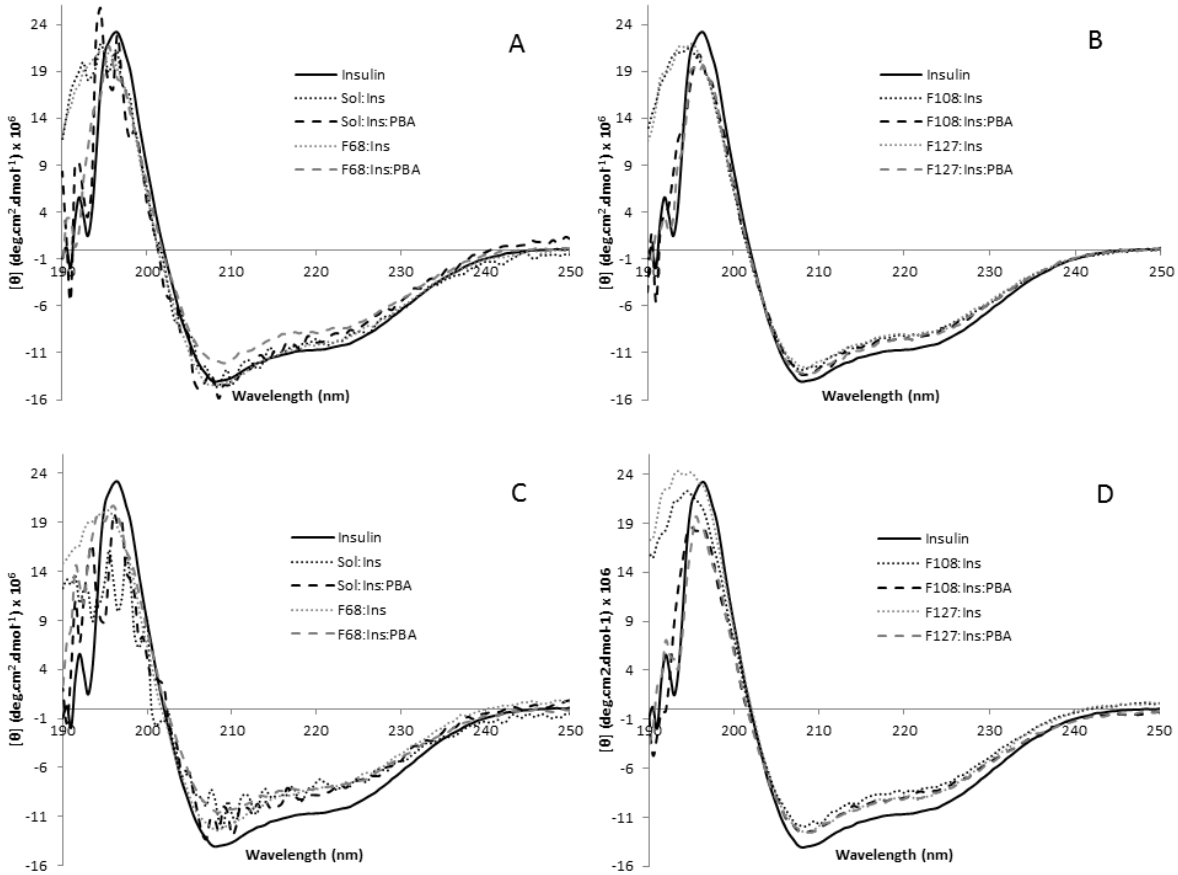

Figure 4.13 far-UV CD spectra of insulin-loaded lyophilized micelles (polymer:Ins) and insulin-loaded lyophilized micelles containing PBA (polymer:Ins:PBA) of SOL and F68 (A and C) and F108 and F127 (B and D) stored for 6 months at 20 ºC (A and B) and 4 ºC (C and D).

4. Discussion

As a consequence of the lack of evident surface charge, after some weeks of storage in liquid state micelles tend to aggregate and suffer deposition (data not shown). In order to improve the storage stability of formulations and to produce powders for inhalation the samples were lyophilized and nanocomposites obtained. Although spray-drying is considered the technique of excellence for the production of inhaled powders, formulations like Afrezza® (insulin dry powder formulation with market authorization) were successfully produced by lyophilization (458).

Nanocomposites of 3-5 µm in diameter can be easily administered by inhalation, reaching the deep lungs and deliver the nanoparticles when in contact to the lung fluids (333, 459). The nanocomposites obtained were easily dispersed in water, producing micelles with mean hydrodynamic diameters and PdI slightly, but not significantly, higher than the fresh samples (Figure 4.1), as consequence of the aggregation promoted by lyophilization. However, excepting for micelles of F68, all the insulin-loaded micelles presented mean

hydrodynamic diameters smaller than 200 nm at both 25 and 37 ºC, being in the desired range of sizes to expect low uptake by alveolar macrophages (460). A slight increase of particle size of Pluronic®-based micelles after lyophilization and redispersion was previously reported by other research groups (461). The produced micelles showed to be easily redispersed without the addition of cryoprotectants. This good redispersion behavior can be related to the capacity of Pluronic® copolymers to protect particles from aggregation during lyophilization when present in the system at high concentrations, working as themselves as cryoprotectants, possibly due to the presence of PEG chains (462). SOL seems to behave the same way as Pluronic® copolymers, since also present PEG in its structure.

Insulin thermogram showed a board endothermic peak that corresponds to the glass transition and denaturation of insulin (Figure 4.2). Contrary to other reports, was not possible to detect the two distinct endothermic peaks corresponding to the biphasic denaturation of insulin (218). PBA showed a sharp endothermic peak that corresponds to its melting point, indicating a high crystallinity degree of the compound. Contrary to SOL, that showed to be amorphous with a glass transition temperature close to 70 ºC (463, 464), Pluronic® copolymers presented a crystalline solid state with melting temperature around 45-60 ºC (465). In both physical mixtures and insulin-loaded micelles the peaks corresponding to insulin glass transition and denaturation and the melting of PBA disappeared, indicating that they are molecularly dispersed in the polymers and in its amorphous state (466). Also, the melting peaks of Pluronic® copolymers suffered a shift when in physical mixtures and micelles, indicating a possible change in its crystallinity.

The results of DSC were corroborated with XRD studies, where is possible to see a disappearance of characteristic peaks of insulin and PBA, indicating a change in its state from crystal to amorphous when formulated into micelles (Figure 4.3). Also, Pluronic® copolymers suffered a reduction in the crystallinity after formulation and lyophilization, revealed by the reduction in the peaks intensity, indicating a successful lyophilization process. The amorphous state of raw SOL was also confirmed by XRD. The diffractograms of the polymers were in good agreement to the ones reported by others (464, 465). Raman spectroscopy was used to study possible interactions between the different components of formulations. The spectra obtained (Figure 4.4) were in close agreement with others already reported (464, 467-469). No visual changes were observed in the Raman spectra of micelles containing insulin compared to the polymers, indicating the absence of significant physical interactions between the protein and the components of the formulation. In addition, the major characteristic peaks of insulin disappeared and small peaks related to the vibration and stretching of the aromatic ring of PBA can be

detected in PBA containing formulations. These results reinforce the association/loading of the protein into the micelles and the amorphous state of both PBA and insulin.

In order to assess the loading and presence of insulin at the surface of particles, both raw materials and formulations were analyzed by XPS (Table 4.2). The photoelectrons binding energy is used to identify and quantify the elements (excepting hydrogen and helium) occurring on the outermost surface layer to a few nm depth (around 7 nm) of powder samples. Nitrogen is one key element used in the identification of proteins in the samples (469). As referred, although the elemental composition of raw material is in agreement with the elements presented in its molecular formula, the differences in the atomic concentrations from the theoretical expected can be explained by the polydispersity of the polymers and by the presence of dimers of PBA and insulin. The absence of boron in the spectra of formulations containing PBA indicates that it is present in the more interior layers of the micelles, probably due to its neutral, and consequently more hydrophobic, conformation at the pH of the micelles at liquid state after formulation. Regarding insulin is possible to detect it in the outermost layer in all formulations, excepting for the formulations composed by F108. Since insulin is hydrophilic in nature, it is expected that remains between the PEG chains in the outer shell of micelles, being detected by the laser at the surface and in few nm depth. As F108 presents the PEG chains with higher number of monomers, and consequently the higher MW (Table 3.3), insulin was possibly entrapped deeper in the PEG chains, not being available to be excited by the laser and detected.

Secondary structure of insulin was assessed using FTIR spectroscopy and far-UV CD. In FTIR studies the amide I region is considered the most representative target in protein spectra and spectral variations can be used for comparison after second-derivative and area-normalization treatment (453). Usually, the lyophilization process is responsible for a decrease in the α-helix and an increase in β-sheet content. This decrease is motivated by protein-protein interactions, leading to the formation of intermolecular β-sheets during water removal. Therefore, the α-helix band is a better indicator of protein structural maintenance (470). Two different spectral similarity approaches, namely the calculation of AO and SCC, were used in this study as indicators of the maintenance of the conformation of the protein. Since SCC values are related to the differences in band positions and not in relative peak width or height, they give an overestimated idea of conformation maintenance. Nevertheless, SCC can be used as complementary indicator of similarity non-intensity related (453). As showed in Figure 4.5, the spectra of native insulin and formulations are not completely overlapped, being the biggest difference observed for SOL micelles. These visual differences are corroborated with the values of

AO and SCC (Table 4.3). After production and lyophilization, insulin loses some of the secondary structure. Still, the secondary structure of protein was maintained at least 50 % after formulation. As referred above, SOL-based formulations presented the higher insulin structural changes and it was noticed a clear modification of its α-helix band into a random coil at 1637 cm^{-1}. These structural modifications seem to be related with some physical interaction between insulin and SOL, leading to a great loss of insulin native structure. Regarding the other tested formulations, just a slight shift on the α-helix band position was noticed; however it remained in the 1660-1655 cm^{-1} characteristic α-helix range of insulin band. These results showed that Pluronic®-based formulations were able to encapsulate and protect insulin structure from lyophilization stresses. The maintenance of the structure of the protein can be partially due to the cryoprotection properties of the PEG chains (471). In addition, it was noticed that for all the polymer formulations the addition of PBA seemed not to affect insulin secondary structure after micelles production, since similar levels of protein structural maintenance were noticed for both containing and not containing PBA formulations. However, precaution should be taken in the analysis of the results regarding SOL micelles, since SOL presents a peak regarding the tertiary amide close to the region of the amide I and some interference of the polymer spectrum during the subtraction can occur. To confirm the results obtained by FTIR, far-UV CD was also used to assess the secondary structure of the protein. As seen in Figure 4.6, the spectrum of standard insulin solution is in accordance with the typical spectra of α+β proteins with the dominance of α-helical secondary structure already reported by others (472-474). It is possible to observe a slight decrease in the intensity of the peaks of both lyophilized insulin and formulations compared to the standard insulin solution, which can indicate change in the ratio of α-helix and β-sheet components or a reduction in the α-helix content and the native conformation as a consequence of the process of lyophilization. In the same way, the shift and noise observed in the positive peak can be due to the presence of the chloride ions in the solution that absorb below 200 nm or interference from the polymers that cannot be completely eliminated during subtraction of empty micelles spectra (454). It should be noted that the spectra of formulations are similar to the spectra of lyophilized insulin, which is in accordance to the results obtained by FTIR for Pluronic®-based micelles but differs in the case of SOL-based micelles.

Regarding the morphology of powders, SEM images (Figure 4.7) showed a polymeric network-like structure typical from hydrogels and solid dispersions obtained with higher percentages of polymers (475, 476). Although micelles were prepared using low concentrated polymer solutions (1% w/v), it seems that during the freeze and drying steps of lyophilization an increase in polymer concentration and/or aggregation of micelles lead

to the formation of the observed structures. Similar network-like structure was observed for freeze-dried PCL–PEG–PCL micelles (< 6% w/v) (112).

Size, density and shape of particles are the main characteristics affecting the aerosolization and deposition properties of particles (449, 477). The theoretical aerodynamic diameter (d_{ae}) of powder particles was calculated using a dynamic shape factor of 1.6 as the mean value described by Hassan and Lau (2009) (477) for needle-shape (χ=1.7) and plate-shape (χ=1.5) particles (Table 4.3). For many years it was assumed that aerosolized dry particles should present a size ranging 1-5 µm for efficient lung deposition. Nowadays is accepted that large porous particles presenting small particle mass density ($p < 0.4$ g/cm^3) and geometric size above 5 µm can be properly released from inhalers and reach the deep lung (449). Despite presenting the same aerodynamic diameter, large porous particles have a lower surface-to-volume ratio compared to small nonporous particles, thus aggregating less and behaving more as single entities during aerosolization. Additionally due to its high geometric size they could avoid more easily phagocytosis by macrophages (301). For example, insulin-encapsulated PLGA/cyclodextrin microspheres presenting geometrical diameter similar to our particles ($D_{0.5}$ of 26 µm) were able to reach the deep lung and promote a significant hypoglycemic effect when tested *in vivo* in rodents (24).

Due to its shape and elevated Carr's index (≥ 26) and Hausner ratio (≥ 1.35) values, formulations could present some limitations regarding flowability and by that, lung deposition. Despite being extensively used to predict the quality of powders regarding flowability and deposition; precaution must be taken during the analysis of Carr's index and Hausner ratio, since for some powders a direct correlation between lower Carr's index and Hausner ratio values and higher FPF was not observed (477, 478). Additionally, non-spherical particles, especially fibers, could present some dispersion limitations due to the attractive forces existent between adjacent particles (269).

Nevertheless, in this study good aerosolization properties were obtained as observed by the low MMAD and high FPF fractions, in spite of the low theoretical flowability. SOL and F127 presented the higher FPF and best aerosolization properties (Table 4.5) correlating to the particle size distribution determined by laser diffraction, were both formulations presented the smallest mean diameter values and absence of large size aggregates. The lower CMC values of SOL and F127 originated more compact, smaller micelles that could lead to small powder particles. The FPF of insulin dry powders varies according to the formulation, the technique and the parameters used to assess it, which turns the comparison between formulations a rather intricate task. A formulation of freeze-dried insulin with lactose as coarse carrier showed a FPF of ~52% at a flow rate of 60 L/min

(479), while spore like particles showed FPF >69% (480), and Exubera® a FPF of 33-45% (481). Unlike many authors that take stage 2 (corresponds to the pharynx with a cutoff diameter of 5.8 µm) and lower into account for the calculation of FPF (482-484), in this work only particles that are able to deposit in the trachea (stage 3 with cutoff diameter of 4.7 µm) or lower airways and alveoli were considered. The pharmacological efficacy and clinical outcome of aerosol formulations is related to its deposition profile in the lungs (449), thus higher amounts of insulin are expected to reach the lungs and become available to be absorbed in SOL and F127-based formulations. Future improvements in the efficiency of the formulations could be explored by screening an inhaler device that best fits the characteristics of the developed powders, since the inhaler device has shown to influence the performance of the formulations (280). Additionally, the incorporation of an appropriate coarse carrier to the formulation could improve the deposition of particles in the deep lung by reducing the particle to particle interaction and aggregation of nanocomposites, as well as their electrostatic interaction with the capsule and the inhaler device (283, 485).

Release studies of insulin from micelles were performed in the absence or presence of 1.2 mM glucose. The concentration of glucose used was based on determinations of lung glucose levels performed in diabetic patients without lung disease (486). Insulin release profiles followed a biphasic pattern (Figure 4.8) as reported by others (333). F68 and F108 showed the faster and higher release of insulin, while SOL and F127 presented a more sustained release of insulin over time, which is related to the higher stability upon dilution of micelles composed of polymers with lower CMC. Therefore, the former could be explored as formulations of rapid-acting insulin, while the latter ones as long-acting insulin powders. Furthermore, with a proper mixture of different micelles a formulation with both post-prandial and long-acting effects could be achieved, which holds an advantage over formulations that only present fast-acting or prolonged released of insulin (334, 481, 487). PBA did not confer glucose-sensitive properties to formulations but promoted a faster *in vitro* release of insulin from the micelles. At pH 7.4, PBA presents mainly neutral hydrophobic moieties (433) (~96 % estimated by *in silico* simulation using the Marvin Suite software from ChemAxon, Hungary), thus potentially being present in the inner core of the micelles as confirmed by XPS analysis, not being able to react with the glucose present in liquid media. Nevertheless, the small percentage of ionic species might increase the hydrophilicity of micelles, promoting some destabilization and a faster release of insulin when compared to the formulations without PBA, even in the absence of glucose. Grafting PBA to the hydrophilic segments of the polymers could ensure the presence PBA at the surface of micelles and provide them with the desired glucose-

sensitive properties (436). Also, a covalent modification of insulin as recently performed by Chou and co-workers (488) prior to its encapsulation into the micelles is other possible approach. Regarding SOL-based formulations, further studies are required to analyze deeply the effect of glucose concentration of the release properties of SOL and study the possible stimuli-responsive properties of the polymer in future applications.

Lyophilized formulations were stored at two different temperatures and characterized in terms of size, surface charge and insulin conformation after 1, 3 and 6 months of storage (Figure 4.9 and 4.10). Excepting for some F68 and F108-based micelles for which time and storage temperature induced some degree of particle aggregation, formulations presented similar particle sizes after dispersion in water compared to recently lyophilized formulations. In addition, no changes in the surface charge of micelles were observed. Redispersed micelles presented particle size lower than 600 nm and neutral surface charge in all formulations. SOL and F127-based micelles presented the best results during the storage period studied. Regarding protein stability, storage seemed to induce, to a small extension, loss on insulin conformation in all formulations as seen by a decrease of AO and SCC values in stored samples (Table 4.7). The higher percentages of conformational loss were observed for insulin-loaded SOL micelles stored at 4ºC, with a reduction of 15.04±0.20% and 22.65±1.15% in AO and SCC values, respectively. The storage temperature did not show to influence to a high extent the secondary structure of insulin. In SOL-based micelles insulin structure was dominated by a random coil and low-frequency β-sheet organization. Considering the Pluronic® formulations it was observed that no significant changes in insulin structure band positions was observed. Indeed, the α-helix band of insulin in all those formulations was maintained in its characteristic band range, maintaining also happened to its high and low β-sheets assignments. The FTIR spectra results for these formulations, justify in fact the high AO and SCC values obtained, since minor band position changes were observed. Pluronic® copolymers showed to enhance the conformational stability of different proteins against different processing methods and thermal stress, including salmon calcitonin (489), interleukin-1 (IL-1) receptor antagonist (490), which can be due to the PEG chains as already mentioned. Nevertheless, for PBA containing formulations although the α-helix and β-sheets high-frequency assignments did not drastically change over the 6 months of storage at both 4 ºC and 20 ºC, the appearance of a band peak at 1600 cm^{-1} suggested that PBA may affect insulin stability during storage. These results regarding PBA containing formulations were not corroborated with the far-UV CD experiments performed to the samples stored during 6 months (Figure 4.13), since no significant differences were observed between

micelles with and without PBA. However, a close attention to the effect of PBA on insulin structure should be paid.

Taking into account the results, lyophilization of insulin-loaded micelles may improve the storage shelf-life of the final product, since the acquisition of amorphous powders will improve the physical and chemical stability of formulations. As referred previously, in liquid state micelles tend to aggregate creating particles on micron size range. Also, powders for pulmonary administration are considered advantageous over liquid formulations for many reasons including higher stability. Regarding the protein, solutions of insulin shown to be more prone to instability due to hydrolytic activity of water, namely with the earlier loss of conformation upon storage (453). In addition, in lyophilized formulations insulin shown to be at amorphous state, which may improve its stability, since contrary to what happens with many proteins, insulin presents greater stability in amorphous state (491). This assumption is supported by the maintenance of high percentages of native-like conformation of insulin in lyophilized formulations upon storage compared to recently formulated samples, as well as taking into consideration the example of Exubera®, a spray-dried insulin formulation in amorphous state that shown to be stable when stored at room-temperature (481).

5. Conclusions

Lyophilization of micelles allowed the production of powder nanocomposites that were easily redispersed when in contact to liquid media, originating micelles smaller than 300 nm and neutral charge at body temperature. This behavior can contribute for an increase in the bioavailability of insulin as micelles should prevent partially the clearance of micelles by alveolar macrophages. Insulin shown to be at amorphous state as evidenced by DSC, XRD and Raman spectroscopy and partially at the surface of micelles as evidenced by XPS. In addition, these formulations can be recovered by dispersion, in a manner of preserving the structure and potentially maintaining the activity of insulin.

Lyophilized low-density powders composed by large-porous particles presented, in general, aerodynamic diameters compatible with good lung deposition patterns. Analysis of powder morphology shown that they are formed by a non-homogenous population of needle-shape particles mixed with a kind of plate-shape structures which could result in limited flowability of powders, as predicted by Carr's index and Hausner ratio. However, the *in vitro* deposition profiles observed presumes interesting *in vivo* performance of some formulations.

PBA did not significantly affect the characteristics of formulations but promote a faster *in vitro* release of insulin from the micelles. However, it did not confer the formulations with glucose-sensitive properties.

Formulations showed to be physically stable upon storage with minimal loss of the insulin's native-like structure. Pluronic®-based formulations presented the best results regarding the maintenance of protein conformation analyzed by FTIR, however, far-UV CD studies showed that SOL-based micelles can also maintain a good amount the native-like structure.

In conclusion, powders formulations have shown promising results as delivery systems of inhaled proteins justifying further *in vitro* and *in vivo* assessment.

Chapter 5

In vitro biological assessment of powder formulations for inhalation of insulin

The information presented in this chapter was partially published in the following publication:

Fernanda Andrade, José das Neves, Petra Gener, Simó Schwartz Jr, Domingos Ferreira, Mireia Oliva, Bruno Sarmento, Biological assessment of self-assembled polymeric micelles for pulmonary administration of proteins, submitted for publication

1. Introduction

Biopharmaceuticals hold the potential for the treatment of numerous diseases, for many of which there is no current available cure provided by small molecule drugs (492). This explains the high demand for research and development of formulations based on biopharmaceuticals and the exponential increase in the approval and market share of these formulations that has been witnessed over the past few years. Since biopharmaceuticals are generally administered by injection, a variety of approaches to develop systems for non-invasive administration of such drugs have been proposed recently. For example, oral and pulmonary administration of insulin is being pursued by many researchers, and positive advances in the field have been achieved (326, 493-495). Inhalation appears as a promising non-invasive route for systemic delivery of biopharmaceuticals, reasoned by characteristics of the respiratory system, such as the high area of absorption and blood supply, and the absence of hepatic first-pass metabolism, thus allowing high bioavailability values compared to other non-invasive routes (213, 492). Additionally, reduced costs associated to the production, transport and administration, as well as higher stability and patient compliance are expected for solid formulations for inhalation as compared to parental administration (492). However, the complexity of inhalation and respiratory system (geometry, humidity, defense mechanisms) allied to the challenges posed by the development of biopharmaceuticals-based inhaled formulations, are underneath the fact that only a very restricted number of these products has reached the market so far (213). Thus, several research groups have developed new and improved formulations based on advances observed in molecular biology and particle engineering technology. Nanocarriers, including polymeric micelles, have been proposed as advanced inhaled drug delivery systems with optimized pharmacokinetics and pharmacodynamics. Among other things, nanocarriers could increase the permeation of compounds through the epithelium, reduce the clearance by mucociliary escalator through the penetration of particles in the mucus as well as reduce the recognition of particles by alveolar macrophages (496).

In this chapter, the suitability of powders developed in *Chapter 4* as delivery systems for inhalation of proteins was assessed *in vitro* using pulmonary epithelial cell lines and macrophages.

2. Experimental

2.1. Materials

SOL, F68, F108, and F127 were kindly provided by BASF (Ludwigshafen, Germany). Lyophilized human insulin (potency ≥ 27.5 units per mg), PBA, PBS, 3-(4,5-Dimethylthiazol-2-yl)-2,5-diphenyltetrazolium bromide (MTT), Triton X-100, β-mercaptoethanol, phorbol 12-myristate 13-acetate (PMA), and 5-([4,6-dichlorotriazin-2-yl] amino)fluorescein hydrochloride (5-DTAF) were purchase from Sigma-Aldrich (St. Louis, MO, USA), while sodium bicarbonate and dimethyl sulfoxide (DMSO) from Merck KGaA (Darmstadt, Germany). The other reagents used were methanol, ethanol and acetic acid from analytical grade; acetonitrile and TFA of HPLC grade (Merck, Germany) and Type 1 ultrapure water (18.2 MΩ.cm at 25 ºC, Milli-Q®, Billerica, MA, USA).

Dulbecco's modified eagle medium (DMEM) supplemented with L-glutamine (DMEM-GlutaMAX®), fetal bovine serum (FBS), non-essential amino acids, 10000 U/mL penicillin and 10000 µg/mL streptomycin, 0.25% Trypsin-EDTA were purchased from Gibco (Life Technologies Ltd., Paisley, UK). CellMask® DeepRed Plasma membrane Stain, 4′,6-diamidino-2-phenylindole (DAPI) and ProLong® Gold Antifade Mountant were purchased from Molecular Probes (Life Technologies Ltd., Paisley, UK). RPMI-1640 was purchased from Lonza (Basel, Switzerland).

2.2. Production of micelles and lyophilization

Micelles were prepared using the thin-film hydration technique. Briefly, each polymer was individually weight and dissolved in a mixture of methanol:ethanol (1:1). Then, the solvent was removed under vacuum and the film was left to dry overnight at room-temperature to eliminate any remained solvent. The film was then hydrated with PBS at 37 ºC in order to obtain a 1 % (w/v) solution and vortexed for 5 min. The obtained dispersion was filtered through a 0.22 µm syringe filter to remove possible dust and aggregates.

PBA containing micelles were prepared by dissolving PBA with the polymers in the solvents prior to the production of the film at a ratio of 10:1 (w/w) (polymer:PBA). Insulin-loaded micelles were prepared by hydrating the polymeric films with an insulin solution in PBS to obtain polymer:insulin ratios of 10:1 (w/w). The other steps were the same as for plain formulations.

After production micelles were lyophilized in an AdVantage 2.0 BenchTop Freeze Dryer (SP Scientific, Warminster, PA, USA). The cycle used was the follow: the samples were

frozen at -30 ˚C and the temperature maintained for 60 min, the primary drying was set at 20 ˚C for 480 min at 150 mTorr and the secondary drying for another 480 min at 30 ˚C and 100 mTorr.

2.3. Conjugation of polymers with 5-DTAF

Polymers were fluorescently conjugated with 5-DTAF in an aqueous medium via nucleophilic aromatic substitution by an addition-elimination pathway as previously described (497). Briefly, a stock solution of 20 g/L 5-DTAF in DMSO was diluted in 0.1M sodium bicarbonate (pH 9.3) and added to a 6 % (w/v) polymer solution in 0.1M sodium bicarbonate (pH 9.3) to a final molar ratio of 1:2 (polymer:5-DTAF). The reaction proceeded overnight in the dark at room-temperature. The labelled polymer was purified from the excess of unreacted 5-DTAF by dialysis (12,000-14,000 MWCO Spectra/Por® membrane from Spectrum Europe BV, The Netherlands) against Type I ultrapure water. The dialyzed polymer solutions were lyophilized as described in the manuscript and stored in closed containers protected from light. A schematic representation of fluorescent-labeled polymers preparation is depicted in Figure 5.1.

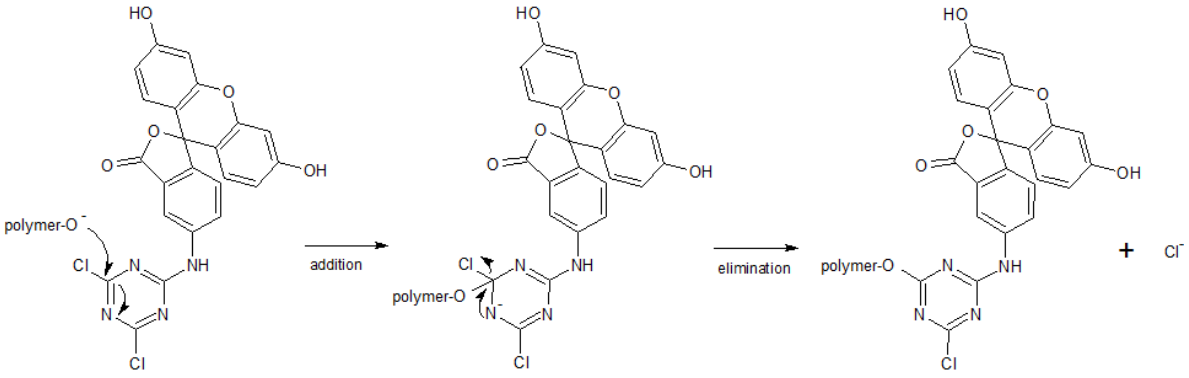

Figure 5.1 Reaction schematic for the conjugation of the polymers with 5-DTAF via nucleophilic aromatic substitution by an addition-elimination mechanism. At basic pH, the terminal hydroxyl group of PEG blocks presented in the polymers, attack the reactive moiety (2-amino-4,6-dichloro-s-triazine) on the 5-DTAF molecule, promoted by strong electron-withdrawing groups (N) of the s-triazine ring.

2.4. Production and characterization of fluorescent micelles

Fluorescent-micelles were produced and lyophilized like empty micelles substituting polymers by 5-DTAF-conjugated polymers. Particle mean hydrodynamic diameter and PdI

was measured without dilution of the samples by DLS at 37 °C using a detection angle of 173° and zeta potential by laser doppler micro-electrophoresis using a NanoZS (Malvern Instruments, UK). For each type of formulation were produced and analyzed at least three replicates.

2.5. Cell lines and culture conditions

Calu-3 (ATCC number HTB-55), A549 (ATCC number CCL-185), RAW 264.7 (ATCC number TIB-71), THP-1 (ATCC number TIB-202) and U937 (ATCC number CRL-1593.2) cell lines were obtained from the American Type Culture Collection (ATCC, Manassas, VA, USA). Calu-3, A549 and RAW 264.7 adherent cells were grown separately in flasks in DMEM-GlutaMAX® while THP-1 and U937 cells were grown separately in suspension in flasks in RPMI-1640 at 37ºC under 5% CO_2 water saturated atmosphere. Both media were supplemented with 10% (v/v) FBS, 1% (v/v) non-essential amino acids and 100 U/mL penicillin and streptomycin. For THP-1 cells, β-mercaptoethanol to a final concentration of 0.05 mM was further added to the medium. The medium was changed every other day and, upon confluence, cells were harvested from flasks with trypsin-EDTA (Calu-3 and A549) or a cell scraper (RAW 264.7) and passed or just passed (THP-1 and U937) to other flasks to continue expansion, be frozen or used in *in vitro* studies.

2.6. Assessment of cytotoxicity

The effect of formulations on cellular viability and membrane integrity of Calu-3, A549 and Raw 246.7 cell after 24h incubation was assessed using the MTT conversion assay and a LDH leakage assay (LDH Cytotoxicity Detection Kit, Takara Bio Inc., Shiga, Japan), respectively.

For MTT assay, cells were seeded separately in 96-well microplates at $5x10^3$ cells/well in 200 µl of complete medium and incubated for 24 hours at 37 ºC in 5% CO_2 environment. The medium was removed and the cells washed with 200 µl of PBS. Then, test solutions, positive control (complete medium) and negative control (2% (w/v) Triton X-100) were added to cells for 24 hours, after which 20 µl of 5mg/ml of MTT solution was added to each well and incubated for 4 hours at 37 ºC. After dissolution of the formed formazan crystals with 200 µl of DMSO, the absorbance was determined at 590 nm with 630 nm background deduction. Each treatment was tested at least in five individual wells.

Regarding LDH release assay, cells were seeded in 96-well microplates at $5x10^3$ cells/well and incubated for 24 hours at 37 ºC in 5% CO_2 environment. The medium was

removed and cells washed with 200 µl of PBS. Test solution, negative control (medium) and positive control (2% (m/v) Triton X-100) in serum free medium were added in at least five wells each and cells incubated for 24 hours. After that, the plates were centrifuged for 10 min at 250xg to remove detached cells and the LDH-content of 100 µl supernatant was measured at 490 nm (and 630 nm for background deduction) in a plate reader using a commercial test kit after incubation for 30 min at room temperature in the dark. The apparent cytotoxicity was calculated according to Equation 5.1.

$$\text{Cytotocxicity } \% = \frac{\text{Experimental value} - \text{Negative control}}{\text{Positive Control} - \text{Negative Control}} \times 100 \qquad \textbf{Equation 5.1}$$

The results of MTT and LDH release assay were used for the determination of half maximal cytotoxic concentration (CC_{50}) index by nonlinear regression of concentration-effect curve fit using Prism 6.02 software (GraphPad Software, Inc., CA, USA).

2.7. Permeability of insulin through pulmonary epithelium

The permeability of free and formulated insulin through alveolar and bronchial epithelium was assessed using A549 and Calu-3 cell monolayers, respectively. Cells were seeded at a density of $8x10^5$ cells/cm^2 onto the apical surface of Transwell® permeable supports (0.33 cm^2 polyester, 0.4 mm pore size, from Costar®, Corning Life Sciences, France) in 0.2 mL complete medium with 0.5 mL medium added to the basolateral chamber. The development of cell monolayers was monitored by measuring the transepithelial electrical resistance (TEER) using chopstick electrodes (STX-2) and an EVOM voltohmmeter from World Precision Instruments (Stevenage, UK). TEER was calculated by subtracting the resistance of a cell-free culture insert and correcting for the surface area of the Transwell® cell culture support. Cell monolayers were used after TEER values reached stable maximum values at 14-15 days in culture. TEER was also measured during experiments as an index of cell viability and monolayer integrity. For all permeability studies, the culture medium was removed and the cell monolayers were washed with 37 ºC PBS. After washing, 0.2 mL of insulin solution or insulin-loaded micelles dispersed in PBS heated at 37 °C and at an initial concentration of 1000 µg/mL was added to the apical (donor) side, while 0.6 mL of PBS at 37 °C was added to the basolateral (receptor) side. At different times (0.25, 0.5, 0.45, 1, 2, 4, 6, 8 hours), 0.2 mL of basolateral samples were collected and replaced by equal volumes of PBS pre-heated at 37 °C, and insulin determined by HPLC as described in *Chapter 3*.

Apparent permeability coefficient (Papp) values (cm/s) were calculated from the measurement of the flow rate of insulin from the donor to the acceptor chambers using Equation 5.2.

$$\mathrm{Papp} = \frac{\mathrm{dQ}}{\mathrm{dt}}(\mathrm{A} \times \mathrm{C0}) \qquad \textbf{Equation 5.2}$$

where dQ is the total amount of permeated insulin (µg), A is the diffusion area (cm^2), C0 is the initial concentration of insulin (µg/mL), and dt is the time of experiment (s). The coefficient dQ/dt represents the steady-state flux of insulin across the monolayer. The permeability enhancement ratio (PER), expressed as the ratio between the Papp of insulin associated with micelles and the Papp of insulin in solution, was also calculated.

2.8. Interaction of micelles with macrophages

The uptake of the 5-DTAF-labelled micelles by PMA-stimulated THP-1 and U937 macrophages was assessed qualitatively by confocal microscopy using a Spectral Confocal Microscope MFV1000 (Olympus Corporation, Japan) and quantitatively by flow cytometry (fluorescence-activated cell sorting (FACS) analysis) in a cytometer Fortessa (BD Biosciences, USA). THP-1 and U937 cells at a density of $5x10^5$ cells/well were seeded separately in 24-well plates in complete medium supplemented with 25 ng/mL of PMA to induce the monocytic differentiation into adherent macrophages. 48 hours after seeding, the medium and non-adherent cells were removed by washing twice with PBS. Particle suspensions in complete medium (1 and 2 mg/mL) were incubated for 4h at 37 ºC and non-internalized fluorescent micelles removed by washing twice with PBS. Cells were detach with trypsin:EDTA (U937 cells) or using a cell scraper (THP-1 cells) and redispersed in PBS, supplemented with 10% FBS. Cells were then analyzed in a cytometer Fortessa (BD Biosciences, USA). Green fluorescence from micelles was detected through the EYG-A channel. The viability of the cells was assessed using DAPI and the cells derbies and doublets of cells were removed by forward and side scatter gating. The analysis of the obtained data was performed with FACS Express 4 software. For each sample, at least 10,000 individual cells were collected and the mean fluorescence intensity was evaluated.

For microscopy studies, 0.1% gelatin-coated coverslips were inserted into the wells prior to cells addition. After 48h of differentiation, the medium containing PMA was removed

and the cells washed twice with PBS to remove non-adherent cells and fluorescent micelles suspension (1 mg/mL) was added to each well. After 4h incubation at 37 ºC, the cells were washed twice with PBS and the membrane stained with CellMask® DeepRed (5 µg/mL) for 5 min at 37 ºC. After washing with PBS (2x), cells were fixed with a mixture of methanol:acetic acid (3:1) for 20 min at room-temperature. Cells were further washed with PBS and the nucleus stained with DAPI (0.2 mg/mL) for 5 min at room-temperature. Before mounting the coverslips into glass slides with ProLong® Gold Antifade Mountant and allowing them to dry, the cells were washed with Type I ultrapure water to remove salt traces. Image analysis of xy planes and z-series scanning was performed using a Spectral Confocal Microscope MFV1000 (Olympus Corporation, Japan). The 561 nm excitation wavelength of the green laser (10mW) was used for selective detection of the red fluorochrome (CellMask® DeepRed). The 488 nm excitation wavelength of Argon multiline laser: 458nm, 488nm and 515nm (40 mW) was used for selective detection of the green fluorochrome (5-DTAF). The nuclear staining DAPI was excited at 405 nm with a violet laser (6 mW). For detecting 3 PMT, detectors for fluorescence (2 plus 1 spectral detection with conventional filters) plus 1 per detector interdifferential contrast were used. Images were acquired with the FluoView FV10-ASW software (Olympus Corporation, Japan), and processed in conjugation with the orthogonals projections using the ImageJ 1.48v software (National Institutes of Health, MD, USA).

2.9. Statistical analysis

One-way ANOVA was used to investigate the differences between the formulations and controls. Post hoc comparisons were performed according to Tukey's HSD test ($p<0.05$ was accepted as denoting significance) using Prism 6.02 software (GraphPad Software, Inc., CA, USA).

3. Results

3.1. *In vitro* assessment of the effect of formulations on cell membrane toxicity and viability

The effect of formulations on cell viability and membrane integrity of pulmonary bronchial (Calu-3) and alveolar (A549) epithelial cell lines, as well as in macrophages (Raw 264.7) after 24h of incubation is presented in Figure 5.2 and 5.3, respectively.

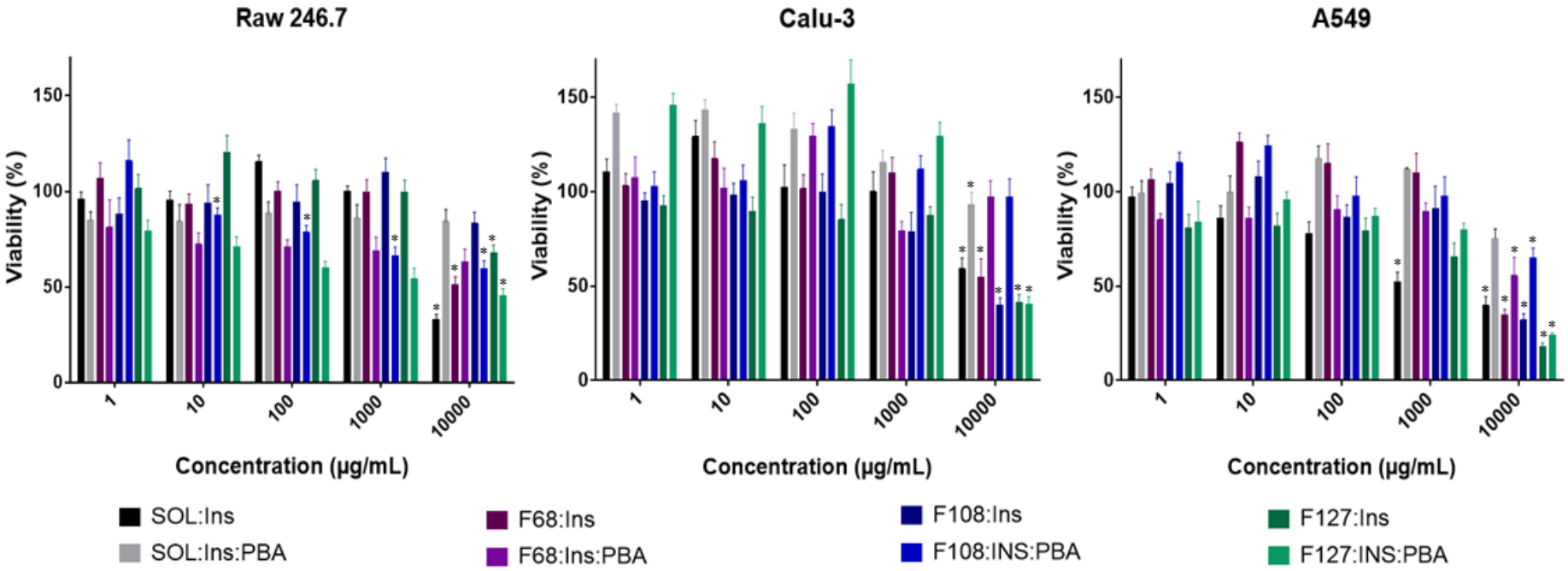

Figure 5.2 Formulations' toxicity profile regarding cell viability of Raw 246.7, Calu.3 and A549 cell lines. Results are expressed as mean ± SEM (n=5). * Denotes a significant ($p<0.05$) lower percentage of viability when compared to lower concentrations of the formulation.

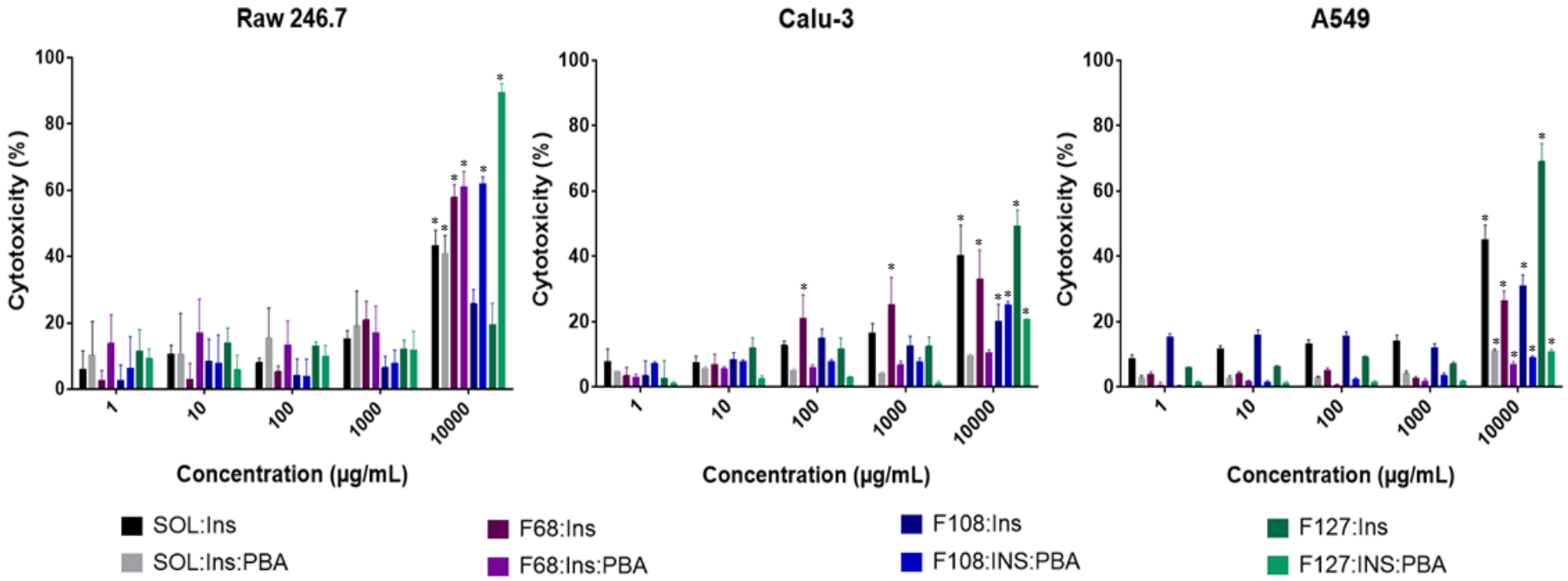

Figure 5.3 Formulations' toxicity profile regarding membrane integrity of Raw 246.7, Calu.3 and A549 cell lines. Results are expressed as mean ± SEM (n=5).

* Denotes a significant ($p<0.05$) higher percentage of cytotoxicity when compared to lower concentrations of the formulation.

Additionally, CC_{50} values are expressed in Table 5.1.

Table 5.1 Half maximal cytotoxic concentration (CC_{50}) values (in mg/mL) of insulin-loaded micelles as determined by lactate dehydrogenase (LDH) leakage and 3-(4,5-dimethylthiazol-2-yl)-2,5-diphenyltetrazolium bromide (MTT) assay in different cell lines. The values presented were obtained through a nonlinear regression of the mean percentage toxicity values versus concentration of formulation using 5 replicates.

Sample	LDH			MTT		
	Raw 264.7	A549	Calu-3	Raw 264.7	A549	Calu-3
SOL:Ins	>10	>10	>10	4.9	1.0	>10
SOL:Ins:PBA	>10	>10	>10	>10	>10	>10
F68:Ins	6.2	>10	>10	>10	7.5	>10
F68:Ins:PBA	8.3	>10	>10	>10	>10	>10
F108:Ins	>10	>10	>10	>10	1.8	1.2
F108:Ins:PBA	8.2	>10	>10	>10	>10	>10
F127:Ins	>10	9.0	>10	>10	1.2	1.2
F127:Ins:PBA	6.0	>10	>10	6.1	3.4	>10

At high concentrations, formulations seemed to exert higher negative effects on the viability of A549 cells (MTT assay), while Raw 264.7 cells seemed to be more prone to suffer membrane damage (LDH leakage assay). The CC_{50} values of all formulations are superior to their concentrations expected in the lungs after administration.

3.2. Determination of the apparent permeability coefficient of insulin through pulmonary epithelium

Permeability of insulin through pulmonary epithelium was assessed using monolayers of A549 or Calu-3 cells. Results as the cumulative percentage of insulin presented in the basolateral chamber of Transwell® systems over time are presented in Figure 5.4 (A and C). Also, values of Papp and PER in both monolayers are presented in Table 5.2. In both models, insulin levels rapidly increased in the first 60 min and continued to be transported at least up to 8h. The total amount of insulin in solution that crossed the cell barrier after 8h was around 5 % and 7 % of the initial concentration in Calu-3 and A549 monolayers, respectively.

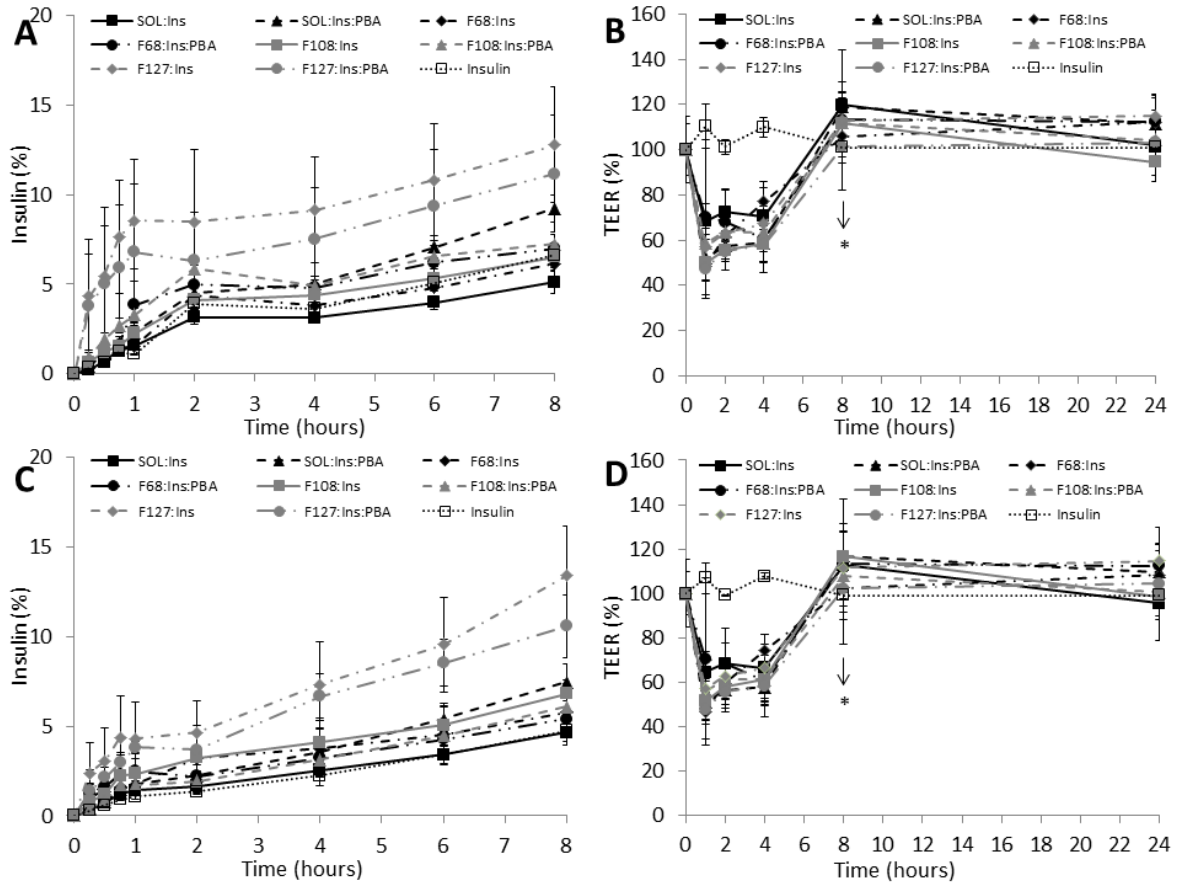

Figure 5.4 Permeability of insulin through A549 (A) and Calu-3 (C) cell monolayers, expressed as the percentage of insulin added to the apical chamber of Transwell® system; and transepithelial electrical resistance (TEER) values as percentage of the of the values prior to experiment during permeability studies across A549 (B) and Calu-3 (D) cell monolayers. Results are presented as mean values ± SD (n=3). * Removal of samples after the 8h of experiment and addition of complete medium.

Some formulations were able to increase the epithelial permeability of insulin, especially through Calu-3 monolayers, as compared to the insulin in solution as evidenced by the PER values. However, only F127-based formulations were able to increase significantly the permeability of insulin through Calu-3 monolayers ($p<0.05$).

Contrasting to insulin solution, the presence of formulations affected the TEER values of cell monolayers (Figure 5.4 B and D). However the decrease in the resistance of the monolayers was reversible, since it recovered to initial values after the substitution of formulations for complete medium. The initial values of TEER remained until at least 24 hours after the beginning of the experiment, indicating integrity of the monolayer after the incubation with the formulations, and that the effects of formulations on tight junctions, if any, were fully reversible.

Table 5.2 Apparent permeability coefficient (Papp) and permeability enhancement ratio (PER) of insulin across A549 and Calu-3 cell monolayers. Results are presented as mean values ± SD (n=3). * Denotes a significant difference ($p<0.05$) when compared to the insulin solution.

Sample	A549		Calu-3	
	Papp (cm/s 10^{-6})	PER	Papp (cm/s 10^{-6})	PER
Insulin solution	1.29±0.06		0.89±0.03	
SOL:Ins	0.94±0.08	0.73	0.82±0.07	0.93
SOL:Ins:PBA	1.76±0.10	1.36	1.41±0.12	1.58
F68:Ins	1.15±0.05	0.89	0.97±0.16	1.08
F68:Ins:PBA	1.29±0.04	1.00	0.79±0.04	0.88
F108:Ins	1.17±0.07	0.91	1.15±0.04	1.29
F108:Ins:PBA	1.21±0.11	0.94	1.09±0.09	1.22
F127:Ins	1.45±0.12	1.13	2.15±0.31*	2.40
F127:Ins:PBA	1.32±0.06	1.02	1.88±0.24*	2.10

3.3. Characterization of fluorescent micelles

Fluorescent-labelled micelles were produced and lyophilized to be used in macrophage uptake experiments. The characteristics of redispersed micelles at 37 ºC are resumed in Table 5.3. The conjugation of polymers with the fluorescent probe did not affect strongly the characteristics of micelles. Only F68 and F108-based micelles showed some differences ($p<0.05$) compared to the non-fluorescent insulin-loaded micelles at the same temperature.

Table 5.3 Mean hydrodynamic diameter, polydispersity index (PdI) and zeta potential of redispersed lyophilized fluorescent-labelled micelles at 37 ºC. Results are presented as mean values ± SD (n=3). * Denotes a significant difference ($p<0.05$) when compared to the insulin-loaded redispersed lyophilized micelles of the same polymer analyzed at 37 ºC.

Sample	Hydrodynamic diameter (nm)	PdI	Zeta potential (mV)
SOL	235.8±12.5	0.19±0.01	0.1±0.11
F68	211.2±7.9*	0.55±0.02	-0.1±0.05
F108	224.9±41.7*	0.40±0.05	-0.3±0.06
F127	39.4±4.5	0.37±0.03	0.1±0.03

3.4. Uptake of micelles by human macrophages

PMA-stimulated THP-1 and U937 cells were used as models to study the uptake of micelles by macrophages.

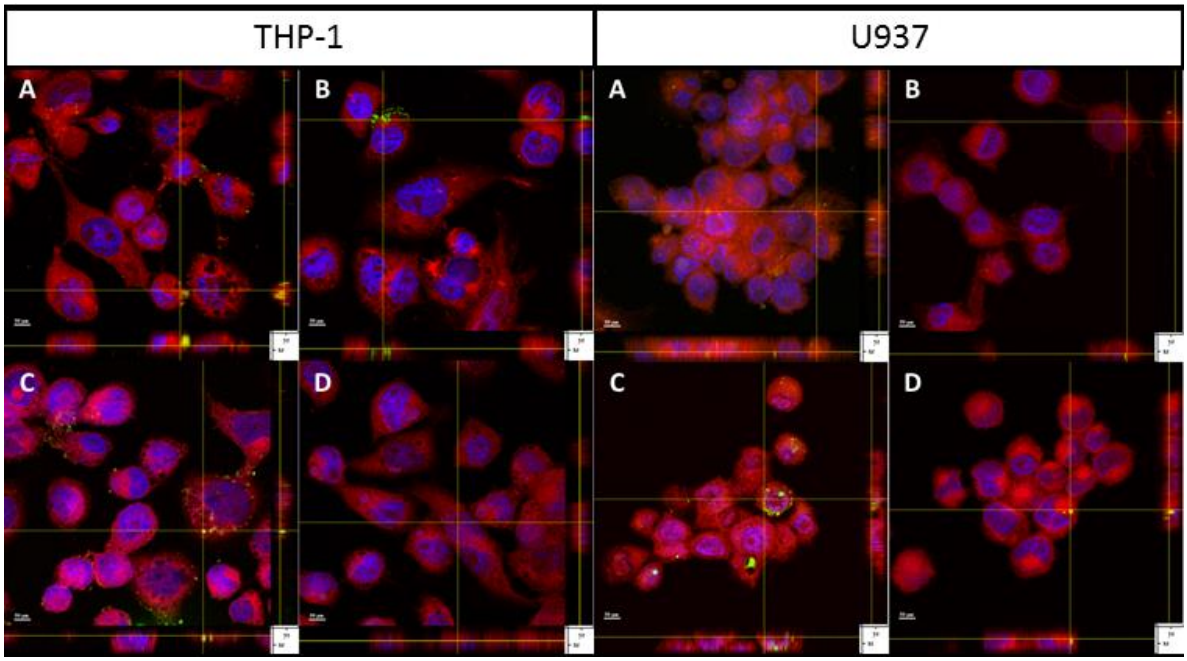

Figure 5.5 Confocal microscopy micrographs of SOL (A), F68 (B), F108 (C) and F127 (D) micelle's internalization by PMA-stimulated THP-1 and U937 macrophages. Each image provides a xy plane through a cell layer, and the cross-sectional view of the same section of the cell layer in the x–y and y–z orientation. Blue, green, and red fluorescence are from DAPI (nucleus), 5-DTAF-polymer (micelles) and CellMask® Deep Red (membrane), respectively.

All the formulations were internalized by the cells after 4h of incubation. Micelles attachment to the surface of cells was not apparent (Figure 5.5).

Table 5.4 FACS quantification of micelles uptake by PMA-stimulated THP-1 and U937 macrophages. The values are expressed as the percentage of cells emitting green fluorescence after 4h incubation with micelles at concentrations of 1 mg/mL and 2 mg/mL.

Sample	THP-1		U937	
	1 mg/mL	2 mg/mL	1 mg/mL	2 mg/mL
SOL	22.47	35.65	36.47	61.63
F68	25.99	45.1	14.92	37.47
F108	75.78	91.83	88.55	98.56
F127	12.08	34.56	13.4	38.86

As seen in Figure 5.6, Figure 5.7, and Table 5.4, the uptake of the micelles by macrophages varied according to the polymer used and was shown to be concentration dependent. An increase in the percentage of cells presenting fluorescence was observed when the concentration of micelles increased from 1 to 2 mg/mL.

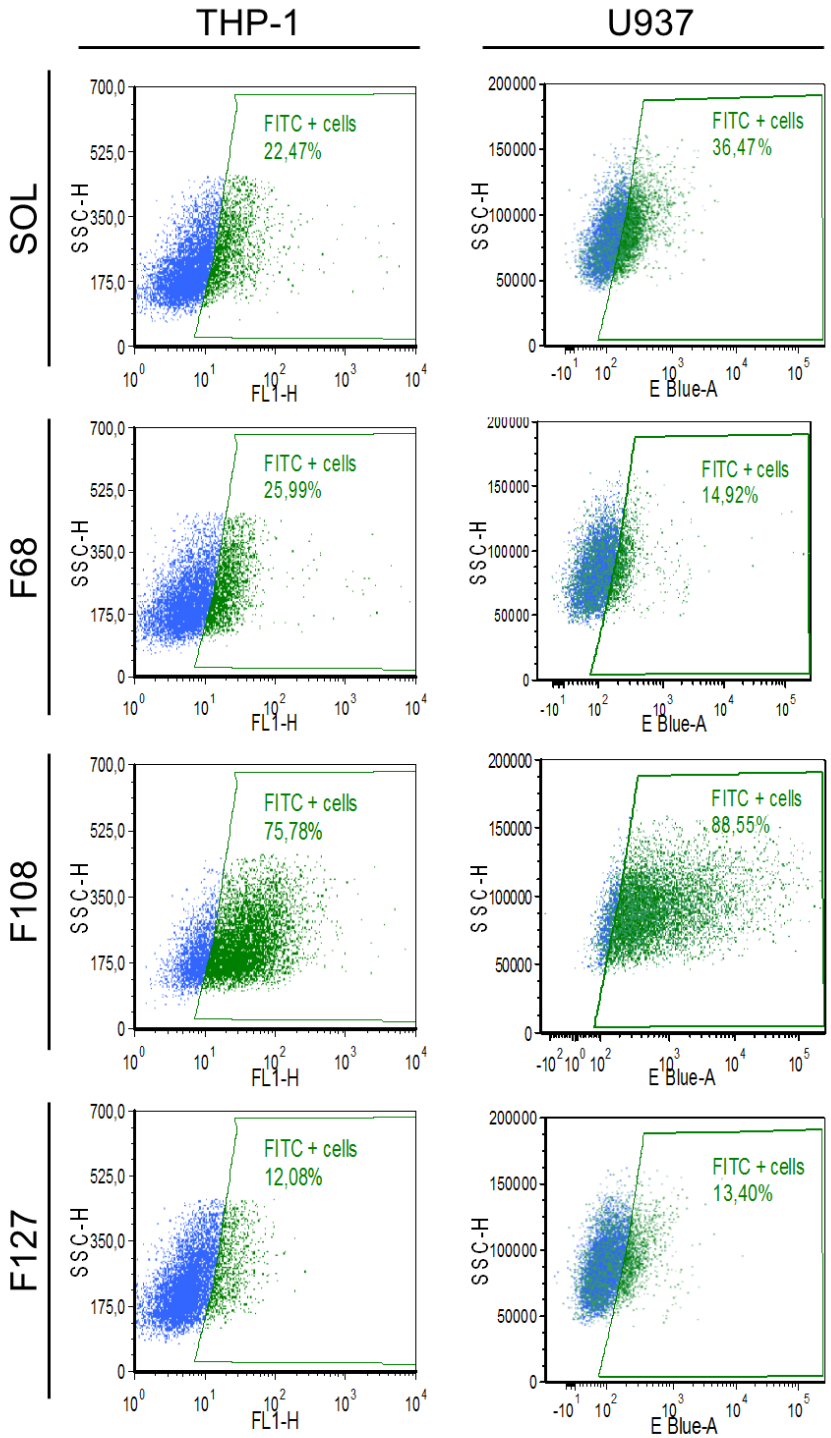

Figure 5.6 FACS quantification of micelles uptake by PMA-stimulated THP-1 and U937 macrophages. The values are expressed as the percentage of cells emitting green fluorescence after 4h incubation with micelles at a concentration of 1 mg/mL.

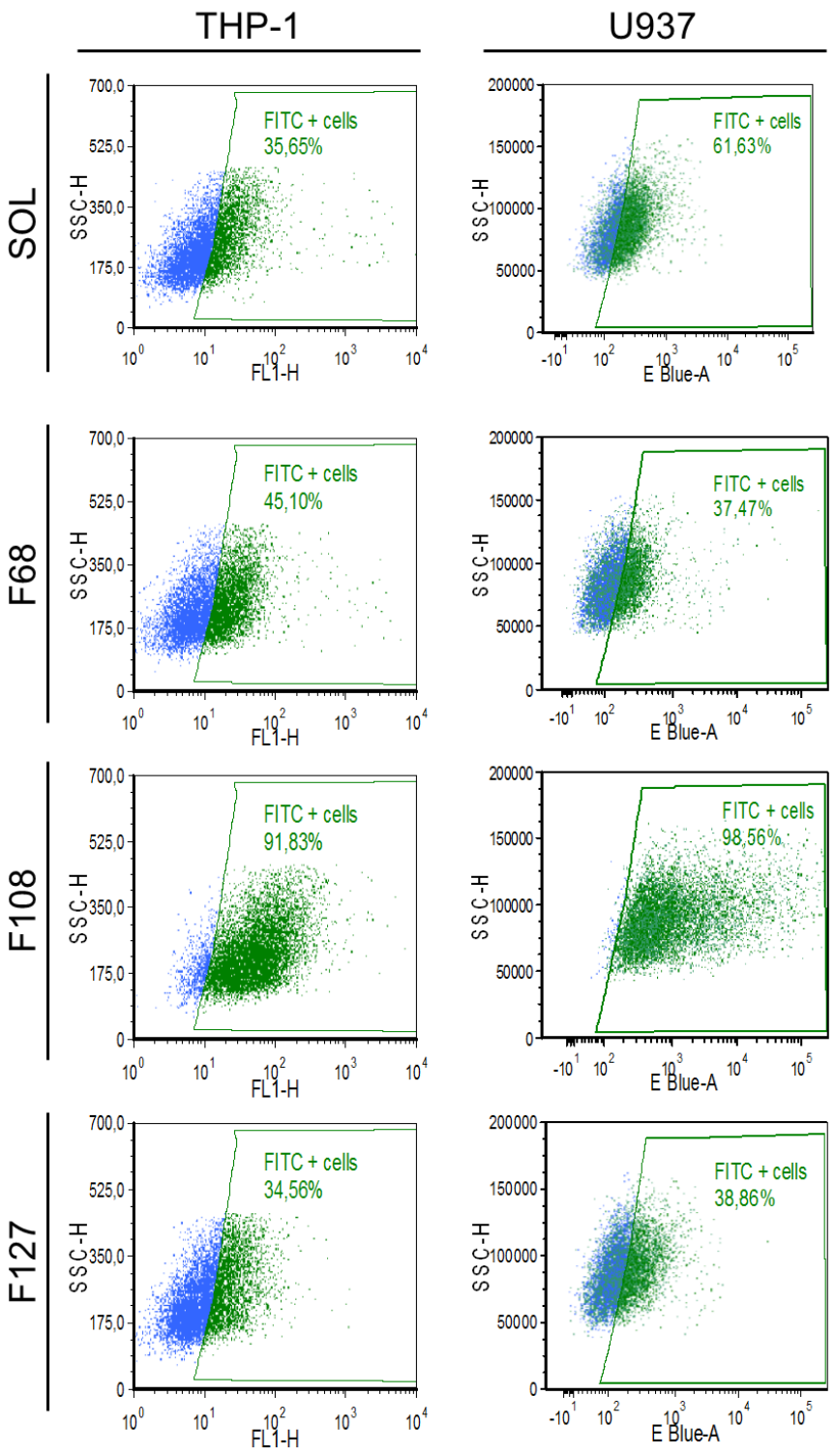

Figure 5.7 FACS quantification of micelles uptake by PMA-stimulated THP-1 and U937 macrophages. The values are expressed as the percentage of cells emitting green fluorescence after 4h incubation with micelles at a concentration of 2 mg/mL.

F127-micelles showed minimal uptake by both PMA-stimulated THP-1 and U937 macrophages while the other formulations underwent higher uptake. F108-micelles suffered the higher uptake by macrophages.

4. Discussion

Pluronic® are considered biocompatible and biodegradable polymers used in many biomedical applications including cell's encapsulation (498, 499). Thus, as expected, no significant signs of toxicity to both pulmonary cell lines and macrophages were observed in the *in vitro* experimental setting used as determined by MTT and LDH leakage assays (Table 5.1). This results are in accordance to other reports where F68 shown a CC_{50} higher than 10 mg/mL in Calu-3 cells (297), and F127 shown negligible toxicity against A549 cell up to 1 mg/mL (56). Some Pluronic® were shown to interact with cell membranes and intracellular organelles such as the mitochondria where it can interfere with metabolic processes (500). Demina and co-workers (2005) reported that Pluronic® presenting higher degree of hydrophobicity are more able to interfere with the membrane (501), which could be somehow related to the lower CC_{50} obtained with F108 and F127 formulations. Still, al the CC_{50} values are superior to 0.84 mg/mL, the concentration of formulation expected in the lungs taking into account basal requirements of insulin. These concentrations were calculated assuming 10 mL as volume of lung epithelial lining fluid (vary from 10 to 40 mL (502, 503)) and 21 IU as daily mean basal requirement for a 70 kg patient according to American Diabetes Association (504). Consequently, no significant pulmonary toxic effects of the formulations should be expected. However, *in vitro/in vivo* extrapolations should be done with caution, and *in vivo* studies are required to assess the pulmonary biocompatibility of formulations in animal models.

Monolayers of A549 or Calu-3 cells were selected as models to assess the permeability of insulin through pulmonary epithelium. Both cell lines have been extensively reported and used for study the drug transport across pulmonary epithelium (505, 506), being *in vitro* models considered a reliable method to predict the permeation behavior and bioavailability of drugs (507, 508). Due to its hydrophilic nature, insulin is expected to permeate monolayers manly via the paracellular route by passive diffusion; however, basolateral to apical transport of insulin have shown higher Papp values from those described to the apical to basolateral direction (508, 509), which could explain partially the low insulin permeability observed in this study and reported by others (510, 511). Nevertheless, both paracellular and transcellular pathways were described for insulin across pulmonary cell monolayers (Calu-3 and 16HBE14o-) (512). The values of Papp

obtained in this study differed from those reported by other groups, which could be explained by differences in the methodology used between studies (e.g. area available for permeation, concentration of protein, number of cells) (506, 513). Amphiphilic polymers, including Pluronic®, have been proposed as excipients for improved delivery of many drugs. Although not completely understood, it seems that this characteristic is related to its capacity to interact with cell membranes and interfere with its structure and microviscosity/fluidity (85, 501). This mechanism is also thought to interfere with the function of P-glycoprotein, explaining the inhibition of this efflux system observed with these polymers (85, 500). Pluronic® with HLB values and number of hydrophobic parts closer to those of F127 (HLB=18-23), reduced the cell membrane microviscosity and increased the fluidity, contrasting to polymers with higher HLB values like F68 and F108 (HLB>24) (85). The increased fluidity of the membrane could increase the transcytosis of insulin through the cells, thus explaining the higher permeation observed with F127 (Table 5.2). Macrogol-15-hydroxystearate (Solutol® HS15) micelles have shown to increase the transepithelial permeation of insulin through Calu-3 cell monolayers by a mechanism dependent on partitioning and changes on cellular membrane structure/fluidity (514). The same polymer also enhanced the nasal permeation of human growth hormone in rats (515). The variation in the TEER *vs* time profile of cell monolayers exposed to micelles (Figure 5.4) compared to insulin solution could be a consequence of the rearrangement of F-actin cellular distribution owing to a change in the membrane lipid environment (516), and not so dependent on effects in zonula occludens-1 (ZO-1) protein, as happens with other permeation enhancers like chitosan (517). Although, since ZO-1 binds directly to F-actin (518), changes in the F-actin could lead at some extent to distortions in ZO-1, contributing to the paracellular transport of insulin. Indeed, Solutol® HS15 micelles have shown to promote a redistribution of F-actin and slight changes in ZO-1 (514), being expected a similar pattern with our formulations.

As expected F127-micelles showed a lower uptake (Table 5.4) by macrophages which is possibly correlated to the small size of redispersed lyophilized micelles at 37 ºC (273, 519), while the other polymers presented larger particles and, consequently, underwent higher uptake. Also, the lower percentage of PEG in the constitution of SOL (13% of the polymer) could be contributing to the higher percentage of uptake when compared to F127-based micelles (70% of PEG), since the density of PEGylation seems to influence the phagocytosis (52, 520). Differences observed between F68 and F127 could also be related to the small MW of the PEG chains presented in F68 (approximately 4000 g/mol for F68 and 5000 g/mol for F127). In other studies, F68-coated particles showed higher uptake by macrophages when compared to F127-coated particles (521, 522). Regarding

F108 micelles, size appears to be the main responsible for the higher uptake compared to F127 micelles. However, there were no apparent differences in size and surface charge of micelles that could explain the high values of uptake observed with F108-micelles. Additionally, confocal microscopy analysis did not reveal a so marked difference between samples. Since the uptake of particles by macrophages is not restricted to phagocytosis (523, 524), and the experiment was run in a static model, it is possible that a percentage of the observed uptake occurred via nonphagocytic. In fact, the experiment was performed in medium supplemented with 10% FBS heat inactivated, which lacks on immunoglobulins and components of the complement system, the main serum opsonins; although presenting serum proteins that could also work as opsonins; which could lead to a reduced activation of the phagocytic pathway (190). However, the alveolar and airway area of lungs contains low levels of complement components, reason why alveolar macrophages seem to primarily execute phagocytosis via opsonin-independent mechanisms (525). SP-A and surfactant protein D (SP-D), member of collectin (collagen-lectin) family that also includes mannose-binding protein and some bovine serum proteins, act as opsonins in lungs (526, 527). SP-A, the most prevalent protein of surfactant, binds preferentially to lipophilic surfaces (528), thus we can speculate that low opsonization derived from SP-A adsorption and consequent low phagocytosis should be expected for small size PEGylated-hydrophilic shell micelles, which are in accordance to the results obtained. For example, Patel and co-workers (2012) showed that the conjugation of PEG to PLGA nanoparticles reduced their internalization by rat alveolar macrophages (529). Nevertheless, since differentiated monocytic cell lines and human macrophages take up particles via different mechanisms (524), and the concentrations tested are above the expected therapeutic concentration requested, the extrapolation of the *in vitro* results to the *in vivo* situation becomes difficulty. Being an *in vitro* model with advantages and drawbacks, this experiment serves as preliminary assessment with a predictive value that needs to be confirmed with further *in vivo* experiments.

5. Conclusions

No significant signs of toxicity on both pulmonary cell lines and macrophages were observed in the *in vitro* experiment setting used as determined by MTT and LDH leakage assays. Additionally, some formulations, namely F108 and F127-based micelles, were able to increase the permeation of insulin across bronchial and alveolar cell monolayers, without damage the membrane integrity. All the formulations were taken up by macrophages, being the degree of internalization dependent on the polymer used. Above

all the polymers, F127 have shown to work as permeability enhancer of insulin and avoid more efficiently to be taken up by macrophages.

Taking into account the results, were managed to achieve formulations with interesting and promising characteristics for pulmonary administration of proteins justifying further *in vivo* studies.

Chapter 6

In vivo pharmacological and toxicological assessment of powder formulations for inhalation of insulin

The information presented in this chapter was partially published in the following publication:

Fernanda Andrade, Pedro Fonte, Ana Costa, Cassilda Cunha Reis, Rute Nunes, Carla Pereira, Domingos Ferreira, Mireia Oliva, Bruno Sarmento, *In vivo* pharmacological and toxicological assessment of self-assembled polymeric micelles as powders for inhalation of proteins, submitted for publication

1. Introduction

Despite the interest in systemic delivery of therapeutic peptides and proteins via inhalation, the accurate assessment of formulation's behavior is a challenging experimental task. Different *in vitro*, *ex vivo* and *in vivo* models have been proposed and used over the years (530). From the works developed in animal models by Schanker and coworkers during the 70´s and 80´s (531-533) up to now, new devices and techniques have been developed and proposed to study drug disposition within and absorption from lungs, their pharmacokinetics, pharmacological efficacy and toxicological profile after pulmonary administration (59, 336, 534-537).

Many methodological variables like animal used, method of anesthesia, administration technique, aerosol generator device, delivery site and animal posture could influence the results, explaining the high intra and inter-laboratory variability observed in inhalation studies (530). For preliminary experiments on pulmonary administration rodents like mice, rats and guinea pigs are employed, being rats and guinea pigs preferred over mice due to easier access to trachea and multiple blood dosing (538). Among the administration techniques used, direct tracheal access by endotracheal instillation using tracheotomy or orotracheal intubation is mainly used due to higher accuracy and reproducibility. Animals are anesthetized and placed in a supine position, then trachea is accessed up to the carina (tracheal bifurcation) and the formulations aerosolized (539, 540). Streptozotocin is an antibiotic that can cause pancreatic β-cell destruction, being capable of inducing type 1 diabetes mellitus (541). Streptozotocin-induced diabetic mice and rats are generally employed as animal models to study the mechanisms of diabetes, screening for potential therapies, and assess the behavior of insulin-based formulations (24, 541-543).

In this chapter it is presented the *in vivo* pharmacological and toxicological assessment of formulations after endotracheal instillation to a streptozotocin-induced murine diabetic model.

2. Experimental

2.1. Materials

SOL, F68, F108, and F127 were kindly provided by BASF (Ludwigshafen, Germany). Lyophilized human insulin (potency ≥ 27.5 IU/mg), PBS, PBA, streptozotocin, LDH, rat cytokine-induced neutrophil chemoattractant 3 (CINC-3) enzyme-linked immunosorbent assay (ELISA) kit, and Eukitt® quick-hardening mounting medium were purchase from

Sigma-Aldrich (St. Louis, MO, USA). Rat tumor necrosis factor alpha (TNF-α) and rat interleukin 6 (IL-6) ELISA kits were purchased from BioLegend (London, UK) while human insulin and insulin autoantibodies (IAA) ELISA kits were purchased from ALPCO Diagnostics (Salem, NH, USA). Pierce® biocinchoninic acid (BCA) Protein Assay and Clear-Rite® 3 were purchased from Thermo Fisher Scientific (Rockford, lL, USA). LDH Cytotoxicity Detection Kit was purchased from Takara Bio Europe/Clontech (France). Ketamine (Clorketam 1000®) was kindly provided by Vétoquinol (Barcarena, Portugal), xylazine (Seton 2 %®) was purchased from Laboratorios Calier (Sintra, Portugal), and isoflurane (Isoflo®) was purchased from Esteve Veterinária (Carnaxide, Portugal). The other reagents used were methanol, ethanol absolute, Turk's solution, sodium citrate, citric acid, paraformaldehyde, paraffin for histology, Gill's hematoxylin II solution, and eosin alcoholic solution (Merck, Germany) and Type 1 ultrapure water (18.2 MΩ.cm at 25 ºC, Milli-Q®, Billerica, MA, USA).

2.2. Production of powder formulations

Micelles were prepared using the thin-film hydration technique. Briefly, each polymer was individually weight and dissolved in a mixture of methanol:ethanol (1:1). Then, the solvent was removed under vacuum and the film was left to dry overnight at room-temperature to eliminate any remained solvent. The film was then hydrated with PBS at 37 ºC in order to obtain a 1 % (w/v) solution and vortexed for 5 min. The obtained dispersion was filtered through a 0.22 µm syringe filter to remove possible dust and aggregates.

PBA containing micelles were prepared by dissolving PBA with the polymers in the solvents prior to the production of the film at a ratio of 10:1 (w/w) (polymer:PBA). Insulin-loaded micelles were prepared by hydrating the polymeric films with an insulin solution in PBS to obtain polymer:insulin ratios of 10:1 (w/w). The other steps were the same as for plain formulations. After production micelles were lyophilized in an AdVantage 2.0 BenchTop Freeze Dryer (SP Scientific, Warminster, PA, USA). The cycle used was the follow: the samples were frozen at -30 ˚C and the temperature maintained for 60 min, the primary drying was set at 20 ˚C for 480 min at 150 mTorr and the secondary drying for another 480 min at 30 ˚C and 100 mTorr.

2.3. Animals

Animals were maintained in accordance with Federation of Laboratory Animal Science Associations (FELASA) recommendations and the European Union legislation (European

Parliament and Council Directive 2010/63/EU). Male Wistar Han rats (150-174g) from Harlan, Spain were kept for seven days after reception for behavioral, physiologic and nutritional stabilization. Animals were provided with food (Diet Standard, Mucedola s.r.l., Italy) and water *ad libitum*. Cages floor were covered with corn cob bedding (Corn Cob ULTRA12, Ultragene, Portugal) and enriched with nesting material. Animals were maintained at 22°C ± 2°C, 55% ± 10% room humidity, and 12h/12h light cycle, and submitted to daily inspection. After quarantine, diabetes was induced in all animals by intraperitoneal injection of streptozocin (10 mg/mL in pH 4.5 citrate buffer) at 60 mg/kg. After one week, animals with fasted blood glucose levels above 250 mg/dL were randomly grouped (n = 6) and used in the experiments.

2.4. *In vivo* pharmacological activity of insulin

Animals were divided into ten groups (n = 6) and fasted 12 hours before and 24 hours during the experiment, but were allowed water *ad libitum*. Prior to the endotracheal administration procedure, rats were anesthetized by inhalation of isoflurane (dose of 5 % for induction) followed by intraperitoneal injection of 100 mg/kg body weight (bw) of ketamine and 10 mg/kg bw of xylazine (for maintenance). Powder formulations (containing around 10 IU/kg bw) were administered endotracheally using a Dry Powder Insufflator® - Model DP-4 (Penn-Century. Inc. Wyndmoor, PA, USA). The delivery tube was introduced into the rat trachea just before the carina and the powder was released after activation of the device with 2 ml of air, which corresponds to the tidal volume of rats. Endotracheal instillation (MicroSprayer® Aerosolizer - Model IA-1B, Penn-Century. Inc. Wyndmoor, PA, USA) and subcutaneous injection of an insulin solution in PBS (10 IU/kg bw) were used as control groups. Blood samples were collected from the tail vein at different time points (15, 30, 45 min, 1, 2, 4, 8 and 24h) and the plasma glucose levels determined using a Precision Xtra blood glucose meter and test strips (Abbot Laboratories, Portugal, range 20-500 mg/dL). Serum insulin levels were determined at 4 and 24h after administration by an ELISA kit according to manufactures' instructions. Serum was obtained after centrifugation (10000 rpm for 20 min) of whole blood and stored at -80 °C until analysis. At the end of the assay, animals were euthanized by exsanguination after intraperitoneal injection of 300 mg/kg bw of ketamine and 30 mg/kg bw of xylazine.

Plasma glucose levels as the percentage of the values prior administration of insulin were plotted against time to evaluate the cumulative hypoglycemic effect over time, quantified by the area above the curve, determined using the trapezoidal method (Prism 6.02, GraphPad Software, Inc., CA, USA). Pharmacological availability (PA) of inhaled insulin-

containing powders and solution as the relative cumulative hypoglycemic effect of inhaled insulin compared to a 100% availability of the control insulin administered subcutaneously was determined according to Equation 6.1.

$$PA = \frac{\frac{AAC\ test}{Dose\ test}}{\frac{AAC\ control}{Dose\ control}} \times 100 \qquad \textbf{Equation 6.1}$$

where AAC test and AAC control are the area above curve values of inhaled insulin groups and subcutaneous control group, respectively; and Dose test and Dose control is the insulin dose (IU/kg bw) administered in inhaled insulin groups and subcutaneous control group, respectively.

2.5. Sub-acute toxicity of insulin-loaded polymeric micelles

Rats were divided into ten groups (5 animals per group) and administered endotracheally with insulin-loaded formulations (containing around 10 IU/kg bw) as described for the pharmacological activity study. Rats administered endotracheally with insulin solution in PBS (10 IU/kg bw) and PBS alone were used as controls. Before insufflation animals were anesthetized by intraperitoneal injection of 100 mg/kg bw of ketamine and 10 mg/kg bw of xylazine. In order to avoid the daily exposure of rats to the anesthesia and reduce the development of tolerance or side effects, the procedure was performed every two days for a period of 14 days. One day after the last administration, the animals were euthanized by exsanguination after intraperitoneal injection of 300 mg/kg bw of ketamine and 30 mg/kg bw of xylazine. Blood samples were collected, the trachea exposed for bronchoalveolar lavage (3 x 5 mL of PBS) and bronchoalveolar lavage fluid (BALF) collected and stored at -80ºC until analysis. BALF was screened for total number of nucleated cells (Turk's solution staining), protein content (BCA assay), relevant inflammatory cytokines and chemokines (TNF-α, IL-6, CINC-3 ELISA kits) and lactate dehydrogenase. Serum samples were screened for the development of insulin autoantibodies using an ELISA kit according to the manufactures' instructions. Serum was obtained after centrifugation (10000 rpm for 20 min) of whole blood and stored at -80 °C until analysis.

2.6. Histological analysis

After euthanasia samples of the lungs, liver and heart were collected and processed for hematoxylin and eosin (H&E) staining and light microscopy histological assessment.

Briefly, the tissues were fixed with 4% paraformaldehyde for 24 hours and processed automatically in a Spin Tissue Processor STP120 (Thermo Scientific, Germany) consisting in graded dehydrations steps in ethanol for 10 minutes each, followed by a diaphanization step using Clear-Rite® 3 for 10 minutes twice. Processing was finished by placing the tissues in liquid paraffin for 2 hours. Tissues were orientated according the plane of cut and, after paraffin solidification, sectioned with a thickness between 5-10 µm using a Leica RM2255 microtome (Leica Biosystems, Germany). The glass slides with the sections were allowed to dry overnight at 37°C before H&E staining.

For the H&E staining, sections were dewaxed in Clear-Rite® 3 for 10 minutes and hydrated through graded alcohols to water for 2 minutes each. After the staining with Gill's hematoxylin II solution for 5 minutes, sections were abundantly washed in tap water for 2 minutes, and dehydration through graded alcohols for 2 minutes each. Then, sections were stained with eosin alcoholic solution for 3 minutes and dipped quickly three times in absolute alcohol. At last, sections were dipped in xylene three times and mount in Eukitt® quick-hardening mounting medium.

2.7. Statistical analysis

One-way ANOVA was used to investigate the differences between the formulations and controls. Post hoc comparisons were performed according to Tukey's HSD test ($p<0.05$ was accepted as significant different) using Prism 6.02 software (GraphPad Software, Inc., CA, USA).

3. Results

3.1. Pharmacological activity of insulin-loaded polymeric micelles

The hypoglycemic effect of powder formulations and insulin solutions administered to fasted diabetic rats was assessed up to 24h. The plasma glucose levels versus time after endotracheal instillation of powders, insulin solution and subcutaneous administration of insulin solution are depicted in Figure 6.1, and the PA values expressed in Figure 6.2. The mean plasma glucose level at time 0 (baseline value) was taken as 100%. Between 8 hours and 24 hours, a drop on the plasma glucose levels was observed for the majority of formulations, which could be related to the fasting state of animals.

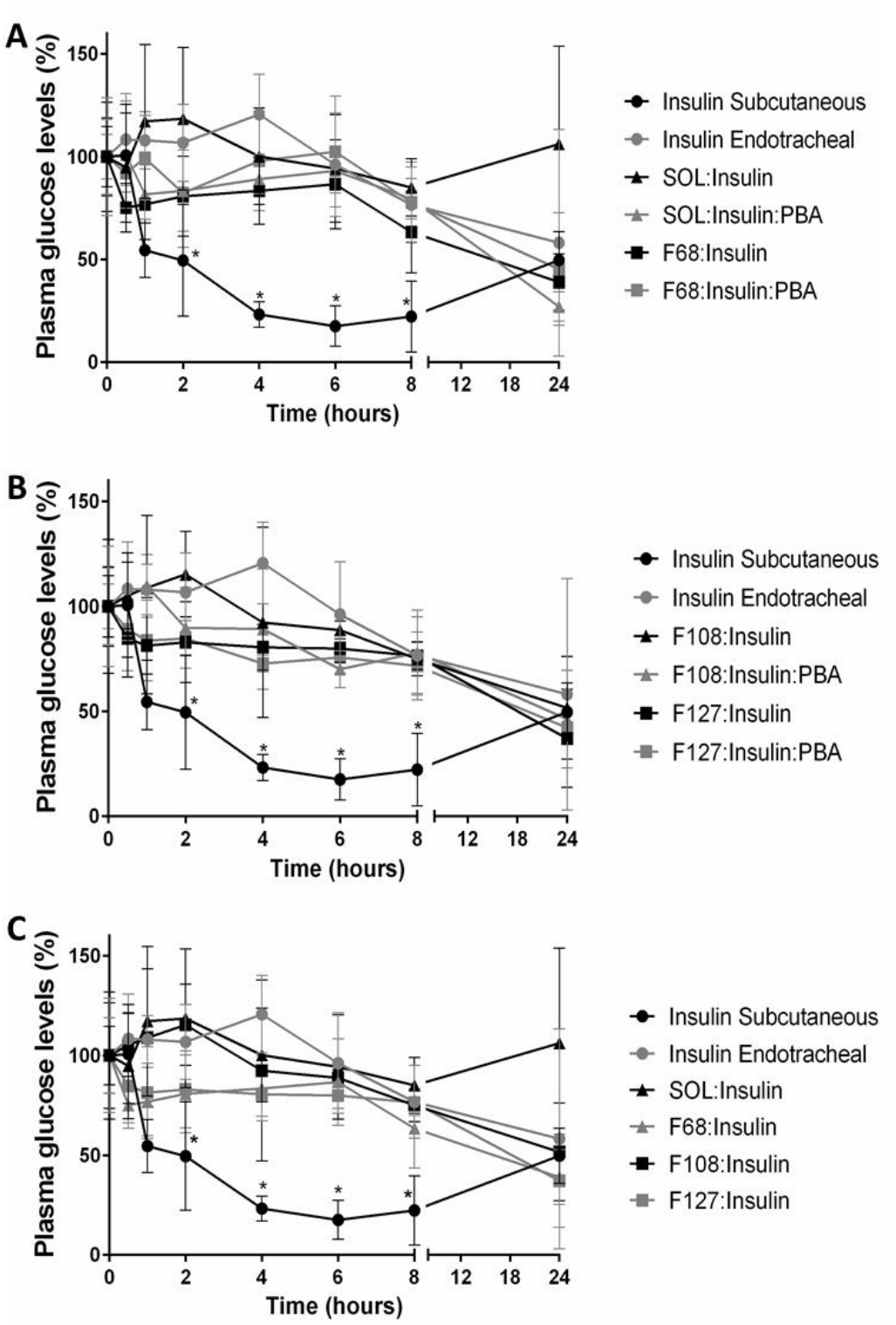

Figure 6.1 Plasma glucose levels as the percentage of the plasma glucose levels at time 0 after subcutaneous administration of insulin solution (10 IU/kg), endotracheal instillation of insulin solution (10 IU/kg) and SOL, F68-based powders (10 IU/kg) (A), F108, F127-based powders (10 IU/kg) (B), and powders without PBA (10 IU/kg) (C). Results are expressed as mean ± SD (n=6). * denotes significant differences of subcutaneous administration compared to endotracheal administration of insulin.

Endotracheal instillation of insulin (10 IU/kg bw) promoted a lower hypoglycemic effect, with an initial reduction at 0.5-1 hours for F68 and F127-based powders, followed by a continuous slow decrease of plasma glucose levels. Insulin solution SOL and F108-based powders didn't promote a significant reduction of glucose levels effect over time. Subcutaneous administration of 10 IU/kg insulin promoted a decrease of plasma glucose levels reaching a minimum decrease to 17.6% of its initial value 6 hours after administration.

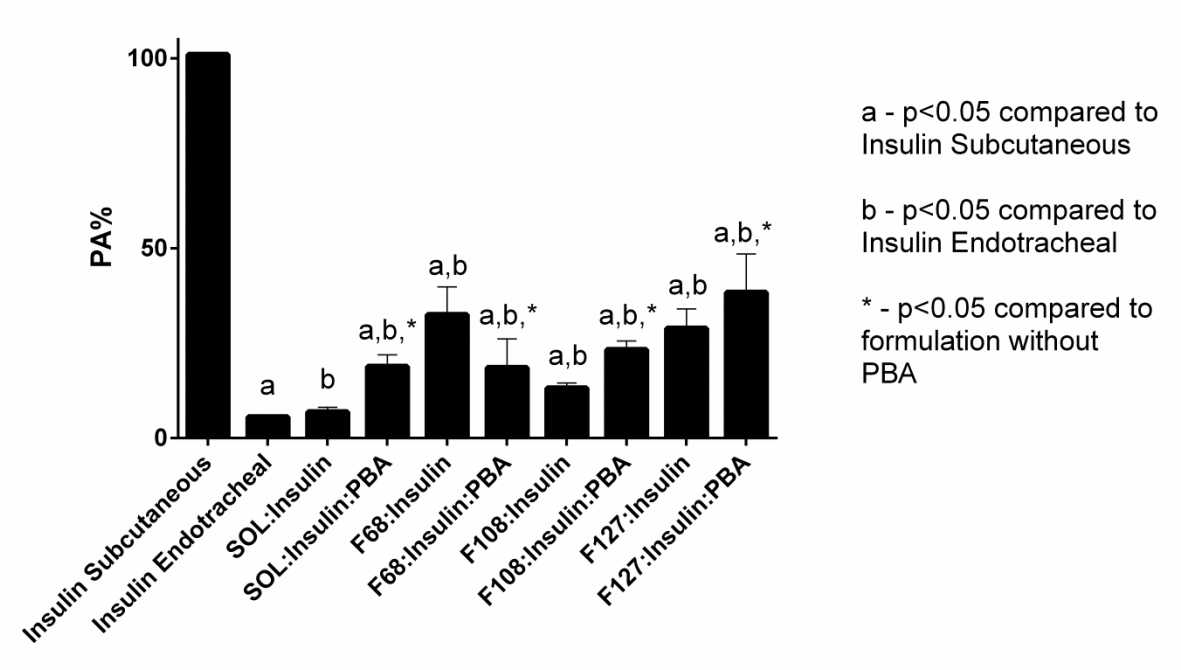

Figure 6.2 Pharmacological availability (PA) values of insulin after subcutaneous administration of insulin solution (10 IU/kg), and endotracheal instillation of insulin solution (10 IU/kg), SOL, F68, F108, and F127-based powders (10 IU/kg). Results are expressed as mean ± SD (n=6).

Excepting for F68-based powders, the presence of PBA significantly increased the PA values, thus increasing the hypoglycemic effects of formulations. Inhaled insulin solution showed the lowest hypoglycemic effect as observed by the plasma glucose profile and the low PA value (5.6%).

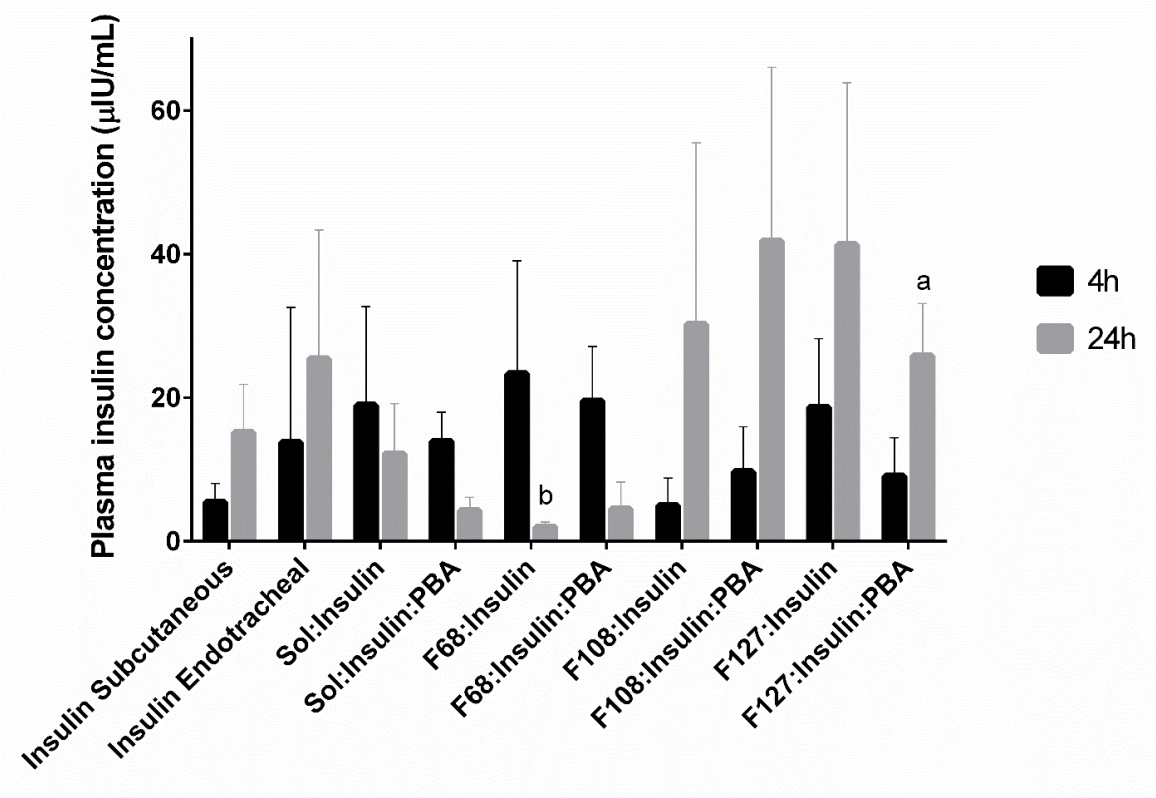

Figure 6.3 Serum insulin levels 4 hours and 24 hours after subcutaneous administration of insulin solution (10 IU/kg) and endotracheal instillation of insulin solution (10 IU/kg) and SOL, F68, F108, F127-based powders (10 IU/kg). Results are expressed as mean ± SD (n=6). a denotes significant differences of subcutaneous administration compared to subcutaneous administration of insulin, and b denotes significant differences of subcutaneous administration compared to endotracheal administration of insulin.

Serum insulin levels of formulations at 4 and 24 hours presented in Figure 6.3 showed small differences that could be related to differences in deposition, release and absorption of insulin, although without statistical significance.

3.2. Sub-acute toxicity

The sub-acute toxicity of formulations was assessed after 14-days of exposure. In general, no differences in cell count, protein content, LDH and TNF-α levels in BALF of animals treated with formulations was observed compared to control animals (Figure 6.4). Additionally, CINC-3 and IL-6 were not detected in the BALF of both treated and control animals.

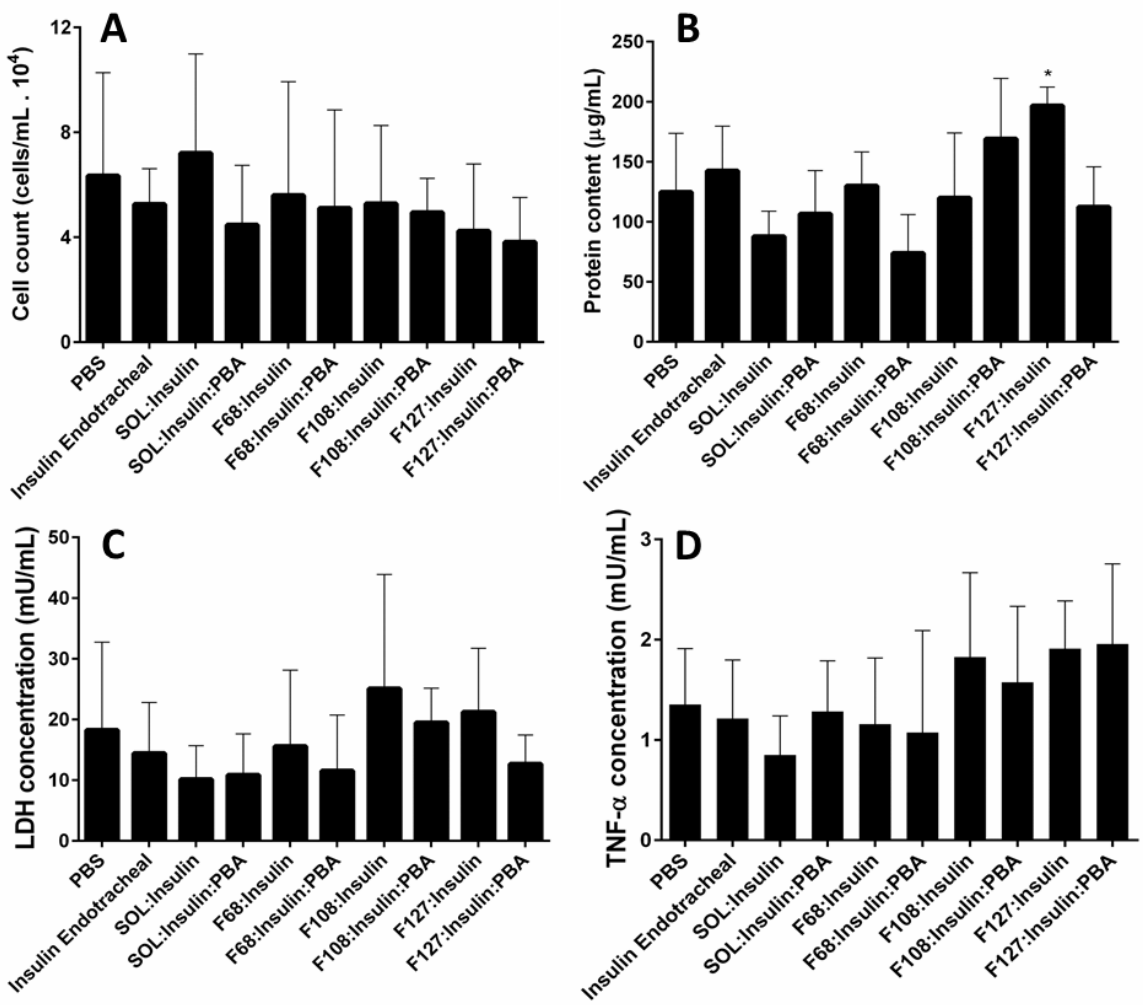

Figure 6.4 Levels of pulmonary toxicity markers in bronchoalveolar lavage fluid (BALF) after 14-days administration of insulin solution (10 IU/kg), insulin-containing SOL, F68, F108, F127-based powders (10 IU/kg), and PBS as negative control: Total nucleated cells (A), total protein content (B), LDH levels (C), and TNF-α levels (D). Results are expressed as mean ± SD (n=5). * denotes significant differences ($p<0.05$) compared to endotracheal administration of PBS.

Also, no changes in the bw of animals was registered during the experimental period (Figure 6.5).

Blood samples were also screened for the development of antibodies against insulin and the results are displayed in Table 6.1. According to the ELISA kit used, all the samples showed to be negative for the presence of IAA (negative <0.95, borderline 0.95-1.05, and positive >1.05).

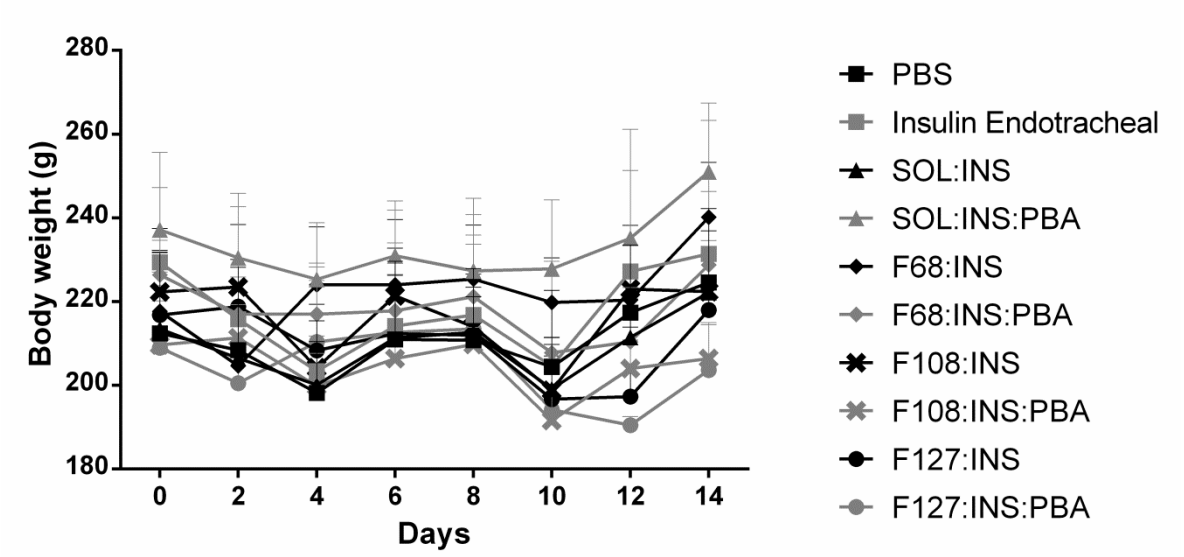

Figure 6.5 Body weight fluctuation of animals during 14 days administration of PBS, insulin solution (10 IU/kg), insulin-containing SOL, F68, F108, and F127-based powders (10 IU/kg). Results are expressed as mean ± SD (n=5).

Table 6.1 Insulin autoantibodies (IAA) ratio value of PBS, insulin solution (10 IU/kg), insulin-containing SOL, F68, F108, and F127-based powders (10 IU/kg) after 14-days administration. Results are expressed as mean ± SD (n=5).

Formulation	IAA ratio value (U/mL)
PBS	0.061±0.004
Insulin solution	0.061±0.007
SOL:Ins	0.065±0.004
SOL:Ins:PBA	0.062±0.006
F68:Ins	0.058±0.005
F68:Ins:PBA	0.061±0.006
F108:Ins	0.055±0.006
F108:Ins:PBA	0.061±0.010
F127:Ins	0.062±0.007
F127:Ins:PBA	0.063±0.010

After euthanasia of animals, selected organs were collected and processed for histological analysis. The histological sections of lungs, liver and heart are displayed in Figure 6.6, 6.7 and 6.8, respectively. No significant histological changes were observed in animals treated with insulin solution and formulations compared to PBS.

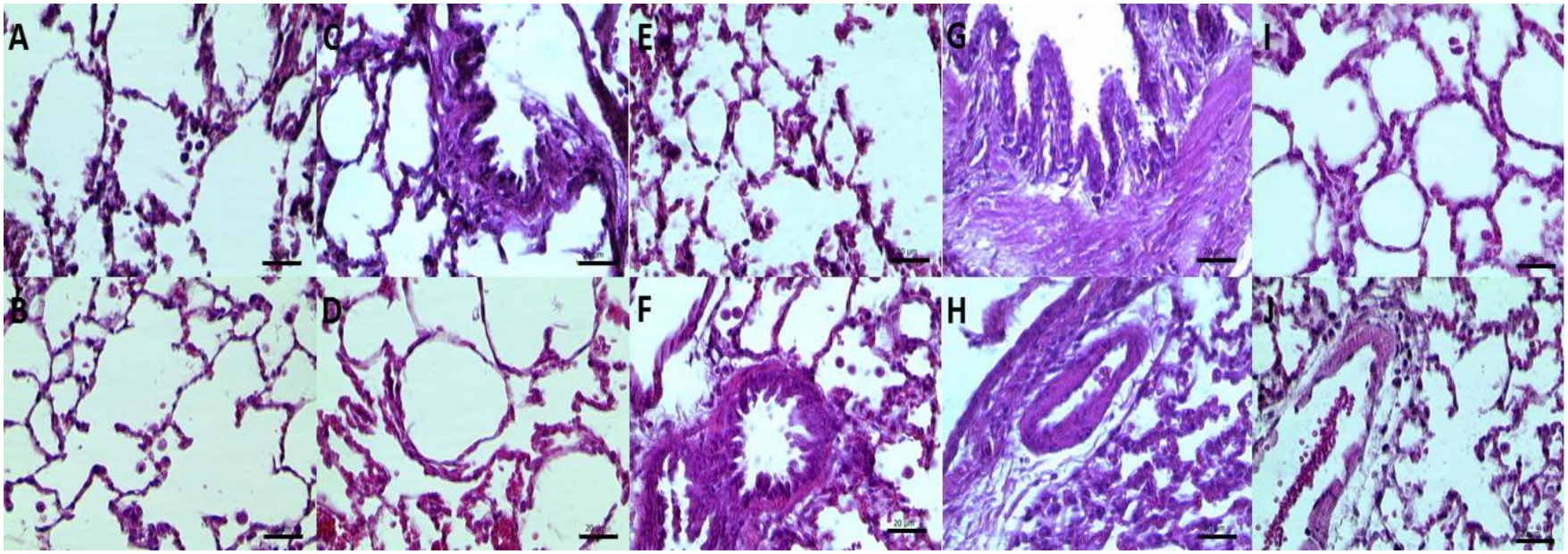

Figure 6.6 Photomicrographs of lung tissue from animals 24 hours after the last administration. Animals treated with PBS (A), insulin solution (B), insulin-loaded SOL (C), SOL:PBA (D), F68 (E), F68:PBA (F) F108 (G), F108:PBA (H), F127 (I), and F127:PBA (J)-based powders. H & E staining with a magnification of 40X. Scale bars are 20 µm.

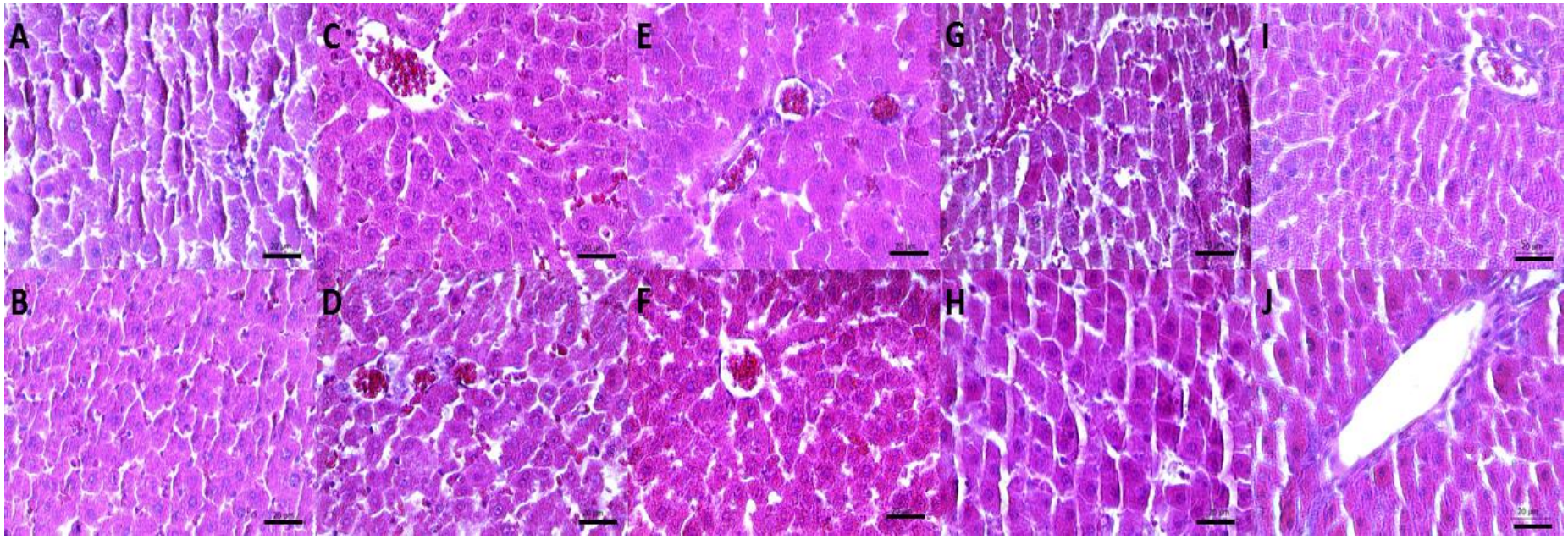

Figure 6.7 Photomicrographs of liver tissue from animals 24 hours after the last administration. Animals treated with PBS (A), insulin solution (B), insulin-loaded SOL (C), SOL:PBA (D), F68 (E), F68:PBA (F) F108 (G), F108:PBA (H), F127 (I), and F127:PBA (J)-based powders. H & E staining with a magnification of 40X. Scale bars are 20 µm.

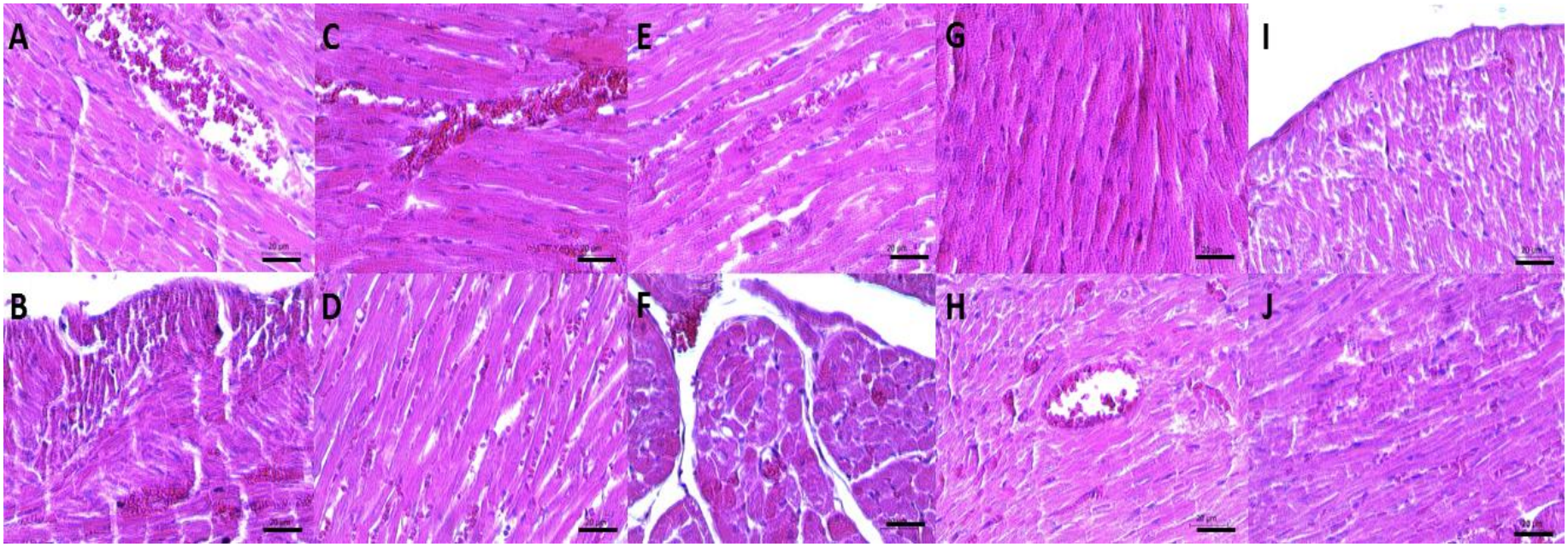

Figure 6.8 Photomicrographs of heart tissue from animals 24 hours after the last administration. Animals treated with PBS (A), insulin solution (B), insulin-loaded SOL (C), SOL:PBA (D), F68 (E), F68:PBA (F) F108 (G), F108:PBA (H), F127 (I), and F127:PBA (J)-based powders. H & E staining with a magnification of 40X. Scale bars are 20 µm.

4. Discussion

The therapeutic effect of inhaled formulations for systemic delivery of proteins is a complex balance between deposition profile of particles in the respiratory system, release from the formulation, degradation, uptake by macrophages and elimination by other defense mechanisms, and absorption to the bloodstream. Encapsulation of proteins for inhalation has been described to increase its bioavailability by protecting from degradation and increasing the transepithelial transport, explaining the higher PA values of powder formulations compared to insulin solution (Figure 6.2). Formulations presented different pharmacological profiles, which are related to its characteristics. The higher PA value of F127-based formulations (28.9%) could be explained by the high FPF (Table 4.4, *Chapter 4*), the low uptake by macrophages (Table 5.4, *Chapter 5*), and the enhanced permeation through pulmonary cell lines (Table 5.2, *Chapter 5*) observed for this formulation. Despite the lower FPF of F68-based powders, the release of >85% of insulin in the first 15 min could be related to the PA values (18.6-32.5%) of these formulations (Figure 4.8, *Chapter 4*). On the other hand, the controlled release of insulin from SOL-based powders (<55% in 24 hours), the low permeation through pulmonary cell monolayers, and the apparent lower maintenance of insulin conformation after lyophilization (Table 4.2, *Chapter 4*), could lead to the low PA value (6.9%) observed, while PBA containing micelles, due to the higher permeation present higher pharmacological activity (PA of 18.9%). Regarding F108-based powders, the PA value of 13.2% could be a result of the lower FPF and a higher uptake by macrophages. The higher release of insulin observed for PBA containing micelles of SOL, F108 and F127, explaining the higher PA values observed when compared to micelles without PBA (18.9%, 23.3% and 38.4%, respectively). On the other hand, the lower permeation of F68 micelles containing PBA could be responsible for its lower PA value.

As referred in *Chapter 5*, Pluronic® polymers have shown to interfere with the cellular membrane and alter its microsviscosity/fluidity (85), influencing the epithelial permeability. It has been demonstrated that the polymers with intermediate length of PEG blocks and lipophilicity interfere at a higher extent with the membrane (85), which could also contribute to the higher permeation and pharmacological availability exhibited by F68 and F127.

Besides alveolar macrophages, the mucus presented in the airways represents an important mechanism of defense that prevents particles from reaching the mucosa by hindering its movement (544). The shell of micelles of both SOL and Pluronic® is composed by PEG, which was shown to provide particles with stealth and mucus penetrating properties when at its surface. Thus, the developed powders could present

some mucus penetrating properties, enabling insulin to be absorbed at bronchial level in addition to the alveolar area. The capacity to avoid interactions with mucins and penetrate through its chain network is dependent on the MW of PEG and the surface coating density, being the mobility inversely proportional to the PEG MW and directly proportional to the PEG surface density (545). F68, F127, SOL and F108 possess PEG chains with approximate 4000, 5000, 6000 and 7000 g/mol, respectively. Additionally, SOL is composed by 13 % of PEG, while Pluronic® possesses a PEG density of 70-80 %. Hence, F68 and F127 should present the highest bronchial absorption, whereas SOL the lowest, in correlation with the observed PA values.

The quicker reduction of plasma glucose levels observed for F68 and F127-based powders indicates that inhaled insulin could be absorbed more rapidly than subcutaneous insulin, and correlates with the serum insulin levels at 4 hours (Figure 6.3). Other inhaled formulations, including Afrezza® and Exubera®, showed faster absorption and onset of action of inhaled insulin over subcutaneous administration (325, 495, 511) that is related to physiologic characteristics of lungs like large surface area, thin epithelial barrier, extensive blood supply, and lower enzymatic activity and efflux systems (224), making them a good place for absorption of compounds, including proteins.

Despite the possible quicker absorption, the lower hypoglycemic effect of inhaled insulin compared to subcutaneous insulin could be explained by the amount of insulin administered and available to be absorbed. Since FPF do not correspond to the total of the aerosolized formulation, the amount of insulin deposited in the peripheral lung and available to be absorbed is far from the theoretical 10 IU/kg administered. Also, after endocytosis by alveolar cells, insulin is partially degraded in the lysosomes by proteolytic enzymes (546). Additionally, the mixture of anesthetics used in this study has been shown to induce glucose intolerance with an increase of plasma glucose levels in rats up to 5 hours after intraperitoneal injection (547). That phenomenon could be behind the observations reported for the animals administered with inhaled insulin, since in that case the administration was performed under anesthesia, unlike in the subcutaneous insulin group.

A variety of formulations intended for pulmonary administration of insulin have been developed and proposed in the last decade, including Exubera® and Afrezza® (392). For example, insulin-loaded PLGA microcapsules promoted a sustained release of insulin and a prolonged hypoglycemic effect compared to subcutaneous administration of 4 IU per animal (495), a higher dose than that tested in this study (2-2.5 IU per animal). The complexity of inhalation, in addition to the differences inherent to each formulation, and

the *in vivo* study design render an adequate comparison of the different formulations very difficult.

The sub-acute toxicity of formulations was assessed after 14 days of exposure. The intraperitoneal injection of the combination of anesthetics at the dose used in this study showed to promote localized tissue damage with muscle necrosis, and a transient increase in serum aspartate transaminase, alanine transaminase, and creatine kinase levels (548). Furthermore, neurotoxicity of ketamine has also been reported (549). For this reason, and since diabetic animals have impaired wound healing, it was decided that the administration of formulations would be performed every two days rather than daily. One day after the last administration, bronchoalveolar lavage was performed and BALF collected for pulmonary toxicity markers screening, namely total nucleated cells, protein content, and LDH, TNF-α, IL-6 and CINC-3 levels. Additionally, blood samples were analyzed for the presence of IAA. F127-based formulations produced an increase of the total protein on BALF compared to PBS, which could be related to the enhanced alveolar-capillary permeability observed *in vitro*. However, no differences on membrane damage (LDH content) and inflammatory induction and response (TNF-α, IL-6, CINC-3, and nucleated cell counts) (Figure 6.4), nor weight loss (Figure 6.5) were observed among controls and experimental groups, indicating the absence of significant toxicity of formulations.

Additional histological evaluations were performed in lung (Figure 6.6), liver (Figure 6.7) and heart (Figure 6.8) tissues. No histopathological changes in lungs as acute infiltration of neutrophils, edema in alveolar sacs or significant alveolar septal thickening, typically observed in acute pulmonary irritation and inflammation (495), were observed in this study. Alterations on liver and heart of treated were also absent. Overall, no signs of tissue damage in important organs were observed in animals treated with inhaled insulin formulations, compared to the negative control (PBS).

Alongside with the low bioavailability of insulin presented by Exubera® or the development of cough and difficulties in managing the inhaler device, the development of antibodies against insulin (319) opened the debate regarding the long-term efficacy and safety of the product (550). In this study, the serum of both treated and control animals was negative for the presence of IAA (Table 6.1), as determined by ELISA for qualitative determination of IgG antibodies to insulin. Although some studies have failed to establish a correlation between increased levels of IAA and clinically relevant alterations in respiratory or metabolic parameters of patients treated with inhaled insulin (551, 552), the development of low levels of antibodies against insulin or their absence could be beneficial parameter in the development of new and improved inhaled formulations.

5. Conclusions

The association of insulin to polymeric micelles improved the efficiency of the protein by increasing its hypoglycemic effect and bioavailability as compared to its free solution form. The higher release of insulin from micelles observed *in vitro* could be related to the higher pharmacological activity presented by PBA-containing formulations. No inflammation induction or cytotoxicity was promoted by pulmonary administration after 14-days of exposure. In addition no weight loss or tissue damage were observed, indicating the absence of significant sub-acute toxicity of the formulations. The presence of PBA did not alter the toxicity profile of micelles. Also, was not observed the development of antibodies against insulin, indicating the absence of significant immunogenicity of insulin when associated to micelles.

In this work, we have achieved formulations with promising pharmacological and toxicological features for inhalation of insulin, especially the ones based on F127, as predicted by *in vitro* assessment. Polymeric micelles have shown to be feasible delivery systems for pulmonary delivery of insulin. These systems could serve as a platform for future development of improved dry powder inhalers of other proteins and biopharmaceuticals.

Chapter 7

General conclusions and future perspectives

The importance of inhalation as a route for both local and systemic administration of drugs, including therapeutic peptides and proteins, gained a new breath in the last decades. This is a result of the important advances observed in the field of molecular biology and particle engineering technology, which in turn, have allowed the development of new and improved formulations. Also, new insights on the understanding of aerosol mechanics boosted the development of innovative inhalation devices with improved aerosolization properties and adapted for the challenges imposed by the new formulations. Still, the development of efficient and safe formulations for pulmonary delivery of drugs imposes numerous challenges.

In these work it was pursued to achieve a formulation for pulmonary administration of insulin based on nanotechnology. Polymeric micelles prepared by thin film hydration technique were chosen owing to its easy production, small size, versatility to encapsulate both hydrophobic and hydrophilic compounds, and higher stability compared to liposomes. Insulin, used as model protein, was associated to polymeric micelles composed by different polymers, namely SOL, F68, F108 and F127 up to a polymer:insulin ratio of 10:1. PBA was added to the system to provide them with glucose sensitive properties. From the different conditions tested, the combination of ethanol and methanol mixed in equal proportions as evaporation solvent, and PBS as hydration solvent was selected to produce micelles of small size (≤ 200 nm for the majority of formulations), neutral surface charge, spherical shape and high protein association.

In order to increase the formulations stability and to produce solid systems for inhalation based on nanocomposites, micelles were lyophilized. Lyophilization promoted a slight aggregation of particles, although, due to the inherent lyoprotectant properties of PEG present in the polymers used, this effect was not significant for the majority of

formulations. By that, no additional cryoprotectans were required, which simplifies the formulation and could impact in their stability and safety profile. Dispersed nanocomposites originate neutral charged micelles generally lower than 300 nm, foreseeing a possible increase in the bioavailability of insulin by a reduction in the recognition of micelles by alveolar macrophages. Importantly, the lyophilized systems preserved the native-like secondary structure of insulin to a good extent, potentially maintaining its activity as assessed by FTIR and far-UV CD.

XPS analysis confirmed the expected core localization of PBA and the shell localization of insulin into micelles, owing to its mainly hydrophobic and hydrophilic nature at neutral pH, respectively. Insulin was also partially detected at the surface of micelles, excepting for F108 micelles, due to the higher MW of PEG portions of the polymer. Also, no significant interactions between the different components of the systems were detected by DSC and micro-Raman spectroscopy.

Nanocomposites of low density and high mean geometrical diameter, presented theoretical aerodynamic diameters compatible with good deposition profiles in the respiratory tract. However, morphological analysis and determination of Carr's index and Hausner ratio predict flowability limitations. Nevertheless, in vitro determination of FPF and MMAD evidenced good aerosolization properties.

Insulin release from the formulations depends on the polymer used, being fast for F68 and controlled for SOL-based systems. Thus, both fast and long-acting insulin formulations were achieved. Despite promote the faster in vitro release of insulin from the micelles, PBA did not modify the release profile of insulin in the presence of glucose. Since PBA was mainly in the core of micelles, it was not available to react with the glucose present in the media.

Regarding the stability of formulations, the lyophilized powders were stored at 4 and 20 ºC for 6 months and the size, surface charge and insulin conformation analyzed over time. No significant differences on the characteristics of micelles were observed up to six months. Additionally, the native-like structure of insulin was maintained, which could be attributed to the amorphous state of the protein in the lyophilized systems as evidenced by XRD, DSC, and micro-Raman spectroscopy.

After production and physical and chemical characterization, biological assessment of formulations was performed resorting pulmonary epithelial cells lines and macrophages. No significant signs of cytotoxicity were observed as determined by MTT and LDH leakage assays, thus, no substantial toxicity is expected at therapeutic doses. Furthermore, some formulations, especially F127-based systems, were able to increase the permeation of insulin across bronchial and alveolar epithelium, without damage the

membrane integrity. All the formulations were partially taken up by macrophages, being the percentage internalization lower to F127-based powders.

Lastly, *in vivo* pharmacological activity and sub-acute toxicity of formulations were assessed through endotracheal instillation to a streptozotocin-induced diabetic murine model. The association of insulin to polymeric micelles improved its therapeutic activity by increasing its hypoglycemic effect and bioavailability as compared to its free solution form. The addition of PBA to micelles, in general increased the PA of formulations, which could be related to the higher release of insulin from the micelles when PBA is present. Sub-acute toxicity of formulations was assessed by quantification of inflammation and toxicity markers present on BALF and histological analysis of selected organs after multiple administrations during 14 days. No signs of inflammation induction, cytotoxicity or tissue damage were observed after 14 days of exposure. Additionally, no weight loss neither the development of antibodies against insulin was detected, indicating the absence of significant sub-acute toxicity of the formulations. The presence of PBA did not affect the toxicity profile of formulations.

In conclusion, solid formulations based on amphiphilic polymers with appropriate characteristics for pulmonary delivery of insulin and good storage stability were achieved. Additionally, they present promising *in vitro* and *in vivo* pharmacological and toxicological features for inhalation of proteins. Above all the polymers, F127 showed to originate powders that redisperse into micelles of small size, present good aerosolization properties, work as permeability enhancer of insulin and efficiently avoid the particles to be taken up by macrophages. These formulations serve as a platform for future development of improved dry powder inhalers of therapeutic peptides and proteins.

Future improvements in the aerodynamic properties of formulations such as addition of a coarse carrier or the use of different inhaler device should be explored. Also a different technique for powder production, namely spray-drying, should be tested to produce spherical solid particles with better aerodynamic properties.

Regarding glucose sensitive properties, grafting PBA to the hydrophilic segments of the polymers could be a possible approach to ensure the presence PBA more at the surface of the micelles. Conjugation of insulin to PBA before association to micelles is also a possibility.

Following the evolution that has been observed in this field during the recent years, is expected in the near future an increase in the development of formulations based on nanocarriers to improve the properties of several drugs. Due to the well-known advantages presented by these systems would not be surprising to see an exponential increase of marketing authorization and commercialization of nanotechnology products,

with particular emphasis for administration of therapeutic peptides and proteins by other routes than the parental one, including the promising inhalation route.

References

1. Kayser O, Lemke A, Hernández-Trejo N. The impact of nanobiotechnology on the development of new drug delivery systems. Curr Pharm Biotechnol 2005; 6(1):3-5.
2. Jain KK. Drug delivery systems - an overview. Methods Mol Biol 2008; 437:1-50.
3. Torchilin V. Multifunctional and stimuli-sensitive pharmaceutical nanocarriers. Eur J Pharm Biopharm 2009; 71(3):431-44.
4. Lammers T, Hennink WE, Storm G. Tumour-targeted nanomedicines: principles and practice. Br J Cancer 2008; 99(3):392-7.
5. Torchilin V. Micellar nanocarriers: pharmaceutical perspectives. Pharm Res 2007; 24(1):1-16.
6. Hartig S, Greene R, DasGupta J, Carlesso G, Dikov M, Prokop A, et al. Multifunctional nanoparticulate polyelectrolyte complexes. Pharm Res 2007; 24(12):2353-69.
7. Hoffman A. The origins and evolution of "controlled" drug delivery systems. J Control Release 2008; 132(3):153-63.
8. Cryan S. Carrier-based strategies for targeting protein and peptide drugs to the lungs. AAPS J 2005; 7(1):E20-41.
9. Wu M, Pasula R, Smith PA, Martin WJ. Mapping alveolar binding sites in vivo using phage peptide libraries. Gene Ther 2003; 10(17):1429-36.
10. Kim HA, Park JH, Cho SH, Lee M. Lung epithelial binding peptide-linked high mobility group box-1 A box for lung epithelial cell-specific delivery of DNA. J Drug Target 2011; 19(7):589-96.
11. Jost PJ, Harbottle RP, Knight A, Miller AD, Coutelle C, Schneider H. A novel peptide, THALWHT, for the targeting of human airway epithelia. FEBS Lett 2001; 489(2-3):263-9.
12. Ross GF, Morris RE, Ciraolo G, Huelsman K, Bruno M, Whitsett JA, et al. Surfactant protein A-polylysine conjugates for delivery of DNA to airway cells in culture. Hum Gene Ther 1995; 6(1):31-40.
13. Rudolph C, Schillinger U, Plank C, Gessner A, Nicklaus P, Müller R, et al. Nonviral gene delivery to the lung with copolymer-protected and transferrin-modified polyethylenimine. Biochim Biophys Acta 2002; 1573(1):75-83.
14. Fajac I, Thévenot G, Bédouet L, Danel C, Riquet M, Merten M, et al. Uptake of plasmid/glycosylated polymer complexes and gene transfer efficiency in differentiated airway epithelial cells. J Gene Med 2003; 5(1):38-48.
15. Goren D, Horowitz AT, Tzemach D, Tarshish M, Zalipsky S, Gabizon A. Nuclear delivery of doxorubicin via folate-targeted liposomes with bypass of multidrug-resistance efflux pump. Clin Cancer Res 2000; 6(5):1949-57.
16. Torchilin VP. Tat peptide-mediated intracellular delivery of pharmaceutical nanocarriers. Adv Drug Deliv Rev 2008; 60(4-5):548-58.
17. Chono S, Tanino T, Seki T, Morimoto K. Efficient drug targeting to rat alveolar macrophages by pulmonary administration of ciprofloxacin incorporated into mannosylated liposomes for treatment of respiratory intracellular parasitic infections. J Control Release 2008; 127(1):50-8.

18. Moretton MA, Chiappetta DA, Andrade F, das Neves J, Ferreira D, Sarmento B, et al. Hydrolyzed galactomannan-modified nanoparticles and flower-like polymeric micelles for the active targeting of rifampicin to macrophages. J Biomed Nanotechnol 2013; 9(6):1076-87.
19. Bailey M, Berkland C. Nanoparticle formulations in pulmonary drug delivery. Med Res Rev 2009; 29(1):196-212.
20. Zhang Y, Chan HF, Leong KW. Advanced materials and processing for drug delivery: the past and the future. Adv Drug Deliv Rev 2013; 65(1):104-20.
21. Yan L, Yang Y, Zhang W, Chen X. Advanced materials and nanotechnology for drug delivery. Adv Mater 2014; 26(31):5533-40.
22. Mishra B, Patel B, Tiwari S. Colloidal nanocarriers: a review on formulation technology, types and applications toward targeted drug delivery. Nanomedicine 2010; 6(1):9-24.
23. Mansour HM, Rhee YS, Wu X. Nanomedicine in pulmonary delivery. Int J Nanomedicine 2009; 4:299-319.
24. Ungaro F, d'Emmanuele di Villa Bianca R, Giovino C, Miro A, Sorrentino R, Quaglia F, et al. Insulin-loaded PLGA/cyclodextrin large porous particles with improved aerosolization properties: in vivo deposition and hypoglycaemic activity after delivery to rat lungs. J Control Release 2009; 135(1):25-34.
25. Bawarski WE, Chidlowsky E, Bharali DJ, Mousa SA. Emerging nanopharmaceuticals. Nanomedicine 2008; 4(4):273-82.
26. Duncan R, Gaspar R. Nanomedicine(s) under the microscope. Mol Pharm 2011; 8(6):2101-41.
27. Bosetti R, Vereeck L. Future of nanomedicine: obstacles and remedies. Nanomedicine (Lond) 2011; 6(4):747-55.
28. Hamburg M. FDA's Approach to Regulation of Products of Nanotechnology. Science 2012; 336(6079):299-300.
29. U.S. Department of Health and Human Services, Food and Drug Administration. Guidance for Industry:Considering Whether an FDA-Regulated Product Involves the Application of Nanotechnology. 2014.
30. BCC Research, Nanotechnology in Medical Applications: The Global Market (HLC069B). 2012.
31. Soppimath K, Aminabhavi T, Kulkarni A, Rudzinski W. Biodegradable polymeric nanoparticles as drug delivery devices. J Control Release 2001; 70(1-2):1-20.
32. Martins S, Sarmento B, Ferreira D, Souto E. Lipid-based colloidal carriers for peptide and protein delivery-liposomes versus lipid nanoparticles. Int J Nanomedicine 2007; 2(4):595-607.
33. Immordino ML, Dosio F, Cattel L. Stealth liposomes: review of the basic science, rationale, and clinical applications, existing and potential. Int J Nanomedicine 2006; 1(3):297-315.
34. Grenha A, Remuñán-López C, Carvalho E, Seijo B. Microspheres containing lipid/chitosan nanoparticles complexes for pulmonary delivery of therapeutic proteins. Eur J Pharm Biopharm 2008; 69(1):83-93.
35. Faraji A, Wipf P. Nanoparticles in cellular drug delivery. Bioorg Med Chem 2009; 17(8):2950-62.
36. Müller R, Petersen R, Hommoss A, Pardeike J. Nanostructured lipid carriers (NLC) in cosmetic dermal products. Adv Drug Deliv Rev 2007; 59(6):522-30.

37. Liu Z, Jiao Y, Wang Y, Zhou C, Zhang Z. Polysaccharides-based nanoparticles as drug delivery systems. Adv Drug Deliv Rev 2008; 60(15):1650-62.
38. Yang Y, Bajaj N, Xu P, Ohn K, Tsifansky M, Yeo Y. Development of highly porous large PLGA microparticles for pulmonary drug delivery. Biomaterials 2009; 30(10):1947-53.
39. Lu Y, Park K. Polymeric micelles and alternative nanonized delivery vehicles for poorly soluble drugs. Int J Pharm 2013; 453(1):198-214.
40. Cabral H, Kataoka K. Progress of drug-loaded polymeric micelles into clinical studies. J Control Release 2014; 190:465-76.
41. Adams ML, Lavasanifar A, Kwon GS. Amphiphilic block copolymers for drug delivery. J Pharm Sci 2003; 92(7):1343-55.
42. Gelderblom H, Verweij J, Nooter K, Sparreboom A. Cremophor EL: the drawbacks and advantages of vehicle selection for drug formulation. Eur J Cancer 2001; 37(13):1590-8.
43. Xiao Y, Lin ZT, Chen Y, Wang H, Deng YL, Le DE, et al. High molecular weight chitosan derivative polymeric micelles encapsulating superparamagnetic iron oxide for tumor-targeted magnetic resonance imaging. Int J Nanomedicine 2015; 10:1155-72.
44. Chen C, Cai G, Zhang H, Jiang H, Wang L. Chitosan-poly(ε-caprolactone)-poly(ethylene glycol) graft copolymers: synthesis, self-assembly, and drug release behavior. J Biomed Mater Res A 2011; 96(1):116-24.
45. Ye YQ, Chen FY, Wu QA, Hu FQ, Du YZ, Yuan H, et al. Enhanced cytotoxicity of core modified chitosan based polymeric micelles for doxorubicin delivery. J Pharm Sci 2009; 98(2):704-12.
46. Bei YY, Yuan ZQ, Zhang L, Zhou XF, Chen WL, Xia P, et al. Novel self-assembled micelles based on palmitoyl-trimethyl-chitosan for efficient delivery of harmine to liver cancer. Expert Opin Drug Deliv 2014; 11(6):843-54.
47. Luppi B, Orienti I, Bigucci F, Cerchiara T, Zuccari G, Fazzi S, et al. Poly(vinylalcohol-co-vinyloleate) for the preparation of micelles enhancing retinyl palmitate transcutaneous permeation. Drug Deliv 2002; 9(3):147-52.
48. Luppi B, Bigucci F, Cerchiara T, Andrisano V, Pucci V, Mandrioli R, et al. Micelles based on polyvinyl alcohol substituted with oleic acid for targeting of lipophilic drugs. Drug Deliv 2005; 12(1):21-6.
49. Zuccari G, Bergamante V, Carosio R, Gotti R, Montaldo PG, Orienti I. Micellar complexes of all-trans retinoic acid with polyvinylalcohol-nicotinoyl esters as new parenteral formulations in neuroblastoma. Drug Deliv 2009; 16(4):189-95.
50. Hu Y, Jiang Z, Chen R, Wu W, Jiang X. Degradation and degradation-induced re-assembly of PVP-PCL micelles. Biomacromolecules 2010; 11(2):481-8.
51. Yuan J, Luo Y, Gao Q. Self-assembled polyion complex micelles for sustained release of hydrophilic drug. J Microencapsul 2011; 28(2):93-8.
52. Essa S, Rabanel JM, Hildgen P. Characterization of rhodamine loaded PEG-g-PLA nanoparticles (NPs): effect of poly(ethylene glycol) grafting density. Int J Pharm 2011; 411(1-2):178-87.
53. Zhan C, Gu B, Xie C, Li J, Liu Y, Lu W. Cyclic RGD conjugated poly(ethylene glycol)-co-poly(lactic acid) micelle enhances paclitaxel anti-glioblastoma effect. J Control Release 2010; 143(1):136-42.

54. Gong CY, Wang YJ, Wang XH, Wei XW, Wu QJ, Wang BL, et al. Biodegradable self-assembled PEG-PCL-PEG micelles for hydrophobic drug delivery, part 2: in vitro and in vivo toxicity evaluation. J Nanopart Res 2011; 13:721–31.
55. Ma M, Li F, Liu XH, Yuan ZF, Chen FJ, Zhuo RX. Self-assembled micellar aggregates based monomethoxyl poly(ethylene glycol)-b-poly(ε-caprolactone)-b-poly(aminoethyl methacrylate) triblock copolymers as efficient gene delivery vectors. J Mater Sci Mater Med 2010; 21(10):2817-25.
56. Chen L, Sha X, Jiang X, Chen Y, Ren Q, Fang X. Pluronic P105/F127 mixed micelles for the delivery of docetaxel against Taxol-resistant non-small cell lung cancer: optimization and in vitro, in vivo evaluation. Int J Nanomedicine 2013; 8:73-84.
57. Wei Z, Hao J, Yuan S, Li Y, Juan W, Sha X, et al. Paclitaxel-loaded Pluronic P123/F127 mixed polymeric micelles: formulation, optimization and in vitro characterization. Int J Pharm 2009; 376(1-2):176-85.
58. Silva M, Ricelli N, El Seoud O, Valentim C, Ferreira A, Sato D, et al. Potential tuberculostatic agent: micelle-forming pyrazinamide prodrug. Archiv Der Pharmazie 2006; 339(6):283-90.
59. Baginski L, Gobbo OL, Tewes F, Salomon JJ, Healy AM, Bakowsky U, et al. In vitro and In vivo characterisation of PEG-lipid-based micellar complexes of salmon calcitonin for pulmonary delivery. Pharm Res 2012; 29(6):1425-34.
60. Abdulla JM, Tan YT, Darwis Y. Rehydrated lyophilized rifampicin-loaded mPEG-DSPE formulations for nebulization. AAPS PharmSciTech 2010; 11(2):663-71.
61. Letchford K, Liggins R, Burt H. Solubilization of hydrophobic drugs by methoxy poly(ethylene glycol)-block-polycaprolactone diblock copolymer micelles: theoretical and experimental data and correlations. J Pharm Sci 2008; 97(3):1179-90.
62. Kwon G, Okano T. Polymeric micelles as new drug carriers. Adv Drug Deliv Rev 1996; 21(2):107-16.
63. Zhang Y, Huang Y, Li S. Polymeric micelles: nanocarriers for cancer-targeted drug delivery. AAPS PharmSciTech 2014; 15(4):862-71.
64. Ohuchi M, Harada M, Amano Y, Kato Y, Physiologically active polypeptide- or protein-encapsulating polymer micelles, and method for production of the same. US2009/02911302009.
65. Matsumura Y. Preclinical and clinical studies of NK012, an SN-38-incorporating polymeric micelles, which is designed based on EPR effect. Adv Drug Deliv Rev 2011; 63(3):184-92.
66. Kato K, Chin K, Yoshikawa T, Yamaguchi K, Tsuji Y, Esaki T, et al. Phase II study of NK105, a paclitaxel-incorporating micellar nanoparticle, for previously treated advanced or recurrent gastric cancer. Invest New Drugs 2012; 30(4):1621-7.
67. Kim DW, Kim SY, Kim HK, Kim SW, Shin SW, Kim JS, et al. Multicenter phase II trial of Genexol-PM, a novel Cremophor-free, polymeric micelle formulation of paclitaxel, with cisplatin in patients with advanced non-small-cell lung cancer. Ann Oncol 2007; 18(12):2009-14.
68. Lee KS, Chung HC, Im SA, Park YH, Kim CS, Kim SB, et al. Multicenter phase II trial of Genexol-PM, a Cremophor-free, polymeric micelle formulation of paclitaxel, in patients with metastatic breast cancer. Breast Cancer Res Treat 2008; 108(2):241-50.
69. Saif MW, Rubin MS, Figueroa JA, Kerr RO. Multicenter phase II trial of Genexol-PM (GPM), a novel Cremophor-free, polymeric micelle formulation of paclitaxel in patients

with advanced pancreatic cancer (APC): Final results. Gastrointestinal Cancers Symposium, Orlando; 2008.
70. Valle JW, Armstrong A, Newman C, Alakhov V, Pietrzynski G, Brewer J, et al. A phase 2 study of SP1049C, doxorubicin in P-glycoprotein-targeting pluronics, in patients with advanced adenocarcinoma of the esophagus and gastroesophageal junction. Invest New Drugs 2011; 29(5):1029-37.
71. Exner AA, Krupka TM, Scherrer K, Teets JM. Enhancement of carboplatin toxicity by Pluronic block copolymers. J Control Release 2005; 106(1-2):188-97.
72. Aliabadi HM, Mahmud A, Sharifabadi AD, Lavasanifar A. Micelles of methoxy poly(ethylene oxide)-b-poly(epsilon-caprolactone) as vehicles for the solubilization and controlled delivery of cyclosporine A. J Control Release 2005; 104(2):301-11.
73. Wang J, Mongayt D, Torchilin VP. Polymeric micelles for delivery of poorly soluble drugs: preparation and anticancer activity in vitro of paclitaxel incorporated into mixed micelles based on poly(ethylene glycol)-lipid conjugate and positively charged lipids. J Drug Target 2005; 13(1):73-80.
74. Benahmed A, Ranger M, Leroux JC. Novel polymeric micelles based on the amphiphilic diblock copolymer poly(N-vinyl-2-pyrrolidone)-block-poly(D,L-lactide). Pharm Res 2001; 18(3):323-8.
75. Watanabe M, Kawano K, Yokoyama M, Opanasopit P, Okano T, Maitani Y. Preparation of camptothecin-loaded polymeric micelles and evaluation of their incorporation and circulation stability. Int J Pharm 2006; 308(1-2):183-9.
76. Liaw J, Chang SF, Hsiao FC. In vivo gene delivery into ocular tissues by eye drops of poly(ethylene oxide)-poly(propylene oxide)-poly(ethylene oxide) (PEO-PPO-PEO) polymeric micelles. Gene Ther 2001; 8(13):999-1004.
77. Torchilin VP. PEG-based micelles as carriers of contrast agents for different imaging modalities. Adv Drug Deliv Rev 2002; 54(2):235-52.
78. Opanasopit P, Yokoyama M, Watanabe M, Kawano K, Maitani Y, Okano T. Block copolymer design for camptothecin incorporation into polymeric micelles for passive tumor targeting. Pharm Res 2004; 21(11):2001-8.
79. Kedar U, Phutane P, Shidhaye S, Kadam V. Advances in polymeric micelles for drug delivery and tumor targeting. Nanomedicine 2010; 6(6):714-29.
80. Le Garrec D, Ranger M, Leroux J-C. Micelles in anticancer drug delivery. Am J Drug Deliv 2004; 2(1):15-42.
81. Rapoport N. Physical stimuli-responsive polymeric micelles for anti-cancer drug delivery. Progress in Polymer Science 2007; 32:962-90.
82. Yuan Q, Venkatasubramanian R, Hein S, Misra RD. A stimulus-responsive magnetic nanoparticle drug carrier: magnetite encapsulated by chitosan-grafted-copolymer. Acta Biomater 2008; 4(4):1024-37.
83. Bae Y, Jang WD, Nishiyama N, Fukushima S, Kataoka K. Multifunctional polymeric micelles with folate-mediated cancer cell targeting and pH-triggered drug releasing properties for active intracellular drug delivery. Mol Biosyst 2005; 1(3):242-50.
84. Smola M, Vandamme T, Sokolowski A. Nanocarriers as pulmonary drug delivery systems to treat and to diagnose respiratory and non respiratory diseases. Int J Nanomedicine 2008; 3(1):1-19.
85. Batrakova EV, Li S, Alakhov VY, Miller DW, Kabanov AV. Optimal structure requirements for pluronic block copolymers in modifying P-glycoprotein drug efflux

transporter activity in bovine brain microvessel endothelial cells. J Pharmacol Exp Ther 2003; 304(2):845-54.
86. Batrakova EV, Kelly DL, Li S, Li Y, Yang Z, Xiao L, et al. Alteration of genomic responses to doxorubicin and prevention of MDR in breast cancer cells by a polymer excipient: pluronic P85. Mol Pharm 2006; 3(2):113-23.
87. Miller DW, Batrakova EV, Kabanov AV. Inhibition of multidrug resistance-associated protein (MRP) functional activity with pluronic block copolymers. Pharm Res 1999; 16(3):396-401.
88. Seoul National University Hospital. A phase II study of Genexol-PM and cisplatin as induction chemotherapy in unresectable, locally advanced head and neck squamous cell carcinoma (HNSCC). NCT01689194: https://clinicaltrials.gov [accessed on April 2015].
89. Samyang Biopharmaceuticals Corporation. Open-label, multicenter, phase I trial to evaluate efficacy and safety of the combination therapy of Genexol®-PM plus carboplatin as a firstline treatment in subjects with advanced ovarian cancer. NCT00877253: https://clinicaltrials.gov [accessed on April 2015].
90. Korean Breast Cancer Study Group. A clinical trial of paclitaxel loaded polymeric micelle (Genexol-PM®) in patients with taxane-pretreated recurrent breast cancer.NCT00912639: https://clinicaltrials.gov [accessed on April 2015].
91. Nippon Kayaku Co. A phase I dose-escalation study of NK012 administered intravenously as a single dose every three weeks in patients with refractory solid tumors. NCT00542958: https://clinicaltrials.gov [accessed on April 2015].
92. Nippon Kayaku Co. A phase II study of NK012 in sensitive relapsed and refractory relapsed small-cell lung cancer (SCLC). NCT00951613: https://clinicaltrials.gov [accessed on April 2015].
93. Nippon Kayaku Co. A multi-national phase III clinical study comparing NK105 versus paclitaxel in patients with metastatic or recurrent breast cancer. NCT01644890: https://clinicaltrials.gov [accessed on April 2015].
94. M.D. Anderson Cancer Center. A phase 1 dose-escalation and pharmacokinetic study of NC-4016 in patients with advanced solid tumors or lymphoma.NCT01999491: https://clinicaltrials.gov [accessed on April 2015].
95. Orient Europharma Co. A phase III, open-label, randomized study of the combination therapy with NC-6004 and gemcitabine versus gemcitabine alone in patients with locally advanced or metastatic pancreatic cancer. NCT02043288: https://clinicaltrials.gov [accessed on April 2015].
96. Nanocarrier Co. A phase 1b/2 dose escalation and expansion trial of NC-6004 (nanoparticle cisplatin) plus gemcitabine in patients with advanced solid tumors or non-small cell lung cancer. NCT02240238: https://clinicaltrials.gov [accessed on April 2015].
97. National Cancer Institute. A pilot open-label single-dose study using intravenous micellar paclitaxel for patients with severe psoriasis. NCT00006276: https://clinicaltrials.gov [accessed on April 2015].
98. Angiotech Pharmaceuticals. A phase 2 open-label clinical study using intravenous Paxceed™ to treat patients with rheumatoid arthritis. NCT00055133: https://clinicaltrials.gov [accessed on April 2015].
99. University of Colorado. Safety and efficacy of a novel antioxidant-rich multivitamin supplement for persons with cystic fibrosis. NCT01018303: https://clinicaltrials.gov [accessed on April 2015].

100. University of Colorado. A multi-center, randomized, controlled, double-blind study of the effects of an antioxidant-enriched multivitamin supplement on inflammation and oxidative stress in cystic fibrosis patients. NCT01859390: https://clinicaltrials.gov [accessed on April 2015].
101. BIND Therapeutics. An open label, multicenter, Phase 2 study to determine the safety and efficacy of BIND-014 (docetaxel nanoparticles for injectable suspension) as a second-line therapy for patients with KRAS mutation positive or squamous cell non-small cell lung cancer. NCT02283320: https://clinicaltrials.gov [accessed on April 2015].
102. BIND Therapeutics. A phase 1 open label, safety, pharmacokinetic and pharmacodynamic dose escalation study of BIND-014 (docetaxel nanoparticles for injectable suspension), given by intravenous infusion to patients with advanced or metastatic cancer. NCT01300533: https://clinicaltrials.gov [accessed on April 2015].
103. BIND Therapeutics. An open label, multicenter, phase 2 study to determine the safety and efficacy of BIND-014 (docetaxel nanoparticles for injectable suspension), administered to patients with metastatic castration-resistant prostate cancer. NCT01812746: https://clinicaltrials.gov [accessed on April 2015].
104. Kataoka K, Harada A, Nagasaki Y. Block copolymer micelles for drug delivery: design, characterization and biological significance. Adv Drug Deliv Rev 2001; 47(1):113-31.
105. Xiong XB, Binkhathlan Z, Molavi O, Lavasanifar A. Amphiphilic block co-polymers: Preparation and application in nanodrug and gene delivery. Acta Biomater 2012; 8(6):2017-33.
106. Hu FQ, Liu LN, Du YZ, Yuan H. Synthesis and antitumor activity of doxorubicin conjugated stearic acid-g-chitosan oligosaccharide polymeric micelles. Biomaterials 2009; 30(36):6955-63.
107. Hu FQ, Ren GF, Yuan H, Du YZ, Zeng S. Shell cross-linked stearic acid grafted chitosan oligosaccharide self-aggregated micelles for controlled release of paclitaxel. Colloids Surf B 2006; 50(2):97-103.
108. Gilani K, Moazeni E, Ramezanli T, Amini M, Fazeli MR, Jamalifar H. Development of respirable nanomicelle carriers for delivery of amphotericin B by jet nebulization. J Pharm Sci 2011; 100(1):252-9.
109. Liu Y, Sun J, Cao W, Yang J, Lian H, Li X, et al. Dual targeting folate-conjugated hyaluronic acid polymeric micelles for paclitaxel delivery. Int J Pharm 2011; 421(1):160-9.
110. Chang Y-C, Chu I-M. Methoxy poly(ethylene glycol)-b-poly(valerolactone) diblock polymeric micelles for enhanced encapsulation and protection of camptothecin. Eur Polym J 2008; 44:3922–30.
111. Moretton MA, Glisoni RJ, Chiappetta DA, Sosnik A. Molecular implications in the nanoencapsulation of the anti-tuberculosis drug rifampicin within flower-like polymeric micelles. Colloids Surf B 2010; 79(2):467-79.
112. Moretton MA, Chiappetta DA, Sosnik A. Cryoprotection-lyophilization and physical stabilization of rifampicin-loaded flower-like polymeric micelles. J R Soc Interface 2012; 9(68):487-502.
113. Ramasamy T, Kim J, Choi HG, Yong CS, Kim JO. Novel dual drug-loaded block ionomer complex micelles for enhancing the efficacy of chemotherapy treatments. J Biomed Nanotechnol 2014; 10(7):1304-12.

114. Matsumoto S, Christie RJ, Nishiyama N, Miyata K, Ishii A, Oba M, et al. Environment-responsive block copolymer micelles with a disulfide cross-linked core for enhanced siRNA delivery. Biomacromolecules 2009; 10(1):119-27.
115. Shahin M, Ahmed S, Kaur K, Lavasanifar A. Decoration of polymeric micelles with cancer-specific peptide ligands for active targeting of paclitaxel. Biomaterials 2011; 32(22):5123-33.
116. Gao ZG, Lee DH, Kim DI, Bae YH. Doxorubicin loaded pH-sensitive micelle targeting acidic extracellular pH of human ovarian A2780 tumor in mice. J Drug Target 2005; 13(7):391-7.
117. Lee ES, Na K, Bae YH. Doxorubicin loaded pH-sensitive polymeric micelles for reversal of resistant MCF-7 tumor. J Control Release 2005; 103(2):405-18.
118. Seo D, Jeong Y, Kim D, Jang M, Jang M, Nah J. Methotrexate-incorporated polymeric nanoparticles of methoxy poly(ethylene glycol)-grafted chitosan. Colloids Surf B 2009; 69(2):157-63.
119. Chen J, Zehtabi F, Ouyang J, Kong J, Zhong W, Xing MMQ. Reducible self-assembled micelles for enhanced intracellular delivery of doxorubicin. J Mater Chem 2012; 22:7121-29.
120. Harada A, Kataoka K. Pronounced activity of enzymes through the incorporation into the core of polyion complex micelles made from charged block copolymers. J Control Release 2001; 72(1-3):85-91.
121. Ramasamy T, Choi JY, Cho HJ, Umadevi SK, Shin BS, Choi HG, et al. Polypeptide-based micelles for delivery of irinotecan: physicochemical and in vivo characterization. Pharm Res 2014; in press.
122. Zhan C, Qian J, Feng L, Zhong G, Zhu J, Lu W. Cyclic RGD-poly(ethylene glycol)-polyethyleneimine is more suitable for glioblastoma targeting gene transfer in vivo. J Drug Target 2011; 19(7):573-81.
123. Mondon K, Zeisser-Labouèbe M, Gurny R, Möller M. Novel cyclosporin A formulations using MPEG-hexyl-substituted polylactide micelles: a suitability study. Eur J Pharm Biopharm 2011; 77(1):56-65.
124. Di Tommaso C, Bourges JL, Valamanesh F, Trubitsyn G, Torriglia A, Jeanny JC, et al. Novel micelle carriers for cyclosporin A topical ocular delivery: In vivo cornea penetration, ocular distribution and efficacy studies. Eur J Pharm Biopharm 2012; 81(2):257-64.
125. Peng T, Su J, Cheng SX, Zhuo RX. Degradation and drug release properties of poly-alpha,beta-[N-(2-hydroxyethyl)-L-aspartamide]-g-poly(2,2-dimethyltrimethylene carbonate). J Mater Sci Mater Med 2007; 18(9):1765-9.
126. Lee ES, Gao Z, Kim D, Park K, Kwon IC, Bae YH. Super pH-sensitive multifunctional polymeric micelle for tumor pH(e) specific TAT exposure and multidrug resistance. J Control Release 2008; 129(3):228-36.
127. Song Z, Feng R, Sun M, Guo C, Gao Y, Li L, et al. Curcumin-loaded PLGA-PEG-PLGA triblock copolymeric micelles: Preparation, pharmacokinetics and distribution in vivo. J Colloid Interface Sci 2011; 354(1):116-23.
128. Jeong JH, Kim SW, Park TG. Biodegradable triblock copolymer of PLGA-PEG-PLGA enhances gene transfection efficiency. Pharm Res 2004; 21(1):50-4.
129. Chang SF, Chang HY, Tong YC, Chen SH, Hsaio FC, Lu SC, et al. Nonionic polymeric micelles for oral gene delivery in vivo. Hum Gene Ther 2004; 15(5):481-93.

130. Chen YC, Jiang LP, Liu NX, Ding L, Liu XL, Wang ZH, et al. Enhanced gene transduction into skeletal muscle of mice in vivo with pluronic block copolymers and ultrasound exposure. Cell Biochem Biophys 2011; 60(3):267-73.
131. Wang Y, Yu L, Han L, Sha X, Fang X. Difunctional Pluronic copolymer micelles for paclitaxel delivery: synergistic effect of folate-mediated targeting and Pluronic-mediated overcoming multidrug resistance in tumor cell lines. Int J Pharm 2007; 337(1-2):63-73.
132. Wang Y, Li Y, Wang Q, Wu J, Fang X. Pharmacokinetics and biodistribution of paclitaxel-loaded pluronic P105/L101 mixed polymeric micelles. Yakugaku Zasshi 2008; 128(6):941-50.
133. Wang Y, Li Y, Wang Q, Fang X. Pharmacokinetics and biodistribution of polymeric micelles of paclitaxel with pluronic P105/poly(caprolactone) copolymers. Pharmazie 2008; 63(6):446-52.
134. Dutta P, Dey J. Drug solubilization by amino acid based polymeric nanoparticles: characterization and biocompatibility studies. Int J Pharm 2011; 421(2):353-63.
135. Dutta P, Dey J, Perumal V, Mandal M. Amino acid based amphiphilic copolymer micelles as carriers of non-steroidal anti-inflammatory drugs: solubilization, in vitro release and biological evaluation. Int J Pharm 2011; 407(1-2):207-16.
136. Dutta P, Shrivastava S, Dey J. Amphiphilic polymer nanoparticles: characterization and assessment as new drug carriers. Macromol Biosci 2009; 9(11):1116-26.
137. Orienti I, Zuccari G, Fini A, Rabasco AM, Carosio R, Raffaghello L, et al. Modified doxorubicin for improved encapsulation in PVA polymeric micelles. Drug Deliv 2005; 12(1):15-20.
138. Zeng X, Li J, Zheng J, Pan Y, Wang J, Zhang L, et al. Amphiphilic cylindrical copolypeptide brushes as potential nanocarriers for the simultaneous encapsulation of hydrophobic and cationic drugs. Colloids Surf B 2012; 94:324-32.
139. Wei Y, Wang Y, Wang L, Hao D, Ma G. Fabrication strategy for amphiphilic microcapsules with narrow size distribution by premix membrane emulsification. Colloids Surf B 2011; 87(2):399-408.
140. Morita T, Horikiri Y, Suzuki T, Yoshino H. Applicability of various amphiphilic polymers to the modification of protein release kinetics from biodegradable reservoir-type microspheres. Eur J Pharm Biopharm 2001; 51(1):45-53.
141. Chen S, Zhang XZ, Cheng SX, Zhuo RX, Gu ZW. Functionalized amphiphilic hyperbranched polymers for targeted drug delivery. Biomacromolecules 2008; 9(10):2578-85.
142. Xu Q, Liu Y, Su S, Li W, Chen C, Wu Y. Anti-tumor activity of paclitaxel through dual-targeting carrier of cyclic RGD and transferrin conjugated hyperbranched copolymer nanoparticles. Biomaterials 2012; 33(5):1627-39.
143. Wong HL, Bendayan R, Rauth AM, Xue HY, Babakhanian K, Wu XY. A mechanistic study of enhanced doxorubicin uptake and retention in multidrug resistant breast cancer cells using a polymer-lipid hybrid nanoparticle system. J Pharmacol Exp Ther 2006; 317(3):1372-81.
144. Shuhendler AJ, Cheung RY, Manias J, Connor A, Rauth AM, Wu XY. A novel doxorubicin-mitomycin C co-encapsulated nanoparticle formulation exhibits anti-cancer synergy in multidrug resistant human breast cancer cells. Breast Cancer Res Treat 2010; 119(2):255-69.

145. Hu Y, Atukorale PU, Lu JJ, Moon JJ, Um SH, Cho EC, et al. Cytosolic delivery mediated via electrostatic surface binding of protein, virus, or siRNA cargos to pH-responsive core-shell gel particles. Biomacromolecules 2009; 10(4):756-65.
146. Chaudhari KR, Ukawala M, Manjappa AS, Kumar A, Mundada PK, Mishra AK, et al. Opsonization, biodistribution, cellular uptake and apoptosis study of PEGylated PBCA nanoparticle as potential drug delivery carrier. Pharm Res 2012; 29(1):53-68.
147. Song N, Liu W, Tu Q, Liu R, Zhang Y, Wang J. Preparation and in vitro properties of redox-responsive polymeric nanoparticles for paclitaxel delivery. Colloids Surf B 2011; 87(2):454-63.
148. Chen J, Tian B, Yin X, Zhang Y, Hu D, Hu Z, et al. Preparation, characterization and transfection efficiency of cationic PEGylated PLA nanoparticles as gene delivery systems. J Biotechnol 2007; 130(2):107-13.
149. Kwon JS, Park IK, Cho AS, Shin SM, Hong MH, Jeong SY, et al. Enhanced angiogenesis mediated by vascular endothelial growth factor plasmid-loaded thermo-responsive amphiphilic polymer in a rat myocardial infarction model. J Control Release 2009; 138(2):168-76.
150. Kamei N, Morishita M, Chiba H, Kavimandan NJ, Peppas NA, Takayama K. Complexation hydrogels for intestinal delivery of interferon beta and calcitonin. J Control Release 2009; 134(2):98-102.
151. Nakamura K, Murray RJ, Joseph JI, Peppas NA, Morishita M, Lowman AM. Oral insulin delivery using P(MAA-g-EG) hydrogels: effects of network morphology on insulin delivery characteristics. J Control Release 2004; 95(3):589-99.
152. Morishita M, Goto T, Nakamura K, Lowman AM, Takayama K, Peppas NA. Novel oral insulin delivery systems based on complexation polymer hydrogels: single and multiple administration studies in type 1 and 2 diabetic rats. J Control Release 2006; 110(3):587-94.
153. Bhattarai N, Ramay HR, Gunn J, Matsen FA, Zhang M. PEG-grafted chitosan as an injectable thermosensitive hydrogel for sustained protein release. J Control Release 2005; 103(3):609-24.
154. Gao Y, Sun Y, Ren F, Gao S. PLGA-PEG-PLGA hydrogel for ocular drug delivery of dexamethasone acetate. Drug Dev Ind Pharm 2010; 36(10):1131-8.
155. Ghahremankhani AA, Dorkoosh F, Dinarvand R. PLGA-PEG-PLGA tri-block copolymers as in situ gel-forming peptide delivery system: effect of formulation properties on peptide release. Pharm Dev Technol 2008; 13(1):49-55.
156. Wenzel J, Balaji K, Koushik K, Navarre C, Duran S, Rahe C, et al. Pluronic F127 gel formulations of deslorelin and GnRH reduce drug degradation and sustain drug release and effect in cattle. J Control Release 2002; 85(1-3):51-9.
157. Pisal S, Paradkar A, Mahadik K, Kadam S. Pluronic gels for nasal delivery of vitamin B-12. Part I: preformulation study. Int J Pharm 2004; 270(1-2):37-45.
158. Escobar-Chavez J, Quintanar-Guerrero D, Ganem-Quintanar A. In vivo skin permeation of sodium naproxen formulated in pluronic F-127 gels: Effect of Azone and Transcutol. Drug Dev Ind Pharm 2005; 31(4-5):447-54.
159. Wang C, Han W, Tang X, Zhang H. Evaluation of drug release profile from patches based on styrene-isoprene-styrene block copolymer: the effect of block structure and plasticizer. AAPS PharmSciTech 2012; 13(2):556-67.

160. Rouxhet L, Dinguizli M, Latere Dwan'isa JP, Ould-Ouali L, Twaddle P, Nathan A, et al. Monoglyceride-based self-assembling copolymers as carriers for poorly water-soluble drugs. Int J Pharm 2009; 382(1-2):244-53.
161. Linn M, Collnot EM, Djuric D, Hempel K, Fabian E, Kolter K, et al. Soluplus® as an effective absorption enhancer of poorly soluble drugs in vitro and in vivo. Eur J Pharm Sci 2012; 45(3):336-43.
162. Zu Y, Gorukanti S, Ahmed SU, inventors; Abon Pharmaceuticals, LLC, assignee. Extended-release oral dosage forms for poorly soluble amine drugs. US20120087979 A1 2012.
163. Moghimi SM, Hunter AC. Poloxamers and poloxamines in nanoparticle engineering and experimental medicine. Trends Biotechnol 2000; 18(10):412-20.
164. Kabanov AV, Batrakova EV, Alakhov VY. Pluronic block copolymers as novel polymer therapeutics for drug and gene delivery. J Control Release 2002; 82(2-3):189-212.
165. Stridsberg K, Ryner M, Albertsson A. Controlled ring-opening polymerization: polymers with designed macromolecular architecture. In: Albertsson A, editor. Degradable Aliphatic Polyesters: Advances in Polymer Science. Springer-Verlag Berlin Heidelberg; 2002. p. 41-65.
166. Albertsson A, Varma I. Recent developments in ring opening polymerization of lactones for biomedical applications. Biomacromolecules 2003; 4(6):1466-86.
167. O'Donnell JM. Reversible addition-fragmentation chain transfer polymerization in microemulsion. Chem Soc Rev 2012; 41:3061–76.
168. Srivastava R, Albertsson A. Enzyme-catalyzed ring-opening polymerization of seven-membered ring lactones leading to terminal-functionalized and triblock polyesters. Macromolecules 2006; 39(1):46-54.
169. Albertsson A, Srivastava R. Recent developments in enzyme-catalyzed ring-opening polymerization. Adv Drug Deliv Rev 2008; 60(9):1077-93.
170. Kumar M, Kumar N, Domb A, Arora M. Pharmaceutical polymeric controlled drug delivery systems. In: Filled Elastomers Drug Delivery Systems: Advances in Polymer Science. Springer-Verlag Berlin Heidelberg; 2002. p. 45-117.
171. Smith A, Xu X, McCormick C. Stimuli-responsive amphiphilic (co)polymers via RAFT polymerization. Prog Polym Sci 2010; 35(1-2):45-93.
172. Ward MA, Georgiou TK. Thermoresponsive polymers for biomedical applications. Polymers 2011; 3:1215-42.
173. Motornov M, Roiter Y, Tokarev I, Minko S. Stimuli-responsive nanoparticles, nanogels and capsules for integrated multifunctional intelligent systems. Prog Polym Sci 2010; 35(1-2):174-211.
174. Hu Y, Litwin T, Nagaraja AR, Kwong B, Katz J, Watson N, et al. Cytosolic delivery of membrane-impermeable molecules in dendritic cells using pH-responsive core-shell nanoparticles. Nano Lett 2007; 7(10):3056-64.
175. Urbani CN, Bell CA, Lonsdale D, Whittaker MR, Monteiro MJ. Self-assembly of amphiphilic polymeric dendrimers synthesized with selective degradable linkages. Macromolecules 2008; 41:76-86.
176. Letchford K, Burt H. A review of the formation and classification of amphiphilic block copolymer nanoparticulate structures: micelles, nanospheres, nanocapsules and polymersomes. Eur J Pharm Biopharm 2007; 65(3):259-69.

177. Myers D. Surfactant science and technology. 3rd ed. USA: Wiley-Interscience; 2006.
178. Jones M, Leroux J. Polymeric micelles - a new generation of colloidal drug carriers. Eur J Pharma Biopharm. 1999; 48:101-11.
179. Malmsten M. Surfactants and polymers in drug delivery. CRC Press; 2002.
180. Babinot J, Guigner JM, Renard E, Langlois V. A micellization study of medium chain length poly(3-hydroxyalkanoate)-based amphiphilic diblock copolymers. J Colloid Interface Sci 2012; 375(1):88-93.
181. Abdekhodaie MJ, Liu Z, Erhan SZ, Wu XY. Characterization of novel soybean-oil-based thermosensitive amphiphilic polymers for drug delivery applications. Polym Int 2012; 61(9):1477-84.
182. Hu Z, Fan X, Wang H, Wang J. Synthesis and characterization of biodegradable and biocompatible amphiphilic block copolymers bearing pendant amino acid residues. Polymer 2009; 50(17):4175–81.
183. Cerritelli S, O'Neil CP, Velluto D, Fontana A, Adrian M, Dubochet J, et al. Aggregation behavior of poly(ethylene glycol-bl-propylene sulfide) di- and triblock copolymers in aqueous solution. Langmuir 2009; 25(19):11328-35.
184. Alexandridis P, Holzwarthf JF, Hatton TA. Micellization of poly(ethylene oxide)-poly(propylene oxide)-poly(ethylene oxide) triblock copolymers in aqueous solutions: thermodynamics of copolymer association. Macromolecules 1994; 27:2414-25.
185. Gu L, Shen Z, Feng C, Li Y, Lu G, Huang X. Synthesis of double hydrophilic graft copolymer containing poly(ethylene glycol) and poly(methacrylic acid) side chains via successive ATRP. J Polym Sci Pol Chem 2008; 46:4056–69.
186. Fournier E, Dufresne MH, Smith DC, Ranger M, Leroux JC. A novel one-step drug-loading procedure for water-soluble amphiphilic nanocarriers. Pharm Res 2004; 21(6):962-8.
187. Dutta P, Dey J, Ghosh G, Nayak RR. Self-association and microenvironment of random amphiphilic copolymers of sodium N-acryloyl-L-valinate and N-dodecylacrylamide in aqueous solution. Polymer 2009; 50:1516–25.
188. Ho K, Li W, Wong C, Li P. Amphiphilic polymeric particles with core-shell nanostructures: emulsion-based syntheses and potential applications. Colloid Polym Sci 2010; 288(16-17):1503-23.
189. Kwon GS. Amphiphilic block copolymer micelles for nanoscale drug delivery. Drug Develop Res 2006; 67(1):15-22.
190. Owens DE, Peppas NA. Opsonization, biodistribution, and pharmacokinetics of polymeric nanoparticles. Int J Pharm 2006; 307(1):93-102.
191. Moghimi SM, Szebeni J. Stealth liposomes and long circulating nanoparticles: critical issues in pharmacokinetics, opsonization and protein-binding properties. Prog Lipid Res 2003; 42(6):463-78.
192. Merrett K, Cornelius RM, McClung WG, Unsworth LD, Sheardown H. Surface analysis methods for characterizing polymeric biomaterials. J Biomater Sci Polym Ed 2002; 13(6):593-621.
193. Morales ME, Ruiz MA, Oliva I, Oliva M, Gallardo V. Chemical characterization with XPS of the surface of polymer microparticles loaded with morphine. Int J Pharm 2007; 333(1-2):162-6.
194. Rösler A, Vandermeulen GW, Klok HA. Advanced drug delivery devices via self-assembly of amphiphilic block copolymers. Adv Drug Deliv Rev 2001; 53(1):95-108.

195. Kamaly N, Xiao Z, Valencia PM, Radovic-Moreno AF, Farokhzad OC. Targeted polymeric therapeutic nanoparticles: design, development and clinical translation. Chem Soc Rev 2012; 41(7):2971-3010.
196. Linkov I, Satterstrom F, Corey L. Nanotoxicology and nanomedicine: making hard decisions. Nanomedicine 2008; 4(2):167-71.
197. Rinaldo M, Andujar P, Lacourt A, Martinon L, Canal Raffin M, Dumortier P, et al. Perspectives in biological monitoring of inhaled nanosized particles. Ann Occup Hyg 2015; in press.
198. Oberdörster G, Oberdörster E, Oberdörster J. Nanotoxicology: an emerging discipline evolving from studies of ultrafine particles. Environ Health Perspect 2005; 113(7):823-39.
199. Möller W, Felten K, Sommerer K, Scheuch G, Meyer G, Meyer P, et al. Deposition, retention, and translocation of ultrafine particles from the central airways and lung periphery. Am J Respir Crit Care Med 2008; 177(4):426-32.
200. Renwick L, Brown D, Clouter A, Donaldson K. Increased inflammation and altered macrophage chemotactic responses caused by two ultrafine particle types. Occup Environ Med 2004; 61(5):442-7.
201. Pickup J, Zhi Z, Khan F, Saxl T, Birch D. Nanomedicine and its potential in diabetes research and practice. Diabetes Metab Res Rev 2008; 24(8):604-10.
202. Tauzin B. Biotechnology Medicines in Development. Washington DC: Pharmaceutical Research and Manufacturers Association, 2008.
203. Tang L, Meibohm B. Pharmacokinetics of peptides and proteins. In: Meibohm B, editor. Pharmacokinetics and pharmacodynamics of biotech drugs - principles and case studies in drug development. Weinheim: Wiley-VCH Verlag GmbH & Co. KGaA; 2006. p. 17-43.
204. PhRMA. 2013 Overview: medicines in development - biologics: http://www.phrma.org [accessed on December 2014].
205. Morishita M, Peppas N. Is the oral route possible for peptide and protein drug delivery? Drug Discov Today 2006; 11(19-20):905-10.
206. Rader RA. FDA biopharmaceutical product approvals and trends in 2012. BioProcess Int 2013; 11(3):18-27.
207. EvaluatePharma. World Preview 2018: http://www.evaluatepharma.com [accessed on June 2014].
208. Albericio F, Kruger HG. Therapeutic peptides. Future Med Chem 2012; 4(12):1527-31.
209. Hillery A. Drug delivery: the basic concepts. In: Hillery A, Lloyd A, Swarbrick J, editors. Drug delivery and targeting for pharmacists and pharmaceutical scientists. First ed. London and New York: Taylor & Francis; 2001. p. 1-48.
210. Craik DJ, Fairlie DP, Liras S, Price D. The future of peptide-based drugs. Chem Biol Drug Des 2013; 81(1):136-47.
211. Antosova Z, Mackova M, Kral V, Macek T. Therapeutic application of peptides and proteins: parenteral forever? Trends Biotechnol 2009; 27(11):628-35.
212. Sharma AR, Kundu SK, Nam JS, Sharma G, Priya Doss CG, Lee SS, et al. Next generation delivery system for proteins and genes of therapeutic purpose: why and how? Biomed Res Int 2014; 2014:327950.
213. Depreter F, Pilcer G, Amighi K. Inhaled proteins: challenges and perspectives. Int J Pharm 2013; 447(1-2):251-80.

214. Quan C, Alcala E, Petkovska I, Matthews D, Canova-Davis E, Taticek R, et al. A study in glycation of a therapeutic recombinant humanized monoclonal antibody: where it is, how it got there, and how it affects charge-based behavior. Anal Biochem 2008; 373(2):179-91.
215. Klingler C, Müller B, Steckel H. Insulin-micro- and nanoparticles for pulmonary delivery. Int J Pharm 2009; 377(1-2):173-9.
216. Amidi M, Mastrobattista E, Jiskoot W, Hennink W. Chitosan-based delivery systems for protein therapeutics and antigens. Adv Drug Deliv Rev 2010; 62(1):59-82.
217. Pinto Reis C, Silva C, Martinho N, Rosado C. Drug carriers for oral delivery of peptides and proteins: accomplishments and future perspectives. Ther Deliv 2013; 4(2):251-65.
218. Sarmento B, Ribeiro A, Veiga F, Ferreira D. Development and characterization of new insulin containing polysaccharide nanoparticles. Colloids Surf B 2006; 53(2):193-202.
219. Bayat A, Dorkoosh F, Dehpour A, Moezi L, Larijani B, Junginger H, et al. Nanoparticles of quaternized chitosan derivatives as a carrier for colon delivery of insulin: ex vivo and in vivo studies. Int J Pharm 2008; 356(1-2):259-66.
220. Kane C, O'Neil K, Conk M, Picha K. Inhalation delivery of protein therapeutics. Inflamm Allergy Drug Targets 2013; 12(2):81-7.
221. Anderson PJ. History of aerosol therapy: liquid nebulization to MDIs to DPIs. Respir Care 2005; 50(9):1139-50.
222. Sanders M. Inhalation therapy: an historical review. Prim Care Respir J 2007; 16(2):71-81.
223. O'Callaghan C, Nerbrink O, Vidgren MT. The history of inhaled drug therapy. In: Bisgaard H, O'Callaghan C, Smaldone GC, editors. Drug delivery to the lung. Lung biology in health and disease. Marcel Dekker; 2002. p. 1-20.
224. Rau JL. The inhalation of drugs: advantages and problems. Respir Care 2005; 50(3):367-82.
225. Dessanges JF. A history of nebulization. J Aerosol Med 2001; 14(1):65-71.
226. Knott FA, Southwell N. Aerosol Penicillin in the Oxygen Tent. Arch Dis Child 1946; 21(105):16-8.
227. Humphrey J, Joules H. Penicillin inhalation in pulmonary disease. Lancet 1946; 2(6416):221-5.
228. Southwell N. Inhaled penicillin in bronchial infections. Lancet 1946; 2(6416):225-7.
229. Hurst A. Penicillin nebulization in bronchopulmonary disease: a preliminary report. Rocky Mt Med J 1946; 43:219-21.
230. O'Riordan T. Inhaled antimicrobial therapy: from cystic fibrosis to the flu. Respir Care 2000; 45(7):836–45.
231. McAllen MK, Kochanowski SJ, Shaw KM. Steroid aerosols in asthma: an assessment of betamethasone valerate and a 12-month study of patients on maintenance treatment. Br Med J 1974; 1(5900):171-5.
232. Muttil P, Wang C, Hickey AJ. Inhaled drug delivery for tuberculosis therapy. Pharm Res 2009; 26(11):2401-16.
233. Geller DE, Flume PA, Staab D, Fischer R, Loutit JS, Conrad DJ, et al. Levofloxacin inhalation solution (MP-376) in patients with cystic fibrosis with Pseudomonas aeruginosa. Am J Respir Crit Care Med 2011; 183(11):1510-6.

234. Bernstein DI, Reuman PD, Sherwood JR, Young EC, Schiff GM. Ribavirin small-particle-aerosol treatment of influenza B virus infection. Antimicrob Agents Chemother 1988; 32(5):761-4.
235. Mohammad RA, Klein KC. Inhaled amphotericin B for prophylaxis against invasive Aspergillus infections. Ann Pharmacother 2006; 40(12):2148-54.
236. Aitken M, Burke W, McDonald G, Shak S, Montgomery A, Smith A. Recombinant human DNase inhalation in normal subjects and patients with cystic fibrosis. A phase 1 study. JAMA 1992; 267(14):1947-51.
237. Jones LH, Baldock H, Bunnage ME, Burrows J, Clarke N, Coghlan M, et al. Inhalation by design: dual pharmacology β-2 agonists/M3 antagonists for the treatment of COPD. Bioorg Med Chem Lett 2011; 21(9):2759-63.
238. de Galan B, Simsek S, Tack C, Heine R. Efficacy and safety of inhaled insulin in the treatment of diabetes mellitus. Neth J Med 2006; 64(9):319-25.
239. Huland E, Burger A, Fleischer J, Fornara P, Hatzmann E, Heidenreich A, et al. Efficacy and safety of inhaled recombinant interleukin-2 in high-risk renal cell cancer patients compared with systemic interleukin-2: an outcome study. Folia Biologica 2003; 49(5):183-90.
240. Videira M, Almeida AJ, Fabra A. Preclinical evaluation of a pulmonary delivered paclitaxel-loaded lipid nanocarrier antitumor effect. Nanomedicine 2011; 8(7):1208-15.
241. Hokey DA, Misra A. Aerosol vaccines for tuberculosis: a fine line between protection and pathology. Tuberculosis (Edinb) 2011; 91(1):82-5.
242. Lu D, Garcia-Contreras L, Muttil P, Padilla D, Xu D, Liu J, et al. Pulmonary immunization using antigen 85-B polymeric microparticles to boost tuberculosis immunity. AAPS J 2010; 12(3):338-47.
243. Todoroff J, Ucakar B, Inglese M, Vandermarliere S, Fillee C, Renauld JC, et al. Targeting the deep lungs, Poloxamer 407 and a CpG oligonucleotide optimize immune responses to Mycobacterium tuberculosis antigen 85A following pulmonary delivery. Eur J Pharm Biopharm 2013; 84(1):40-8.
244. Cryan S, Sivadas N, Garcia-Contreras L. In vivo animal models for drug delivery across the lung mucosal barrier. Adv Drug Deliv Rev 2007; 59(11):1133-51.
245. Stocks J, Hislop AA. Structure and function of the respiratory system-developmental aspects and their relevance to aerosol therapy. In: Bisgaard H, O'Callaghan C, Smaldone GC, editors. Drug delivery to the lung. Lung biology in health and disease. New York: Marcel Dekker; 2001. p. 47-104.
246. Widmaier E, Raff H, Strang K, editors. Vander's Human Physiology - The Mechanisms of Body Function. 10th ed: McGraw-Hill Higher Education; 2006.
247. Groneberg D, Fischer A, Chung K, Daniel H. Molecular mechanisms of pulmonary peptidomimetic drug and peptide transport. Am J Respir Cell Mol Biol 2004; 30(3):251-60.
248. Kim K, Malik A. Protein transport across the lung epithelial barrier. Am J Physiol Lung Cell Mol Physiol 2003; 284(2):L247-59.
249. Vlahovic G, Russell ML, Mercer RR, Crapo JD. Cellular and connective tissue changes in alveolar septal walls in emphysema. Am J Respir Crit Care Med 1999; 160(6):2086-92.
250. Yang W, Peters J, Williams Rr. Inhaled nanoparticles - a current review. Int J Pharm 2008; 356(1-2):239-47.
251. Rytting E, Nguyen J, Wang X, Kissel T. Biodegradable polymeric nanocarriers for pulmonary drug delivery. Expert Opin Drug Deliv 2008; 5(6):629-39.

252. Tomoda K, Ohkoshi T, Nakajima T, Makino K. Preparation and properties of inhalable nanocomposite particles: effects of the size, weight ratio of the primary nanoparticles in nanocomposite particles and temperature at a spray-dryer inlet upon properties of nanocomposite particles. Colloids Surf B 2008; 64(1):70-6.
253. Scheuch G, Kohlhaeufl MJ, Brand P, Siekmeier R. Clinical perspectives on pulmonary systemic and macromolecular delivery. Adv Drug Deliv Rev 2006; 58(9-10):996-1008.
254. Hastings R, Folkesson H, Matthay M. Mechanisms of alveolar protein clearance in the intact lung. Am J Physiol Lung Cell Mol Physiol 2004; 286(4):L679-89.
255. Berthiaume Y, Albertine K, Grady M, Fick G, Matthay M. Protein clearance from the air spaces and lungs of unanesthetized sheep over 144 h. J Appl Physiol 1989; 67(5):1887-97.
256. Patton JS, Fishburn CS, Weers JG. The lungs as a portal of entry for systemic drug delivery. Proc Am Thorac Soc 2004; 1(4):338-44.
257. Folkesson H, Weström B, Karlsson B. Permeability of the respiratory tract to different-sized macromolecules after intratracheal instillation in young and adult rats. Acta Physiol Scand 1990; 139(2):347-54.
258. Conhaim R, Watson K, Lai-Fook S, Harms B. Transport properties of alveolar epithelium measured by molecular hetastarch absorption in isolated rat lungs. J Appl Physiol 2001; 91(4):1730-40.
259. Holter J, Weiland J, Pacht E, Gadek J, Davis W. Protein permeability in the adult respiratory distress syndrome. Loss of size selectivity of the alveolar epithelium. J Clin Invest 1986; 78(6):1513-22.
260. Siekmeier R, Scheuch G. Systemic treatment by inhalation of macromolecules-principles, problems, and examples. J Physiol Pharmacol 2008; 59 Suppl 6:53-79.
261. Bitonti AJ, Dumont JA. Pulmonary administration of therapeutic proteins using an immunoglobulin transport pathway. Adv Drug Deliv Rev 2006; 58(9-10):1106-18.
262. Bitonti A, Dumont J, Low S, Peters R, Kropp K, Palombella V, et al. Pulmonary delivery of an erythropoietin Fc fusion protein in non-human primates through an immunoglobulin transport pathway. PNAS 2004; 101(26):9763-8.
263. Morris CJ, Smith MW, Griffiths PC, McKeown NB, Gumbleton M. Enhanced pulmonary absorption of a macromolecule through coupling to a sequence-specific phage display-derived peptide. J Control Release 2011; 151(1):83-94.
264. Jeong SH. Analytical methods and formulation factors to enhance protein stability in solution. Arch Pharm Res 2012; 35(11):1871-86.
265. Frokjaer S, Otzen DE. Protein drug stability: a formulation challenge. Nat Rev Drug Discov 2005; 4(4):298-306.
266. de Boer AH, Gjaltema D, Hagedoorn P, Frijlink HW. Characterization of inhalation aerosols: a critical evaluation of cascade impactor analysis and laser diffraction technique. Int J Pharm 2002; 249(1-2):219-31.
267. Pilcer G, Amighi K. Formulation strategy and use of excipients in pulmonary drug delivery. Int J Pharm 2010; 392(1-2):1-19.
268. Heyder J. Deposition of inhaled particles in the human respiratory tract and consequences for regional targeting in respiratory drug delivery. Proc Am Thorac Soc 2004; 1(4):315-20.
269. Crowder T, Rosati J, Schroeter J, Hickey A, Martonen T. Fundamental effects of particle morphology on lung delivery: predictions of Stokes' law and the particular

relevance to dry powder inhaler formulation and development. Pharm Res 2002; 19(3):239-45.
270. Champion JA, Walker A, Mitragotri S. Role of particle size in phagocytosis of polymeric microspheres. Pharm Res 2008; 25(8):1815-21.
271. Chono S, Tanino T, Seki T, Morimoto K. Uptake characteristics of liposomes by rat alveolar macrophages: influence of particle size and surface mannose modification. J Pharm Pharmacol 2007; 59(1):75-80.
272. Al-Qadi S, Grenha A, Carrión-Recio D, Seijo B, Remuñán-López C. Microencapsulated chitosan nanoparticles for pulmonary protein delivery: in vivo evaluation of insulin-loaded formulations. J Control Release 2012; 157(3):383-90.
273. Yu SS, Lau CM, Thomas SN, Jerome WG, Maron DJ, Dickerson JH, et al. Size- and charge-dependent non-specific uptake of PEGylated nanoparticles by macrophages. Int J Nanomedicine 2012; 7:799-813.
274. Yue H, Wei W, Yue Z, Lv P, Wang L, Ma G, et al. Particle size affects the cellular response in macrophages. Eur J Pharm Sci 2010; 41(5):650-7.
275. Telko MJ, Hickey AJ. Dry powder inhaler formulation. Respir Care 2005; 50(9):1209-27.
276. Dolovich MB, Dhand R. Aerosol drug delivery: developments in device design and clinical use. Lancet 2011; 377(9770):1032-45.
277. Islam N, Gladki E. Dry powder inhalers (DPIs)-a review of device reliability and innovation. Int J Pharm 2008; 360(1-2):1-11.
278. Muralidharan P, Malapit M, Mallory E, Hayes D, Mansour HM. Inhalable nanoparticulate powders for respiratory delivery. Invited review. Nanomedicine 2015; in press.
279. Shoyele SA, Cawthorne S. Particle engineering techniques for inhaled biopharmaceuticals. Adv Drug Deliv Rev 2006; 58(9-10):1009-29.
280. Donovan MJ, Kim SH, Raman V, Smyth HD. Dry powder inhaler device influence on carrier particle performance. J Pharm Sci 2012; 101(3):1097-107.
281. Pitchayajittipong C, Price R, Shur J, Kaerger JS, Edge S. Characterisation and functionality of inhalation anhydrous lactose. Int J Pharm 2010; 390(2):134-41.
282. Kaialy W, Ticehurst M, Nokhodchi A. Dry powder inhalers: mechanistic evaluation of lactose formulations containing salbutamol sulphate. Int J Pharm 2012; 423(2):184-94.
283. Kaialy W, Alhalaweh A, Velaga SP, Nokhodchi A. Influence of lactose carrier particle size on the aerosol performance of budesonide from a dry powder inhaler. Powder Technol 2012; 227:74–85.
284. Young PM, Cocconi D, Colombo P, Bettini R, Price R, Steele DF, et al. Characterization of a surface modified dry powder inhalation carrier prepared by "particle smoothing". J Pharm Pharmacol 2002; 54(10):1339-44.
285. Schiavone H, Palakodaty S, Clark A, York P, Tzannis ST. Evaluation of SCF-engineered particle-based lactose blends in passive dry powder inhalers. Int J Pharm 2004; 281(1-2):55-66.
286. Le VN, Hoang Thi TH, Robins E, Flament MP. Dry powder inhalers: study of the parameters influencing adhesion and dispersion of fluticasone propionate. AAPS PharmSciTech 2012; 13(2):477-84.
287. Le VN, Hoang Thi TH, Robins E, Flament MP. In vitro evaluation of powders for inhalation: the effect of drug concentration on particle detachment. Int J Pharm 2012; 424(1-2):44-9.

288. Dickhoff BH, de Boer AH, Lambregts D, Frijlink HW. The effect of carrier surface and bulk properties on drug particle detachment from crystalline lactose carrier particles during inhalation, as function of carrier payload and mixing time. Eur J Pharm Biopharm 2003; 56(2):291-302.
289. Dickhoff BH, de Boer AH, Lambregts D, Frijlink HW. The effect of carrier surface treatment on drug particle detachment from crystalline carriers in adhesive mixtures for inhalation. Int J Pharm 2006; 327(1-2):17-25.
290. U.S. Department of Health and Human Services Food and Drug Administration, Guidance for Industry: Nonclinical Studies for the Safety Evaluation of Pharmaceutical Excipients. 2005.
291. ICH M3 (R2), Non-Clinical Safety Studies for the Conduct of Human Clinical Trials and Marketing Authorization for Pharmaceuticals. CPMP/ICH/286/95. 2009.
292. ICH S3A, Note for Guidance on Toxicokinetics: The Assessment of Systemic Exposure in Toxicity Studies. CPMP/ICH/384/95. 1994.
293. Zaru M, Mourtas S, Klepetsanis P, Fadda AM, Antimisiaris SG. Liposomes for drug delivery to the lungs by nebulization. Eur J Pharm Biopharm 2007; 67(3):655-66.
294. FDA. GRAS Notice Inventory. http://www.fda.gov/Food/IngredientsPackagingLabeling/GRAS/NoticeInventory [Accessed on March 2015].
295. de Jesús Valle MJ, Dinis-Oliveira RJ, Carvalho F, Bastos ML, Sánchez Navarro A. Toxicological evaluation of lactose and chitosan delivered by inhalation. J Biomater Sci Polym Ed 2008; 19(3):387-97.
296. Grenha A, Grainger C, Dailey L, Seijo B, Martin G, Remuñán-López C, et al. Chitosan nanoparticles are compatible with respiratory epithelial cells in vitro. Eur J Pharm Sci 2007; 31(2):73-84.
297. Mura S, Hillaireau H, Nicolas J, Le Droumaguet B, Gueutin C, Zanna S, et al. Influence of surface charge on the potential toxicity of PLGA nanoparticles towards Calu-3 cells. Int J Nanomedicine 2011; 6:2591-605.
298. Davis ME, Brewster ME. Cyclodextrin-based pharmaceutics: past, present and future. Nat Rev Drug Discov 2004; 3(12):1023-35.
299. Bailey MM, Gorman EM, Munson EJ, Berkland C. Pure insulin nanoparticle agglomerates for pulmonary delivery. Langmuir 2008; 24(23):13614-20.
300. Pilcer G, Vanderbist F, Amighi K. Spray-dried carrier-free dry powder tobramycin formulations with improved dispersion properties. J Pharm Sci 2009; 98(4):1463-75.
301. Garcia-Contreras L, Fiegel J, Telko MJ, Elbert K, Hawi A, Thomas M, et al. Inhaled large porous particles of capreomycin for treatment of tuberculosis in a guinea pig model. Antimicrob Agents Chemother 2007; 51(8):2830-6.
302. Mueannoom W, Srisongphan A, Taylor KM, Hauschild S, Gaisford S. Thermal ink-jet spray freeze-drying for preparation of excipient-free salbutamol sulphate for inhalation. Eur J Pharm Biopharm 2012; 80(1):149-55.
303. Sharma G, Mueannoom W, Buanz AB, Taylor KM, Gaisford S. In vitro characterisation of terbutaline sulphate particles prepared by thermal ink-jet spray freeze drying. Int J Pharm 2013; 447(1-2):165-70.
304. DeHaan WH, Finlay WH. In vitro monodisperse aerosol deposition in a mouth and throat with six different inhalation devices. J Aerosol Med 2001; 14(3):361-7.

305. Coates MS, Fletcher DF, Chan HK, Raper JA. Effect of design on the performance of a dry powder inhaler using computational fluid dynamics. Part 1: Grid structure and mouthpiece length. J Pharm Sci 2004; 93(11):2863-76.
306. Labiris NR, Dolovich MB. Pulmonary drug delivery. Part II: the role of inhalant delivery devices and drug formulations in therapeutic effectiveness of aerosolized medications. Br J Clin Pharmacol 2003; 56(6):600-12.
307. Alexander BD, Winkler TP, Shi S, Dodds Ashley ES, Hickey AJ. In vitro characterization of nebulizer delivery of liposomal amphotericin B aerosols. Pharm Dev Technol 2011; 16(6):577-82.
308. Heinemann L. The failure of exubera: are we beating a dead horse? J Diabetes Sci Technol 2008; 2(3):518-29.
309. Kriksunov LB, Gumaste AV, inventors; Microdose Technologies, Inc assignee. US20080202514 A1. Inhaler 2008.
310. Crowder TM. Highly reproducible powder aerosolisation for lung delivery using powder-specific electromechanical vibration. Expert Opin Drug Deliv 2005; 2(3):579-85.
311. Wakefield K, Genova PA, inventors; IEP Pharmaceutical Devices Inc., assignee. WO2001085245 A1. Pneumatic breath actuated inhaler 2001.
312. Brunton L, Lazo J, Parker K, editors. Goodman & Gilman's the pharmacological basis of therapeutics. 11th ed. McGraw-Hill Professional; 2006.
313. Katzung B, editor. Basic & clinical pharmacology. 8th ed. Lange Medical Books/McGraw-Hill; 2001.
314. Agu R, Ugwoke M, Armand M, Kinget R, Verbeke N. The lung as a route for systemic delivery of therapeutic proteins and peptides. Respir Res 2001; 2(4):198-209.
315. Cheng K, Mahato R. Biopharmaceutical challenges: pulmonary delivery of proteins and peptides. In: Meibohm B, editor. Pharmacokinetics and pharmacodynamics of biotech drugs - principles and case studies in drug development. 1st ed. Weinheim: WILEY-VCH Verlag GmbH & Co. KGaA; 2006. p. 209-42.
316. Fineberg SE, Kawabata T, Finco-Kent D, Liu C, Krasner A. Antibody response to inhaled insulin in patients with type 1 or type 2 diabetes. An analysis of initial phase II and III inhaled insulin (Exubera) trials and a two-year extension trial. J Clin Endocrinol Metab 2005; 90(6):3287-94.
317. Wolzt M, de la Peña A, Berclaz P, Tibaldi F, Gates J, Muchmore D. AIR inhaled insulin versus subcutaneous insulin: pharmacokinetics, glucodynamics, and pulmonary function in asthma. Diabetes Care 2008; 31(4):735-40.
318. Skyler J, Cefalu W, Kourides I, Landschulz W, Balagtas C, Cheng S, et al. Efficacy of inhaled human insulin in type 1 diabetes mellitus: a randomised proof-of-concept study. Lancet 2001; 357(9253):331-5.
319. Rosenstock J, Cefalu W, Hollander P, Belanger A, Eliaschewitz F, Gross J, et al. Two-year pulmonary safety and efficacy of inhaled human insulin (Exubera) in adult patients with type 2 diabetes. Diabetes Care 2008; 31(9):1723-8.
320. Soares S, Costa A, Sarmento B. Novel non-invasive methods of insulin delivery. Expert Opin Drug Deliv 2012; 9(12):1539-58.
321. Karathanasis E, Bhavane R, Annapragada A. Glucose-sensing pulmonary delivery of human insulin to the systemic circulation of rats. Int J Nanomedicine 2007; 2(3):501-13.
322. Nyambura B, Kellaway I, Taylor K. Insulin nanoparticles: stability and aerosolization from pressurized metered dose inhalers. Int J Pharm 2009; 375(1-2):114-22.

323. Opar A. Another blow for inhaled protein therapeutics. Nat Rev Drug Discov 2008; 7:189-90.
324. Angelo R, Rousseau K, Grant M, Leone-Bay A, Richardson P. Technosphere insulin: defining the role of Technosphere particles at the cellular level. J Diabetes Sci Technol 2009; 3(3):545-54.
325. Pfützner A, Mann A, Steiner S. Technosphere/Insulin-a new approach for effective delivery of human insulin via the pulmonary route. Diabetes Technol Ther 2002; 4(5):589-94.
326. Zisser H, Jovanovic L, Markova K, Petrucci R, Boss A, Richardson P, et al. Technosphere insulin effectively controls postprandial glycemia in patients with type 2 diabetes mellitus. Diabetes Technol Ther 2012; 14(11):997-1001.
327. Potocka E, Amin N, Cassidy J, Schwartz SL, Gray M, Richardson PC, et al. Insulin pharmacokinetics following dosing with Technosphere insulin in subjects with chronic obstructive pulmonary disease. Curr Med Res Opin 2010; 26(10):2347-53.
328. Raskin P, Heller S, Honka M, Chang PC, Boss AH, Richardson PC, et al. Pulmonary function over 2 years in diabetic patients treated with prandial inhaled Technosphere Insulin or usual antidiabetes treatment: a randomized trial. Diabetes Obes Metab 2012; 14(2):163-73.
329. Liu J, Gong T, Fu H, Wang C, Wang X, Chen Q, et al. Solid lipid nanoparticles for pulmonary delivery of insulin. Int J Pharm 2008; 356(1-2):333-44.
330. Huang X, Du Y, Yuan H, Hu F. Preparation and pharmacodynamics of low-molecular-weight chitosan nanoparticles containing insulin. Carbohydr Polym 2009; 76(3):368–73.
331. Yamamoto H, Hoshina W, Kurashima H, Takeuchi H, Kawashima Y, Yokoyama T, et al. Engineering of poly(DL-lactic-co-glycolic acid) nanocomposite particles for dry powder inhalation dosage forms of insulin with the spray-fluidized bed granulating system. Adv Powder Technol 2007; 18(2):215-28.
332. Kawashima Y, Yamamoto H, Takeuchi H, Fujioka S, Hino T. Pulmonary delivery of insulin with nebulized DL-lactide/glycolide copolymer (PLGA) nanospheres to prolong hypoglycemic effect. J Control Release 1999; 62(1-2):279-87.
333. Grenha A, Seijo B, Remuñán-López C. Microencapsulated chitosan nanoparticles for lung protein delivery. Eur J Pharm Sci 2005; 25(4-5):427-37.
334. Zhang Q, Shen Z, Nagai T. Prolonged hypoglycemic effect of insulin-loaded polybutylcyanoacrylate nanoparticles after pulmonary administration to normal rats. Int J Pharm 2001; 218(1-2):75-80.
335. Huang Y, Wang C. Pulmonary delivery of insulin by liposomal carriers. J Control Release 2006; 113(1):9-14.
336. Bi R, Shao W, Wang Q, Zhang N. Spray-freeze-dried dry powder inhalation of insulin-loaded liposomes for enhanced pulmonary delivery. J Drug Target 2008; 16(9):639-48.
337. Chono S, Fukuchi R, Seki T, Morimoto K. Aerosolized liposomes with dipalmitoyl phosphatidylcholine enhance pulmonary insulin delivery. J Control Release 2009; 137(2):104-9.
338. Marino MT, Costello D, Baughman R, Boss A, Cassidy J, Damico C, et al. Pharmacokinetics and pharmacodynamics of inhaled GLP-1 (MKC253): proof-of-concept studies in healthy normal volunteers and in patients with type 2 diabetes. Clin Pharmacol Ther 2010; 88(2):243-50.

339. Wenzel S, Wilbraham D, Fuller R, Getz EB, Longphre M. Effect of an interleukin-4 variant on late phase asthmatic response to allergen challenge in asthmatic patients: results of two phase 2a studies. Lancet 2007; 370(9596):1422-31.
340. Getz EB, Fisher DM, Fuller R. Human pharmacokinetics/pharmacodynamics of an interleukin-4 and interleukin-13 dual antagonist in asthma. J Clin Pharmacol 2009; 49(9):1025-36.
341. Bridges RJ, Newton BB, Pilewski JM, Devor DC, Poll CT, Hall RL. Na+ transport in normal and CF human bronchial epithelial cells is inhibited by BAY 39-9437. Am J Physiol Lung Cell Mol Physiol 2001; 281(1):L16-23.
342. Moss RB, Hansen C, Sanders RL, Hawley S, Li T, Steigbigel RT. A phase II study of DAS181, a novel host directed antiviral for the treatment of influenza infection. J Infect Dis 2012; 206(12):1844-51.
343. Chan RW, Chan MC, Wong AC, Karamanska R, Dell A, Haslam SM, et al. DAS181 inhibits H5N1 influenza virus infection of human lung tissues. Antimicrob Agents Chemother 2009; 53(9):3935-41.
344. Drozd DR, Limaye AP, Moss RB, Sanders RL, Hansen C, Edelman JD, et al. DAS181 treatment of severe parainfluenza type 3 pneumonia in a lung transplant recipient. Transpl Infect Dis 2013; 15(1):E28-32.
345. Aerovance. A phase I/II study to investigate the efficacy and safety of AER 002 in cystic fibrosis given at 3 mg, 10 mg, and 30 mg doses in single then multiple ascending doses and to determine efficacy of the highest tolerable dose in a 4-Week proof of concept study. 2005-000313-35: https://www.clinicaltrialsregister.eu [accessed on December 2014].
346. APTPharmaceuticals. CIS001 extension study of cyclosporine inhalation solution (CIS002). NCT00938236: http://clinicaltrials.gov [accessed on December 2014].
347. University Medical Centre Groningen. Pilot study of cyclosporine A dry powder inhalation in lung transplant patients with bronchiolitis obliterans syndrome. NCT00378677: https://clinicaltrials.gov [accessed on December 2014].
348. Moss RB, Mayer-Hamblett N, Wagener J, Daines C, Hale K, Ahrens R, et al. Randomized, double-blind, placebo-controlled, dose-escalating study of aerosolized interferon gamma-1b in patients with mild to moderate cystic fibrosis lung disease. Pediatr Pulmonol 2005; 39(3):209-18.
349. Hallstrand TS, Ochs HD, Zhu Q, Liles WC. Inhaled IFN-gamma for persistent nontuberculous mycobacterial pulmonary disease due to functional IFN-gamma deficiency. Eur Respir J 2004; 24(3):367-70.
350. Kim D, Mudaliar S, Chinnapongse S, Chu N, Boies SM, Davis T, et al. Dose-response relationships of inhaled insulin delivered via the Aerodose insulin inhaler and subcutaneously injected insulin in patients with type 2 diabetes. Diabetes Care 2003; 26(10):2842-7.
351. DancePharmaceuticals. A phase 1/2 trial investigating the pharmacokinetics, pharmacodynamics and safety of inhaled insulin in subjects with type 1 diabetes. 2012-002071-34: https://www.clinicaltrialsregister.eu [accessed on December 2014].
352. Rave KM, Nosek L, de la Peña A, Seger M, Ernest CS, Heinemann L, et al. Dose response of inhaled dry-powder insulin and dose equivalence to subcutaneous insulin lispro. Diabetes Care 2005; 28(10):2400-5.
353. QDose. Investigating the pharmacokinetics and pharmacodynamics of recombinant human insulin administered by dry powder inhaler. NCT00426920: http://clinicaltrials.gov [accessed on December 2014].

354. Garcia-Contreras L, Morçöl T, Bell SJ, Hickey AJ. Evaluation of novel particles as pulmonary delivery systems for insulin in rats. AAPS PharmSci 2003; 5(2):E9.
355. Heise T, Brugger A, Cook C, Eckers U, Hutchcraft A, Nosek L, et al. PROMAXX inhaled insulin: safe and efficacious administration with a commercially available dry powder inhaler. Diabetes Obes Metab 2009; 11(5):455-9.
356. Eichelberg C, Andreas A, Heuer R, Huland H, Heinzer H, Huland E. Long-term tumor control with inhalational interleukin 2 therapy in cardiac high risk patients with metastatic renal carcinoma. J Urol 2008; 179(4):167.
357. Tazawa R, Nakata K, Inoue Y, Nukiwa T. Granulocyte-macrophage colony-stimulating factor inhalation therapy for patients with idiopathic pulmonary alveolar proteinosis: a pilot study; and long-term treatment with aerosolized granulocyte-macrophage colony-stimulating factor: a case report. Respirology 2006; 11 Suppl:S61-4.
358. CSLBehring. Safety and tolerability study of liquid alpha1 proteinase inhibitor (API) in subjects with cystic fibrosis. NCT01347190: http://clinicaltrials.gov [accessed on October 2014].
359. Kobayashi S, Kondo S, Juni K. Pulmonary delivery of salmon calcitonin dry powders containing absorption enhancers in rats. Pharm Res 1996; 13(1):80-3.
360. Yamamoto A, Okumura S, Fukuda Y, Fukui M, Takahashi K, Muranishi S. Improvement of the pulmonary absorption of (Asu1,7)-eel calcitonin by various absorption enhancers and their pulmonary toxicity in rats. J Pharm Sci 1997; 86(10):1144-7.
361. Yang M, Velaga S, Yamamoto H, Takeuchi H, Kawashima Y, Hovgaard L, et al. Characterisation of salmon calcitonin in spray-dried powder for inhalation. Effect of chitosan. Int J Pharm 2007; 331(2):176-81.
362. Shoyele SA, Sivadas N, Cryan SA. The effects of excipients and particle engineering on the biophysical stability and aerosol performance of parathyroid hormone (1-34) prepared as a dry powder for inhalation. AAPS PharmSciTech 2011; 12(1):304-11.
363. Schreier H, McNicol K, Bennett D, Teitelbaum Z, Derendorf H. Pharmacokinetics of detirelix following intratracheal instillation and aerosol inhalation in the unanesthetized awake sheep. Pharm Res 1994; 11(7):1056-9.
364. Bennett D, Tyson E, Nerenberg C, Mah S, de Groot J, Teitelbaum Z. Pulmonary delivery of detirelix by intratracheal instillation and aerosol inhalation in the briefly anesthetized dog. Pharm Res 1994; 11(7):1048-55.
365. van Zandwijk N, Jassem E, Dubbelmann R, Braat M, Rumke P. Aerosol application of interferon-alpha in the treatment of bronchioloalveolar carcinoma. Eur J Cancer 1990; 26(6):738-40.
366. Low S, Nunes S, Bitonti A, Dumont J. Oral and pulmonary delivery of FSH-Fc fusion proteins via neonatal Fc receptor-mediated transcytosis. Hum Reprod 2005; 20(7):1805-13.
367. Onoue S, Yamamoto K, Kawabata Y, Hirose M, Mizumoto T, Yamada S. Novel dry powder inhaler formulation of glucagon with addition of citric acid for enhanced pulmonary delivery. Int J Pharm 2009; 382(1-2):144-50.
368. Roy I, Vij N. Nanodelivery in airway diseases: challenges and therapeutic applications. Nanomedicine 2010; 6(2):237-44.
369. Alpar HO, Somavarapu S, Atuah KN, Bramwell VW. Biodegradable mucoadhesive particulates for nasal and pulmonary antigen and DNA delivery. Adv Drug Deliv Rev 2005; 57(3):411-30.

370. Lai S, Wang Y, Hanes J. Mucus-penetrating nanoparticles for drug and gene delivery to mucosal tissues. Adv Drug Deliv Rev 2009; 61(2):158-71.
371. Tang BC, Dawson M, Lai SK, Wang YY, Suk JS, Yang M, et al. Biodegradable polymer nanoparticles that rapidly penetrate the human mucus barrier. PNAS 2009; 106(46):19268-73.
372. Suk JS, Boylan NJ, Trehan K, Tang BC, Schneider CS, Lin JM, et al. N-acetylcysteine enhances cystic fibrosis sputum penetration and airway gene transfer by highly compacted DNA nanoparticles. Mol Ther 2011; 19(11):1981-9.
373. Suk JS, Lai SK, Wang YY, Ensign LM, Zeitlin PL, Boyle MP, et al. The penetration of fresh undiluted sputum expectorated by cystic fibrosis patients by non-adhesive polymer nanoparticles. Biomaterials 2009; 30(13):2591-7.
374. Shahiwala A, Misra A. A preliminary pharmacokinetic study of liposomal leuprolide dry powder inhaler: a technical note. AAPS PharmSciTech 2005; 6(3):E482-6.
375. Letsou G, Safi H, Reardon M, Ergenoglu M, Li Z, Klonaris C, et al. Pharmacokinetics of liposomal aerosolized cyclosporine A for pulmonary immunosuppression. Ann Thorac Surg 1999; 68(6):2044-8.
376. Waldrep J, Arppe J, Jansa K, Vidgren M. Experimental pulmonary delivery of cyclosporin A by liposome aerosol. Int J Pharm 1998; 160(2):239-49.
377. Gilbert B, Knight C, Alvarez F, Waldrep C, Rodarte J, Knight V, et al. Tolerance of volunteers to cyclosporine A-dilauroylphosphatidylcholine liposome aerosol. Am J Respir Crit Care Med 1997; 156(6):1789-93.
378. Khanna C, Hasz D, Klausner J, Anderson P. Aerosol delivery of interleukin 2 liposomes is nontoxic and biologically effective: canine studies. Clin Cancer Res 1996; 2(4):721-34.
379. Khanna C, Anderson P, Hasz D, Katsanis E, Neville M, Klausner J. Interleukin-2 liposome inhalation therapy is safe and effective for dogs with spontaneous pulmonary metastases. Cancer 1997; 79(7):1409-21.
380. Skubitz K, Anderson P. Inhalational interleukin-2 liposomes for pulmonary metastases: a phase I clinical trial. Anticancer Drugs 2000; 11(7):555-63.
381. Ten R, Anderson P, Zein N, Temesgen Z, Clawson M, Weiss W. Interleukin-2 liposomes for primary immune deficiency using the aerosol route. Int Immunopharmacol 2002; 2(2-3):333-44.
382. Kaipel M, Wagner A, Wassermann E, Vorauer-Uhl K, Kellner R, Redl H, et al. Increased biological half-life of aerosolized liposomal recombinant human Cu/Zn superoxide dismutase in pigs. J Aerosol Med Pulm Drug Deliv 2008; 21(3):281-90.
383. Lange C, Hancock R, Samuel J, Finlay W. In vitro aerosol delivery and regional airway surface liquid concentration of a liposomal cationic peptide. J Pharm Sci 2001; 90(10):1647-57.
384. Menon JU, Ravikumar P, Pise A, Gyawali D, Hsia CC, Nguyen KT. Polymeric nanoparticles for pulmonary protein and DNA delivery. Acta Biomater 2014; 10(6):2643-52.
385. Kunda NK, Alfagih IM, Dennison SR, Tawfeek HM, Somavarapu S, Hutcheon GA, et al. Bovine serum albumin adsorbed PGA-co-PDL nanocarriers for vaccine delivery via dry powder inhalation. Pharm Res 2015; 32(4):1341-53.
386. Tawfeek HM, Evans AR, Iftikhar A, Mohammed AR, Shabir A, Somavarapu S, et al. Dry powder inhalation of macromolecules using novel PEG-co-polyester microparticle carriers. Int J Pharm 2013; 441(1-2):611-9.

387. Grenha A. Microencapsulación de nanopartículas de quitosano para la administración pulmonar de macromoléculas terapéuticas. Santiago de Compostela: Universidad de Santiago de Compostela, Facultad de Farmacia; 2006.
388. Yamamoto H, Kuno Y, Sugimoto S, Takeuchi H, Kawashima Y. Surface-modified PLGA nanosphere with chitosan improved pulmonary delivery of calcitonin by mucoadhesion and opening of the intercellular tight junctions. J Control Release 2005; 102(2):373-81.
389. Yang M, Yamamoto H, Kurashima H, Takeuchi H, Yokoyama T, Tsujimoto H, et al. Design and evaluation of poly(DL-lactic-co-glycolic acid) nanocomposite particles containing salmon calcitonin for inhalation. Eur J Pharm Sci 2012; 46(5):374-80.
390. Yang M, Yamamoto H, Kurashima H, Takeuchi H, Yokoyama T, Tsujimoto H, et al. Design and evaluation of inhalable chitosan-modified poly (DL-lactic-co-glycolic acid) nanocomposite particles. Eur J Pharm Sci 2012; 47(1):235-43.
391. Sinsuebpol C, Chatchawalsaisin J, Kulvanich P. Preparation and in vivo absorption evaluation of spray dried powders containing salmon calcitonin loaded chitosan nanoparticles for pulmonary delivery. Drug Des Devel Ther 2013; 7:861-73.
392. Klingler C, Müller B, Steckel H. Insulin-micro- and nanoparticles for pulmonary delivery. Int J Pharm 2009; 377(1-2):173-9.
393. Cipolla D, Gonda I, Chan HK. Liposomal formulations for inhalation. Ther Deliv 2013; 4(8):1047-72.
394. Willis L, Hayes D, Mansour HM. Therapeutic liposomal dry powder inhalation aerosols for targeted lung delivery. Lung 2012; 190(3):251-62.
395. Insmed Incorporated. Phase 1b/2a multidose safety and tolerability study of liposomal amikacin for inhalation (Arikace™) in cystic fibrosis patient with chronic infections due to Pseudomonas aeruginosa. NCT00558844: https://clinicaltrials.gov [accessed on February 2015].
396. Aradigm Corporation. A multicenter, randomized, double-blind, placebo-controlled study to evaluate the safety and efficacy of Pulmaquin® in the management of chronic lung infections with Pseudomonas aeruginosa in patients with non-cystic fibrosis bronchiectasis, including 28 day open-label extension. NCT02104245: https://clinicaltrials.gov [accessed on January 2015].
397. Chen CH, Cuong NV, Chen YT, So RC, Liau I, Hsieh MF. Overcoming multidrug resistance of breast cancer cells by the micellar doxorubicin nanoparticles of mPEG-PCL-graft-cellulose. J Nanosci Nanotechnol 2011; 11(1):53-60.
398. Rijnders BJ, Cornelissen JJ, Slobbe L, Becker MJ, Doorduijn JK, Hop WC, et al. Aerosolized liposomal amphotericin B for the prevention of invasive pulmonary aspergillosis during prolonged neutropenia: a randomized, placebo-controlled trial. Clin Infect Dis 2008; 46(9):1401-8.
399. Barwicz J, Christian S, Gruda I. Effects of the aggregation state of amphotericin B on its toxicity to mice. Antimicrob Agents Chemother 1992; 36(10):2310-5.
400. Moazeni E, Gilani K, Najafabadi AR, Reza Rouini M, Mohajel N, Amini M, et al. Preparation and evaluation of inhalable itraconazole chitosan based polymeric micelles. Daru 2012; 20(1):85.
401. Vadakkan MV, Annapoorna K, Sivakumar KC, Mundayoor S, Kumar GS. Dry powder cationic lipopolymeric nanomicelle inhalation for targeted delivery of antitubercular drug to alveolar macrophage. Int J Nanomedicine 2013; 8:2871-85.

402. Gill KK, Nazzal S, Kaddoumi A. Paclitaxel loaded PEG(5000)-DSPE micelles as pulmonary delivery platform: formulation characterization, tissue distribution, plasma pharmacokinetics, and toxicological evaluation. Eur J Pharm Biopharm 2011; 79(2):276-84.
403. Garbuzenko OB, Mainelis G, Taratula O, Minko T. Inhalation treatment of lung cancer: the influence of composition, size and shape of nanocarriers on their lung accumulation and retention. Cancer Biol Med 2014; 11(1):44-55.
404. Gaber N, Darwis Y, Peh K, Tan Y. Characterization of polymeric micelles for pulmonary delivery of beclomethasone dipropionate. J Nanosci Nanotechnol 2006; 6(9-10):3095-101.
405. Sahib MN, Abdulameer SA, Darwis Y, Peh KK, Tan YT. Solubilization of beclomethasone dipropionate in sterically stabilized phospholipid nanomicelles (SSMs): physicochemical and in vitro evaluations. Drug Des Devel Ther 2012; 6:29-42.
406. Sahib MN, Darwis Y, Peh KK, Abdulameer SA, Tan YT. Rehydrated sterically stabilized phospholipid nanomicelles of budesonide for nebulization: physicochemical characterization and in vitro, in vivo evaluations. Int J Nanomedicine 2011; 6:2351-66.
407. Craparo EF, Teresi G, Bondi' ML, Licciardi M, Cavallaro G. Phospholipid-polyaspartamide micelles for pulmonary delivery of corticosteroids. Int J Pharm 2011; 406(1-2):135-44.
408. Hu FQ, Zhao MD, Yuan H, You J, Du YZ, Zeng S. A novel chitosan oligosaccharide-stearic acid micelles for gene delivery: properties and in vitro transfection studies. Int J Pharm 2006; 315(1-2):158-66.
409. Hu FQ, Wu XL, Du YZ, You J, Yuan H. Cellular uptake and cytotoxicity of shell crosslinked stearic acid-grafted chitosan oligosaccharide micelles encapsulating doxorubicin. Eur J Pharm Biopharm 2008; 69(1):117-25.
410. Laouini A, Andrieu V, Vecellio L, Fessi H, Charcosset C. Characterization of different vitamin E carriers intended for pulmonary drug delivery. Int J Pharm 2014; 471(1-2):385-90.
411. Laouini A, Koutroumanis KP, Charcosset C, Georgiadou S, Fessi H, Holdich RG, et al. pH-sensitive micelles for targeted drug delivery prepared using a novel membrane contactor method. ACS Appl Mater Interfaces 2013; 5(18):8939-47.
412. Wu Y, Li M, Gao H. Polymeric micelle composed of PLA and chitosan as a drug carrier. J Polym Res 2009; 16(1):11-8.
413. Chen L, Xie Z, Hu J, Chen X, Jing X. Enantiomeric PLA-PEG block copolymers and their stereocomplex micelles used as rifampin delivery. J Nanopart Res 2007; 9(5):777-85.
414. Silva M, Lara A, Leite C, Ferreira E. Potential tuberculostatic agents: Micelle-forming copolymer poly(ethylene glycol)-poly(aspartic acid) prodrug with isoniazid. Arch Pharm 2001; 334(6):189-93.
415. McConville JT, Overhoff KA, Sinswat P, Vaughn JM, Frei BL, Burgess DS, et al. Targeted high lung concentrations of itraconazole using nebulized dispersions in a murine model. Pharm Res 2006; 23(5):901-11.
416. Vaughn JM, McConville JT, Burgess D, Peters JI, Johnston KP, Talbert RL, et al. Single dose and multiple dose studies of itraconazole nanoparticles. Eur J Pharm Biopharm 2006; 63(2):95-102.

417. Alvarez CA, Wiederhold NP, McConville JT, Peters JI, Najvar LK, Graybill JR, et al. Aerosolized nanostructured itraconazole as prophylaxis against invasive pulmonary aspergillosis. J Infect 2007; 55(1):68-74.
418. Hoeben BJ, Burgess DS, McConville JT, Najvar LK, Talbert RL, Peters JI, et al. In vivo efficacy of aerosolized nanostructured itraconazole formulations for prevention of invasive pulmonary aspergillosis. Antimicrob Agents Chemother 2006; 50(4):1552-4.
419. Vaughn JM, Wiederhold NP, McConville JT, Coalson JJ, Talbert RL, Burgess DS, et al. Murine airway histology and intracellular uptake of inhaled amorphous itraconazole. Int J Pharm 2007; 338(1-2):219-24.
420. Liu D, Hsieh J, Fan X, Yang J, Chung T. Synthesis, characterization and drug delivery behaviors of new PCP polymeric micelles. Carbohydr Polym 2007; 68(3):544-54.
421. Kontoyianni C, Sideratou Z, Theodossiou T, Tziveleka LA, Tsiourvas D, Paleos CM. A novel micellar PEGylated hyperbranched polyester as a prospective drug delivery system for paclitaxel. Macromol Biosci 2008; 8(9):871-81.
422. Yang Y, Chen C, Yang J, Tsai T. Spray-dried microparticles containing polymeric micelles encapsulating hematoporphyrin. AAPS J 2010; 12(2):138-46.
423. Roesler S, Koch FP, Schmehl T, Weissmann N, Seeger W, Gessler T, et al. Amphiphilic, low molecular weight poly(ethylene imine) derivatives with enhanced stability for efficient pulmonary gene delivery. J Gene Med 2011; 13(2):123-33.
424. Chao Y, Chang S, Lu S, Hwang T, Hsieh W, Liaw J. Ethanol enhanced in vivo gene delivery with non-ionic polymeric micelles inhalation. J Control Relesease 2007; 118(1):105-17.
425. Umashankar M, Sachdeva R, Gulati M. Aquasomes: a promising carrier for peptides and protein delivery. Nanomedicine 2010; 6(3):419-26.
426. Liechty WB, Kryscio DR, Slaughter BV, Peppas NA. Polymers for drug delivery systems. Annu Rev Chem Biomol Eng 2010; 1:149-73.
427. Wang Y, Li Y, Zhang L, Fang X. Pharmacokinetics and biodistribution of paclitaxel-loaded pluronic P105 polymeric micelles. Arch Pharm Res 2008; 31(4):530-8.
428. Sundar S, Kundu J, Kundu S. Biopolymeric nanoparticles. Sci Technol Adv Mater 2010; 11(1):1-13.
429. Sung J, Pulliam B, Edwards D. Nanoparticles for drug delivery to the lungs. Trends Biotechnol 2007; 25(12):563-70.
430. Panyam J, Labhasetwar V. Biodegradable nanoparticles for drug and gene delivery to cells and tissue. Adv Drug Deliv Rev 2003; 55(3):329-47.
431. Gaucher G, Dufresne MH, Sant VP, Kang N, Maysinger D, Leroux JC. Block copolymer micelles: preparation, characterization and application in drug delivery. J Control Release 2005; 109(1-3):169-88.
432. Sarmento B, Ribeiro A, Veiga F, Ferreira D. Development and validation of a rapid reversed-phase HPLC method for the determination of insulin from nanoparticulate systems. Biomed Chromatogr 2006; 20(9):898-903.
433. Cambre JN, Sumerlin BS. Biomedical applications of boronic acid polymers. Polymer 2011; 52(21):4631-43.
434. Yang T, Ji R, Deng XX, Du FS, Li ZC. Glucose-responsive hydrogels based on dynamic covalent chemistry and inclusion complexation. Soft Matter 2014; 10(15):2671-8.
435. Yang H, Zhang C, Li C, Liu Y, An Y, Ma R, et al. Glucose-responsive polymer vesicles templated by α-CD/PEG inclusion complex. Biomacromolecules 2015; 16(4):1372–1381.

436. Yao Y, Shen H, Zhang G, Yang J, Jin X. Synthesis of poly(N-isopropylacrylamide)-co-poly(phenylboronate ester) acrylate and study on their glucose-responsive behavior. J Colloid Interface Sci 2014; 431:216-22.
437. Samad A, Sultana Y, Aqil M. Liposomal drug delivery systems: an update review. Curr Drug Deliv 2007; 4(4):297-305.
438. ICH. Impurities: Guideline for Residual Solvents Q3C (R5). 2011.
439. Tsui H-W, Wang J-H, Hsu Y-H, Chen L-J. Study of heat of micellization and phase separation for Pluronic aqueous solutions by using a high sensitivity differential scanning calorimetry. Colloid Polym Sci 2010; 288:1687-96.
440. Lin Y, Alexandridis P. Temperature-dependent adsorption of Pluronic F127 block copolymers onto carbon black particles dispersed in aqueous media. J Phys Chem B 2002; 106:10834-44.
441. Desai PR, Jain NJ, Sharma RK, Bahadur P. Effect of additives on the micellization of PEO/PPO/PEO block copolymer F127 in aqueous solution. Colloids Surf A 2001; 178(1-3):57-69.
442. Wu Y, Sprik R, Poon W, Eiser E. Effect of salt on the phase behaviour of F68 triblock PEO/PPO/PEO copolymer. J Phys: Condens Matter 2006; 18(19):4461–70.
443. Batrakova EV, Kabanov AV. Pluronic block copolymers: evolution of drug delivery concept from inert nanocarriers to biological response modifiers. J Control Release 2008; 130(2):98-106.
444. Alexandridis P, Hatton TA. Poly(ethylene oxide)-poly(propylene oxide)-poly (ethylene oxide) block copolymer surfactants in aqueous solutions and at interfaces: thermodynamics, structure, dynamics, and modeling. Colloids Surf A 1995; 96(1-2):1-46.
445. Jokerst JV, Lobovkina T, Zare RN, Gambhir SS. Nanoparticle PEGylation for imaging and therapy. Nanomedicine (Lond) 2011; 6(4):715-28.
446. Ibricevic A, Guntsen SP, Zhang K, Shrestha R, Liu Y, Sun JY, et al. PEGylation of cationic, shell-crosslinked-knedel-like nanoparticles modulates inflammation and enhances cellular uptake in the lung. Nanomedicine 2013; 9(7):912-22.
447. Wood GC. Aerosolized antibiotics for treating hospital-acquired and ventilator-associated pneumonia. Expert Rev Anti Infect Ther 2011; 9(11):993-1000.
448. Rubin BK, Williams RW. Emerging aerosol drug delivery strategies: from bench to clinic. Adv Drug Deliv Rev 2014; 75:141-8.
449. Yang MY, Chan JG, Chan HK. Pulmonary drug delivery by powder aerosols. J Control Release 2014; 193:228-240.
450. Carvalho TC, Peters JI, Williams RO. Influence of particle size on regional lung deposition-what evidence is there? Int J Pharm 2011; 406(1-2):1-10.
451. Newman SP, Chan HK. In vitro/in vivo comparisons in pulmonary drug delivery. J Aerosol Med Pulm Drug Deliv 2008; 21(1):77-84.
452. Dong A, Huang P, Caughey WS. Protein secondary structures in water from second-derivative amide I infrared spectra. Biochemistry 1990; 29(13):3303-8.
453. Soares S, Fonte P, Costa A, Andrade J, Seabra V, Ferreira D, et al. Effect of freeze-drying, cryoprotectants and storage conditions on the stability of secondary structure of insulin-loaded solid lipid nanoparticles. Int J Pharm 2013; 456(2):370-81.
454. Kelly SM, Jess TJ, Price NC. How to study proteins by circular dichroism. Biochim Biophys Acta 2005; 1751(2):119-39.
455. European Pharmacopoeia 8th edition. Strasbourg: EDQM, Council of Europe; 2014.

456. Holt J. MMADcalculator. http://www.mmadcalculator.com [accessed on February 2015].
457. Moore JW, Flanner HH. Mathematical comparison of dissolution profiles. Pharm Tech 1996; 20:64-74.
458. Rave K, Potocka E, Heinemann L, Heise T, Boss AH, Marino M, et al. Pharmacokinetics and linear exposure of AFRESA compared with the subcutaneous injection of regular human insulin. Diabetes Obes Metab 2009; 11(7):715-20.
459. Lebhardt T, Roesler S, Uusitalo HP, Kissel T. Surfactant-free redispersible nanoparticles in fast-dissolving composite microcarriers for dry-powder inhalation. Eur J Pharm Biopharm 2011; 78(1):90-6.
460. Makino K, Yamamoto N, Higuchi K, Harada N, Ohshima H, Terada H. Phagocytic uptake of polystyrene microspheres by alveolar macrophages: effects of the size and surface properties of the microspheres. Colloids Surf B 2003; 27(1):33–9.
461. Liu Z, Liu D, Wang L, Zhang J, Zhang N. Docetaxel-loaded pluronic P123 polymeric micelles: in vitro and in vivo evaluation. Int J Mol Sci 2011; 12(3):1684-96.
462. Hirsjärvi S, Peltonen L, Hirvonen J. Effect of sugars, surfactant, and tangential flow filtration on the freeze-drying of poly(lactic acid) nanoparticles. AAPS PharmSciTech 2009; 10(2):488-94.
463. Djuris J, Nikolakakis I, Ibric S, Djuric Z, Kachrimanis K. Preparation of carbamazepine-Soluplus solid dispersions by hot-melt extrusion, and prediction of drug-polymer miscibility by thermodynamic model fitting. Eur J Pharm Biopharm 2013; 84(1):228-37.
464. Thakral NK, Ray AR, Bar-Shalom D, Eriksson AH, Majumdar DK. Soluplus-solubilized citrated camptothecin-a potential drug delivery strategy in colon cancer. AAPS PharmSciTech 2012; 13(1):59-66.
465. Albertini B, Passerini N, Di Sabatino M, Monti D, Burgalassi S, Chetoni P, et al. Poloxamer 407 microspheres for orotransmucosal drug delivery. Part I: formulation, manufacturing and characterization. Int J Pharm 2010; 399(1-2):71-9.
466. Gill P, Moghadam TT, Ranjbar B. Differential scanning calorimetry techniques: applications in biology and nanoscience. J Biomol Tech 2010; 21(4):167-93.
467. Guo C, Liu H, Wang J, Chen J. Conformational structure of triblock copolymers by FT-Raman and FTIR spectroscopy. J Colloid Interface Sci 1999; 209(2):368-73.
468. Piergies N, Proniewicz E, Ozaki Y, Kim Y, Proniewicz LM. Influence of substituent type and position on the adsorption mechanism of phenylboronic acids: infrared, Raman, and surface-enhanced Raman spectroscopy studies. J Phys Chem A 2013; 117(27):5693-705.
469. Vanea E, Simon V. XPS and Raman study of zinc containing silica microparticles loaded with insulin. Appl Surf Sci 2013; 280:144–50.
470. Griebenow K, Klibanov A. On protein denaturation in aqueous−organic mixtures but not in pure organic solvents. J Am Chem Soc 1996; 118(47):11695-700.
471. Mi Y, Wood G, Thoma L. Cryoprotection mechanisms of polyethylene glycols on lactate dehydrogenase during freeze-thawing. AAPS J 2004; 6(3):e22.
472. Sarmento B, Ferreira D, Jorgensen L, van de Weert M. Probing insulin's secondary structure after entrapment into alginate/chitosan nanoparticles. Eur J Pharm Biopharm 2007; 65(1):10-7.
473. Martin SR, Schilstra MJ. Circular dichroism and its application to the study of biomolecules. Methods Cell Biol 2008; 84:263-93.

474. Lu X, Gao H, Li C, Yang YW, Wang Y, Fan Y, et al. Polyelectrolyte complex nanoparticles of amino poly(glycerol methacrylate)s and insulin. Int J Pharm 2012; 423(2):195-201.
475. Fang JY, Hsu SH, Leu YL, Hu JW. Delivery of cisplatin from Pluronic co-polymer systems: liposome inclusion and alginate coupling. J Biomater Sci Polym Ed 2009; 20(7-8):1031-47.
476. Shamma RN, Basha M. Soluplus®: a novel polymeric solubilizer for optimization of carvedilol solid dispersions: formulation design and effect of method of preparation. Powder Technol 2013; 237:406–14.
477. Hassan MS, Lau RW. Effect of particle shape on dry particle inhalation: study of flowability, aerosolization, and deposition properties. AAPS PharmSciTech 2009; 10(4):1252-62.
478. Kaialy W, Martin GP, Ticehurst MD, Royall P, Mohammad MA, Murphy J, et al. Characterisation and deposition studies of recrystallised lactose from binary mixtures of ethanol/butanol for improved drug delivery from dry powder inhalers. AAPS J 2011; 13(1):30-43.
479. Kumar TM, Misra A. Formulation and evaluation of insulin dry powder for inhalation. Drug Dev Ind Pharm 2006; 32(6):677-86.
480. Shen ZG, Chen WH, Jugade N, Gao LY, Glover W, Shen JY, et al. Fabrication of inhalable spore like pharmaceutical particles for deep lung deposition. Int J Pharm 2012; 430(1-2):98-103.
481. White S, Bennett DB, Cheu S, Conley PW, Guzek DB, Gray S, et al. EXUBERA: pharmaceutical development of a novel product for pulmonary delivery of insulin. Diabetes Technol Ther 2005; 7(6):896-906.
482. Johal B, Howald M, Fischer M, Marshall J, Venthoye G. Fine particle profile of fluticasone propionate/formoterol fumarate versus other combination products: the DIFFUSE study. Comb Prod Ther 2013; 3:39-51.
483. Shi S, Ashley ES, Alexander BD, Hickey AJ. Initial characterization of micafungin pulmonary delivery via two different nebulizers and multivariate data analysis of aerosol mass distribution profiles. AAPS PharmSciTech 2009; 10(1):129-37.
484. Kisich KO, Higgins MP, Park I, Cape SP, Lindsay L, Bennett DJ, et al. Dry powder measles vaccine: particle deposition, virus replication, and immune response in cotton rats following inhalation. Vaccine 2011; 29(5):905-12.
485. Telko MJ, Hickey AJ. Aerodynamic and electrostatic properties of model dry powder aerosols: a comprehensive study of formulation factors. AAPS PharmSciTech 2014; 15(6):1378-97.
486. Baker EH, Clark N, Brennan AL, Fisher DA, Gyi KM, Hodson ME, et al. Hyperglycemia and cystic fibrosis alter respiratory fluid glucose concentrations estimated by breath condensate analysis. J Appl Physiol (1985) 2007; 102(5):1969-75.
487. Amancha KP, Balkundi S, Lvov Y, Hussain A. Pulmonary sustained release of insulin from microparticles composed of polyelectrolyte layer-by-layer assembly. Int J Pharm 2014; 466(1-2):96-108.
488. Chou DH, Webber MJ, Tang BC, Lin AB, Thapa LS, Deng D, et al. Glucose-responsive insulin activity by covalent modification with aliphatic phenylboronic acid conjugates. PNAS 2015; 112(8):2401-6.

489. Lee TH, Lin SY. Pluronic F68 enhanced the conformational stability of salmon calcitonin in both aqueous solution and lyophilized solid form. Biopolymers 2011; 95(11):785-91.
490. Akash MS, Rehman K, Sun H, Chen S. Assessment of release kinetics, stability and polymer interaction of poloxamer 407-based thermosensitive gel of interleukin-1 receptor antagonist. Pharm Dev Technol 2014; 19(3):278-84.
491. Pikal MJ, Rigsbee DR. The stability of insulin in crystalline and amorphous solids: observation of greater stability for the amorphous form. Pharm Res 1997; 14(10):1379-87.
492. McElroy MC, Kirton C, Gliddon D, Wolff RK. Inhaled biopharmaceutical drug development: nonclinical considerations and case studies. Inhal Toxicol 2013; 25(4):219-32.
493. Sarmento B, Martins S, Ferreira D, Souto EB. Oral insulin delivery by means of solid lipid nanoparticles. Int J Nanomedicine 2007; 2(4):743-9.
494. Fonte P, Nogueira T, Gehm C, Ferreira D, Sarmento B. Chitosan-coated solid lipid nanoparticles enhance the oral absorption of insulin. Drug Deliv and Transl Res 2011; 1(4):299–308.
495. Hamishehkar H, Emami J, Najafabadi AR, Gilani K, Minaiyan M, Hassanzadeh K, et al. Pharmacokinetics and pharmacodynamics of controlled release insulin loaded PLGA microcapsules using dry powder inhaler in diabetic rats. Biopharm Drug Dispos 2010; 31(2-3):189-201.
496. Kaur G, Narang RK, Rath G, Goyal AK. Advances in pulmonary delivery of nanoparticles. Artif Cells Blood Substit Immobil Biotechnol 2012; 40(1-2):75-96.
497. Ahmed F, Alexandridis P, Neelamegham S. Synthesis and application of fluorescein-labeled pluronic block copolymers to the study of polymer−surface interactions. Langmuir 2001; 17(2):537–46.
498. Jung HH, Park K, Han DK. Preparation of TGF-β1-conjugated biodegradable pluronic F127 hydrogel and its application with adipose-derived stem cells. J Control Release 2010; 147(1):84-91.
499. Lippens E, Swennen I, Gironès J, Declercq H, Vertenten G, Vlaminck L, et al. Cell survival and proliferation after encapsulation in a chemically modified Pluronic F127 hydrogel. J Biomater Appl 2013; 27(7):828-39.
500. Batrakova EV, Li S, Vinogradov SV, Alakhov VY, Miller DW, Kabanov AV. Mechanism of pluronic effect on P-glycoprotein efflux system in blood-brain barrier: contributions of energy depletion and membrane fluidization. J Pharmacol Exp Ther 2001; 299(2):483-93.
501. Demina T, Grozdova I, Krylova O, Zhirnov A, Istratov V, Frey H, et al. Relationship between the structure of amphiphilic copolymers and their ability to disturb lipid bilayers. Biochemistry 2005; 44(10):4042-54.
502. Widdicombe JG. Airway liquid: a barrier to drug diffusion? Eur Respir J 1997; 10(10):2194-7.
503. Rennard SI, Basset G, Lecossier D, O'Donnell KM, Pinkston P, Martin PG, et al. Estimation of volume of epithelial lining fluid recovered by lavage using urea as marker of dilution. J Appl Physiol (1985) 1986; 60(2):532-8.
504. Herbst KL, Hirsch IB. Insulin strategies for primary care providers. Clin Diabetes 2002; 20(1):11-7.
505. Foster KA, Avery ML, Yazdanian M, Audus KL. Characterization of the Calu-3 cell line as a tool to screen pulmonary drug delivery. Int J Pharm 2000; 208(1-2):1-11.

506. Wang Z, Zhang Q. Transport of proteins and peptides across human cultured alveolar A549 cell monolayer. Int J Pharm 2004; 269(2):451-6.
507. Antunes F, Andrade F, Araújo F, Ferreira D, Sarmento B. Establishment of a triple co-culture in vitro cell models to study intestinal absorption of peptide drugs. Eur J Pharm Biopharm 2013; 83(3):427-35.
508. Mathia NR, Timoszyk J, Stetsko PI, Megill JR, Smith RL, Wall DA. Permeability characteristics of Calu-3 human bronchial epithelial cells: in vitro-in vivo correlation to predict lung absorption in rats. J Drug Target 2002; 10(1):31-40.
509. Sarmento B, Andrade F, Silva SB, Rodrigues F, das Neves J, Ferreira D. Cell-based in vitro models for predicting drug permeability. Expert Opin Drug Metab Toxicol 2012; 8(5):607-21.
510. Zheng J, Zheng Y, Chen J, Fang F, He J, Li N, et al. Enhanced pulmonary absorption of recombinant human insulin by pulmonary surfactant and phospholipid hexadecanol tyloxapol through Calu-3 monolayers. Pharmazie 2012; 67(5):448-51.
511. Rave K, Bott S, Heinemann L, Sha S, Becker R, Willavize S, et al. Time-action profile of inhaled insulin in comparison with subcutaneously injected insulin lispro and regular human insulin. Diabetes Care 2005; 28(5):1077-82.
512. Hussain A, Ahsan F. Indication of transcytotic movement of insulin across human bronchial epithelial cells. J Drug Target 2006; 14(4):181-90.
513. Pezron I, Mitra R, Pal D, Mitra A. Insulin aggregation and asymmetric transport across human bronchial epithelial cell monolayers (Calu-3). J Pharm Sci 2002; 91(4):1135-46.
514. Shubber S, Vllasaliu D, Rauch C, Jordan F, Illum L, Stolnik S. Mechanism of mucosal permeability enhancement of CriticalSorb® (Solutol® HS15) investigated In vitro in cell cultures. Pharm Res 2015; 32(2):516-27.
515. Illum L, Jordan F, Lewis AL. CriticalSorb: a novel efficient nasal delivery system for human growth hormone based on Solutol HS15. J Control Release 2012; 162(1):194-200.
516. Caroni P. New EMBO members' review: actin cytoskeleton regulation through modulation of PI(4,5)P(2) rafts. EMBO J 2001; 20(16):4332-6.
517. Vllasaliu D, Exposito-Harris R, Heras A, Casettari L, Garnett M, Illum L, et al. Tight junction modulation by chitosan nanoparticles: comparison with chitosan solution. Int J Pharm 2010; 400(1-2):183-93.
518. Fanning AS, Ma TY, Anderson JM. Isolation and functional characterization of the actin binding region in the tight junction protein ZO-1. FASEB J 2002; 16(13):1835-7.
519. Xiao K, Li Y, Luo J, Lee JS, Xiao W, Gonik AM, et al. The effect of surface charge on in vivo biodistribution of PEG-oligocholic acid based micellar nanoparticles. Biomaterials 2011; 32(13):3435-46.
520. Shan X, Liu C, Yuan Y, Xu F, Tao X, Sheng Y, et al. In vitro macrophage uptake and in vivo biodistribution of long-circulation nanoparticles with poly(ethylene-glycol)-modified PLA (BAB type) triblock copolymer. Colloids Surf B 2009; 72(2):303-11.
521. Besheer A, Vogel J, Glanz D, Kressler J, Groth T, Mäder K. Characterization of PLGA nanospheres stabilized with amphiphilic polymers: hydrophobically modified hydroxyethyl starch vs pluronics. Mol Pharm 2009; 6(2):407-15.
522. Jain TK, Foy SP, Erokwu B, Dimitrijevic S, Flask CA, Labhasetwar V. Magnetic resonance imaging of multifunctional pluronic stabilized iron-oxide nanoparticles in tumor-bearing mice. Biomaterials 2009; 30(35):6748-56.

523. Geiser M. Update on macrophage clearance of inhaled micro- and nanoparticles. J Aerosol Med Pulm Drug Deliv 2010; 23(4):207-17.
524. Lunov O, Syrovets T, Loos C, Beil J, Delacher M, Tron K, et al. Differential uptake of functionalized polystyrene nanoparticles by human macrophages and a monocytic cell line. ACS Nano 2011; 5(3):1657-69.
525. Patel B, Gupta N, Ahsan F. Particle engineering to enhance or lessen uptake by alveolar macrophages and to influence therapeutic outcomes. Eur J Pharm Biopharm 2014; 89:163-74.
526. McCormack FX, Whitsett JA. The pulmonary collectins, SP-A and SP-D, orchestrate innate immunity in the lung. J Clin Invest 2002; 109(6):707-12.
527. Heale JP, Pollard AJ, Stokes RW, Simpson D, Tsang A, Massing B, et al. Two distinct receptors mediate nonopsonic phagocytosis of different strains of Pseudomonas aeruginosa. J Infect Dis 2001; 183(8):1214-20.
528. Seaton BA, Crouch EC, McCormack FX, Head JF, Hartshorn KL, Mendelsohn R. Review: structural determinants of pattern recognition by lung collectins. Innate Immun 2010; 16(3):143-50.
529. Patel B, Gupta V, Ahsan F. PEG-PLGA based large porous particles for pulmonary delivery of a highly soluble drug, low molecular weight heparin. J Control Release 2012; 162(2):310-20.
530. Sakagami M. In vivo, in vitro and ex vivo models to assess pulmonary absorption and disposition of inhaled therapeutics for systemic delivery. Adv Drug Deliv Rev 2006; 58(9-10):1030-60.
531. Schanker LS. Drug absorption from the lung. Biochem Pharmacol 1978; 27(4):381-5.
532. Brown RA, Schanker LS. Absorption of aerosolized drugs from the rat lung. Drug Metab Dispos 1983; 11(4):355-60.
533. Schanker LS, Mitchell EW, Brown RA. Species comparison of drug absorption from the lung after aerosol inhalation or intratracheal injection. Drug Metab Dispos 1986; 14(1):79-88.
534. Codrons V, Vanderbist F, Ucakar B, Préat V, Vanbever R. Impact of formulation and methods of pulmonary delivery on absorption of parathyroid hormone (1-34) from rat lungs. J Pharm Sci 2004; 93(5):1241-52.
535. Suarez S, O'Hara P, Kazantseva M, Newcomer CE, Hopfer R, McMurray DN, et al. Airways delivery of rifampicin microparticles for the treatment of tuberculosis. J Antimicrob Chemother 2001; 48(3):431-4.
536. Herber-Jonat S, Mittal R, Gsinn S, Bohnenkamp H, Guenzi E, Schulze A. Comparison of lung accumulation of cationic liposomes in normal rats and LPS-treated rats. Inflamm Res 2010; 60(3):245-53.
537. Pauluhn J. Acute nose-only inhalation exposure of rats to di- and triphosgene relative to phosgene. Inhal Toxicol 2011; 23(2):65-73.
538. Phalen RF, Oldham MJ, Wolff RK. The relevance of animal models for aerosol studies. J Aerosol Med Pulm Drug Deliv 2008; 21(1):113-24.
539. Driscoll KE, Costa DL, Hatch G, Henderson R, Oberdorster G, Salem H, et al. Intratracheal instillation as an exposure technique for the evaluation of respiratory tract toxicity: uses and limitations. Toxicol Sci 2000; 55(1):24-35.
540. Lizio R, Westhof A, Lehr CM, Klenner T. Oral endotracheal intubation of rats for intratracheal instillation and aerosol drug delivery. Lab Anim 2001; 35(3):257-60.

541. Wu KK, Huan Y. Streptozotocin-induced diabetic models in mice and rats. Curr Protoc Pharmacol 2008; 40:5.47.1-5.47.14.
542. Sarmento B, Ribeiro A, Veiga F, Sampaio P, Neufeld R, Ferreira D. Alginate/chitosan nanoparticles are effective for oral insulin delivery. Pharm Res 2007; 24(12):2198-206.
543. Sajeesh S, Bouchemal K, Marsaud V, Vauthier C, Sharma CP. Cyclodextrin complexed insulin encapsulated hydrogel microparticles: an oral delivery system for insulin. J Control Release 2010; 147(3):377-84.
544. Cu Y, Saltzman WM. Drug delivery: stealth particles give mucus the slip. Nat Mater 2009; 8(1):11-3.
545. Wang YY, Lai SK, Suk JS, Pace A, Cone R, Hanes J. Addressing the PEG mucoadhesivity paradox to engineer nanoparticles that "slip" through the human mucus barrier. Angew Chem Int Ed Engl 2008; 47(50):9726-9.
546. Oda K, Yumoto R, Nagai J, Katayama H, Takano M. Mechanism underlying insulin uptake in alveolar epithelial cell line RLE-6TN. Eur J Pharmacol 2011; 672(1-3):62-9.
547. Hindlycke M, Jansson L. Glucose tolerance and pancreatic islet blood flow in rats after intraperitoneal administration of different anesthetic drugs. Ups J Med Sci 1992; 97(1):27-35.
548. Wellington D, Mikaelian I, Singer L. Comparison of ketamine-xylazine and ketamine-dexmedetomidine anesthesia and intraperitoneal tolerance in rats. J Am Assoc Lab Anim Sci 2013; 52(4):481-7.
549. Venâncio C, Félix L, Almeida V, Coutinho J, Antunes L, Peixoto F, et al. Acute ketamine impairs mitochondrial function and promotes superoxide dismutase activity in the rat brain. Anesth Analg 2015; 120(2):320-8.
550. Stoever JA, Palmer JP. Inhaled insulin and insulin antibodies: a new twist to an old debate. Diabetes Technol Ther 2002; 4(2):157-61.
551. Heise T, Bott S, Tusek C, Stephan JA, Kawabata T, Finco-Kent D, et al. The effect of insulin antibodies on the metabolic action of inhaled and subcutaneous insulin: a prospective randomized pharmacodynamic study. Diabetes Care 2005; 28(9):2161-9.
552. Sarmiento EG. Inhaled insulin and its effects on the lungs. Arch Bronconeumol 2007; 43(12):643-5.